DM

Preparation and Characterization of Anionic PPI Dendrimers for Delivery of the Hydroxychloroquine Into Tumor Cells

MASTER DISSERTATION

Ana Filipa Gonçalves Rodrigues
MASTER IN APPLIED BIOCHEMISTRY

UNIVERSIDADE da MADEIRA
A Nossa Universidade
www.uma.pt

September | 2022

Preparation and Characterization of Anionic PPI Dendrimers for Delivery of the Hydroxychloroquine Into Tumor Cells

MASTER DISSERTATION

Ana Filipa Gonçalves Rodrigues
MASTER IN APPLIED BIOCHEMISTRY

ORIENTATION
João Manuel Cunha Rodrigues

CO-ORIENTATION
Dina Maria Sousa Maciel

Preparation and Characterization of Anionic PPI Dendrimers for Delivery of the Hydroxychloroquine Into Tumor Cells

Ana Filipa Gonçalves Rodrigues

Master's in Applied Biochemistry

Supervisor: Professor João Manuel Cunha Rodrigues

Co-Supervisor: Doctor Dina Maria Sousa Maciel

Faculdade de Ciências Exatas e da Engenharia

Centro de Química da Madeira

Funchal-Portugal

September 2022

This master thesis was carried out in the Molecular Materials Research Group (MMRG) of Centro de Química da Madeira (CQM), which I thank for providing the equipment and materials.

This work was financially supported by the Fundação para a Ciência e Tecnologia (FCT) through the CQM Base Fund - UIDB/00674/2020, and Programmatic Fund - UIDP/00674/2020, and Agência Regional para o Desenvolvimento da Investigação Tecnologia e Inovação (ARDITI) through the projects M1420-01-0145-FEDER-000005 - CQM^{+}.

Acknowledgments

This work was not have been possible without the help and support of my family, colleagues, and professors. I want to thank everyone who was involved, directly and indirectly, in this project.

First, I want to thank my supervisor, Professor João Rodrigues, for all the availability, patience, support, knowledge sharing, and guidance. I want to knowledge my co-supervisor Drª Dina Maciel, for all their help, support, motivation, guidance, suggestions, generosity, availability, patience, and for helping me with the NMR experiments. I am very grateful, and I miss your company in the lab.

To my colleagues at Centro Química da Madeira (CQM), especially Nádia Nunes, Drª Rita Castro, and Drª Mara Gonçalves, for always being available to help me and share ideas. To Drª Rosa Perestrelo for the Mass Spectroscopy analyses. Moreover, also to Duarte and Lydia for supporting me with the fluorescence spectrometer equipment.

To my friends Patrícia and Ivana, I am very grateful for all the support, friendship, patience, company, and motivation, for all laughs and coffee breaks.

Finally, to my parents, Martinho and Natália, my aunt Eulália, and my boyfriend Pedro, for being my inspiration, for the care, for love, for the comprehension, and for always believing in me.

Thank you for all!

Abstract

Cancer is one of the most lethal diseases worldwide. In 2020, 19.3 million new cancer cases were reported, with approximately 10 million deaths. Female breast cancer was the most diagnosed, with 2.3 million new cases.

Hydroxychloroquine (HCQ) is an immunomodulatory drug used to treat malaria and has been shown to have therapeutic potential in oncology. It has been proven that HCQ increases tumor cell death alone or combined with targeted agents or cytotoxic chemotherapy. By combining HCQ and a nanocarrier, it is possible to direct the drug to the tumor tissues, reducing the side effects and enhancing the bioavailability.

Based on the previous experience of our group, the main goal of this master thesis was to prepare anionic carboxylate and sulfonate PPI dendrimers to transport and deliver the HCQ into tumor cells. First, amine-terminated PPI dendrimers, generation 0 to 3 (G0-G3), were synthesized, with a yield in the range of 57% -99%, and characterized by ^{1}H- and ^{13}C- NMR. After the G0 to G3 amine-terminated PPI dendrimers were prepared and obtained, the functionalization of the terminal groups with carboxylate and sulfonate dendrimers was done. Additionally, for the first time, the carboxylate- and sulfonate-terminated dendrimers G4 was synthesized. The anionic dendrimers have the advantage of being less cytotoxic, hemotoxic, and immunogenicity than cationic dendrimers. After G1 to G3 characterization by ^{1}H- ^{13}C- NMR, ATR-FTIR, DLS, zeta potential, and MS, HCQ was encapsulated. Following this, the *in vitro* drug release was performed in PBS with a pH 5 and 7.4, since the cumulative release is slightly higher in PBS with a pH 5. In general, all dendrimers showed a sustained release of HCQ in both pHs. The hemotoxicity of the dendrimers and the HCQ were also evaluated and showed no hemotoxicity. Finally, the cytotoxicity of the synthesized dendrimers, non-loaded and loaded with HCQ, was evaluated in a cancer cell line (MCF-7) and a non-cancer cell line (BJ cells). The HCQ in a range of concentration between 0.5 and 50 µM are highly cytotoxic for BJ cells and less cytotoxic for MCF-7 cells. The HCQ was further tested with the CACO-2 cells and showed to be less sensitive to the drug than with the MCF-7 cells. In order to

improve the cytotoxicity of the prepared dendrimers, an assay with doxorubicin (DOX) was performed, but no synergetic effect was observed.

Keywords: PPI dendrimers; Hydroxychloroquine; Drug release; Cytotoxicity; MCF-7 cells; CACO-2 cells; BJ cells.

Resumo

O cancro é uma das doenças mais letais em todo o mundo. Em 2020, foram reportados 19.3 milhões de novos casos, com aproximadamente 10 milhões de mortes. O cancro de mama feminino foi o mais diagnosticado, com 2.3 milhões de novos casos.

A hidroxicloroquina (HCQ) é um fármaco imunomodulador utilizado no tratamento da malária, e tem demostrado potencial terapêutico em oncologia. Foi provado que a HCQ aumenta a morte das células tumorais isoladamente ou em combinação com outros agentes ou quimioterapia. Combinando a HCQ a um nanotransportador, é possível direcionar o fármaco para os tecidos tumorais, reduzindo os efeitos secundários e aumentando a biodisponibilidade.

Baseado na experiência do nosso grupo, o principal objetivo desta tese de mestrado foi preparar dendrímeros aniónicos de poli(alquilidenamina) com terminações carboxilato e sulfonato para transportar e entregar a HCQ nas células tumorais. Em primeiro lugar, os dendrímeros de poli(alquilidenamina), geração 0 a 3 (G0 a G3) com terminações amina foram sintetizados, com um rendimento entre 57%-99%, e caracterizados por ^{1}H- e ^{13}C- NMR. De seguida procedeu-se à funcionalização dos grupos terminais do dendrímero com grupos carboxilato e sulfonato. Pela primeira vez, foi preparada a G4 dos dendrímeros com terminações carboxilato e sulfonato.

Os dendrímeros aniónicos têm a vantagem de ser menos citotóxicos, hemotóxicos e, imunogénicos, em comparação com os dendrímeros catiónicos. Após a caracterização das G1 a G3 por ^{1}H- ^{13}C- NMR, ATR-FIR, DLS, zeta potencial e MS, foi realizado o encapsulamento da HCQ. Seguidamente, a libertação do fármaco *in vitro* foi realizada em PBS a pH 5 e 7.4, sendo que, em PBS a pH 5, a libertação cumulativa é ligeiramente superior. Em geral, todos os dendrímeros apresentaram libertação sustentada da HCQ em ambos os pHs. A hemotoxicidade dos dendrímeros e da HCQ foi também avaliada. Globalmente, os dendrímeros e a HCQ não apresentaram hemotoxicidade. A citotoxicidade dos dendrímeros com HCQ e sem HCQ encapsulada foi avaliada numa linhagem celular cancerígena (MCF-7) e numa linhagem celular não cancerígena (células BJ). A HCQ numa faixa de concentração de 0.5-50 µM é

altamente citotóxica para as células BJ e menos citotóxica para as MCF-7. A HCQ foi ainda testada nas células CACO-2 que mostraram ser menos sensíveis ao fármaco, em comparação com as MCF-7. Com o objetivo de aumentar a citotoxicidade dos dendrímeros preparados foi realizado um ensaio com doxorrubicina (DOX), mas não se observou nenhum efeito sinergético digno de registo.

Palavras-chave: Dendrímeros PPI; Hidroxicloroquina; Libertação do fármaco; Citotoxicidade; Células MCF-7; Células CACO-2; Células BJ.

List of abbreviations

2,5-DHB	2,5- dihydroxybenzoic acid
AA	Antibiotic-antimycotic
AFM	Atomic force microscopy
ATR-FTIR	Attenuated total reflectance - Fourier transform infrared spectroscopy
BJ	Fibroblast cells
CACO-2	Colorectal adenocarcinoma cells
CQ	Chloroquine
C-reagent	Cyanmethemoglobin reagent
DAB	Diaminobutane
DLS	Dynamic light scattering
D-MEM	Dulbecco's modified eagle medium
DOX	Doxorubicin
DSM	Dutch state mines
EDA	Ethylenediamine
EE	Encapsulation efficiency
EGFR	Epidermal growth factor receptor
EMA	European Medicine Agency
EPR	Enhanced permeability and retention
ESI-TOF-MS	Electrospray ionization time-of-flight mass spectroscopy
FAR	Folate receptor
FBS	Fetal bovine serum
FDA	Food and Drug Administration
G6PD	Glucose-6-phosphate dehydrogenase
GHS	Glutathione
GxCN	Nitrile dendrimers (x=G0,G1,G2,G3)
$GxCO_2Me$	Methyl ester dendrimers (x=G0,G1,G2,G3)
GxC	Carboxylate dendrimers (x=G0,G1,G2,G3…)
$GxNH_2$	Amine dendrimer (x=G0,G1,G2,G3)
GxS	Sulfonate dendrimers (x=G0,G1,G2,G3…)

HA	Hyaluronic acid
HCQ	Hydroxychloroquine
HER2	Human epidermal growth factor receptor 2
Hg	Hemoglobin
HIV	Human immunodeficiency virus
HPV	Human papillomavirus infection
LC	Loading capacity
MCF-7	Breast cancer cells
MEM	Minimum essential medium
MPS	Mononuclear phagocytic system
MS	Mass spectroscopy
NEAA	Non-essential amino acids
NMR	Nuclear magnetic resonance
NNI	National Nanotechnology Initiative
NSAIDs	Non-steroidal anti-inflammatory drugs
PAMAM	Polyamidoamine
PBS	Phosphate buffered saline
PEG	Polyethylene glycol
PET	Positron emission tomography
PLGA	Poly (lactic-*co*-glycolic acid)
PLL	Poly-L-lysine
PLLA	Poly-(L)-glutamic acid
PPI	Poly (propyleneimine)
PSMA	Prostate-specific membrane antigen
PTK-7	Protein tyrosine kinase-like 7
RES	Reticuloendothelial system
RPMI	Roswell park memorial institute 1640 medium
RSV	Respiratory syncytial virus
SD	Standard deviation
sHCQ	Hydroxychloroquine sulfate
TEM	Transmission electron microscopy

Contents

Figures Index

Table Index

Chapter I: Introduction

1 Nanotechnology and nanomaterials

Nanotechnology is defined by the National Nanotechnology Initiative (NNI) as the science, engineering, and technology conducted at the nanoscale, which is about 1 to 100 nm.[1] The development of nanotechnology has proven to be a multidisciplinary scientific field, with applications in the most diverse areas, including chemistry, biology, medicine, physics, materials science, and engineering.[2]

Particles in the nanoscale range (nanoparticles) present unique physical and chemical properties.[3] One of the most important properties is that the nanoparticles have a maximum surface/volume ratio. This particular characteristic of the nanoparticles allows chemical reactions to occur on the surface of the particles, wich is ideal for surface functionalization and the incorporation of a therapeutic load.[3,4] The creation of materials at the nanometer scale can be made by scaling up from single groups of atoms or by refining or reducing bulk material into nanoparticles.[5]

The nanoparticles can be classified based on their properties as organic and inorganic nanoparticles. Organic nanoparticles include liposomal nanoparticles, nanocrystals, polymeric nanoparticles, protein-based nanoparticles, star-shaped dendrimers, micelle nanoparticles, silicon- and carbon-based nanoparticles, carbon nanotubes, and carbon nanoshells. While the inorganic nanoparticles comprise different agents such as quantum dots, superparamagnetic iron oxide nanoparticles, nanobots, and metallic nanoparticles (gold, silver, and titanium nanoparticles).[6-8]

The convergence of nanotechnology and medicine has led to the interdisciplinary field of nanomedicine.[9] A variety of nanomaterials and nanostructures are involved in nanomedicine for diagnostic, imaging, controlled and targeted therapeutic drugs, and gene delivery.[10,11] Due to its size, it is ideal for penetrating cells, circulating in the bloodstream, and crossing tissues.[12]

2 Dendrimers

The 20th century focused on polymer synthesis and the design of biodegradable polymeric macromolecules.[13] Polymers are macromolecules made from many molecular units denominated monomers that, by a polymerization process, form a chain linked by covalent bonds. They usually represent organic

molecules containing carbon, hydrogen, oxygen, nitrogen, halogens, etc.[14] They can have a natural origin, such as rubber, cellulose, and starch, or they can be synthesized.[14]

As a result of these, dendrimers emerged as an innovation in the field of polymer science.[13] Derived from the Greek word "dendron", which means tree, the dendrimers are a particular class of synthetic polymers defined as synthetic macromolecules and characterized by an abundant number of branching points, a three-dimensional globular shape, monodispersity, and a nanometric size range.[13,15]

The first described dendrimer, a polypropylenimine (PPI) of low generation, was reported by Vögtle and co-workers in 1978.[15,16] Later, in the mid-1980, Tomalia and co-workers synthesized dendrimers with higher generations with well-defined structures.[15,17-19]

2.1 Structure of dendrimers

The dendrimers are composed of several perfectly branched monomers (dendrons) that diffuse radially from a central nucleus (core).[20,21] So, the structure can be divided into three regions: the core; the interior layers or branches; and the periphery or terminal groups (figure 1).[21]

The number of branching points, when going from the core to the surface, will define the generation. The nucleus is simply referred to as generation 0 (G0) since no cascade points are present.[22]

The core and number/type of branched monomers are responsible for the tridimensionality structure and the overall morphology and rigidity of the dendrimer.[23] In other words, the morphology depends on the chemical composition and generation number. Dendrimers of a lower generation have a floppy asymmetrical shape and an open disc-like structure. They have fewer branches and, consequently, fewer terminal groups, which confer a more open structure. On the other hand, in higher generations (> G4), the hyperbranched polymer adopts a more globular or even spherical conformation. Moreover, as the dendrimers' molecular weight and generation increase, the terminal units double in number, making the structure more compact.[21,24]

The terminal groups are responsible for the interaction of the dendrimer with the external groups or molecules.[25]

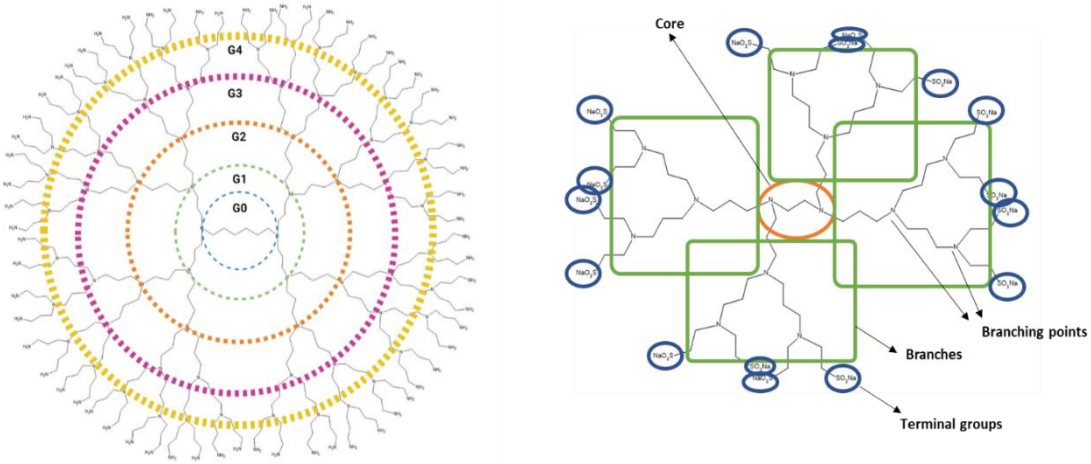

Figure 1- Schematic representation of the structure of dendrimers.

2.2 Properties of dendrimers

As the generation of the dendrimer increases, the composition of the core, branches, and terminal groups, will significantly affect its physical and chemical properties and, thus, its utility in specific biomedical applications.[26] Some important dendrimers properties are discussed in the following sections.

2.2.1 Monodispersity

One of the most important properties of dendrimers, and what sets them apart from hyperbranched polymers, is that they possess monodispersed properties, which means that all molecules are alike in structure and molecular weight. This is a result of stringent control of all synthesis steps, unlike the hyperbranched polymers, which are produced by a relatively simplified single-step reaction.[27]

2.2.2 Solubility

In general, dendrimers are water-soluble, and as a result, these nanoparticles have been studied as molecule carriers with low solubility.[28]

The terminal groups of the dendrimers strongly influence their solubility. A dendrimer with hydrophilic end groups can make a dendrimer with a hydrophobic

core, soluble in water (polar solvent), while hydrophobic terminal groups can make a dendrimer with a hydrophilic core, soluble in non-polar solvents.[29,30]

However, the nature of the branches, the generation number, and the core also influence the solubility of the dendrimer.[25] As the generation of the dendrimer increases, the hydrophobicity decreases.[31] In addition, temperature, pH, nature of the solvent, presence of salts, and concentration, also affect the dendrimer's solubility.[31,32]

2.2.3 Multivalency

Multivalency is one of the most important properties of dendrimers. Also called polyvalency, it refers to the number of reactive sites that the dendrimer presents on its surface (terminal groups).[25] The terminal reactive zones are important for interacting with biological receptors and membranes and forming complexes or conjugating with drugs or ligands.[25]

In turn, the number of terminal groups depends on the multivalency of both the core and the branching points. A change in the multivalency of the core impacts the total number of terminal groups.[33]

2.2.4 End groups and toxicity

When designing dendrimers for application *in vivo*, they should be non-toxic, non-immunogenic, able to cross biobarriers (biopermeable), able to stay in circulation for the necessary time for a clinical effect, and be able to target specific structures.[22,24]

In general, cationic macromolecules interact with the cell membrane's negative charge, leading to their destabilization.[22] The same occurs with dendrimers with a positive charge (cationic dendrimers) that adhere and damage the cell membranes, causing their lysis.[34]

Some studies were carried out about how these dendrimers interact with the cells. The cell line and the type of dendrimer influenced this interaction.[35,36] Zhang *et al.,* showed that using high-generation dendrimers with high cationic profiles strongly interacts with the cell membranes through electrostatic forces, inducing lipid mixing and leakage from the membranes.[37] Mecke *et al.,* proposed another mechanism that

defends the formation of nanoholes (15-40 nm) upon dendrimer-membrane interaction and, consequently, cell lysis.[38]

Dendrimers like PPI and PAMAM exert significant cytotoxicity due to the terminal NH_2 groups, which confer a positive surface charge.[39] Svenson concluded that amine-terminated PPI and PAMAM dendrimers present similar behaviour regarding cytotoxicity and hemolytic effect.[40] With the increase in generation, both dendrimers become more cytotoxic and hemolytic.[41,42] This was also confirmed by Malik *et al.,* who investigated the hemotoxicity of cationic PAMAM dendrimer.[43] In addition, Jones *et al.,* observed significant cytotoxicity in various cell lines and hemolytic activity in the blood.[44] Thus, generally speaking, PAMAM and PPI dendrimers display concentration- and generation number-dependent toxicity and hemolysis.[42,43,45,46]

Contrarily, neutral and anionic dendrimers have proven to be less toxic or even non-toxic.[39] To overcome the toxicity and make the dendrimers more biocompatible, their surface amine groups can be functionalized with negatively charged or neutral groups.[34]

A comparative study between anionic and cationic PAMAM dendrimers demonstrated that anionic carboxyl functionalized PAMAM dendrimers present significantly lower cytotoxicity than amine-terminated dendrimers in CACO-2 cells.[46]

The addition of polyethylene glycol (PEG) chains (entitled PEGylation method) to the surface of dendrimers decreases immunogenicity, overcoming cytotoxicity and hemolytic toxicity and increasing blood circulation.[47] Initially, a review reported that unmodified G3 to G7 amino-terminated PAMAM dendrimers displayed little to no immunogenicity. Later, it was demonstrated that the immunogenicity of these dendrimers is affected by the PEGylation, which reduces and increases their lifetime in the blood.[48]

Research also showed that the structure of amino-terminated PAMAM dendrimers influences their toxicity. The globular and less flexible structure is less toxic than more flexible amino functionalized linear polymers because of their lower adherence to cellular surfaces.[22]

The core can also influence the biocompatibility of dendrimers. For instance, dendrimers with an aromatic polyether skeleton and anionic carboxylate groups on

the surface show hemolytic activity. The aromatic interior of the dendrimer may cause hemolysis through hydrophobic membrane contact. The influence of the core can be minimized with the increase of generation and rigidity of the branches. In fact, how more protected the core unit is, the lower is the interaction of the core and the cell surface.[22,47]

2.3 Synthesis

The synthesis of the traditional macromolecule structures (linear, cross-linked, and branched) originate products with different molecular weights and high polydispersity. Conversely, dendrimers can be prepared with a level of control that results in monodisperse, structure-controlled macromolecular architectures like those observed in biological systems.[49] Two major strategies have evolved for synthesizing dendrimers: the divergent and convergent methods. Other approaches have also been developed, including “Hypercore and branched monomers”, “Double exponential”, “Lego chemistry,” and “Click chemistry”.[50]

2.3.1 Divergent method

The first proposed method, the divergent method, introduced by Tomalia,[23] is currently the most widely used.[25] In this approach, the synthesis starts from the central core, and repeated monomeric molecules that possess reactive groups are successively added and diverge radially towards the exterior (figure 2).[49,50]

This method implies two essential steps, the coupling of monomers and the activation of the monomer end-group, to promote the reaction with a new monomer.[25] This process is repeated until the obtention of the desired dendrimer generation. After each step, a purification method must be applied. Because of the higher number of reactions performed at the same time, defective monomers assembly are produced, originating secondary products.[26]

This method presents a set of attractive advantages, including rapid synthesis, cheap reagents, exponential growth, attainable large dendrimers, highly symmetric dendrimers, and a major yield compared with the convergent method.[19,51]

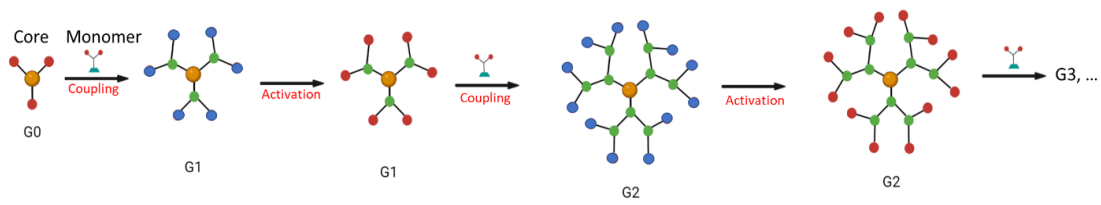

Figure 2- Schematic representation of the divergent method.

2.3.2. Convergent method

The convergent method, reported by Fréchet and Hawker,[19] consists of synthesizing first the various dendrons (that will constitute the dendrimer) and attaching them to a central nucleus (figure 3).[20,49]

In the first step, the surface groups are coupled to a monomer, originating a segment that will be activated for a subsequent reaction with another monomer. This sequence is repeated until obtained the largest dendron generation, which will be coupled in the final step to a core, producing the final dendrimer.[25]

One of the advantages of this method is that only a limited number of active sites are present per reaction, reducing structural defects in the final products.[26,52] The ability to precisely control the molecular weight creates a monodisperse product that is easy to purify and characterize.[24,51] Unlike the divergent method, this approach does not require purification after each step.[26] Another advantage is the possibility of linking different types of dendrons to one dendrimer and choosing the connection positions.[24,51] However, it is complicated to produce dendrimers of higher generations due to the steric hindrance between the dendrons.[26]

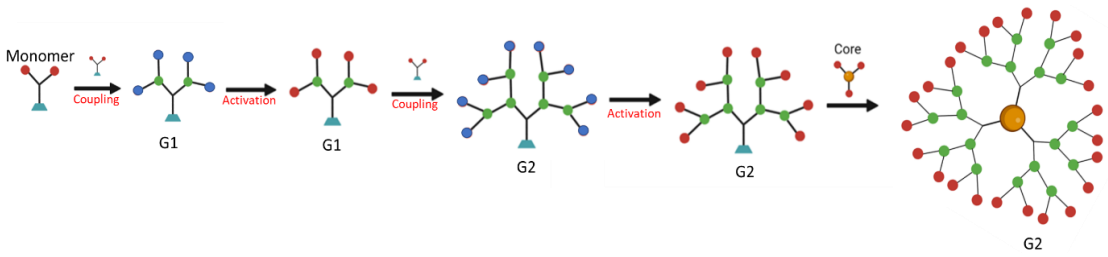

Figure 3- Schematic representation of the convergent method.

2.3.3 Other approaches

To overcome some of the problems of the classical synthesis pathways, enhanced approaches were developed to minimize: the number of reaction steps, the time, the starting materials, and the costs.[25]

The “Hypercore and branched monomers” method is similar to the convergent method. It consists of linking pre-assembly oligomeric species in fewer steps to accelerate production.[50]

Another approach, the “Double exponential method”, enables the preparation of monomers from a single functionalized group that can react to each other to give an orthogonally protected trimer. Further, these can be used to increase growth. One advantage of this method is its fast synthesis of dendrimers, which can be applied in convergent and divergent methods.[24]

The “Lego chemistry” strategy, developed by Tomalia and Svenson for the preparation of phosphorous dendrimers, uses highly functionalized cores and branch monomers to produce dendrimers quickly. Some variations in the scheme of reaction allow, in only one step, to multiply the number of terminal surface groups from 48 to 250.[23]

The "Click chemistry” method, also developed by Tomalia and Svenson, successfully produced triazole dendrimers using Cu(I)-catalyzed with various surface groups, with high purity and excellent yields.[23] This methodology is applied in divergent approaches, using two different monomeric units of complementary functionalities that render spontaneous synthesis, reducing the number of steps.[26]

2.4 Types of dendrimers

Despite de different types of dendrimers produced over the years, like liquid crystalline dendrimers, glycodendrimers, metallodendrimers, silicon-based dendrimers, phosphorus-based dendrimers, our focus in the next section goes to the PAMAM and PPI dendrimers. [34,53]

2.4.1 PAMAM dendrimers

The PAMAM dendrimers family was developed by Tomalia and co-workers during the 1980s.[17] These molecules were the first dendritic structures exhaustively

investigated and have received widespread attention over the years.[34] Also, it was the first complete dendrimer family to be synthesized, characterized, and commercialized.[54]

Generally, these dendrimers are synthesized *via* a divergent approach, and the core molecule can vary. The most basic initiators are ammonia and ethylenediamine (EDA).[16,55,56] They comprise polyamide branches and tertiary amines as branching units (figure 4).[17] Products up to generation 10 have been obtained with a low polydispersity index for each generation.[57]

They are used in many biological applications due to their unique architecture, solubility in water, and biocompatibility.[54] They can host metals or guest molecules in their internal cavities and bind to various targeting molecules.[24] PAMAM dendrimers are available in the market at the following companies, NanoSynthons (Mt. Pleasant, USA), Polysciences (Warrington, USA), Dendritech (Midland, USA), and Aldrich chemical company (Milwaukee, USA).[58]

2.4.2 PPI dendrimers

The first PPI dendrimer was reported by Fritz Vögtle *et al.* and consisted of a hyperbranched macromolecule.[16,59] In comparison with PAMAM dendrimers (figure 4), they are non-polar in nature, mainly because they do not have polyamide groups, are more hydrophobic, and have different bond lengths with results in different sizes. In the case of PPI dendrimers, they have four bonds, in contrast with the seven bonds present in PAMAM dendrimers. Therefore, they are smaller in size. Both dendrimers have the same number of end groups, but they do not share the same generations. For example, the G3 of PPI dendrimers have 32 amino-terminal groups, and the G3 of PAMAM dendrimers have 16 amino-terminal groups.[58,60-63]

The PPI dendrimers are mainly synthesized by the divergent method, employing cores such as EDA and 1,4-diaminobutane (DAB).[59,64,65] However, various other molecules with primary or secondary amine groups can also be used as the core.[66] They are formed by an interior of tertiary tris-propyleneamines containing poly(alkylamines) and primary amines.[67,68] The highest generation synthesized was G5.[64,65]

These dendrimers have good advantages and characteristics for biological applications and are extensively used for drug delivery. PPI dendrimers are available in the market from Dutch State Mines (DSM) (Netherlands), and Aldrich Chemical Company (Milwaukee, USA).[34]

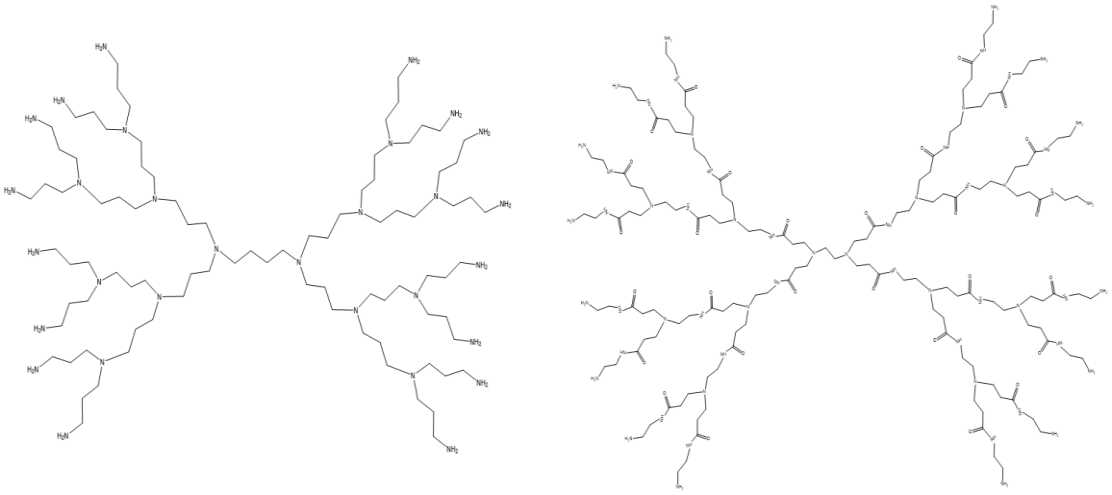

Figure 4- Schematic representation of the structure of a PPI dendrimer (left) and a PAMAM dendrimer (right).

3 Applications of dendrimers

The distinctive properties of dendrimers - monodispersity, nanometric size range, permeability across the biological membrane, multifunctional end groups, and numerous internal cavities - make these suitable for potential biomedical applications.[34]

In 1982, for the first time, Maciejewski proposed the utilization of dendrimers as molecular carriers.[69] Some applications of dendrimers include drug delivery, gene delivery (transfection), imaging and diagnostic contrast agents, and tissue engineering. Furthermore, they can directly act as drugs, such as antimicrobial and antiviral agents (particularly against HIV).[26,70]

From the point of view of medical applications, a dendrimer carrying a molecule or nanoparticle must be present in the bloodstream long enough to reach or recognize its therapeutic site of action.[71] The major obstacle to overcome is the opsonization by the mononuclear phagocytic system (MPS), also known as the reticuloendothelial system (RES). Opsonization consists of a process in which a foreign organism or particle becomes covered with opsonin proteins present in the blood serum, and phagocytosis can occur, destroying or removing the foreign

material from de bloodstream.[71] These two processes can occur separately or together, making it the main clearance mechanism for removing strange components.[71] A non-treat polymeric nanoparticle is often removed from the bloodstream in a few minutes by opsonization and sequestration in MPS organs, usually in the liver and spleen.[71] As previously seen, one of the methods to go around this problem is by adding PEG chains on the dendrimers' surface. These will create a hydrophilic protective layer that avoids opsonins' adhesion, making the nanoparticles "invisible" to phagocytic cells.[72] In general, nanoparticles coated with a hydrophilic polymer, such as poloxamines, poloxamers, polysaccharides, or PEG, prevent washing out, and remain in the bloodstream for a longer time, repelling plasma proteins and escaping from the opsonization and clearance.[73-75] A study carried out by Peracchia *et al.* showed that 24h after injection, 40% of the PEGylated particles were found in the liver, while 90% of the "naked" particles were found in the liver after 3 min.[76]

The size of the dendrimer also influences biodistribution. Macromolecules with a molecular weight lower than 30-50 kDa or a diameter of 5-6 nm are rapidly cleared from the blood and are facile eliminated in the urine by filtration at the renal glomerulus.[77,78] However, studies have shown that particles with a hydrodynamic radius of over 200 nm typically exhibit a more rapid rate of clearance than particles with a radius under 200 nm, regardless of whether they are PEGylated or not.[79] Research undertaken by Porter *et al.* demonstrated that PEGylated nanoparticles with a diameter of 250 nm were mostly sequestered in the spleen and liver. In contrast, particles with a hydrodynamic radius lower than 150 nm were shown to produce an increased uptake of particles in the bone marrow of rabbits. Therefore, the size influences not only the half-time of nanoparticles circulation but also the final biodistribution.[80]

Additionally, it has been reported that the surface charge will determine the destination *in vivo* of the nanoparticles. Dendrimers with neutral or anionic surface charges reduce the nonspecific interaction or opsonization. It has been reported that large molecules with neutral or weak anionic charges tend to escape the opsonization.[71] Malik *et al.* claimed that anionic and neutral PAMAM dendrimers had a lower accumulation in the liver and higher blood circulation.[81] On the other hand,

cationic PAMAM dendrimers are quickly cleared from the body with a low blood level and high accumulation in the liver, kidney, spleen, lung, and pancreas.[43,45,82] Further, Xiao *et al.* demonstrated that nanoparticles with higher surface charge, either positive or negative, tend to get caught up by the macrophages. So, the surface charge had to be slightly negative to minimize the rapid clearance from the blood circulation and facilitate the accumulation at the tumor sites.[83] Maeda confirmed this by concluding that the RES in the liver and spleen had swiftly taken up highly negatively charged nanoparticles.[84]

To summarize, for the delivery systems to achieve the tumor site, they must persist in the systemic circulation and avoid renal excretion and the cells and organs of the RES.

The following sections will discuss the dendrimers' applications as carriers for drug delivery, gene delivery, and imaging agents.

3.1 Dendrimers in drug delivery

As stated before, due to the particular properties of dendrimers, they are considered excellent potential carriers in drug delivery. Some advantages of using them include: enhancing the solubility of hydrophobic drugs and directing the drug to specific tissues, minimizing undesired interactions with healthy tissues (*i.e.* reducing the side effects). Further, these increase bioavailability.

Also, dendrimers could protect the drug molecule from the biological environment, increasing their stability. Moreover, they allow the delivery of more than one molecule simultaneously, improve the drug passage through biological barriers, increase the half-time in circulation and achieve controlled and specific drug delivery. Furthermore, they can conjugate or encapsulate high molecular weight drugs and exhibit a high uptake by the cells. Finally, they provide the chance to passively target tumor tissues *via* the enhanced permeability and retention (EPR) effect.[21,52,58,85-87]

3.1.1 Mechanism of drug-dendrimer interaction

The structure of the dendrimers influences the number and type of drug molecules, which can be complexed with the dendrimer or incorporated into them.

As mentioned previously, as the molecular weight and generation of the dendrimer increases, the terminal units become more compact, which facilitates the encapsulation of molecules or nanoparticles in the channels within the globular dendrimer system.[21] Plus, the higher dendrimer generations possess more functional groups for drug conjugation than lower generations.[21,88]

Therefore, these allow the encapsulation of small molecules and nanoparticles in the channels within the sphere (physical encapsulation) or chemically fixate on the terminal groups covalently or *via* non-covalent interactions (hydrogen bonding and electrostatic attractions). Also, the drug can interact with various dendrimers forming a dendrimer-drug network (figure 5).[70,89]

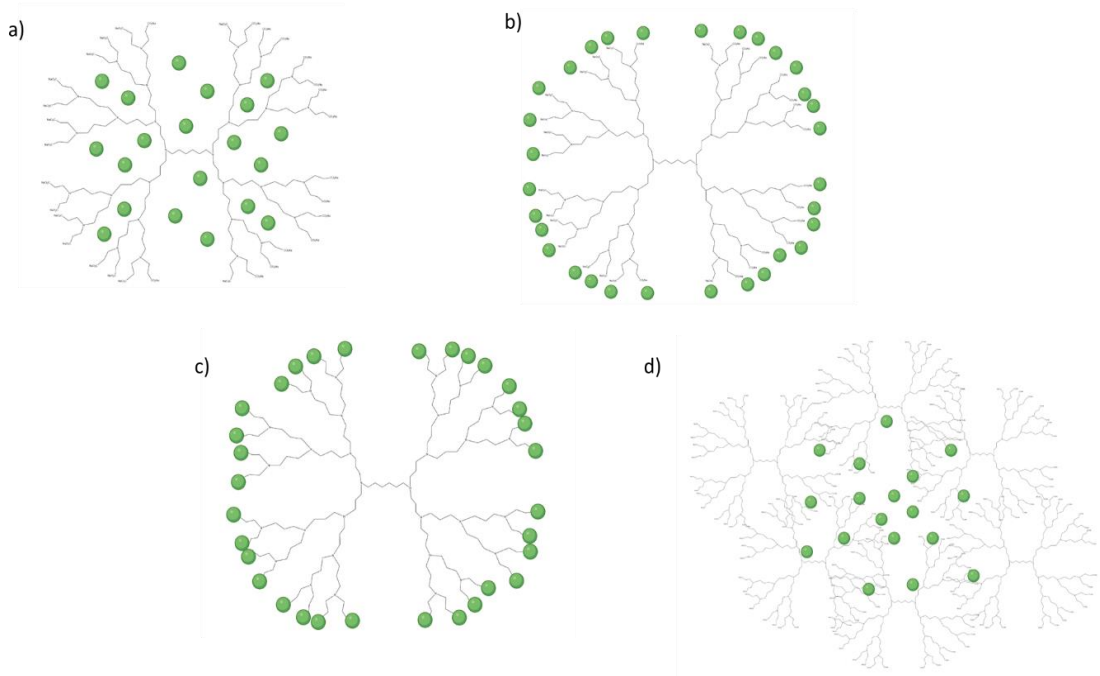

Figure 5- Schematic representations of how the drug interacts with the dendrimer: a) encapsulation; b) electrostatic interactions; c) covalent binding; d) dendrimer-drug networks.

3.1.1.1 Physical encapsulation

Dendrimers have the ability to encapsulate drugs physically. The empty internal cavities of the dendrimers are mostly hydrophobic, so poorly soluble drugs can interact through hydrophobic interactions.[90,91] Moreover, the presence of nitrogen or oxygen atoms in the dendrimer branches can interact with the drug through hydrogen bond formations.[92]

Physical encapsulation has the advantage of a rapid and simple preparation without affecting the pharmacological drug activity. However, some disadvantages include low stability in terms of storage and premature drug release, batch-to-batch variation in concentration of a solubilized drug, and low-drug loading capacity.[93,94]

3.1.1.2 Electrostatic interactions

The high density of the functional groups on the surface of dendrimers (such as amine or carboxyl groups) can interact with hydrophobic drugs by electrostatic interaction. The ionizable functional groups attract drug molecules with opposite charges, providing an electrostatic bonding.[90,95] Also, the primary amine and tertiary amine groups present within the core of PAMAM and PPI dendrimers are ionizable groups and offer potential sites for drug interaction.[50]

3.1.1.3 Covalent conjugation

The presence of numerous functional groups on the dendrimers surface makes them suitable for interacting with drugs through covalent bonds.[96] Despite the last two approaches preserving the chemical integrity and pharmacological properties of the drug, the covalent attachment through chemical bonds allows better control over drug release.[89] The drugs can be directly covalently conjugated to the dendrimers; through spacers, such as PEG and aminobenzoic acid, or by biodegradable linkages like ester or amide bonds.[97]

3.1.2 Routes of administration

Drugs are introduced into the body by various routes such as enteral (oral, sublingual, and rectum administration), parental (intravascular, intramuscular, subcutaneous, and inhalation administration), or topical (skin and mucosal membranes). The route of administration strongly influences the speed and efficacy of what the drug acts.[98]

Dendrimers have been applied using different routes for drug delivery, including intravenous, intratumoral, intraperitoneal, oral, nasal, intravaginal, transdermal, pulmonary, and ocular routes. According to several studies, the intravenous route is the preferred way to deliver drugs using dendrimers.[90,98]

3.1.2.1 Intravenous/intraperitoneal/intratumoral drug delivery

The intravenous route is the most rapid and straightforward method for delivering drugs into systemic circulation.[99] But, some drugs, especially anti-cancer drugs, have poor water solubility, resulting in several side effects, such as hemolysis and phlebitis.[100] These problems limit, in some cases, the application of the intravenous administration route.

Dendrimers are a good alternative to solve these problems. As so, before applying dendrimers using the intravenous route, some considerations including the knowledge of the biodistribution in the body and the toxicity, need to be known.[99,100]

3.1.2.2 Oral drug delivery

The oral delivery system is the most common route of drug administration preferred by patients and clinicians. This route requires reduced administration costs for anticancer agents and facilitates the use of more chronic treatment regimens. However, some problems, like low aqueous solubility and poor permeability across the biological membrane, restricts its intake and application.[101-103]

To overcome these problems, the drug is loaded into drug carriers, which should protect them from degradation and reduce the nonspecific interactions with food proteins. In addition, they should increase the absorption *via* intestinal epithelium.[90,104] Further, they solve the solubility problem and improve the stability of drugs in the biological environment.[90] Some studies have proven the potential of dendrimers as oral drug deliveries.[105,106]

3.1.2.3 Transdermal drug delivery

Transdermal drug delivery has revolutionized the pharmaceutical industry because it is a non-invasive method that allows the penetration of therapeutic agents through the skin.[107] This route of administration eliminates the degradation in the gastrointestinal tract and maintains a constant therapeutic blood concentration of the drug for a longer time.[90,108,109] Also, the sustained/prolonged delivery of therapeutic agents with this approach simplifies the dosing schedule.[110] However, this administration method is limited due to the poor transcutaneous drug delivery rates because of the skin's barrier function.[109]

The dendrimers have been investigated for transdermal delivery of drugs due to their high water-solubility and biocompatibility, and given that they improve drug properties, such as solubility and plasma circulation time, for the efficient delivery of drugs.[24] The dendrimer's permeability through the skin depends on physicochemical properties such as composition, size, concentration, molecular weight, and surface charge.[111] These carriers are proving to be efficient as a transdermal delivery system of anticancer, antiviral, antimicrobial, non-steroidal anti-inflammatory (NSAIDs), or antihypertensive drugs.[112-114]

3.1.3 Mechanisms of drug delivery through dendrimers

When the dendrimers-drug conjugate is administrated, there are three mechanisms for drug delivery: the *in vivo* degradation of covalent bonds between drugs and dendrimers (dependent on the existence of enzymes); or an alteration in the biological microenvironment that's able to break the chemical bond (like pH and temperature); or the release of the drug from the dendrimer through a physical change or stimulus that leads to the release (see section 4.2).[88,96]

3.2 Dendrimers in gene delivery

Gene therapy involves the introduction of new genetic material into the cells for the treatment of diseases.[50,115] However, the delivery of genes into the nucleus and cytoplasm of a cell remains a challenge for researchers due to the necessity of a vector that can deliver the genetic material without deactivating or damaging the DNA.[50]

The traditional method to introduce a therapeutic gene into cells involves the use of viral vectors, such as lentivirus, retrovirus, adeno-associated virus, and adenovirus-derived vectors. Despite this method achieving rapid and efficient gene transfection, some problems, like oncogenic transformation, pathogenic risk, and the induction of immune responses, limited their application.[116]

So, natural and synthetic molecules (non-viral vectors) were implemented to deliver genetic material. Some advantages of this method include low production costs, easy fabrication and targeting ability, lower immune response, and no risk of transmission of infectious diseases.[50,117-119]

Dendrimers like PAMAM and PPI with terminal amino groups are good candidates for DNA delivery since they interact with the phosphate groups of nucleic acids by electrostatic interactions, helping the DNA to enter the internal structure of the dendrimer. So, the genetic material is protected from degradation by nucleases during delivery.[120,121] Moreover, it is possible to deliver drugs and genes simultaneously using a suitable carrier.[122] Numerous reports, including from our group, have been published about the successful utilization of dendrimers to deliver DNA into cells.[123-127]

3.3 Dendrimers as imaging and diagnostic agents

Imaging modalities can be used in oncology to diagnose, locate, and plan treatment.[128] Dendrimers have been used as imaging agents in radiotherapy, as X-ray and Magnetic Resonance Imaging (MRI).[129,130]

MRI is a non-invasive technique that provides high-quality-three-dimensional images to diagnose diseases. This technique is based on different relaxation times of protons in different tissues. Additionally, a contrast agent is added to increase the signal intensity.[34,131] Different groups of contrast agents are established for clinical application, with gadolinium (Gd^{3+}) chelates constituting the largest group of MRI contrast agents.[131] Gadolinium-based contrast agents were approved by U.S. Food and Drug Administration (FDA) and European Medicine Agency (EMA) for MRI since they provided a greater contrast between normal and abnormal tissues in the brain and the body.[132] Some issues with using these particles include no tissue specificity, low contrast efficiency, and fast excretion from the body. The concentration of the contrast agents could be increased to avoid these problems, although doing so could result in some unintended side effects. Additionally, they are also toxic due to their strong affinity for serum protein. So, researchers have been focusing on adding contrast agents in carriers, such as dendrimers.[26,130] In the early 1990s, Lauterbur and colleagues demonstrated the first *in vivo* diagnostic imaging applications using dendrimer-based MRI contrast agents.[133]

X-ray is an imaging device for organs and tissues, used in many clinical trials.[134] Normally, iodinated contrast agents are used. The conjugation of these with dendrimers has shown a greater retention time, permits targeted delivery, and

reduces toxicity.[128] Furthermore, dendrimers conjugated with gold or silver nanoparticles were successfully used as contrast agents for X-rays imaging and proven to be more effective than iodine-based contrast agents.[135-140]

4 Dendrimers in cancer diagnosis and treatment

Cancer is one of the most lethal diseases in the world and causes over 10 million deaths annually. In 2020, 19.3 million new cases were reported, with approximately 10 million deaths. Female breast cancer was the most diagnosed cancer type, with 2.3 million new cases, and lung cancer was the most mortal, with 1.8 million deaths. In 2040, it is expected 28,4 million cases per year, an increment of 47% when compared with 2020.[141,142]

In a simplified way, cancer consists of an uncontrolled proliferation of abnormal cells, and because of the complexity of genetic and phenotypic levels, a permanent cure for cancer is yet to be discovered. The treatments involve the use of chemotherapeutic drugs, radiation therapy, surgical treatment, or biotherapy involving cancer immunotherapy.[141,143] Sometimes, surgery cannot be employed, and radiotherapy can damage healthy cells around the tumor.[144] Chemotherapy, introduced in 1950, is the most common therapeutic approach and consists of delivering anticancer drugs systemically to kill cancer cells by drug toxicity or by preventing cell division, either by discontinuing nutrient uptake or inhibiting the mechanism responsible for cell division.[145-147] Nevertheless, one of the challenges is the capacity of anticancer drugs to distinguish a transformed cell from the healthy one and then provide a sufficiently high dose of toxic agent to selectively kill the cells without affecting the healthy cells around.[52] Chemotherapy presents these adverse side effects because the free drug can circulate to most tissues in the body and accumulate at toxic levels in healthy tissues (such as the liver, spleen, kidney, and bone marrow).[26,128] Moreover, the drug cannot penetrate and reach the core of solid tumors, failing to kill the cancerous cells.[148] Another problem of most chemotherapeutic drugs is hydrophobicity, which results in low water solubility and, consequently, difficulties in the efficient delivery into cells.[24] Furthermore, low molecular weight drugs, when in the bloodstream, are quickly filtered and removed

through the kidneys.[26,52] So, applying nanoparticle technology to cancer therapies might overcome these obstacles. Further, it is possible to combine both diagnostics capabilities and therapy within a single entity, using nanoparticles - theranostic.[149]

Currently, some based drug delivery systems for cancer treatments that are on the market or under research and evaluation include dendrimers, polymeric micelles, liposomes, nanocapsules, nanospheres, and nanotubes.[150,151]

4.1 Strategies for delivery of the drug-nanoparticle conjugate into tumor

There are two strategies for delivering the drug-nanoparticle conjugates in cancer tissues: passive targeting and active targeting.

4.1.1 Passive targeting (Enhanced Permeability and Retention (EPR) effect)

As the tumor size increases, a natural phenomenon called angiogenesis is induced. It consists of creating new blood vessels to supply oxygen and nutrients to the tumor cells.[152] These new blood vessels within the tumor are irregular in shape, dilated, leaky, or defective, and the endothelial cells are poorly aligned or disorganized with large spaces between them.[153] These defects allow leakage of the blood plasma components, such as macromolecules, nanoparticles, and lipidic particles, and their accumulation in the tumor tissue due to the limited lymphatic drainage. This event is termed the EPR effect (figure 6).[153] The EPR effect was first reported by Matsumura and Maeda, in 1986, during an experiment using polymer-protein conjugates with approximately 80 kDa, and they verified the preferential accumulation of these materials in the tumor tissues.[154]

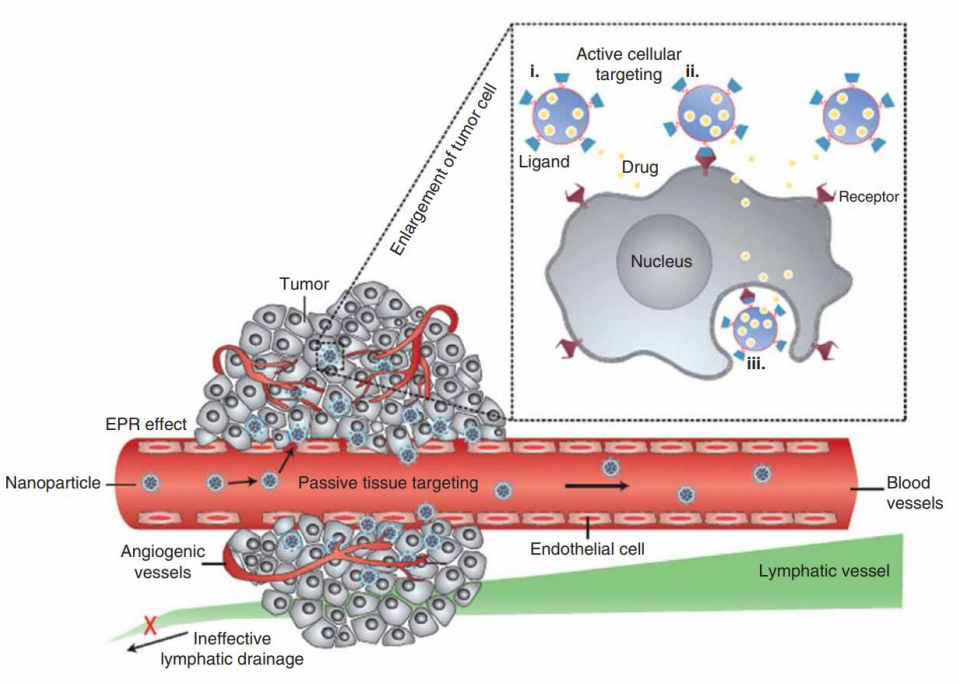

Figure 6- Schematic representation of the EPR Effect in solid tumors.[155]

The drug—encapsulated nanoparticles utilise the EPR effect for the passive delivery of the drugs in the tumor cells. It is possible to attain very high concentrations at the tumor site - 10–50-fold higher than in normal tissue, within 1–2 days. This results in an increment of bioavailability of the drug to the diseased tissues resulting in a decrease in the side effects.[153] It is currently thought that the diameter of nanoparticle therapeutics for cancer should be between 10-100 nm to achieve the EPR effect. Particles with a diameter lower than 10 nm tend to be secreted by the kidney, and with a diameter superior to 100 nm are susceptible to phagocytic by the RES.[156-158] However, the porosity of vasculature varies depending on the cancer type and the affected organ and can vary from patient to patient.[159] A review published in 1992 establishes that liposomes with a size range between 70-200 nm accumulate in the tumor cells by EPR effect. Increasing the size over 200 nm, the liposomes are uptake in the spleen. This is in concordance with what was previously stated: particles with a size superior to 200 nm are most facile captured by the RES.[160] Another study showed that liposomes loaded with daunorubicin, an antibiotic belonging to the anthracycline group used in cancer therapy, with a diameter of 142 nm, exhibited an inhibitory effect against Yoshida sarcoma. In contrast, liposomes with diameters 57–58 nm and 272 nm had little to no effect.[161]

The FDA has approved a conjunct of nanoparticles for chemotherapeutic delivery, such as a liposomal delivery system of doxorubicin (DOX), the Doxil (approved 1995); an albumin-based nanoparticle delivery system of paclitaxel, the Abraxane (approved 2005); and in South Korea and Europe a polymeric micelle delivery vehicle of paclitaxel, the Genexol-PM (approved in Korea 2007), has been approved for the treatment of breast cancer.[143,157,162] These delivery systems are passively targeted formulations and can suffer a few limitations.

Some problems with passive targeting include the eventual delivery off target, resulting in multidrug resistance in later stages, and some cancers do not exhibit the EPR effect.[135,163,164] Additionally, passive targeting cannot promote the uptake of nanoparticles by the cancer cells, staying in the tumor interstitium.[165] To overcome these problems, the active targeting strategy was introduced.

4.1.2 Active targeting

In the case of active targeting, a targeting moiety is added to the nanoparticle system to bind and deliver the drug to the right cells based on molecular recognition processes, such as ligand-receptor, antibody-antigen, or any other form of molecular recognition. Due to their genetic defects, tumor cells have highly expressed receptors on their surface compared to restricted expression in normal cells.[77,143,149,157]

A diversity of tumor-targeting ligands, like antibodies, folate or growth factors, and cytokines, have been used to facilitate the uptake of carriers into cells.[166] The first agents used for targeting nanocarriers were antibodies. In 1975, a monoclonal antibody was introduced to bind to specific tumor antigens.[167] The first one approved by the FDA for clinical applications was the murine monoclonal antibody Muromonab CD3 (OrthoClone OKT3®). These reverse graft rejections by probably blocking the T cells' function, which plays a major role in acute allograft rejection.[168,169] Artificially engineered antibodies have also been reported.[170,171] In addition, monoclonal antibodies or antibody fragments can reduce immunogenicity and improve pharmacokinetics.[170,171]

Furthermore, the drug-encapsulated nanoparticle must enter the cell before starting the drug dispersal.[146] Sometimes, it is necessary to utilize strategies for receptor-mediated cell internalization.[73] The specific receptors overexpression is

dependent on the type of tumor. Human cancers, like the ovary, lung, breast, endometrium, kidney, and brain, greatly express folate receptors (FAR). The folate molecules can bind to these receptors with high affinity when conjugated in a nanoparticle system and be shuttled into the cell *via* an endocytic mechanism.[172,173]

The Human epidermal growth factor 2 (HER2) receptor is overexpressed in approximately 25% of invasive breast cancers.[174] Nanoparticles conjugated with humanized monoclonal antibody trastuzumab, have been shown to target these receptors. These are able to internalize after antibody binding HER2.[175,176]

The epidermal growth factor receptor (EGFR) is frequently overexpressed in many cancers like colon, lung, ovarian, neck, head, pancreatic, kidney, prostate, and especially breast cancer.[177] A chimeric human-murine monoclonal antibody, cetuximab, can bind competitively with a high affinity to the EGFR, rendering it a potential target for anticancer therapy.[178]

In prostate cancer, the tumor antigen overexpressed is the Prostate-specific membrane antigen (PSMA). Through the monoclonal antibody J591, nanoparticle systems can deliver the drug or detect prostate cancer.[165,179,180]

Furthermore, it is possible to add aptamers to the nanocarriers. This consists of short single-stranded DNA or RNA oligonucleotides capable of binding to specific biological targets, most often proteins.[181]

4.2 Stimuli-responsive nanoparticles

The activation or release of a compound out of a tumor site can result in side effects and a reduction of the therapeutic potential of a drug. The development of smart systems allows control over this through either the difference between cancerous and normal cells (internal stimuli) or by activation through a source outside of the cell (external stimuli).[182] In the following sections, examples of each of these stimuli are presented.

4.2.1 Internal stimuli

Some internal stimuli include alterations in pH, enzymatic activity, and potential redox.

Under normal conditions, the pH of the blood and tissues is tightly controlled at around 7.4. On the other hand, cancer cells have an extracellular acidic environment, between 6.5 to 7.0.[183,184] The main reason for that is that with the lack of oxygen, the tumor cells produce energy through anaerobic glycolysis, which results in lactate secretion.[185] However, the intracellular cytoplasm in cancer cells has a higher pH than normal cells, which has been demonstrated to facilitate cell proliferation and tumor growth.[183] The lysosomal compartment within the cell has an acidic environment. However, while normal cells have a pH between 4.5-6.5, in cancer cells pH can be below 4.5.[186] This difference makes the lysosomes good targets for internal release.[187] Exploring the pH differences makes it is possible to allow external drug release in the tumor microenvironment, or intracellular drug release in the lysosomes or endosomes (pH≈5).[187] The release in the acidic microenvironment of the tumor, sometimes might result in penetration problems when the tumor mass is too dense. In most cases, the nanoparticle system needs a targeting ligand to release in the cytoplasm.[157]

The differences in pH between these compartments has become an attractive strategy for drug delivery, and extensive studies have been carried out exploring this approach. Muniswamy *et al.* created a DOX-loaded PLGA (Poly-(lactic-co-glycolic acid)) nanoparticle core that, when in the endosome, the polymer is degraded and the DOX is released.[188] Kim *et al.* developed a FAR-targeted-DOX-loaded polymeric micelle for targeting the folate receptors in ovarian tumors. After endocytosis, the drug was released into the acidic environment of the endosome.[189]

Another characteristic of tumor tissues is the higher expression of enzymes when compared with normal tissues.[182] The breast, ovarian, and pancreatic cancers show the expression of cathepsins. Polymers such as poly-L-lysine hydrobromide (PLL) can be used for coating particles that incorporate a drug since they are degraded by lysosomal cathepsin B.[190-192] The intracellular class of enzymes glycosyl hydrolases, that catalyse the hydrolyses of glycosidic bonds, can degrade the dextrin molecule inducing drug release.[193,194] Protein tyrosine kinase-like 7 (PTK-7) has been shown to have significantly high expression levels in some specific cancer types. They follow a subgroup of kinases without catalytic activity but have a significant role in signal transduction. Huang *et al.* reported an aptamer-lipid-PLGA hybrid for the delivery of

DOX and paclitaxel. The aptamer interacts with the PTK-7, and a modification in the structure of the carrier releases the drug.[195,196] In the clinical context, Xyotax® is a pioneer protease-reactive drug for the release of paclitaxel. The release depends on the enzyme's degradation of the poly-(L)-glutamic acid (PLLA).[197]

Another stimulus uses the differences in the redox potential between the extracellular and intracellular spaces. Once intracellular cytoplasm has more reducing species, mainly glutathione (GHS), it is more reducing than the outside of the cell. Taking advantage of this, redox-activated drug delivery systems can release or activate the drug in the intracellular space.[181-200] One experiment using smart release nanoparticles combined HA (hyaluronic acid)-based active and redox-responsive targeting achieved a release of up to 92% by using the characteristic reductive conditions of the intracellular space.[201]

4.2.2 External stimuli

Applying heat, light, or a magnetic field makes it possible to release or activate the compound at a specific time and location.[157] These are applied from outside the body with spatial and temporal control.[202]

Cancer cells are more sensitive to changes in temperature. The application of mild heat (up to 41°C-43°C) to the body, or hyperthermia, represents a potential cancer treatment.[203] Temperature-responsive drug delivery systems have been explored. In the case of temperature-responsive polymers, these can change their characteristics, such as solubility, or conformation, in response to the environmental temperatures.[204]

Magforce developed the NanoTherm™ therapy, which has been tested in clinical trials for glioblastoma. They convert electromagnetic energy into heat by applying a magnetic field in magnetic nanoparticles. The magnetic field causes a rapid change in the nanoparticle's magnetic orientation, activating the particles and resulting in heat. The temperature in the tissues can achieve 80°C and destroy the cancer cells.[182] A heat-activated DOX liposome, ThermoDox®, is in Phase III of clinical trials. This system allows the release of DOX into and around the tumor, with heat and ultrasound activation.[205,206]

The use of light, UV/visible or near-infrared light, has been used in biomedical applications. They can induce a change in the structure of the delivery system or the cleavage of chemical bonds. Photochromic compounds have been extensively applied to create light-responsive nanoparticles. These molecules show the reversible isomeric transformation.[204] Zhao and co-workers created a system that changes its morphology through photo-isomerization of azobenzene units, using UV-visible light with a certain wavelength.[207]

5 Dendrimers in the market and clinical trials

Although dendrimers have all these promising characteristics, few dendrimer-based products are on the market. One of the most popular products in the market is VivaGel®, developed by Starpharma, an antiviral that also blocks bacteria. Several clinical studies have successfully tested the safety and efficacy of VivaGel® for treating and preventing bacterial vaginosis. Further, laboratories studies have proven the antiviral activity of VivaGel® against HIV, herpes simplex, hepatitis B, human papillomavirus infection (HPV), Zika, adenovirus, respiratory syncytial virus (RSV), and SARS-CoV-2 (the coronavirus that causes COVID-19).[208]

Dendrins, a molecular diagnostic company, developed DendrisChip technology for DNA microarray tests. It consists in functionalizing supports with phosphorous dendrimers to fix oligonucleotides in special probes, allowing higher detection sensitivity. This product is useful for respiratory and sexual diseases, medical diagnosis, and food pathogen detection.[209]

Genisphere and ChemBio Diagnostic Systems Inc., created the 3DNA Dendrimer for fast diagnostic tests for infectious diseases. Thus, dendrimers have been employed to enhance the sensibility of numerous assay platforms for protein and acid nucleic detection.[210]

Other products available include the Stratus® CS Accurate Care TM for cardiac diagnostic testings and the Superfect®, which is a transfection agent.[211,212]

In clinical trials are the DEP® docetaxel and DEP® cabazitaxel, from Starpharma, which consist of drug carriers that increase the drug water solubility of docetaxel and cabazitaxel.[213,214] Docetaxel is a drug for solid tumor, incluiding breast,

prostate, and lung cancers. DEP® systems allow obtaining controlled release and present a plasma half-time 40x longer than free docetaxel.[210] This system is currently in phase II studies, which focuses on determining the anti-tumor activity, overall safety, tolerability, and pharmacokinetics parameters.[213] Cabazitaxel is a drug for advanced prostate cancer usage. Conjugated with the DEP®, it increases the therapeutic window, decreases bone marrow toxicity, and enhances drug efficacy. Currently, DEP® cabazitaxel is in clinical phase I/II for solid tumors.[210,214]

The PLL dendrimer functionalized with 24 macrocyclic complexes of Gd^{3+} on the surface, named Gadomer-17, provides a high-relaxivity agent for MRI. This compound has been injected for imaging of the aortoiliac region and then into patients with coronary artery disease, allowing an improved detection.[215,216]

AstraZeneca is currently in phase I of clinical trials as an inhibitor of Bcl2/xL protein, the AZD 0466, based on DEP® technology of Starpharma, for the treatment of solid tumors and hematological malignancies.[210,217]

Also, in phase I for breast cancer is MAG-Tn 3, which consists of a dendrimer-based vaccine .[218]

A fourth-generation PAMAM functionalized with OH and N-acetyl cysteine, labelled OP-101, has shown anti-inflammatory and anti-oxidant activity against microglia cells.[219,220]

A third-generation PAMAM- hydroxyl dendrimer was used in clinical phase I trials for specific positron emission tomography (PET) imaging and radiotherapy to detect inflammatory sites or tumors. They have radionuclides, in particular, ^{18}F.[220]

More recently, a nasal spray to prevent COVID-19 infections was created. VIRALEZE™ is based on a generation-four dendrimer bearing 32 Sodium 1-(Carboxymethoxy)naphthalene-3,6-disulfonate on the surface. This product is in clinical trials in Australia.[221,222]

6 Hydroxychloroquine for the treatment of cancer

Hydroxychloroquine (HCQ) is an immunomodulatory drug that has been used for 60 years to treat malaria and autoimmune diseases, and potential new uses and benefits continue to emerge from it.[223] This drug has shown to be beneficial for many

rheumatological, cardiovascular, and dermatological conditions, and there is growing evidence that supports its therapeutic potential in oncology, HIV infection, chronic kidney disease, and a variety of nonmalarial infections.[224] Some side effects can be associated with the use of HCQ, including retinopathy, hyperpigmentation, myopathy, and skin reactions.[223]

In cancer treatment, the HCQ acts as an inhibitor of autophagy. Autophagy is a natural process by which cellular material is delivered to the lysosome for degradation and recycling to maintain cell and tissue homeostasis in all eukaryotes. It plays an important role in multiple physiological processes, including differentiation, normal growth, development, and immunity.[225-228] Under normal conditions, autophagy can prevent the development of malignant transformations. However, once cancer is established, autophagy supports the progression and metastatic dissemination, increasing the ability of cells to adapt to adverse microenvironmental conditions and chemotherapy treatments.[229-234] It has been reported that autophagy induction is a mechanism of chemoresistance.[235] Moreover, it has been proven that several tumor types use autophagy as a survival mechanism.[236-238] The relationship between autophagy and cancer is complex and may depend on the tumor type, stage of tumorigenesis, and environment.[230,239,240] It has been reported by various studies that the combination of anticancer drugs with pharmacologic or genetic autophagy inhibition can improve antitumor effects.[229,235,241]

The HCQ and chloroquine (CQ) are the only available autophagy inhibitors in the clinical market.[242] The HCQ, compared to CQ, is less toxic in long-term dosing and exhibits similar potency.[240] However, the mechanism of how these drugs inhibit autophagy is not fully understood. We know these drugs are weak bases that accumulate in the acidic environment of lysosomes, increasing the pH of these compartments and blocking the fusion with autophagosomes.[235,243] The HCQ molecule has three nitrogens with pKa values of 4.0, 8.3, and 9.7. In the lysosome, it can be protonated and cannot easily diffuse back into the cytosol.[244-246] Nonetheless, in the acid tumor microenvironment, the HCQ has difficulty crossing the cell membrane. This difficult cellular uptake limits the efficacy of HCQ in autophagy

inhibition.[247] To overcome these limitations, HCQ could be encapsulated into a nanocarrier and target the drug to the tumor.[248,249]

Preclinical studies showed that HCQ increases tumor cell death by itself or by enhancing tumor death in combination with targeted agents or cytotoxic chemotherapy.[250] This lysosomotropic agent induces lysosomal membrane permeabilization, activating the mitochondrial pathway of apoptosis.[251,252] Some studies showed that the inhibition of autophagy using HCQ could induce cell death of myeloma, lymphoma, and hepatocellular carcinoma cells.[253,254] A study carried out by Bray *et al.* has proven that HCQ enhances the cytotoxicity of temsirolimus against renal cell carcinoma cell lines *in vitro*.[255,256] The same synergetic effect was observed when administered HCQ with gefitinib, which resulted in a significant increase in cell death of breast cancer cell lines.[257] Some studies conclude that autophagy can promote the therapeutic activity of specific antineoplastic agents.[253,254,258-264] However, there is no agreement about it. Some studies also show that tumor cell death decreases by inhibiting autophagy, and tumor growth increases after drug treatment.[235] In addition, the whole-body inhibition of autophagy may favour the insurgence of treatment-related neoplasms, infectious diseases, neurodegenerative conditions and promote immunosuppression.[265]

So, the inhibition of autophagy *per se* can positively or negatively affect cancer therapies. There is evidence that autophagy can prevent or promote cancer and kill or protect cancer cells after treatment with anti-cancer drugs and radiation.[241]

Based on the previous evidence, the HQC encapsulation in nanocarriers, like dendrimers, could lead to a different *in situ* behavior of this autophagy inhibitor, with reflexes in the control of cancer cell progression and tumor evasion.

7 Doxorubicin for the treatment of cancer

The DOX is an anthracycline antibiotic approved by the FDA that has been the base of cancer therapy for a long time. It has commonly used in chemotherapy to treat breast, lung, stomach, bladder, ovaries, thyroid, soft tissue sarcoma, multiple myeloma, and Hodgkin´s lymphoma cancers.[266,267]

The antitumor activity of DOX is associated with the ability to intercalate into the DNA helix and/or bind covalently to proteins involved in DNA replication and transcription. This results in the inhibition of DNA, RNA, and protein synthesis, resulting in cell death.[268,269]

A range of side effects, including stomatitis, alopecia, anemia, neurologic disturbances, cumulative cardiotoxicity, and gastrointestinal disturbances, are associated with the use of DOX.[270] So, several efforts, including the development of novel anthracycline analogues, low-dose usage, and co-administration with cardioprotective agents and nanocarriers for encapsulation, have been made to reduce the toxicity of conventional anthracyclines.[271-273]

There are several liposomal systems for DOX carriers, such as Doxil® (previously cited), Myocet®, and Nudoxa®. Several studies using dendrimers for encapsulated DOX have been reported, including some by our team.[274-277]

8 Goals and objectives of the thesis

The objective of this thesis was to prepare and characterize anionic poly (alkylidenamine) carboxylate and sulfonate dendrimers for the transport and delivery of the HCQ into cancer cells. The specific aims to achieve were:

- Synthesize and characterize by NMR the G0 to G3 PPI nitrile dendrimers from 1,6-hexanediamine (core);
- Synthesize and characterize by NMR the G0 to G3 PPI amine dendrimers;
- Synthesize and characterize by NMR, ATR-FTIR, DLS, Zeta Potential, and MS the G1 to G4 anionic sulfonate and carboxylate PPI dendrimers;
- Encapsulate the drug into the anionic dendrimers (G1, G2, and G3), and characterized by NMR, ATR-FTIR, and zeta potential;
- Evaluate the cumulative release of sHCQ *in vitro* in PBS at pH 7.4 and 5;
- Determine the hemolysis of the anionic dendrimers and sHCQ;
- Evaluate the cytotoxicity of the compounds in a cancer cell line (MCF-7) and a non-cancer cell line (BJ cells).
- Evaluate the cytotoxicity of the compounds in combination with the free DOX in the cell line MCF-7 and the eventual synergistic effect.

Chapter II: Materials and methods

9 Materials and methods

9.1 Materials and reagents

All solvents and reagents were purchased from commercial sources and used as received unless otherwise reported. The 1,6-hexanediamine 99.5+%, acrylonitrile 99+%, borane dimethyl sulfide complex 94%, methanol 99.8% extra dry, methyl acrylate 99%, and hydroxychloroquine sulfate (sHCQ) 98%, were obtained from Acros Organics. Anhydrous tetrahydrofuran (THF) was obtained from a solvent purification system (mBraun MB SPS-800) and stored in a nitrogen atmosphere shortly before use. Sodium vinyl sulfonate was acquired from TCl. Sodium hydroxide was obtained from Fisher Scientific. Methanol was acquired from Chem-Lab. Chloroform, n-hexane, and diethyl ether were from AnalaR NORMAPUR VWR. Ethyl acetate was from PanReac AppliChem. DOX was purchased from the Biosynth Carbonsynth.

Dialysis membranes were obtained from Spectrumlabs (MWCO 100-500 Da, MWCO 500-1000 Da).

The RPMI (Roswell Park Memorial Institute) 1640 medium, MEM (Minimum Essential Medium) medium, and D-MEM (Dulbecco's Modified Eagle Medium) medium were obtained from Gibco, as well the antibiotic-antimycotic (AA), the fetal bovine serum (FBS), the non-essential amino acids (NEAA) and the human insulin. The sodium pyruvate is from Sigma-Aldrich.

9.2 Dendrimers synthesis and characterization

All the dendrimers were characterized by ^{1}H- NMR and ^{13}C- NMR, ATR- FTIR, dynamic light scattering (DLS), and mass spectroscopy (MS) to confirm the successfulness of the reactions.

The NMR (Nuclear Magnetic Resonance) characterization was performed using Bruker Avance ll+ 400 MHz equipment with a probe temperature of 25°C. The chemical shifts (δ, ppm) were measured relative to residual ^{1}H and ^{13}C, and deuterated water (D_2O) and deuterated chloroform ($CDCl_3$) were used as solvents. About 20 mg of the samples were dissolved in 540 µL of the respective solvent. The amine-, carboxylate- and sulfonate- terminated dendrimers were dispersed in D_2O.

The methyl ester dendrimers and the nitrile-terminated dendrimers were dissolved in $CDCl_3$.

The ATR-FTIR (Attenuated total reflectance - Fourier transform infrared spectroscopy) spectra were obtained using a Perkin Elmer Spectrum Two™ spectrometer in the range of 400 - 4000 cm^{-1}, with a number of 32 scans.

The size and zeta potential were measured using a Zetasizer Nano ZS with a He-Ne laser with a 633 nm wavelength from Malvern lnstruments Ltd. UK, at 25°C. The samples were dissolved in filtrated distilled water (0.2 µm filter) to measure the zeta potential and, to determine the size in one solution of 100 mM of NaCl (using filtrated distilled water (0.2 µm filter)), at a concentration of 0.5 mg/mL. Before measurements, all samples were filtrated with a 0.2 µm filter. Three measurements were done for the zeta potential analysis, corresponding to 30 runs each, and for the size experiments, 20 runs for each sample were done. Disposable folded capillary cells were used for the zeta potential analysis.

Mass Spectrometry (MS) spectra were obtained by a Bruker Autoflex maX Matrix-Assisted Laser Desorption and Ionization (Time-of-Flight) 2 Mass Spectrometer. The 2,5- dihydroxybenzoic acid (2,5- DHB) dissolved in methanol was used as the matrix.

9.2.1 Synthesis of nitrile poly(alkylidenamine) dendrimers (GxCN)

The synthesis of nitrile poly(alkylidenamine) dendrimers (GxCN) was performed following an experimental procedure previously developed by our team, with some modifications.[278] Firstly, 1,6- hexanediamine was dissolved in distilled water at room temperature. Acrylonitrile was added dropwise, stirring the mixture for 3h at 48 °C under a nitrogen atmosphere. After this, the temperature was increased to 80°C, and acrylonitrile was added dropwise. The reaction was carried out for 3h, after which the solvent was removed by vacuum. For the next generations the reaction was carried out for 4h at 48°C and then 4h at 80 °C, under a nitrogen atmosphere. In the case of G2 and G3, methanol was used as the solvent. The obtained yellow oil was dissolved in chloroform (20 mL) and washed seven times with distilled water (7 x 15 mL). The highest generation was washed less times (5x) and

with less solvent (5-20 mL), depending on the amount of product. The final product was obtained after drying under vacuum (figure 7).

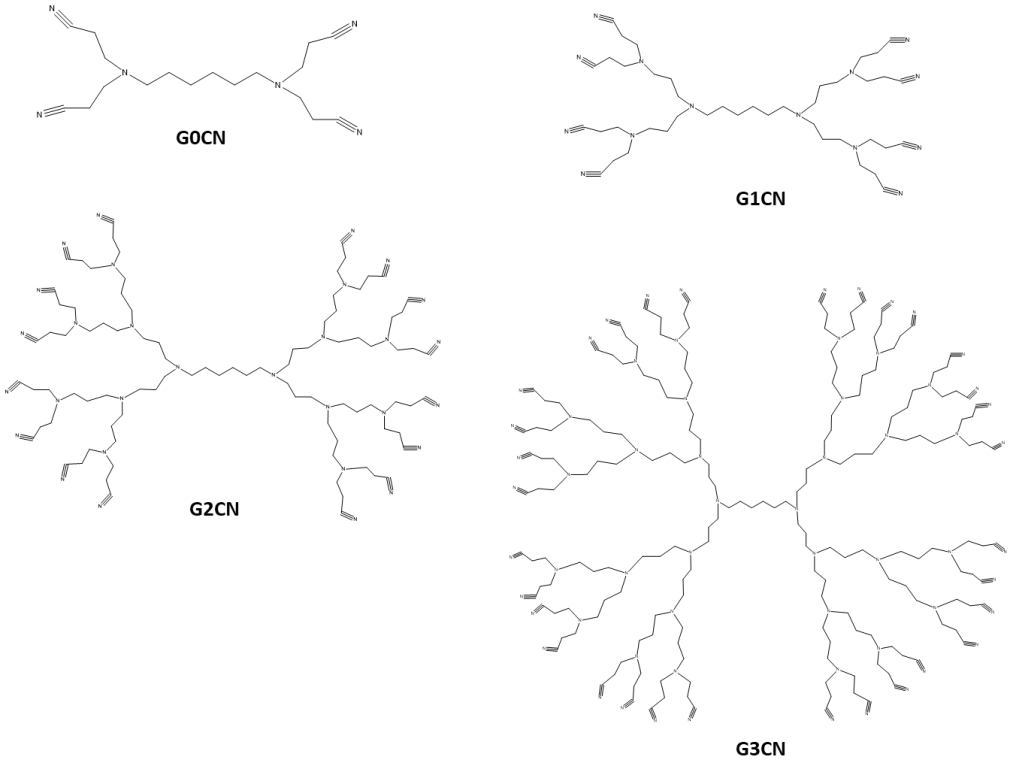

Figure 7- Structures of nitrile dendrimers synthesized (G0-G3).

9.2.1.1 G0CN dendrimer

For the synthesis of G0 nitrile dendrimer (G0CN), 10.82 g of 1.6-hexanediamine (93.1 mmol) was dissolved in 90 mL of distilled water. 23.1 mL of acrylonitrile (353.7 mmol, 3.8 eq. mol) was added twice to obtain 26.8 g of G0CN with a yield of 88%. ^{1}H NMR (400 MHz, $CDCl_3$) δ= 2.85-2.81 (-C**H**$_2$CN). ^{13}C NMR (100 MHz, $CDCl_3$) = 118.31 (-CH_2**C**N).

9.2.1.2 G1CN dendrimer

First batch: To obtain G1 nitrile dendrimer (G1CN), 2.07 g of G0NH_2 dendrimer (6.0 mmol) dissolved in 60 mL of distilled water, reacted with 2.99 mL of acrylonitrile (45.6 mmol, 7.6 eq. mol), added twice, to obtain 2.65 g of G1CN with a yield of 57%. ^{1}H NMR (400 MHz, $CDCl_3$) δ= 2.86-2.82 (-C**H**$_2$CN). ^{13}C NMR (100 MHz, $CDCl_3$) = 118.93 (-CH_2**C**N).

Second batch: G1CN was obtained using 1.13 g of G0NH_2 dendrimer (3.3 mmol) dissolved in 50 mL of distilled water and 1.49 mL of acrylonitrile (25 mmol, 7.6

eq. mol), added twice, to obtain 1.28 g of G1CN with a yield of 55%. ^{1}H NMR (400 MHz, $CDCl_3$) δ= 2.86-2.82 (-C**H**$_2$CN). ^{13}C NMR (100 MHz, $CDCl_3$) = 118.38 (-CH_2**C**N).

Third batch: 1.98 g of G0NH_2 dendrimer (5.8 mmol) was dissolved in 60 mL of distilled water, and 2.9 mL of acrylonitrile (43.7 mmol, 7.6 eq. mol), added twice, to obtain 2.21 g of G1CN with a yield of 50%. ^{1}H NMR (400 MHz, $CDCl_3$) δ= 2.86-2.83 (-C**H**$_2$CN). ^{13}C NMR (100 MHz, $CDCl_3$) = 118.37 (-CH_2**C**N).

Fourth batch: 2.61 g of G0NH_2 dendrimer (7.6 mmol) dissolved in 60 mL of distilled water reacted with 3.77 mL of acrylonitrile (57.6 mmol, 7.6 eq. mol), added twice, to obtain 2.99 g of G1CN with a yield of 51%. ^{1}H NMR (400 MHz, $CDCl_3$) δ= 2.86-2.83 (-C**H**$_2$CN). ^{13}C NMR (100 MHz, $CDCl_3$) = 118.36 (-CH_2**C**N).

9.2.1.3 G2CN dendrimer

First batch: To obtain the G2 nitrile dendrimer (G2CN), 1.5 g of G1NH_2 dendrimer (1.9 mmol) dissolved in 50 mL of distilled water and 1.86 mL of acrylonitrile (28.4 mmol, 15.2 eq. mol), added twice, resulted in 1.15 g of G2CN with a yield of 37%. ^{1}H NMR (400 MHz, $CDCl_3$) δ= 2.86-2.83 (-C**H**$_2$CN). ^{13}C NMR (100 MHz, $CDCl_3$) = 118.42 (-CH_2**C**N).

Second batch: 0.77 g of G1NH_2 dendrimer (1.0 mmol) dissolved in 40 mL of distilled water reacted with 0.96 mL of acrylonitrile (14.7 mmol, 15.2 eq. mol), added twice, to obtain 0.34 g of G2CN with a yield of 21%. ^{1}H NMR (400 MHz, $CDCl_3$) δ= 2.86-2.83 (-C**H**$_2$CN). ^{13}C NMR (100 MHz, $CDCl_3$) = 118.4 (-CH_2**C**N).

Third batch: 2.16 g of G1NH_2 (2.7 mmol) dendrimer was dissolved in 60 methanol, and 2.69 mL of acrylonitrile (41 mmol, 15.2 eq. mol) was added twice. We obtained 1.83 g of G2CN with a yield of 41%. ^{1}H NMR (400 MHz, $CDCl_3$) δ= 2.86-2.83 (-C**H**$_2$CN). ^{13}C NMR (100 MHz, $CDCl_3$) = 118.51 (-CH_2**C**N).

9.2.1.4 G3CN dendrimer

First batch: The G3 nitrile dendrimer (G3CN) was obtained using 0.48 g of G2NH_2 (0.3 mmol) dendrimer dissolved in 30 mL of methanol and 0.55 mL of acrylonitrile (8.4 mmol, 30.4 eq. mol) was added twice, to obtain 0.5 g of G3CN with a yield of 54%. ^{1}H NMR (400 MHz, $CDCl_3$) δ= 2.83 (-C**H**$_2$CN). ^{13}C NMR (100 MHz, $CDCl_3$) = 116.21 (-CH_2**C**N).

Second batch: 0.22 g of $G2NH_2$ (0.1 mmol) dendrimer was dissolved in 30 mL of methanol, and 0.25 mL of acrylonitrile (3.8 mmol, 30.4 eq. mol) was added twice, and 0.22 g of G3CN was obtained with a yield of 51%. ^{1}H NMR (400 MHz, $CDCl_3$) δ= 2.82 (-C**H**$_2$CN). ^{13}C NMR (100 MHz, $CDCl_3$) = 118.7 (-CH_2**C**N).

9.2.2 Synthesis of amine poly(alkylidenamine) dendrimers (GxNH$_2$)

According to the procedure of Pan *et al*.,[279] the nitrile-terminated dendrimers were dissolved in anhydrous THF under a nitrogen atmosphere, and borane dimethyl sulfide complex (5 eq. per nitrile group) was added using a syringe. The reaction was carried out for 48h at room temperature. Then, extra dry methanol was added slowly at 0°C, until no reaction was observed. The volatiles were removed by vacuum, and the final product was dissolved in fresh extra dry methanol and heated to reflux overnight at 70°C. Some modifications were done, including increasing the reaction time to 72h and reducing the reagent to 2.5 eq. per nitrile group in the G2 and G3. After this, the solvent was removed, and the residual oil was dissolved in water (50 mL) and washed with diethyl ether (7 x 20 mL), hexane (7 x 20 mL), and ethyl acetate (1 x 20 mL). The highest generation was washed less times (5x) and with less solvent (5-15 mL). The final product was dried under a vacuum (figure 8).

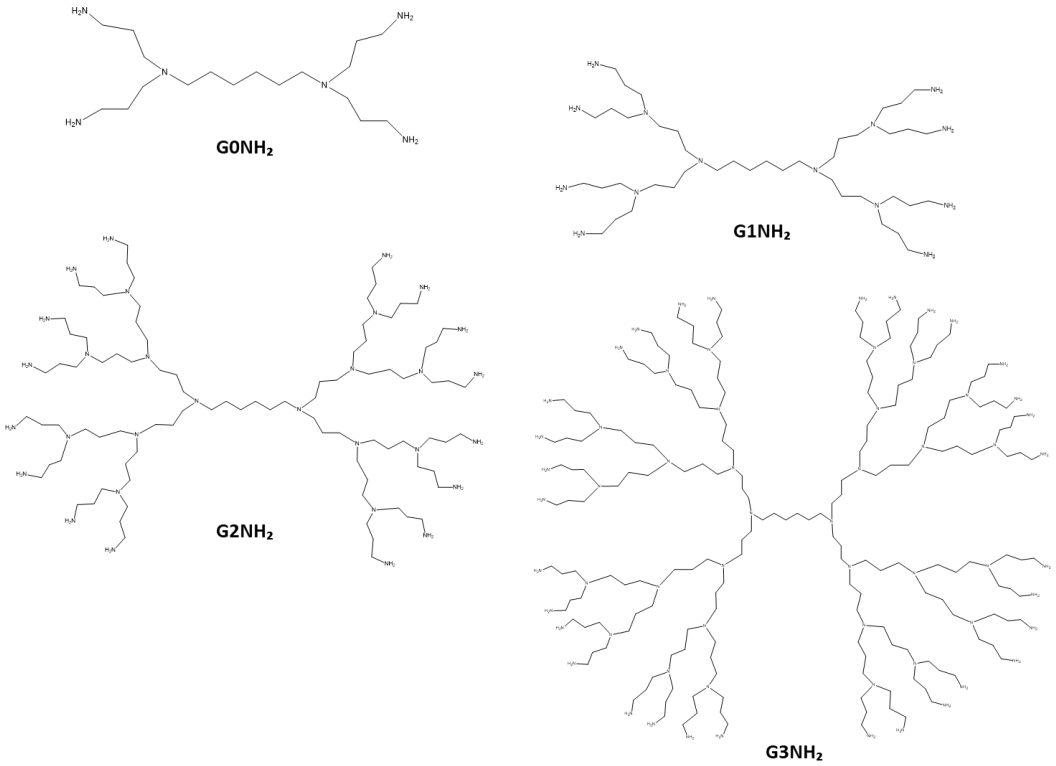

Figure 8- Structures of amine dendrimers synthesized (G0-G3).

9.2.2.1 G0NH_2 dendrimer

First batch: The synthesis of G0 amine dendrimer (G0NH_2) started with 5.03 g of G0CN dendrimer (15.3 mmol), and 100 mL of anhydrous THF was added. Then, 29.01 mL of borane dimethyl sulfide complex (306.3 mmol, 5 eq. per nitrile group) was added to obtain 5.22 g of G0NH_2 with a yield of 99%. ^{1}H NMR (400 MHz, D_2O) δ= 1.90 (-$CH_2N\mathbf{H}_2$), 2.79-2.76(-$C\mathbf{H}_2NH_2$). ^{13}C NMR (100 MHz, D_2O) = 38.17 (-$\mathbf{C}H_2NH_2$).

Second batch: 5.06 g of G0CN (15.4 mmol) was dissolved in 100 mL of anhydrous THF, and 29.2 mL of borane dimethyl sulfide complex (308.2 mmol, 5 eq. per nitrile group) was added to obtain 4.59 g of G0NH_2 dendrimer with a yield of 87%. ^{1}H NMR (400 MHz, D_2O) δ= 1.91 (-$CH_2N\mathbf{H}_2$), 2.83-2.79(-$C\mathbf{H}_2NH_2$). ^{13}C NMR (100 MHz, D_2O) = 37.99 (-$\mathbf{C}H_2NH_2$).

9.2.2.2 G1NH_2 dendrimer

First batch: To obtain the G1 amine dendrimer (G1NH_2), 1.74 g of G1CN (2.3 mmol) dissolved in 40 mL of anhydrous THF, reacted with 8.53 mL of borane dimethyl sulfide complex (90.3 mmol, 5 eq. per nitrile group), to obtain 1.21 g of G1NH_2 dendrimer with a yield of 67%. ^{1}H NMR (400 MHz, D_2O) δ= 1.91 (-$CH_2N\mathbf{H}_2$), 2.83 (-$C\mathbf{H}_2NH_2$). ^{13}C NMR (100 MHz, D_2O) = 37.99 (-$\mathbf{C}H_2NH_2$).

Second batch: 0.88 g of G1CN (1.1. mmol) dissolved in 20 mL of anhydrous THF, 4.32 mL of borane dimethyl sulfide complex (45.7 mmol, 5 eq. per nitrile group) was added. We obtained 0.77 g of G1NH_2 with a yield of 85%. ^{1}H NMR (400 MHz, D_2O) δ= 1.90 (-$CH_2N\mathbf{H}_2$), 2.91-2.88 (-$C\mathbf{H}_2NH_2$). ^{13}C NMR (100 MHz, D_2O) = 37.71 (-$\mathbf{C}H_2NH_2$).

Third batch: 1.76 g of G1CN (2.3 mmol) dissolved in 40 mL of anhydrous THF was added 8.8 mL of borane dimethyl sulfide complex (91.7 mmol, 5 eq. per nitrile group), to obtain 1.5 g of G1NH_2 with a yield of 82%. ^{1}H NMR (400 MHz, D_2O) δ= 1.90 (-$CH_2N\mathbf{H}_2$), 2.88-2.86 (-$C\mathbf{H}_2NH_2$). ^{13}C NMR (100 MHz, D_2O) = 37.87 (-$\mathbf{C}H_2NH_2$).

Fourth batch: 2.99 g of G1CN (3.9 mmol) dispersed in 40 mL of anhydrous THF, 15 mL of borane dimethyl sulfide complex (155.5 mmol, 5 eq. per nitrile group) was added to obtain 2.16 g of G1NH_2 with a yield of 69%. ^{1}H NMR (400 MHz, D_2O) δ= 1.93 (-$CH_2N\mathbf{H}_2$), 2.91-2.89 (-$C\mathbf{H}_2NH_2$). ^{13}C NMR (100 MHz, D_2O) = 37.9 (-$\mathbf{C}H_2NH_2$).

9.2.2.3 G2NH_2 dendrimer

First batch: To obtain the G2 amine dendrimer (G2NH_2), 1.12 g of G2CN (0.7 mmol) dissolved in 40 mL of anhydrous THF, and 5.23 mL of borane dimethyl sulfide

complex (54.4 mmol, 5 eq. per nitrile group) was added to obtain 0.18 g of G2NH₂ with a yield of 16%.

Second batch: 0.51 g of G2CN (0.3 mmol) in 40 mL of anhydrous THF reacted with 1.19 mL of borane dimethyl sulfide complex (12.4 mmol, 2.5 eq. per nitrile group), to obtain 0.48 g of G2NH₂ with a yield of 89%. ^{1}H NMR (400 MHz, D_2O) δ= 1.92 (-$CH_2N\mathbf{H}_2$), 2.98 (-$C\mathbf{H}_2NH_2$). ^{13}C NMR (100 MHz, D_2O) = 37.65 (-$\mathbf{C}H_2NH_2$).

Third batch: 0.62 g of G2CN (0.4 mmol) was dissolved in 40 mL of anhydrous THF, and 1.44 mL of borane dimethyl sulfide complex (15 mmol, 2.5 eq. per nitrile group) was added, to obtain 0.51 g of G2NH₂ with a yield of 80%. ^{1}H NMR (400 MHz, D_2O) δ= 1.92 (-$CH_2N\mathbf{H}_2$), 2.92 (-$C\mathbf{H}_2NH_2$). ^{13}C NMR (100 MHz, D_2O) = 37.85 (-$\mathbf{C}H_2NH_2$).

Fourth batch: 0.7 g of G2CN (0.4 mmol) in 40 mL of anhydrous THF, 1.61 mL of borane dimethyl sulfide complex (16.9 mmol, 2.5 eq. per nitrile group) was added to obtain 0.49 g of G2NH₂ with a yield of 67%. ^{1}H NMR (400 MHz, D_2O) δ= 1.91 (-$CH_2N\mathbf{H}_2$), 2.92-2.89 (-$C\mathbf{H}_2NH_2$). ^{13}C NMR (100 MHz, D_2O) = 37.76 (-$\mathbf{C}H_2NH_2$).

9.2.2.4 G3NH₂ dendrimer

First batch: The G3 amine dendrimer (G3NH₂) was obtained using 0.46 g of G3CN (0.1 mmol) in 30 mL of anhydrous THF and 1.04 mL of borane dimethyl sulfide complex (10.9 mmol, 2.5 eq. per nitrile group). Then, 0.39 g of G3NH₂ was obtained with a yield of 82%. ^{1}H NMR (400 MHz, D_2O) δ= 1.92 (-$CH_2N\mathbf{H}_2$), 2.84 (-$C\mathbf{H}_2NH_2$). ^{13}C NMR (100 MHz, D_2O) = 38.11 (-$\mathbf{C}H_2NH_2$).

Second batch: 0.22 g of G3CN (0.06 mmol) dissolved in 30 mL of anhydrous THF reacted with 0.5 mL of borane dimethyl sulfide complex (5.2 mmol, 2.5 eq. per nitrile group) to obtain 0.21 g of G3NH₂ with a yield of 92%. ^{1}H NMR (400 MHz, D_2O) δ= 1.91 (-$CH_2N\mathbf{H}_2$), 2.89 (-$C\mathbf{H}_2NH_2$). ^{13}C NMR (100 MHz, D_2O) = 38.25 (-$\mathbf{C}H_2NH_2$).

9.2.3 Synthesis of carboxylate dendrimers (GxCO₂Na)

The synthesis of carboxylate dendrimers was performed following the experimental procedure by García-Gallego *et al.,*[280] with adaptations. At room temperature, the amine-terminated dendrimers were dissolved in 5 mL methanol, and methyl acrylate (2.8 eq. per amine group) was added. The solution was stirred for 18 h at 80°C, under a nitrogen atmosphere. After this, the solvent was removed under a vacuum to obtain the methyl ester dendrimer ($GxCO_2Me$) as a clear oil.

Then, the methyl ester dendrimers were dissolved in 3 mL of methanol, and a solution of sodium hydroxide (1.1 eq. per amine group) in 4 mL of methanol was added to the previous solution. The reaction was carried out at room temperature for 48h. In the case of the G4, the reaction was carried out for 72h. The solvent was removed under reduced pressure, and the product was purified using a dialysis membrane (100-500 Da (G1, G2) and 500-1000 Da (G3, G4)) for several hours (6h-8h). The carboxylate dendrimers were obtained after lyophilization as white solids (figure 9).

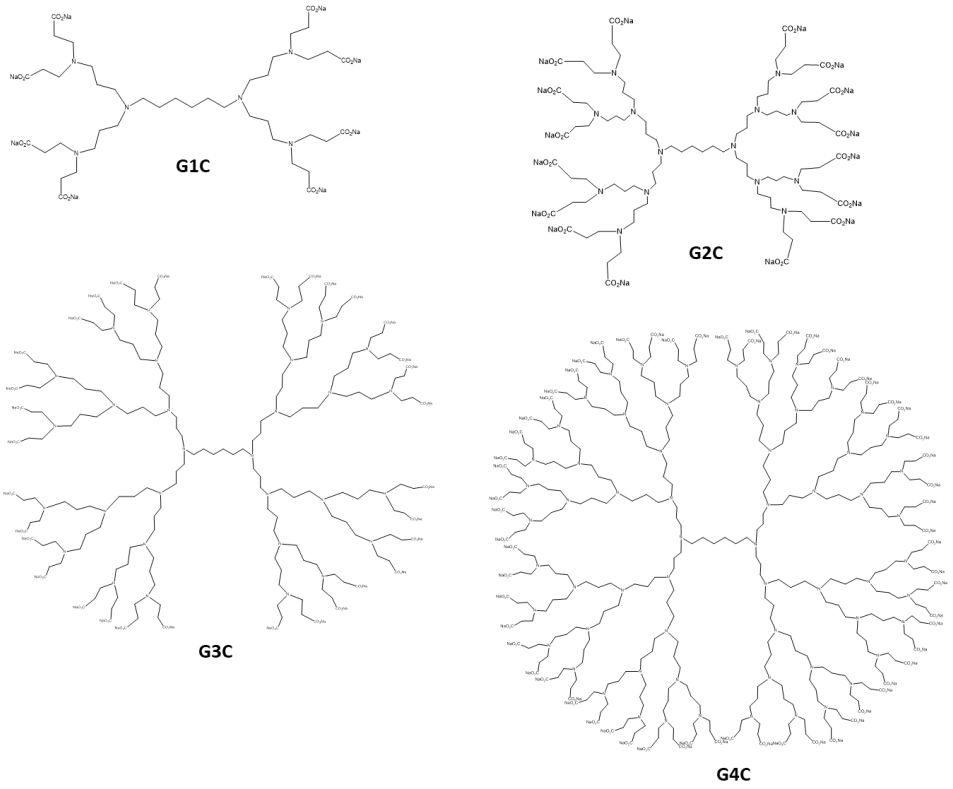

Figure 9- Structures of carboxylate dendrimer synthesized (G1-G4).

9.2.3.1 G1C dendrimer

For the preparation of G1 carboxylate dendrimer (G1C), we started with 0.54 g $G0NH_2$ (1.6 mmol) and added 1.6 mL of methyl acrylate (17.7 mmol), to obtain 1.16 g of $G1CO_2Me$ with a yield of 71%. ^1H NMR (400 MHz, $CDCl_3$) δ= 3.64 (-CO_2**Me**), 2.76-2.72 (-C**H**$_2CO_2Me$). ^{13}C NMR (100 MHz, $CDCl_3$) δ= 172.55 (-**C**O_2Me), 51.07 (-CO_2**Me**).

After ^1H NMR characterization, 0.81 g of $G1CO_2Me$ (0.8 mmol) was dissolved in methanol and sodium hydroxide was added (0.28 g, 6.9 mmol) in methanol, to obtain 0.81 g of G1C with a yield of 94%. ^1H NMR (400 MHz, D_2O) δ= 2.86-2.82 (-

C**H**$_2$CO$_2$Na). ^{13}C NMR (100 MHz, D_2O) = 179.91 (-**C**O_2Na). ATR-FTIR: ν= 2933.1 cm^{-1} (ν_{O-H}), 1394.54 cm^{-1} (ν_{c-o}). TOF-MS (ESI-): m/z= 727.17 [M- $C_9H_{14}NNa_2O_4$ – 6 Na +1H]$^{5-}$.

9.2.3.2 G2C dendrimer

To obtain G2 carboxylate dendrimer (G2C), to 0.52 g G1NH_2 (0.6 mmol) ,1.3 mL of methyl acrylate (14.5 mmol) was added, to achieve 1.04 g of G2CO_2Me with a yield of 74%. ^{1}H NMR (400 MHz, $CDCl_3$) δ= 3.65 (-CO_2**Me**), 2.76-2.73 (-C**H**$_2$$CO_2$Me).

To 0.62 g of G2CO_2Me (0.3 mmol) dissolved in methanol, a solution of NaOH (0.2 g, 5.0 mmol) in methanol was added, and we achieved 0.61 g of G2C with a yield of 93%. ^{1}H NMR (400 MHz, D_2O) δ= 2.64 (-C**H**$_2$$CO_2$Na). ^{13}C NMR (100 MHz, D_2O) = 179.89 (-**C**O_2Na). ATR-FTIR: ν= 2939.8 cm^{-1} (ν_{O-H}), 1396.54 cm^{-1} (ν_{c-o}). TOF-MS (ESI-): m/z= 985.31[M- $C_{45}H_{74}N_7Na_8O_{16}$ – 8 Na + 2H]$^{6-}$.

9.2.3.3 G3C dendrimer

For the synthesis of G3 carboxylate dendrimer (G3C), to 0.24g of G2NH_2 (0.1 mmol), 0.56 mL of methyl acrylate (6.2 mmol) was added, obtaining 0.42 g of G3CO_2Me with a yield of 68 %. ^{1}H NMR (400 MHz, $CDCl_3$) δ= 3.64 (-CO_2**Me**), 2.75-2.72 (-C**H**$_2$$CO_2$Me).

Then, to 0.42 g of G3CO_2Me (0.1 mmol) in methanol, a solution of NaOH (0.16 g, 3.3 mmol) was added to obtain 0.29 g of G3C with a yield of 65%. ^{1}H NMR (400 MHz, D_2O) δ= 2.63 (-C**H**$_2$$CO_2$Na). ^{13}C NMR (100 MHz, D_2O) = 179.83 (-**C**O_2Na). ATR-FTIR: ν= 2945.1 cm^{-1} (ν_{O-H}), 1721.2 cm^{-1} ($\nu_{c=o}$), 1398.7 cm^{-1} (ν_{c-o}).

9.2.3.4 G4C dendrimer

To synthesize G4 carboxylate dendrimer (G4C), 0.21 g of G3NH_2 dendrimer (0.06 mmol) reacted with 0.48 mL of methyl acrylate (5.2 mmol) to obtain 0.2 g of G4CO_2Me with a yield of 38 %. ^{1}H NMR (400 MHz, $CDCl_3$) δ= 3.64 (-CO_2**Me**), 2.73 (-C**H**$_2$$CO_2$Me).

After this, to 0.2 g of G4CO_2Me dendrimer (0.02 mmol) dissolved in methanol, a solution of NaOH (0.06 g, 1.6 mmol) was added, to obtain 0.11 g of G4C dendrimer with a yield of 50%. ^{1}H NMR (400 MHz, D_2O) δ= 2.67 (-C**H**$_2$$CO_2$Na). ^{13}C NMR (100 MHz, D_2O) = 181.09 (-**C**O_2Na). ATR-FTIR: ν= 2944.3 cm^{-1} (ν_{O-H}), 1725.7 cm^{-1} ($\nu_{c=o}$), 1397.7 cm^{-1} (ν_{c-o}).

9.2.4 Synthesis of sulfonate dendrimers (GxSO₃Na)

The experimental procedure of García-Gallego *et al.*,[280] was also used with adaptations for the synthesis of sulfonate dendrimers. At room temperature, the amine-terminated dendrimers were dissolved in 3 mL of methanol. To this solution, sodium vinyl sulfonate (2 eq. per amine group) was added, and the mixture was stirred for 48 h at 120°C under a nitrogen atmosphere. In the case of the G4, the mixture was stirred for 72h. After this, the solvent was removed under reduced pressure, and the final product was purified using a dialysis membrane (100-500 Da (G1, G2) and 500-1000 Da (G3, G4)) for several hours. The sulfonate dendrimers were obtained after lyophilization as white solids (figure 10).

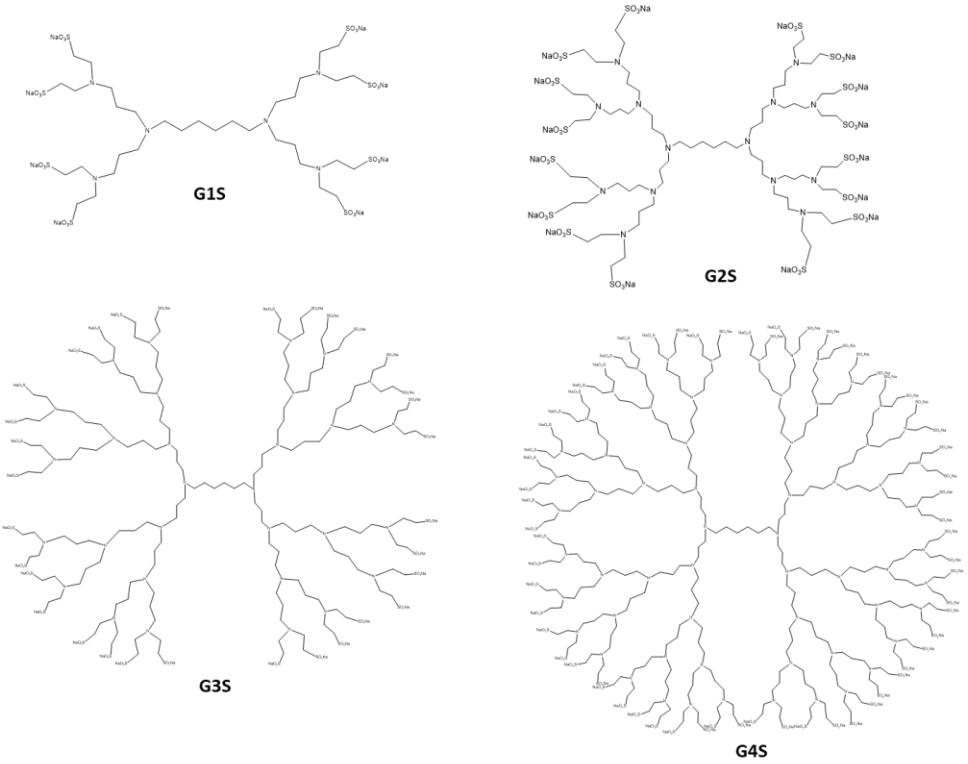

Figure 10- Structures of the sulfonate dendrimers synthesized (G1-G4).

9.2.4.1 G1S dendrimer

To synthesize G1 sulfonate dendrimers (G1S), to 0.5 g of G0NH_2 dendrimer (1.5 mmol), 5.1 mL of sodium vinyl sulfonate (11.7 mmol) was added, and 1.6 g of G1S dendrimer was obtained with a yield of 78%. ^{1}H NMR (400 MHz, D_2O) δ= 3.25-3.22 ppm (-C**H**$_2$$SO_3$Na). ^{13}C NMR (100 MHz, D_2O) = 46.67 ppm (-**C**$H_2$$SO_3$Na) ATR-FTIR:

ν= 1175.5 cm^{-1} ($\nu_{s=o}$), 1044 cm^{-1} ($\nu_{s=o}$). TOF-MS (ESI-): m/z= 971.36 [M- $C_5H_{10}Nna_2O_6S_2$ – 6 Na]$^{6-}$.

9.2.4.2 G2S dendrimer

The G2 sulfonate dendrimer (G2S) was synthesized using 0.5 g of $G1NH_2$ dendrimer (0.6 mmol) and 4.4 mL of sodium vinyl sulfonate (10.0 mmol) to obtain 1.1 g of G2S dendrimer with a yield of 60%. ^{1}H NMR (400 MHz, D_2O) δ= 3.24-3.21 ppm (-C**H**$_2SO_3Na$). ^{13}C NMR (100 MHz, D_2O) = 46.63 ppm (-**C**H_2SO_3Na) ATR-FTIR: ν= 1176.5 cm^{-1} ($\nu_{s=o}$), 1042.2 cm^{-1} ($\nu_{s=o}$). TOF-MS (ESI-): m/z= 2190.62 [M- $C_{17}H_{34}N_3Na_4O_{12}S_4$].

9.2.4.3 G3S dendrimer

For the synthesis of G3 sulfonate dendrimer (G3S), to 0.24 g of $G2NH_2$ dendrimer (0.1 mmol), 1.96 mL of sodium vinyl sulfonate (4.5 mmol) was added and obtained 0.65 g of G3S dendrimer with a yield of 79%. ^{1}H NMR (400 MHz, D_2O) δ= 3.27-3.23 ppm (-C**H**$_2SO_3Na$). ^{13}C NMR (100 MHz, D_2O) = 46.05 ppm (-**C**H_2SO_3Na) ATR-FTIR: ν= 1171.4 cm^{-1} ($\nu_{s=o}$), 1039.4 cm^{-1} ($\nu_{s=o}$).

9.2.4.4 G4S dendrimer

To synthesize G4 sulfonate dendrimer (G4S), 0.11 g of $G3NH_2$ dendrimer (0.03 mmol) reacted with 0.87 mL of sodium vinyl sulfonate (2.0mmol) to obtain 0.35 g of G4S dendrimer with a yield of 94%. ^{1}H NMR (400 MHz, D_2O) δ= 3.22-3.18 ppm (-C**H**$_2SO_3Na$). ^{13}C NMR (100 MHz, D_2O) = 46.6 ppm (-**C**H_2SO_3Na) ATR-FTIR: ν= 1175.5 cm^{-1} ($\nu_{s=o}$), 1041.6 cm^{-1} ($\nu_{s=o}$).

9.3 Drug encapsulation of Hydroxychloroquine sulfate (sHCQ)

The encapsulation of sHCQ was done following the experimental procedure of Agrawal *et al*.[281] For drug loading, an aqueous solution of sHCQ in 1 mL of distilled water (10mg/ml and 5 mg/ml) was prepared and slowly added to each dendrimer's solution (1mL, 100mg/ml and 50 mg/mL), under magnetic agitation. Each microtube was washed with 1 mL of distilled water and added to the respective dendrimer flasks. The solutions were stirred at room temperature for 24h. After this, these were centrifuged (SIGMA 3-30KS centrifuge) for 5 minutes, 15938*g*, at room temperature. The precipitate was washed three times with 3 mL of distilled water, and the supernatant was collected and lyophilized to obtain the drug-entrapped final product. To determine indirectly the amount of drug-loaded, a calibration curve of

sHCQ in distilled water was prepared using known concentrations, through UV-vis spectroscopy (Lambda25 spectrophotometer from PerkinElmer). The precipitate was dissolved in distilled water, and the absorbance measured at 343 nm. The encapsulation efficiency (EE) and the loading capacity (LC) was calculated using the 343 nm absorbance values, through the equations below[282]:

$$(eq.1)\ EE\ (\%) = \frac{total\ HCQ\ amount - free\ HCQ\ amount}{Initial\ mass\ of\ HCQ} \times 100$$

$$(eq.\ 2)\ LC(\%) = \frac{mass\ of\ loaded\ HCQ}{mass\ of\ HCQ\ loaded\ dendrimers} \times 100$$

Additionally, the dendrimers with the encapsulated sHCQ were characterized by ^{1}H- NMR and ^{13}C -NMR, ATR- FTIR, and DLS to measure the zeta potential and to confirm the successfulness of the encapsulation.

9.4 Drug release studies

The drug-encapsulated dendrimers were dissolved in 300 µL of PBS at pH 7.4 or PBS at pH 5. We weighed 129 µg of sHCQ. This solution was transferred to a dialysis device (Slide-A-Lyzer™ MINI Dialysis Device, 2000 MWCO) and placed in a glass flask with 7 mL of the respective PBS. The assays were done in triplicate, and sHCQ dissolved in PBS was used as a control. The samples were placed in the incubator (Wisd Laboratory instruments) at a constant temperature of 37°C. After 1h, 2h, 4h, 6h, 24h, 48h, and 1 week, 1 mL of the supernatant was removed, and replaced with 1 mL of fresh PBS, for fluorescence spectroscopy analysis (LS55 fluorescence spectrometer equipment from PerkinElmer). The cumulative release was calculated by the following equation[283]:

$$(eq.3)\ Cr\ (\%) = \frac{Vr\ \sum_{n}^{n-1} Ci + Vo\ Cn}{m\ HCQ} \times 100$$

where mHCQ represents the amount of sHCQ encapsulated in the dendrimers used in the study, V_o is the volume of the release medium (V_o = 7 mL), V_r is the volume of the replaced medium (V_r = 1 mL), and C_n represents the concentration of sHCQ in the sample. The results are presented as a percentage of cumulative release (mean of three independent assays) ± standard deviation (SD).

A calibration curve of sHCQ in PBS at pH 5 and pH 7.4 was previously prepared, using standards of the known concentration by fluorescence spectroscopy to measure the concentration of sHCQ released.

9.5 Hemotoxicity evaluation

Samples of fresh and healthy human blood were obtained from donors at Hospital Dr. Nélio Mendonça to determine the compounds' hemotoxicity through the cyanmethemoglobin method.[284] A 250-fold dilution of blood in cyanmethemoglobin reagent (C-reagent) was prepared to evaluate the blood's total hemoglobin (Hg) concentration. The C-reagent was previously prepared using 50 mg of potassium ferricyanide, 12.5 mg of potassium cyanide, 35 mg of potassium dihydrogen phosphate in 250 mL of distilled water with 250 µL of Triton-X, and the pH was adjusted to 7.4.

A standard curve for Hg was prepared using Hg from bovine blood. A stock solution of 1.5 mg/ml was prepared, and from this, successive dilutions were done in a range of 0.2-1.39 mg/ml, to obtain standards of known concentrations. The C-reagent was used as a blank, and the absorbance was measured at 550 nm.

The dendrimers were dissolved in PBS 7.4 (Mg^{2+}/Ca^{2+} free), in the same concentrations used for the cells (0.5-50 µM), and 70 µL were transferred into Eppendorf type vials, one for each compound and concentration to be tested. For controls, distilled water (positive control) and PBS 7.4 (Mg^{2+}/Ca^{2+} free) (negative control) were used. A solution of 10% (v/v) of blood was prepared in PBS 7.4 (Mg^{2+}/Ca^{2+} free), and 10 µL was added into Eppendorf type vials containing the compounds. Subsequently, the samples were incubated at 37°C for 3h, and centrifuged at 1324*g* for 5 min. After this, 40 µL of each supernatant was transferred to 96-well plates, and 160 µL of C -reagent was added.

In the end, the absorbance was measured at 550 nm using a Perkin Elmer VICTOR^3 ™ Multilabel Reader spectrophotometer. The results are presented as a percentage of hemolysis (mean of three independent assays) ± standard deviation (SD), following the next equation:

$$(eq. 4)\ \%\ hemolysis = \frac{S}{T} \times 100$$

where, S is the value of the concentration of Hg supernatant, and T is the total Hg concentration in the test tubes, which is obtained by dividing the Hg concentration in whole blood by the dilution factor.

9.6 Cytotoxicity evaluation of dendrimers and dendrimers-HCQ conjugates

For the evaluation of cytotoxicity, three different cell lines were used: breast cancer cells (MCF-7), colorectal adenocarcinoma cells (CACO-2), and fibroblast cells (BJ, a non-cancer cell line). The cryopreserved tubes containing the cells were centrifuged at 300*g* for 8 min at 4 °C, and the pallet was resuspended in 1 mL of the respective medium. Then, the resuspended cells were transferred to a culture dish with 9 mL of medium (v_f = 10 mL). All mediums contained 10% (v/v) FBS and 1% (v/v) AA (from 100x solution).

The MCF-7 cells were cultured in RPMI 1640 Medium supplemented with 1% (v/v) NEAA (from 100× solution), 1 mM sodium pyruvate, and 3.3 µg/mL human insulin. The CACO-2 cells were cultured in MEM medium supplemented with 1% (v/v) NEAA. And the BJ cells were cultured in D-MEM medium.

The culture dishes were incubated at 37°C in a humidified atmosphere with 5% carbon dioxide (DH Autoflow Automatic CO2 Air Jacked Incubator, Nuaire). The medium was replaced every 2-3 days.

For the cell culture experiments, the cells were cultured in 96-well plates with a density of 1.5 x 10^4 cells *per* well, in the respective medium. The cytotoxicity of the dendrimers was indirectly quantified by measuring the metabolic activity of cells through a resazurin reduction assay. The dendrimers, dendrimers-HCQ conjugates, and sHCQ were prepared in filtered distilled water within the concentration range of 0.5-50 µM. From this solution, 20 µL were added to the cells and incubated at 37°C for 48h. After, the cell culture medium was replaced with a complete fresh medium containing 10% (v/v) of a resazurin solution (0.1% (w/v) in PBS), and the cells were incubated for 3h at 37°C. Then, the supernatant was transferred to 96-well opaque plates, and the fluorescence of the resorufin ((λ_{ex} = 530 nm, λ_{em} = 590 nm) was measured using a microplate reader (Perkin Elmer VICTOR^3 ™ Multilabel Reader

spectrophotometer). A DOX assay was performed, dissolving the drug in distilled water with concentrations of 100 µM and 0.1 µM. The experiments were done in triplicate, and all samples were carried out in quadruplicate. The results are expressed as a percentage of cell viability in relation to the control (cells not exposed to sHCQ).

Chapter III: Results and discussion

10 Results and discussion

10.1 Synthesis and characterization of the nitrile dendrimers

This work uses the divergent method to synthesize the G0-G3 amine- and nitrile- PPI dendrimers. The PPI dendrimers are constituted by a 1,6-hexanediamine core, and the interior contains only alkyl and tertiary amine groups.[60] The primary amines are on the periphery, which allows the occurrence of chemical reactions required for surface functionalization, generation increase, and attaching a molecule or a ligand to the terminal groups.[285]

The first step for synthesizing the G0CN consists of a double Michael addition of acrylonitrile to the primary amines of the 1,6- hexanediamine (figure 11). The Michael reaction is a nucleophilic addition, where the amine group acts like a nucleophile since it donates an electron pair to the carbon atom from the acrylonitrile to form a bond. So, the acrylonitrile acts like an electrophile, and the double C=C bond becomes a simple C-C bond.[286]

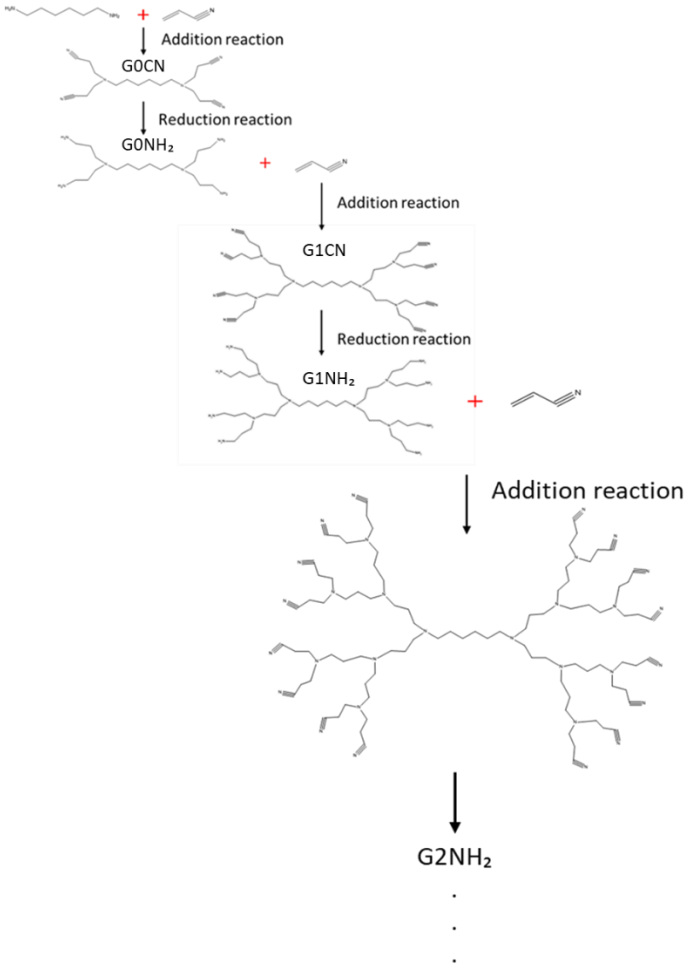

Figure 11- Scheme of the synthesis of PPI dendrimers

Table 1 displays the results of the yields obtained for the nitrile dendrimers preparation. Considering the published results,[287] the G0CN was synthesized with a yield within the expected, achieving 88%. To prepare G0CN, the reaction was carried out for 6h in total. For the other generations, the dendrimers were prepared using a total time of 8h, because we have more amine groups to react. In the G1CN the yield decreases drastically, around 50%-60%, and, in the G2 we obtained yields of 21% and 37%. So, in the preparation of G2 and G3, instead of water, methanol was used as a solvent, since this solvent facilitates solubilization and purification in the higher generation. The yields did not vary too much and remained at around 50%. The yields reported in the literature are 61% and 56% for the synthesis of G1 and G2, respectively.[287] Our yields, although slightly lower, remained, in most of the cases, at the same order of magnitude. The most plausible explanation for these differences can be explained by the different experimental conditions, mainly in the purification process (washes with distilled water to eliminate some excess of acrylonitrile and the formed secondary products) and in the effectiveness of vacuum drying of the prepared dendrimers.

Table 1- Yields obtained for the synthesis of nitrile dendrimers*.

	First batch	Second batch	Third batch	Fourth batch
G0CN	η=88%	-	-	-
G1CN	η=57%	η=51%	η=50%	η=51%
G2CN	η=37%	η=21%	η=41% (using methanol as solvent)	---
G3CN	η=54% (using methanol as solvent)	η=51% (using methanol as solvent)	---	---

* Unless stated, reactions were done in water

The obtained G0-G3 nitrile dendrimers were characterized by ^{1}H- and ^{13}C - NMR, which allowed us to obtain information about the structure and chemical transformations that occurred in the end groups during the synthesis steps.[288]

The NMR analyses of G0CN (figure 12) showed the expected signals in the ^{1}H-NMR spectrum. Signals corresponding to the core can be observed between 1.47 and

1.32 ppm, and at 2.85-2.70 ppm. The protons corresponding to the branches are shown as a triplet at 2.53-2.50 ppm and 2.47-2.44 ppm. In the ^{13}C-NMR spectrum (figure 13) the carbon signal corresponding to the nitrile group is displayed at 118.31 ppm, and the carbon signals of the core are shown at 26.39 ppm, 26.9 ppm, and 52.81 ppm. At 16.53 ppm and 49.16 ppm, it is possible to observe the signals of the carbons of the dendrimer branches .[66,252,278-291]

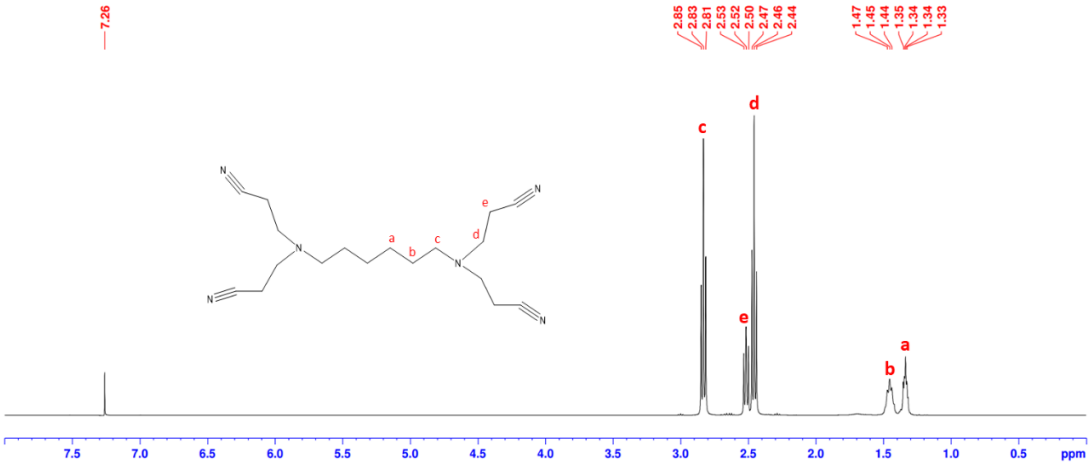

Figure 12- ^{1}H-NMR spectrum of the G0CN in $CDCl_3$.

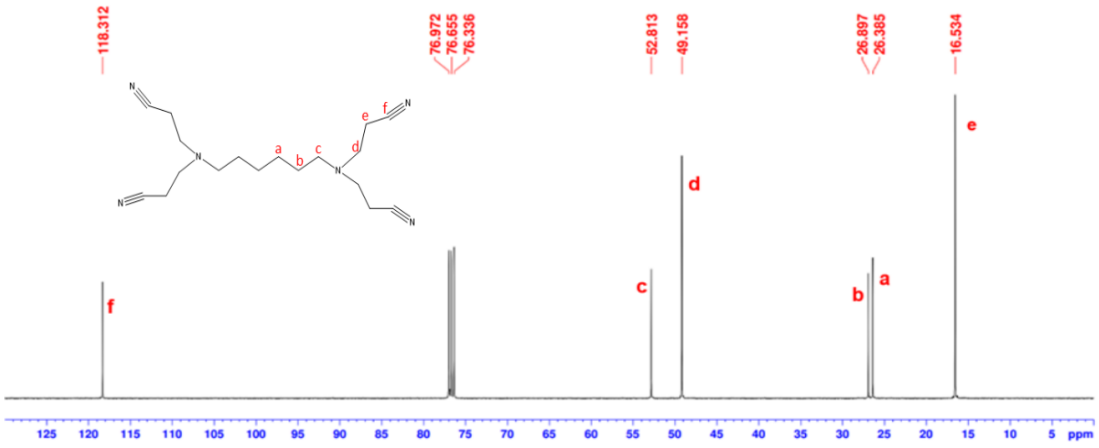

Figure 13- ^{13}C-NMR spectrum of G0CN in $CDCl_3$.

For G1CN, the ^{1}H-NMR spectrum (figure 14) shows the signals corresponding to the core between 1.42 ppm and 1.28 ppm, and at 2.86-2.82 ppm. Further, this signal also includes the protons near the nitrile group. The protons of the branches are shown as a quintet between 1.62-1.55 ppm and as two triplets between 2.50-2.46 ppm and 2.57- 2.54 ppm. In the ^{13}C-NMR spectrum (figure 15), the carbon that corresponds to the nitrile group is observed at 118.93 ppm, and the core signals are

displayed at 27.16 ppm, 27.84 ppm, and 54.12 ppm. The branches' carbon signals are presented at 17.08, 25.16, 49.75, 51.53, and 51.70 ppm.

Regarding the second, third, and fourth batches of G1CN, the ^{1}H-NMR spectrum (see annex figures A1, A3, and A5) and ^{13}C-NMR spectrum (see annex figures A2, A4, and A6) showed the same expected signals as observed in the first synthesis.

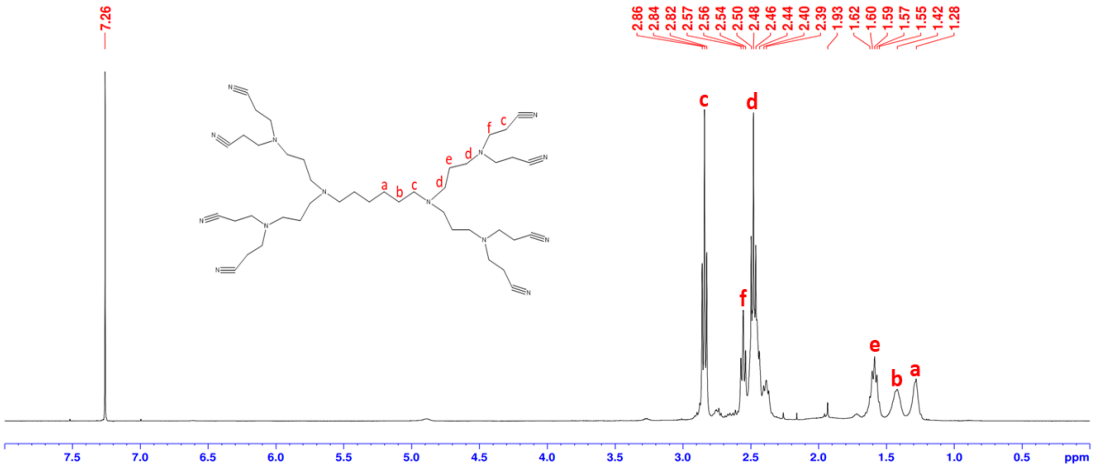

Figure 14- ^{1}H-NMR spectrum of G1CN in $CDCl_3$.

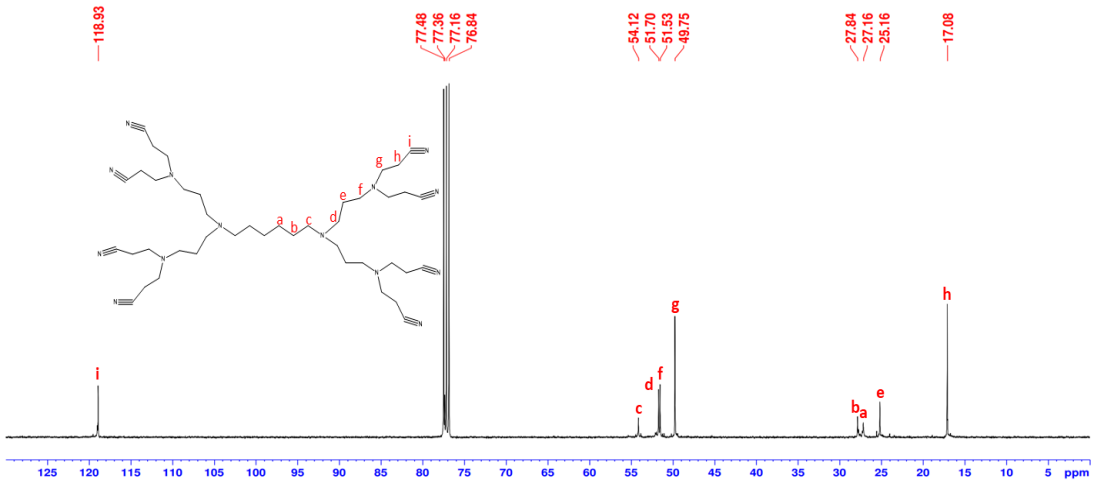

Figure 15- ^{13}C-NMR spectrum of G1CN in $CDCl_3$.

The G2CN dendrimers showed the expected signals for the ^{1}H-NMR spectrum (figure 16). The core signals occurred at 1.29 ppm, 1.43 ppm and 2.86-2.83 ppm. These include the protons near the nitrile. The protons of the branches are shown as a quintet between 1.61-1.58 ppm and two triplets between 2.50-2.47 ppm and 2.57-2.54 ppm. In the ^{13}C-NMR spectrum (figure 17), the carbon corresponding to the nitrile group presents itself at 118.42 ppm, and the core signals are displayed at 26.66

ppm and 27.37, and 53.69 ppm. The carbon signals of the branches are presented at 16.53, 24.62, 49.18, 51.02, and 51.77 ppm.

As expected, the ^{1}H-NMR spectrum (see annex figures A7 and A9) and 13C-NMR spectrum (see annex figures A8 and A10) for the subsequent batches present the same signals.

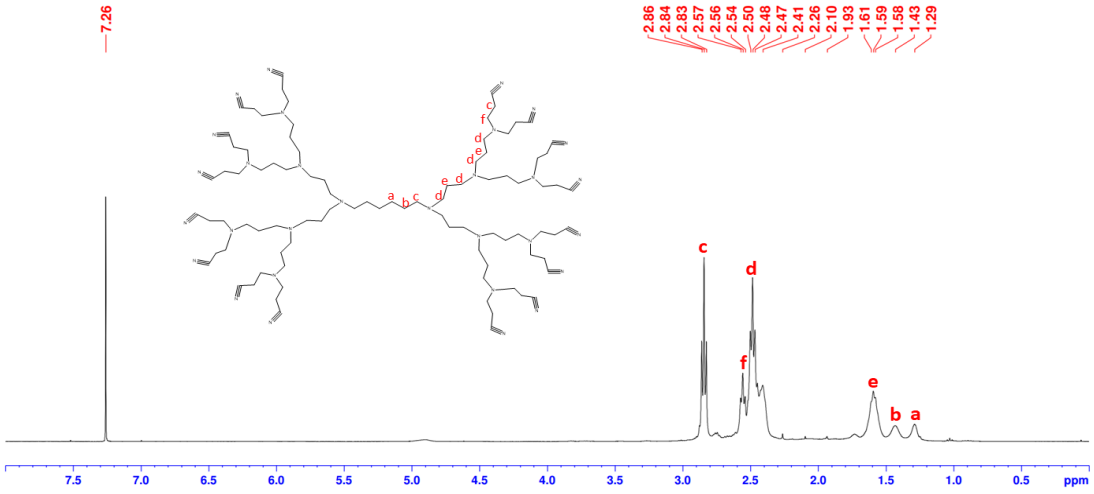

Figure 16- ^{1}H-NMR spectrum of G2CN in $CDCl_3$.

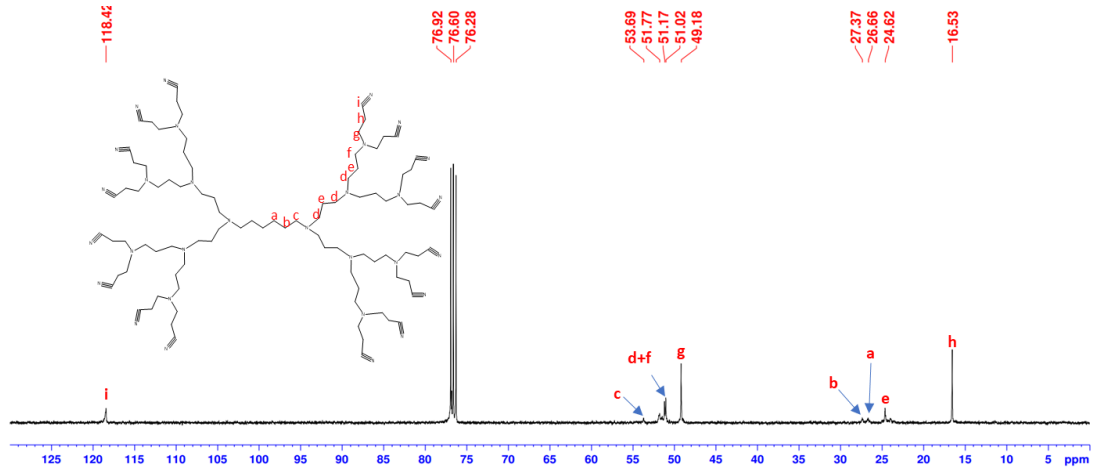

Figure 17- ^{13}C-NMR spectrum of G2CN in $CDCl_3$.

In the NMR spectrums of G3CN, the signals are more difficult to discriminate, which is probably due to the dendrimer's size and defects (the purification is more demanding) and sample concentration. In fact, when performing the divergent synthesis in the higher generations, it is difficult to separate the desired product from the reactants. This is because of its molecular similarity with the final product and the formation of dendrimers with structural defects.[292]

In the ^{1}H-NMR spectrum (figure 18), the signals of the core appear at 1.24 ppm and 1.36 ppm. The signals of the core protons and near the terminal nitrile group are displayed as a triplet around 2.87-2.83 ppm. The protons of the branches appear at 1.80 ppm and between 2.67 ppm and 2.53 ppm. Some methanol residues also appeared at 3.46 ppm. In the ^{13}C -NMR (figure 19), the carbon of the nitrile group is displayed at 116.21 ppm. This signal is a 2 ppm shift to the upfield (lower energy) compared with the previous generations. However, the NMR spectra resolution is not comparable. The signals of the core are at 27.93 ppm and at 48.25 ppm. The other carbons of the structure appear at 14.12 ppm, 26.93 ppm, and between 47.76 and 41.87 ppm.

In the second bath, the ^{1}H- and ^{13}C- NMR spectra (see annex figures A11 and A12) are very similar, with the signals occurring around the same values identified.

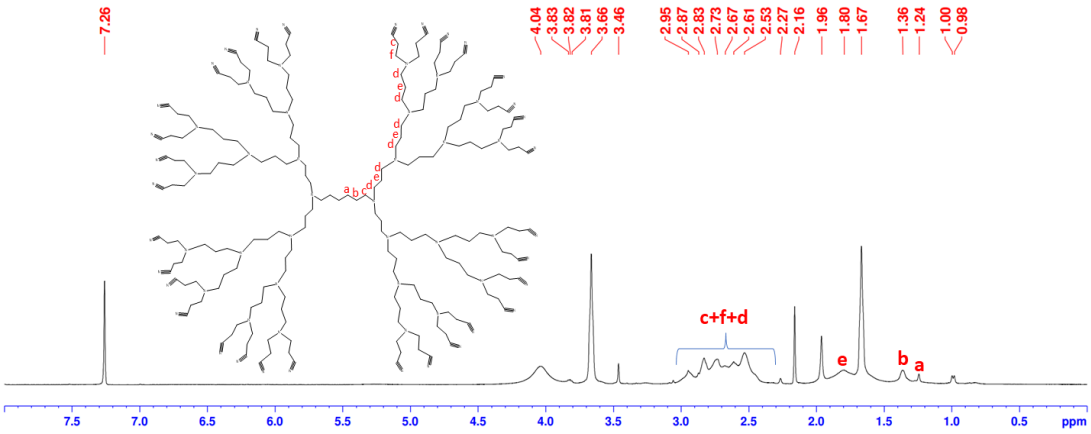

Figure 18- ^{1}H-NMR spectrum of G3CN in $CDCl_3$.

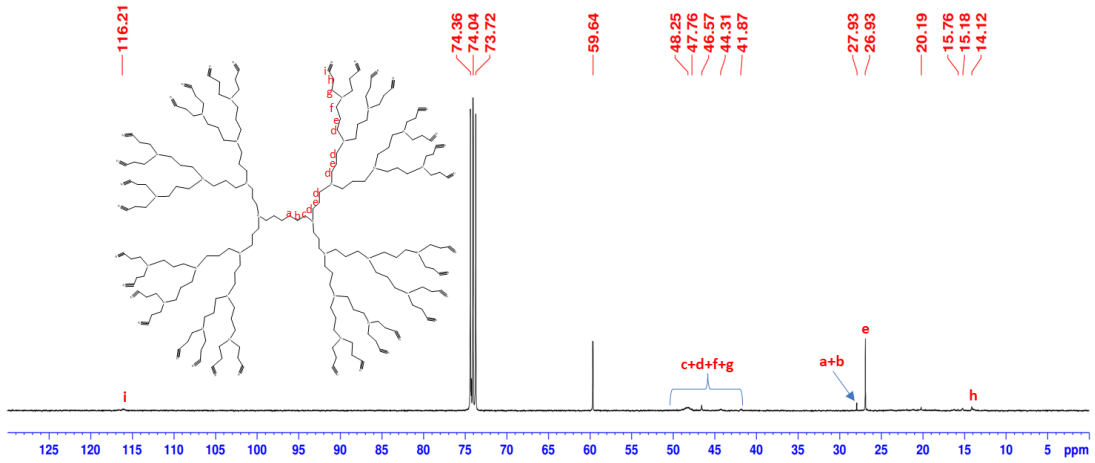

Figure 19- ^{13}C-NMR spectrum of G3CN in $CDCl_3$.

10.2 Synthesis and characterization of the amine dendrimer

The amine dendrimers are obtained by reduction of the terminal nitrile groups in anhydrous THF using borane dimethyl sulfide complex as a reducing agent (figure 11). Starting with the G0CN, we obtained the $G0NH_2$ dendrimer with a yield of 99% and 86% (table 2). Values in line with what has been reported previously, respectively 95% and 84%.[66,279,291]

The $G1NH_2$ was synthesized as described in the experimental procedure, with a yield of 67%, 85%, 82% and 69% (average value 76%), also in line with previous reports.[279,291]

In relation to the synthesis of $G2NH_2$, in the first attempt, we extended the reaction time to 72h. However, the yield obtained was unsatisfactory (16%). So, we reduced the amount of reagent to 2.5 eq. per nitrile group and kept the reaction time at 72h. The yields obtained increased to 89%, 80%, and 67% (average of 79%). The first unsuccessful result was because we faced a problem with Tandem Michael addition/amino-nitrile cyclization. Although a similar reaction was reported with a yield of 82%,[279] the same compound ($G2NH_2$) had a much lower yield (only 15%).[291] So, the introduced synthesis modification represented a significant increase in the final yield on the preparation of higher dendrimers generation (ca. of 5 times).

Based on the approach used in the preparation of ($G2NH_2$), the last generation amine dendrimers synthesized, $G3NH_2$, was done using 2.5 eq. of reagent per nitrile group and a time of reaction of 72h. The dendrimer obtained presented with very good yields (82% and 92%).

Table 2- Yields obtained for the synthesis of amine dendrimers*.

	First batch	Second batch	Third batch	Fourth batch
$G0NH_2$	η=99%	η=86%	---	---
$G1NH_2$	η=67%	η=85%	η=82%	η=69%
$G2NH_2$	η=16%	η=89% (2.5 eq. reagent)	η=80% (2.5 eq. reagent)	η=67% (2.5 eq. reagent)
$G3NH_2$	η=82% (2.5 eq. reagent)	η=92% (2.5 eq. reagent)	---	---

* Unless stated, reactions were done with 5 eq. per group nitrile of reagent

The ^{1}H-NMR spectrum of G0NH$_2$ (figure 20) gives us information about the synthesis and compound purity. The protons of the core are displayed between 1.49 and 1.31 ppm, and 2.67-2.59 ppm. The signal at 1.90 ppm could be attributed to the protons of the amine terminal groups. The protons of the dendrimer branches are presented as a quintet at 1.78-1.70 ppm and as two triplets between 2.79-2.51 and 2.79-2.76 ppm. In the ^{13}C-NMR spectrum (figure 21), the signals of the core carbons are presented at 22.83 ppm, 26.13 ppm, and 52.5 ppm. The carbon signals of the dendrimer branches are observed at 25.53 ppm and 50.05 ppm. The carbons near the amine group are observed at 38.08 ppm. The signals at 180.91 ppm,173.2 ppm, and 61.01 ppm correspond to the solvent (e.g., diethyl ether and ethyl acetate) or residuals of the initial product. Therefore, the final product still needed more purification steps.

We could identify the same expected signals with the synthesis repetition and through the ^{1}H- and ^{13}C -NMR spectrum (see annex figures A13 and A14).[66,290,293,294]

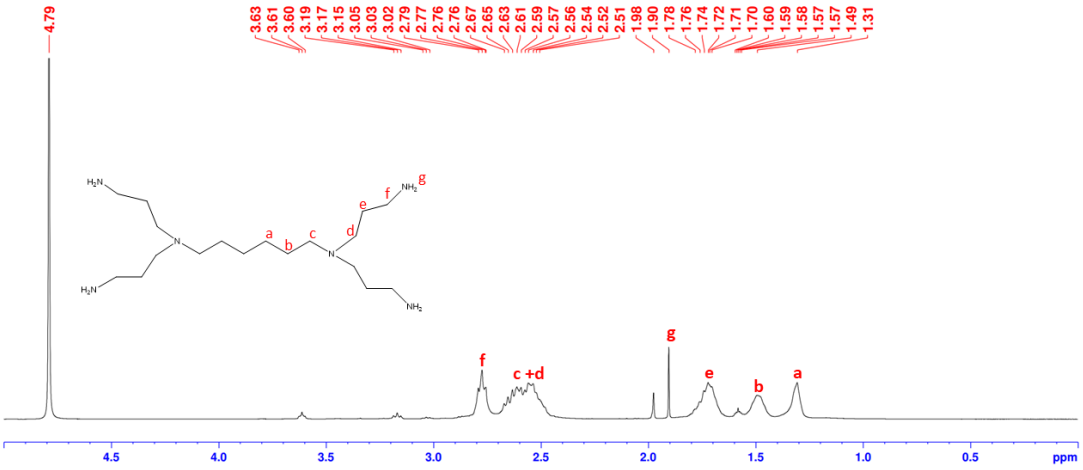

Figure 20- ^{1}H-NMR spectrum of G0NH$_2$ in D$_2$O.

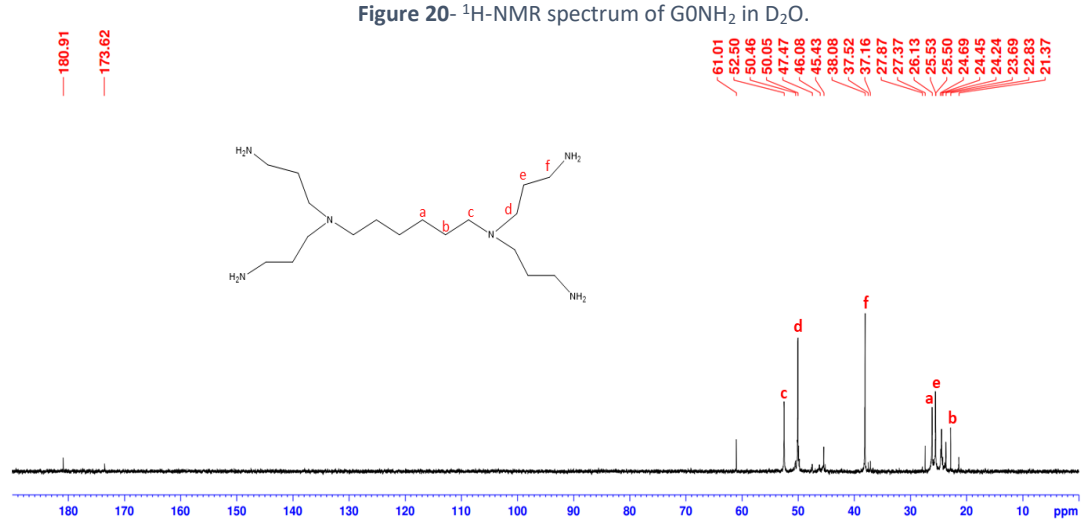

Figure 21- ^{13}C-NMR spectrum of G0NH$_2$ in D$_2$O.

The HSQC-NMR spectrum (figure 22) also helped to identify the signals of the protons through the ^{13}C-NMR spectrum. The core carbons had signals at 1.31 ppm, 1.49 ppm, and 2.67-2.59 ppm in the ^{1}H-NMR spectrum. The signals of the branches in the ^{13}C-NMR spectrum are related to the signals at 1.78-170 ppm, 1.90 ppm, and 2.79-2.51 ppm in the ^{1}H-NMR spectrum, corresponding to the protons.

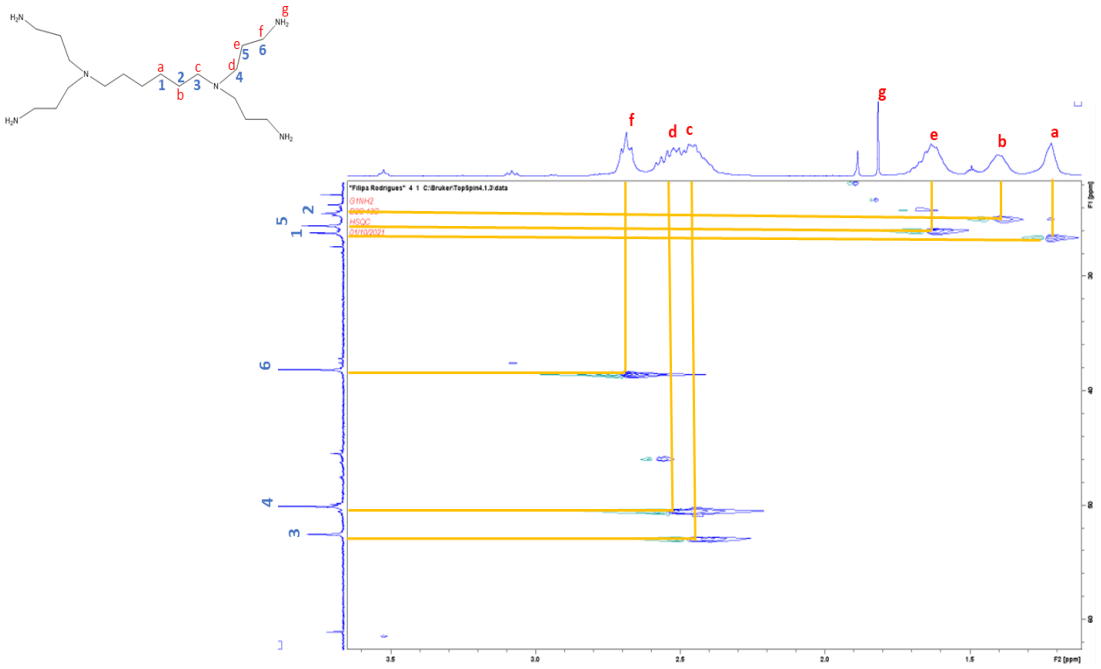

Figure 22- HSQC-NMR spectrum of G0NH$_2$ in D$_2$O.

The G1NH$_2$ showed the expected signals for the ^{1}H-NMR spectrum (figure 23). The core signals are observed at 1.24 ppm, 1.33 ppm, and 2.69-2.65 ppm. The signal at 1.91 ppm can be attributed to the protons in the amine terminal groups. The signals of the branches are displayed at 1.50 ppm, 1.75 ppm, 2.56 ppm, and 2.89 ppm. In the ^{13}C-NMR spectrum (figure 24), the carbon signals, between 23.67-26.29 ppm and 52.59 ppm are assigned to the core. The carbon near the amine group is shown at 37.99 ppm. At 22.83, 27.36, 45.67 ppm, and 50.59 ppm are the signals of the dendrimer branches.

The second, third, and fourth batches of G1NH$_2$ showed the expected signals on the ^{1}H- and ^{13}C-NMR spectrum (see annex A15, A15, A17, A18, A19, A20).

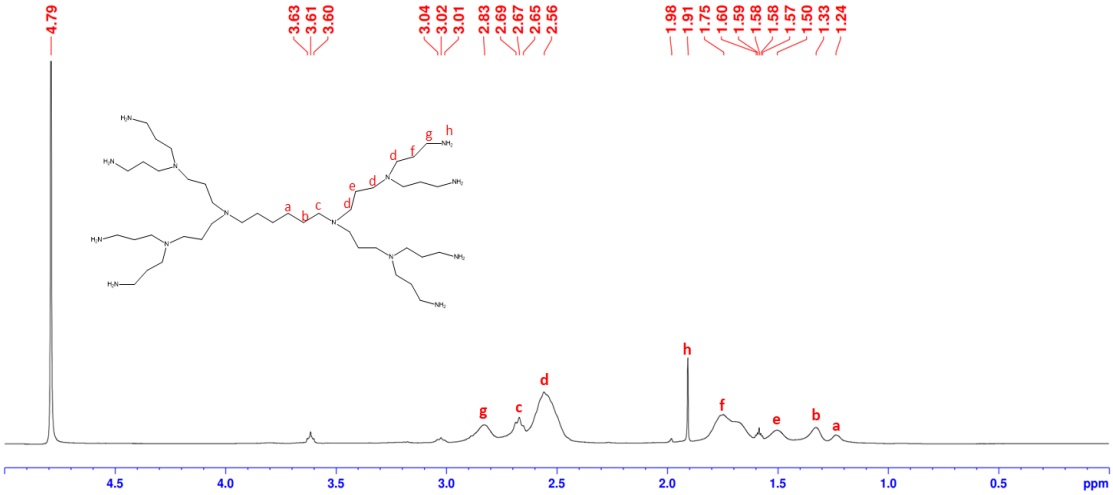

Figure 23- ^{1}H- NMR spectrum of $G1NH_2$ in D_2O.

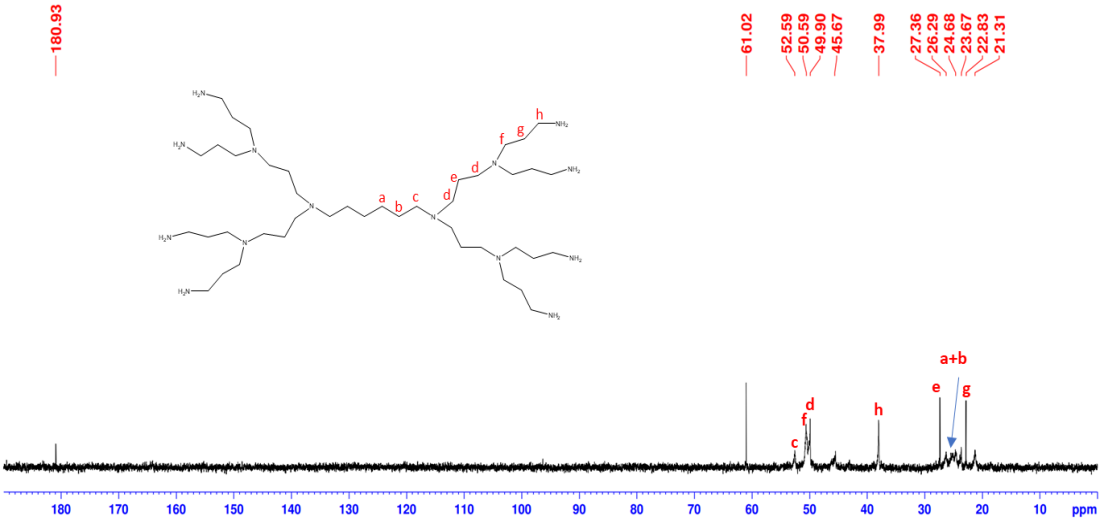

Figure 24- ^{13}C- NMR spectrum of $G1NH_2$ in D_2O.

Regarding $G2NH_2$, in the ^{1}H-NMR spectrum (figure 25) we predicted that the core signals would be observed at the beginning of the spectrum, at 1.30 ppm, 1.32 ppm, and between 2.67-2.73 ppm. The protons next to the amine group were displayed as a singlet at 1.92 ppm. The protons near the amine group appeared as a triplet around 3.03-2.98 ppm. The other protons could not be that easily identified, but we supposed they appeared around 1.40 ppm, 1.80 ppm, and 2.60 ppm. For the ^{13}C-NMR spectrum (figure 26), the carbons of the core continued to be seen at approximately 23.50 ppm and 58.12 ppm. The carbons near to amine group were shown at 37.65 ppm. The carbons of the branches were displayed at the expected values, at 22.86 ppm and between 50.50 ppm and 49.61 ppm.

The NMR spectrums of the other batches (see annex figures A21, A22, A23, and A24) presented the same signals mentioned previously.

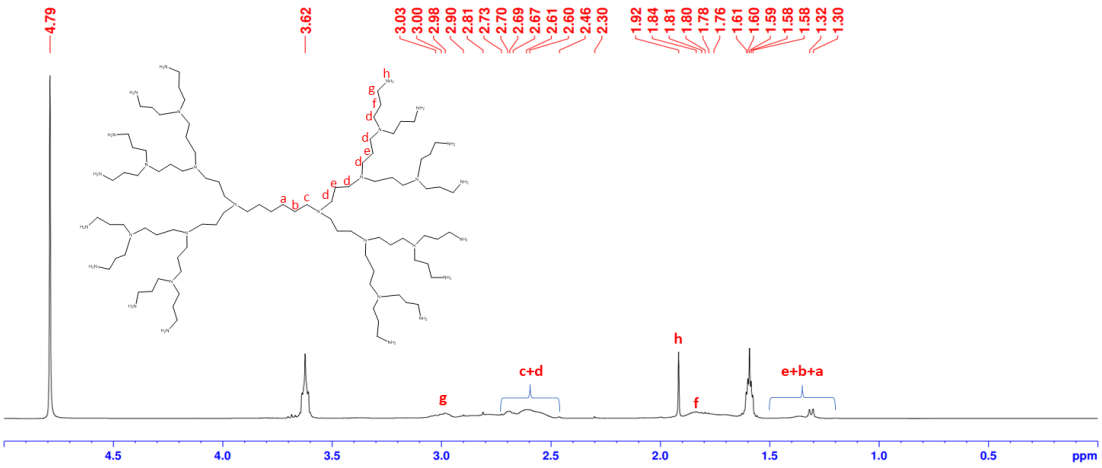

Figure 25- ^{1}H- NMR spectrum of $G2NH_2$ in D_2O.

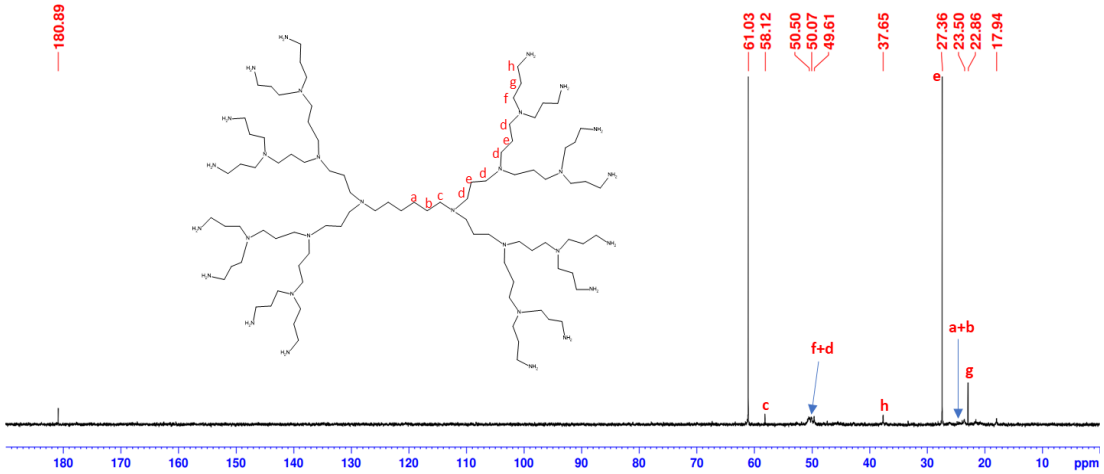

Figure 26- ^{13}C-NMR spectrum of $G2NH_2$ in D_2O.

Only two signals are clearly identified in the $G3NH_2$ ^{1}H-NMR spectrum (figure 27). The protons of the amine group continued to appear at 1.92 ppm. The terminal branches' protons, which are supposed to appear as a quintet, surge around 1.80 and 1.68 ppm. In the ^{13}C-NMR spectrum (figure 28), the carbons of the core are displayed at 24.79 ppm and 58.14 ppm. The carbons near to amine group showed at 38.11 ppm. The rest of the carbon signals surged at 21.57 ppm, 46.21 ppm, and 50.75 ppm.

In the second batch, the ^{1}H- and ^{13}C-NMR spectrums were very similar, with the signals within the expected (see annex figures A25 and A26).

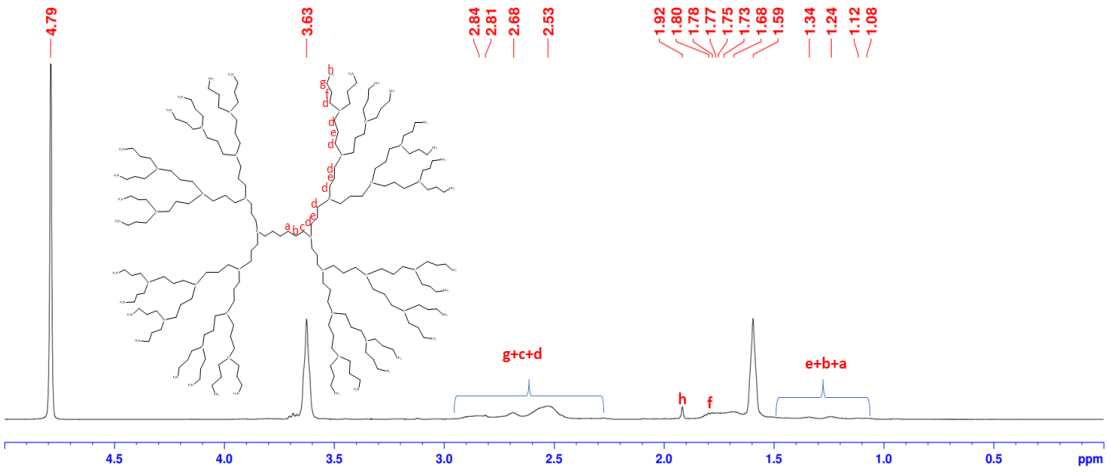

Figure 27- ^{1}H- NMR spectrum of $G3NH_2$ in D_2O.

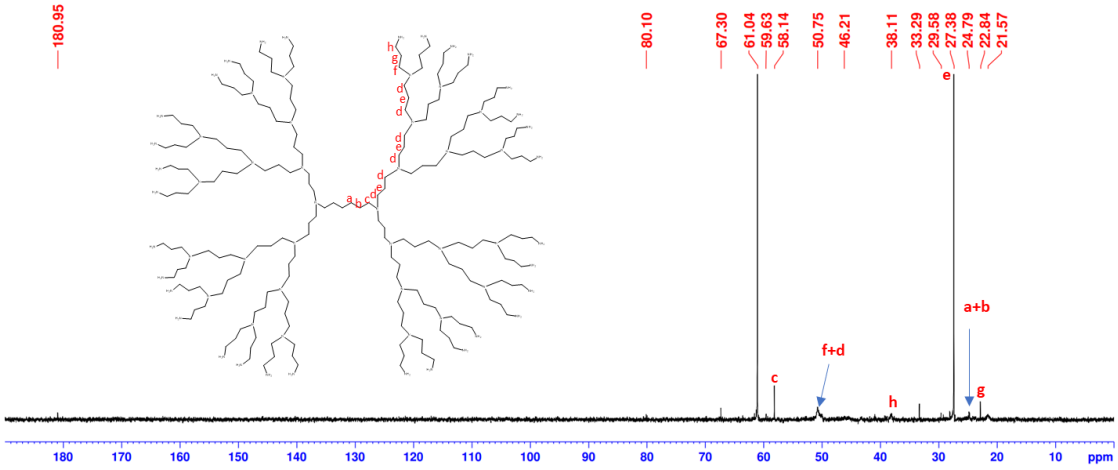

Figure 28- ^{13}C- NMR spectrum of $G3NH_2$ in D_2O.

10.3 Synthesis and characterization of the carboxylate dendrimers

The G1 to G3 were synthesized as described in the experimental section. In the synthesis of G4C, the second reaction step was prolonged to 72h. This reaction time extension is because we have more groups to react, so more time is required with the generation increase.

The addition of the terminal methyl ester groups occurred through a Michael-type addition,[295] and when the solution of NaOH was added, the methyl groups were left with the hydroxyl as methanol.

The yield obtained for G1, G2, G3 and G4 of carboxylate dendrimers was 94%, 93%, 65%, and 50 %, respectively. In line with what was previously reported (yields of 98% and 87% for the G1, 96% and 60% for the G2, and 95% and 47% for the

G3).[280,296] With the increase of generations, the yield naturally decreases because we have more groups for reacting, and some steric effects can occur, making it difficult to add new terminal groups.

In the synthesis of G1C, after the addition of methyl acrylate, the obtained product, G1 methyl ester dendrimer ($G1CO_2Me$), was characterized by ^{1}H- and ^{13}C-NMR to see if the addition reaction occurred. In the ^{1}H-NMR spectrum of the compound $G1CO_2Me$ (figure 29), the singlet at 3.64 ppm corresponds to the protons of methyl group, confirming the compound synthesis. The presence of the methyl ester groups is relevant since they are the precursors for the synthesis of carboxylate dendrimers. In the ^{13}C- NMR spectrum (figure 30), the main signal is at 172.55 ppm, corresponding to the carbon of the terminal group.[280,297]

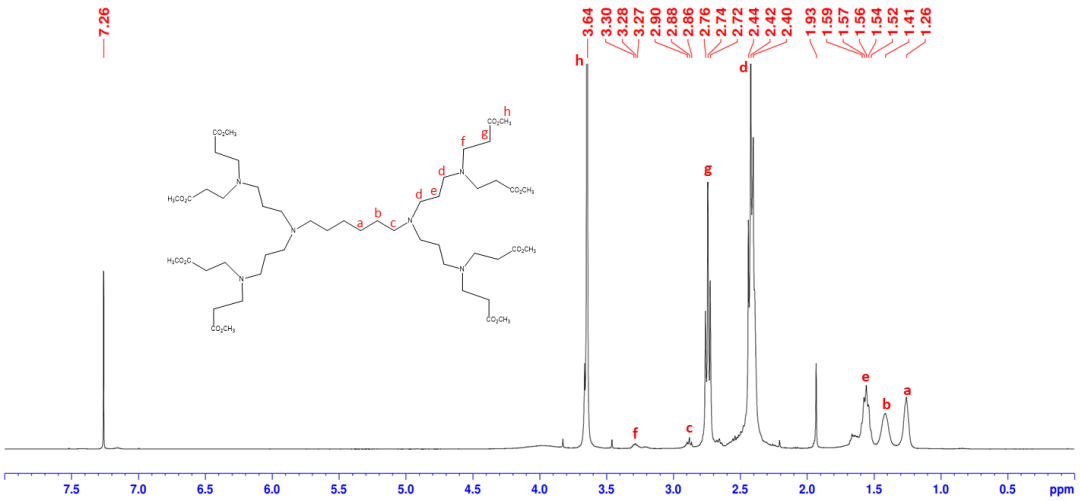

Figure 29- ^{1}H-NMR spectrum of $G1CO_2Me$ in $CDCl_3$.

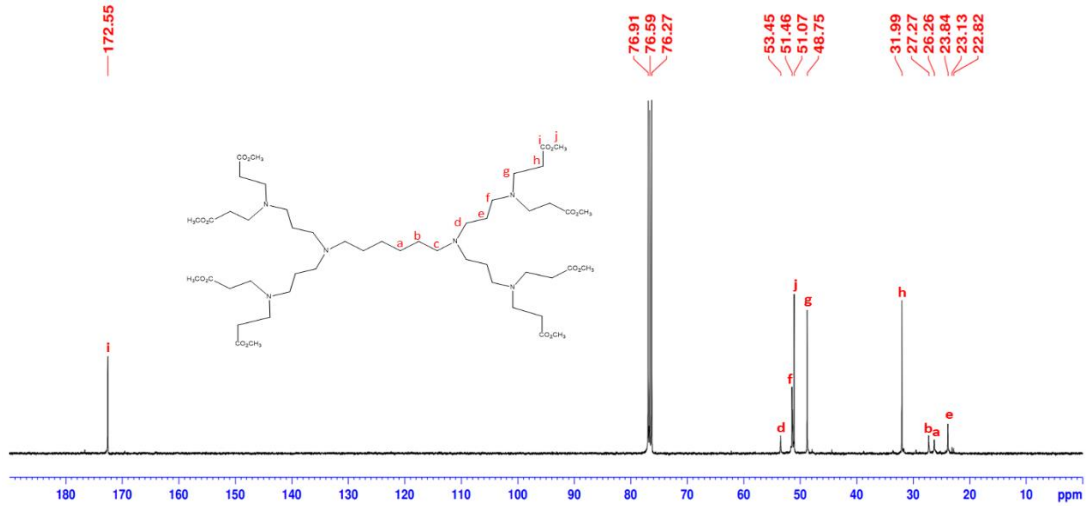

Figure 30- ^{13}C-NMR spectrum of $G1CO_2Me$ in $CDCl_3$.

In the final reaction, we obtained the G1C that was characterized by ^{1}H- ^{13}C-NMR. The absence of the signal of the methyl group protons in the ^{1}H- NMR (figure 31), indicated that the functionalization of the terminal groups happened. The protons beside the carboxylate group appeared as a triplet at 2.86-2.82 ppm. The core protons continued to appear at 1.34 ppm, 1.55 ppm, and 2.97-2.94 ppm. The remaining signals at 1.78-1.77 ppm, 2.41-2.37 ppm and 3.69- 3.66 ppm correspond to the branches' protons. Concerning the ^{13}C- NMR (figure 32), the signal of the carbon of the terminal group appeared at 180.4 ppm. The carbons of the core were detected at 24.02 ppm and 25.85 ppm. The carbon of the core next to the amine should have appeared around 57 ppm. However, in some cases, the core signals can be covered up. The signal around 33.08 ppm corresponded to the carbon next to the terminal group. Finally, the carbon of the branches was displayed at 20.60 ppm, 49.63 ppm, 50.51 ppm, and 52.42 ppm.[280,296,297]

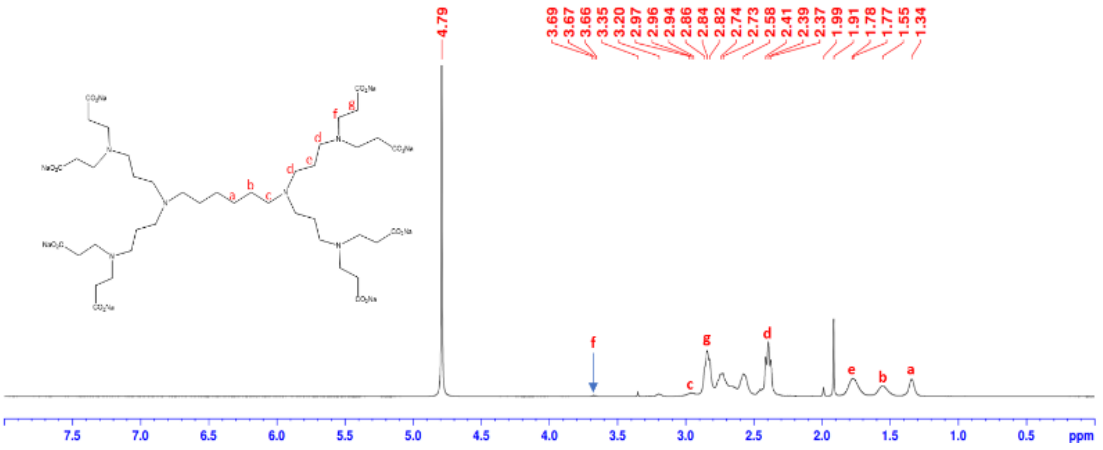

Figure 31- ^{1}H- NMR spectrum of G1C in D_2O.

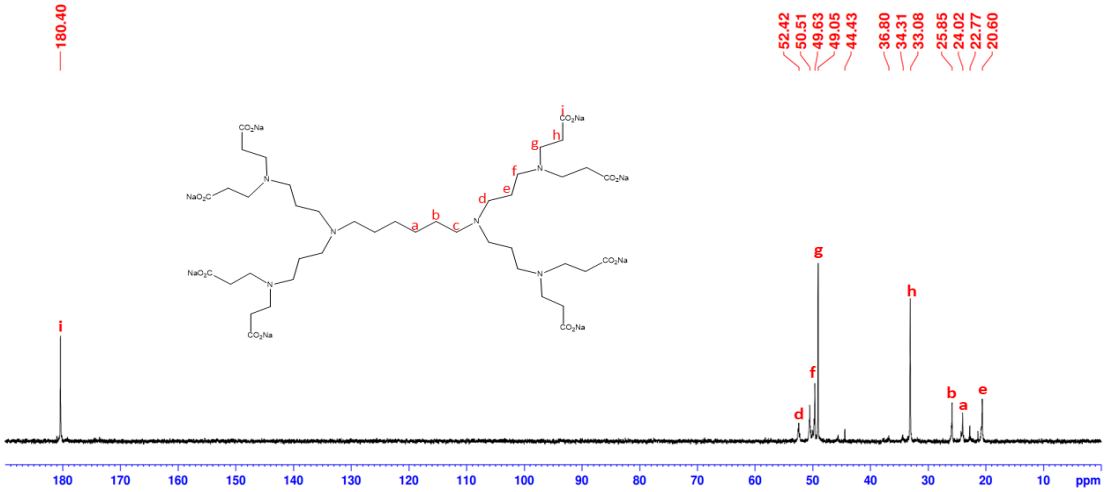

Figure 32- ^{13}C-NMR spectrum of G1C in D_2O.

The ^{1}H-NMR spectrum of G2C presented the expected signals (figure 32), including the protons next to the terminal group at 2.64 ppm and the core protons at 1.37 ppm, 1.61 ppm, and 2.95 ppm. The other signals corresponding to the branches' protons were displayed at 1.79 ppm, 2.45 ppm, and 3.70-3.69 ppm. In the ^{13}C- NMR spectrum (figure 34), the primary signal at 179.89 ppm indicated the existence of the terminal groups. The carbon next to the terminal group exhibited a signal at 32.74 ppm. The carbons of the core continued to appear at 24.21 ppm, 25.98 ppm, and 57.41 ppm. The signals of the branches appeared at 21.02 ppm, 49.27 ppm, 50.06 ppm, and 52.85 ppm.

So, with the presence of the signal corresponding to the carbon of the terminal group in the ^{13}C- NMR spectrum and, the absence of the signal relative to the methyl group in the ^{1}H-NMR spectrum (see annex figure A27), we can conclude that the final product was synthesized successfully.

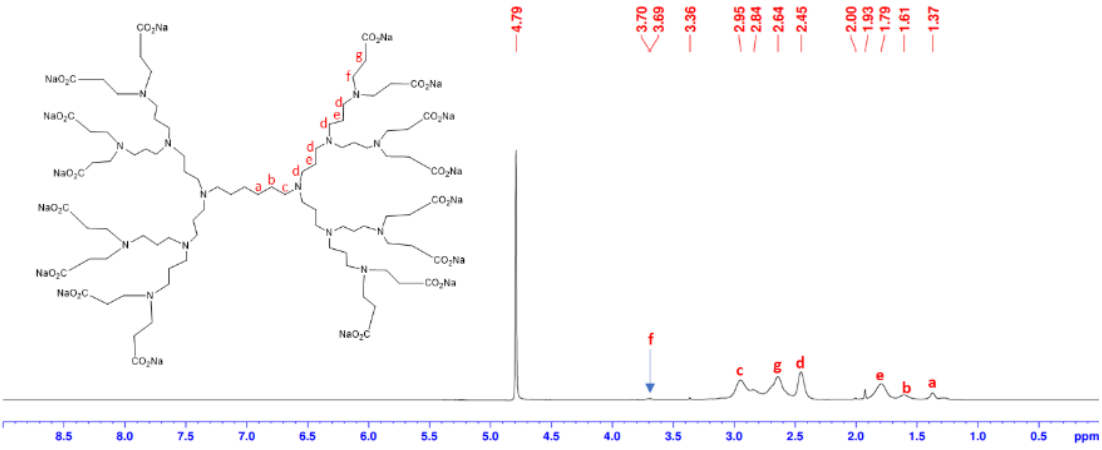

Figure 33- ^{1}H- NMR spectrum of G2C in D_2O.

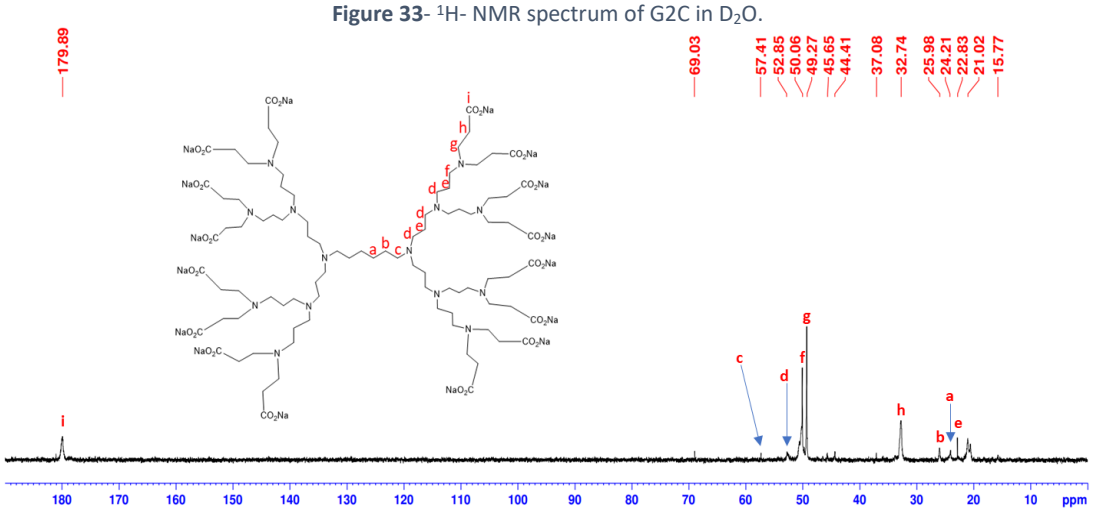

Figure 34- ^{13}C- NMR spectrum of G2C in D_2O.

Relatively to the G3C, the absence of the signal at 3.64 ppm in the ^{1}H-NMR spectrum (see figure 35 and annex figure A28) indicates that functionalization has occurred. Moreover, the protons of the core appeared at 1.36 ppm, 1.60 ppm, and as a triplet at 3.68-3.65 ppm. The remaining signals corresponding to the branches' protons, which appeared at 1.81 ppm, 2.46-2.45 ppm, 2.63 ppm, and 3.68-3.65 ppm. Relatively to the ^{13}C-NMR spectrum (figure 36), the presence of the signal at 179.83 ppm suggested the presence of the terminal groups. The carbon next to the terminal group was displayed at 32.47 ppm. The core's carbon signals appeared around 20 ppm, 22 ppm, and at 57.31 ppm. Finally, the signals at 49.35 ppm, 50.02 ppm and 52.71 ppm corresponded to the carbons of the branches.

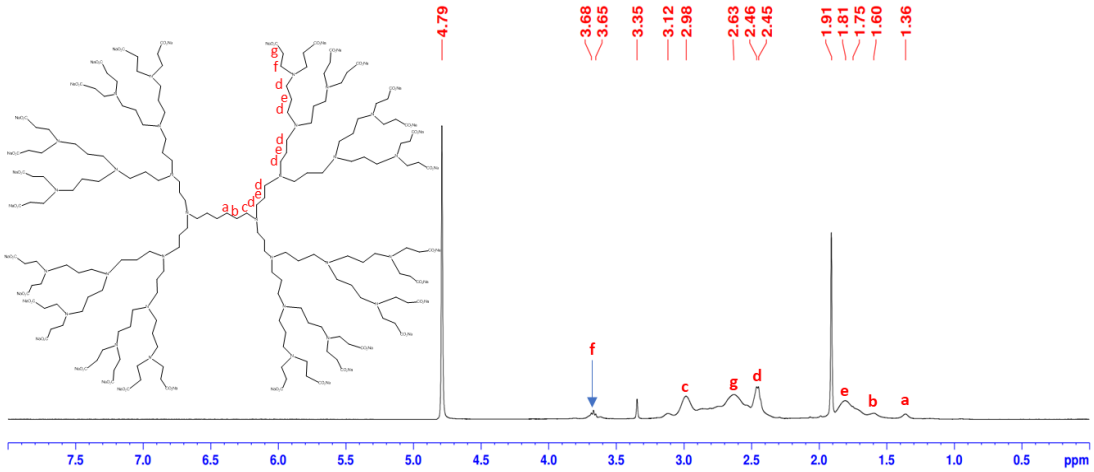

Figure 35- ^{1}H- NMR- spectrum of G3C in D_2O.

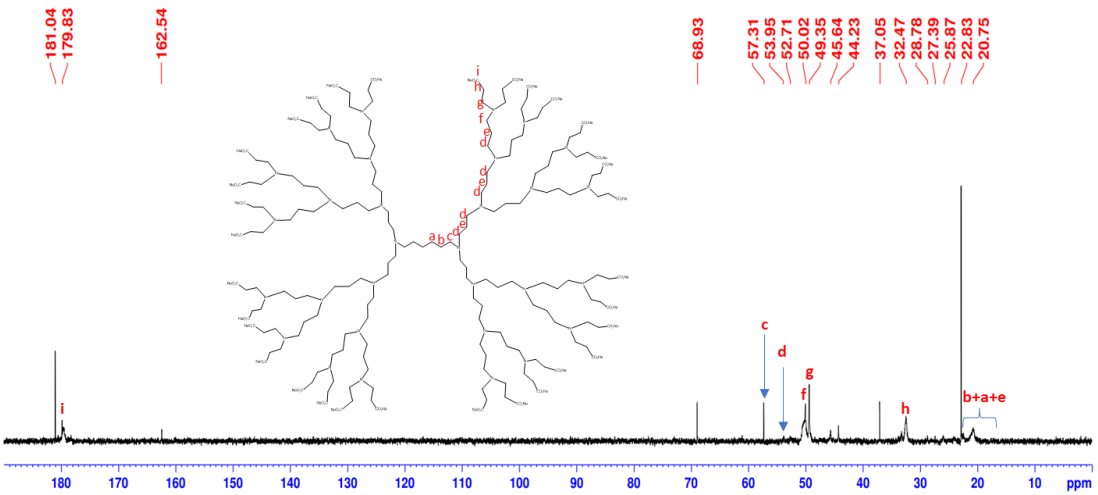

Figure 36- ^{13}C- NMR spectrum of G3C in D_2O.

The signals in the G4C dendrimer ^{1}H-NMR spectrum (figure 37) were not well discriminated. Also, the two signals at 3.60 ppm and 3.66 ppm suggest that some methyl groups could be in the structure (see figure 38 and annex figure A29). The protons next to the terminal group appeared around 2.67 ppm. The protons of the core should have appeared in the initial part of the spectrum around 3.00 ppm. The remaining signals identified corresponded to the protons of the branches. In the ^{13}C-NMR spectrum (figure 38), the signal of the carbon to the terminal group should have been at 181.09 ppm. The carbon next to the terminal group appeared at 33.57 ppm. The core signals have appeared to around 27.98 ppm and at 57.35 ppm. The carbons of the branches appeared at 14.25 ppm, 50.18 ppm, 50.63 ppm, and 52.68 ppm.

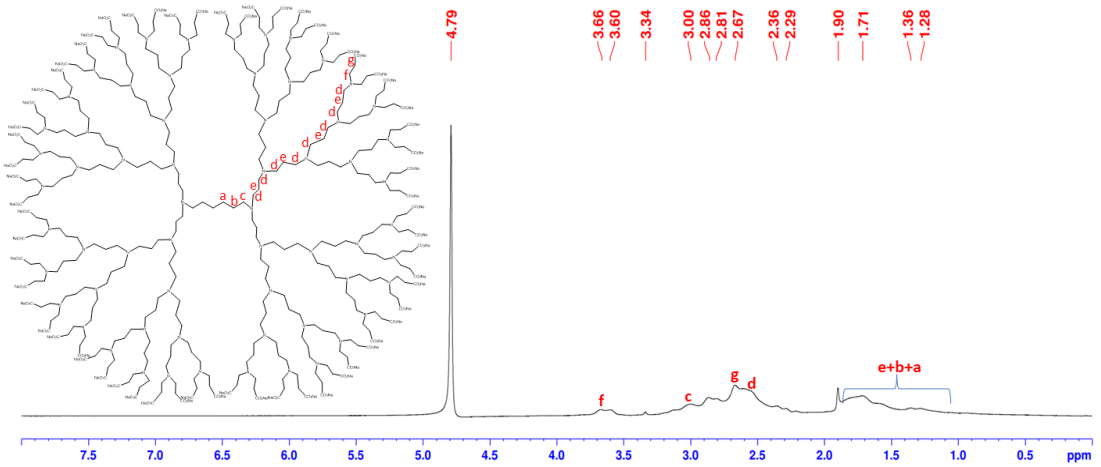

Figure 37- ^{1}H- NMR spectrum of G4C in D_2O.

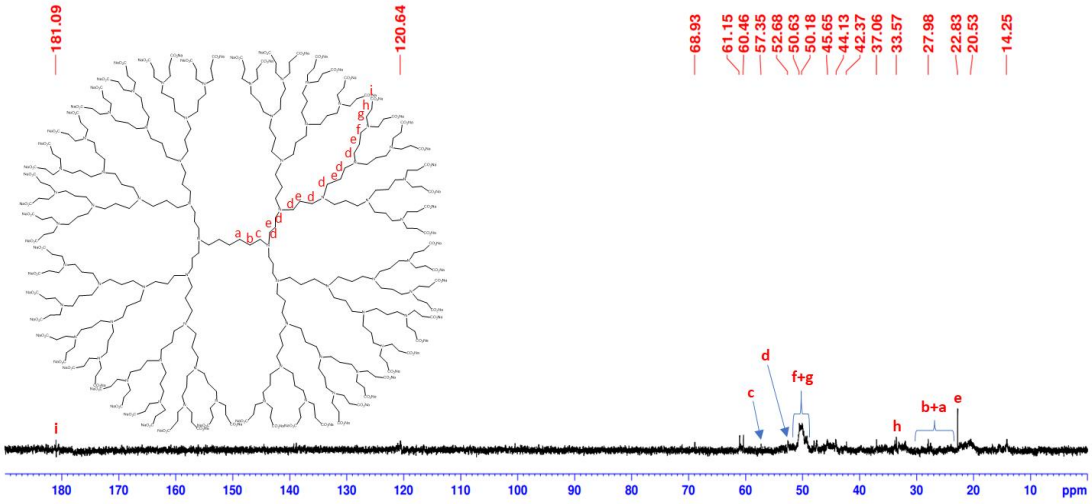

Figure 38- ^{13}C- NMR spectrum of G4C in D_2O.

The ATR-FTIR analyses were done to complement the characterization obtained by the NMR. This technique provided information about the chemical transformations that occurred in the terminal groups of dendrimers. The spectrums of carboxylate dendrimers presented the expected characteristics bands (figure 39 and table 3). The stretch bands of O-H group were observed at 2933.1 cm^{-1}, 2939.8 cm^{-1}, 2945.1 cm^{-1}, and 2944.3 cm^{-1}, for the G1C, G2C, G3C, and G4C dendrimers respectively. In the G3C and G4C dendrimers, the bands at 1721.2 cm^{-1} and 1725.7 cm^{-1}, respectively, corresponded to the stretch of the C=O group. In the lower generations, this band was not observed. Also, the C-O stretch band was identified in all spectra at 1395.5 cm^{-1}, 1396.5 cm^{-1}, 1398.7 $cm^{-1,}$ and 1397.7 cm^{-1}, for the G1C, G2C, G3C, and G4C dendrimers, respectively.[296,297]

Table 3- Main characteristic bands for each functional group of the G1C, G2C, G3C, and G4C, obtained by ATR-FTIR.

Functional group	band (cm^{-1})				Type of vibration
	G1C	G2C	G3C	G4C	
O-H	2933.1	2939.8	2945.1	2944.3	str
C=O	---	---	1721.2	1725.7	str
C-O	1394.5	1396.5	1398.7	1397.7	str

* Str: stretch

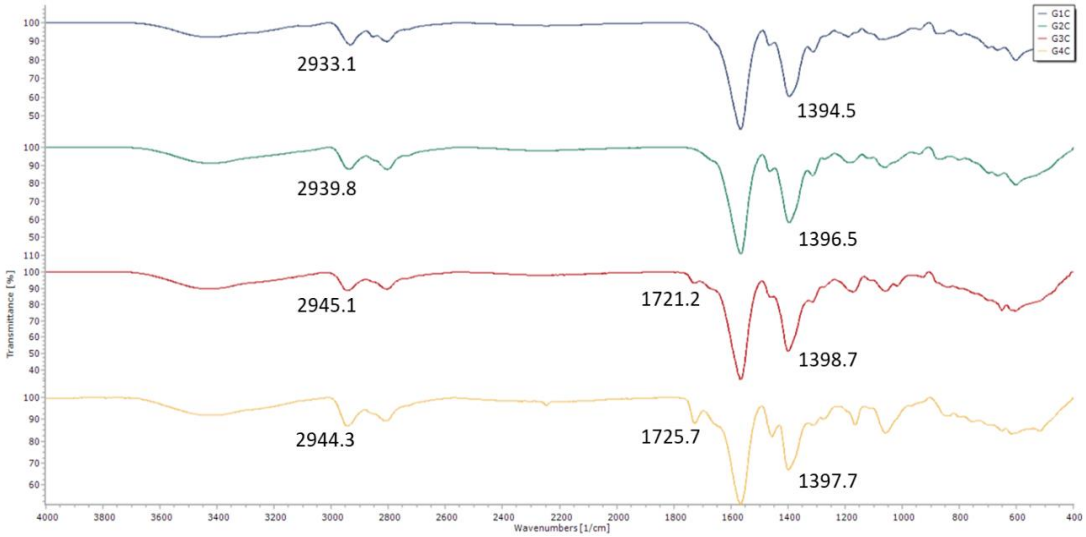

Figure 39- ATR-FTIR spectra of G1C, G2C, G3C and G4C, respectively.

TOF-MS (ESI) analyses were performed to confirm the carboxylate dendrimers' synthesis (table 4), detect some structural defects, and determine

molecular weights. Only for G1 and G2 the analysis were performed because in the highest generations (G3C and G4C), under the experimental conditions used, no peak was found. When the sample was ionized, fragmentation of the structure occurred in most cases because they are large molecules. So, in the G1C, a peak at m/z=727.17 [M- $C_9H_{14}NNa_2O_4$ – 6 Na +1H]$^{5-}$ was found, corresponding to the structure without one branch (figure 40). Since they are counter-ion, Na^+ was not detected, so they are not directly linked to the dendrimer's structure.

In G2C, only half of the structure was found at 985.31 [M- $C_{45}H_{74}N_7Na_8O_{16}$ - 8 Na + 2H]$^{6-}$ (figure 41), without the Na^+ ions.

Table 4- Molecular weight, m/z calculated, and m/z found in the MS spectra for the G1C and G2C (2,5- DHB dissolved in methanol was used as matrix).

	G1C	G2C
Molecular weight	1096.95	2306.08
M/z calculated	727. 85	985.16
M/z found	727.17 [M- $C_9H_{14}NNa_2O_4$ – 6 Na +1H]$^{5-}$	985.31 [M- $C_{45}H_{74}N_7Na_8O_{16}$ - 8 Na + 2H]$^{6-}$

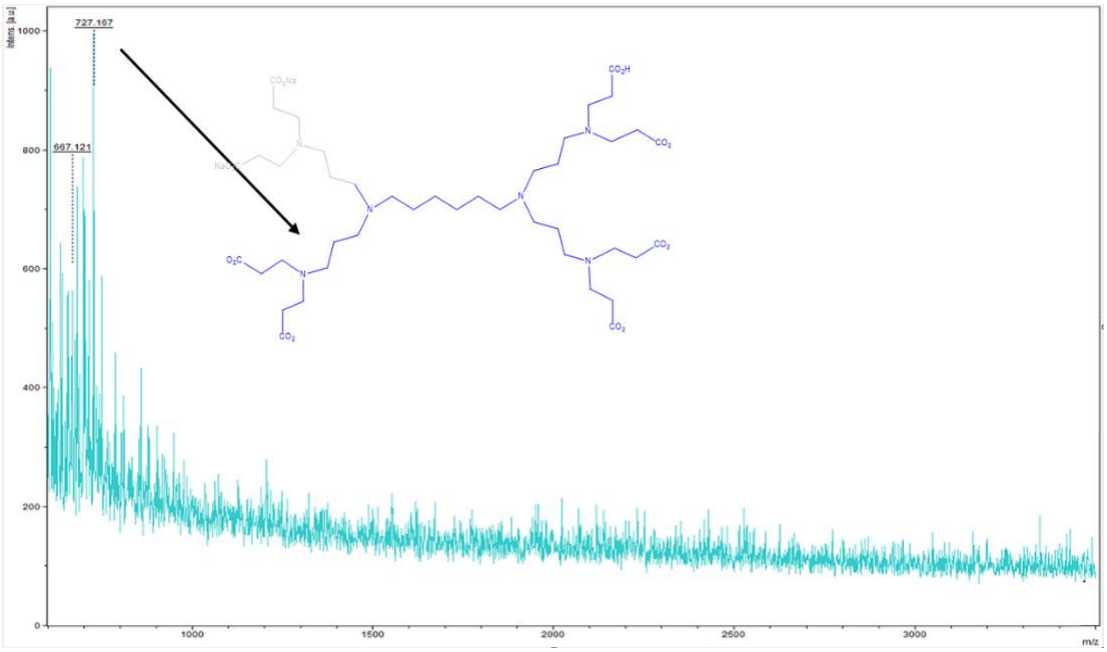

Figure 40- MS spectrum of G1C (matrix: 2,6- DHB dissolved in methanol).

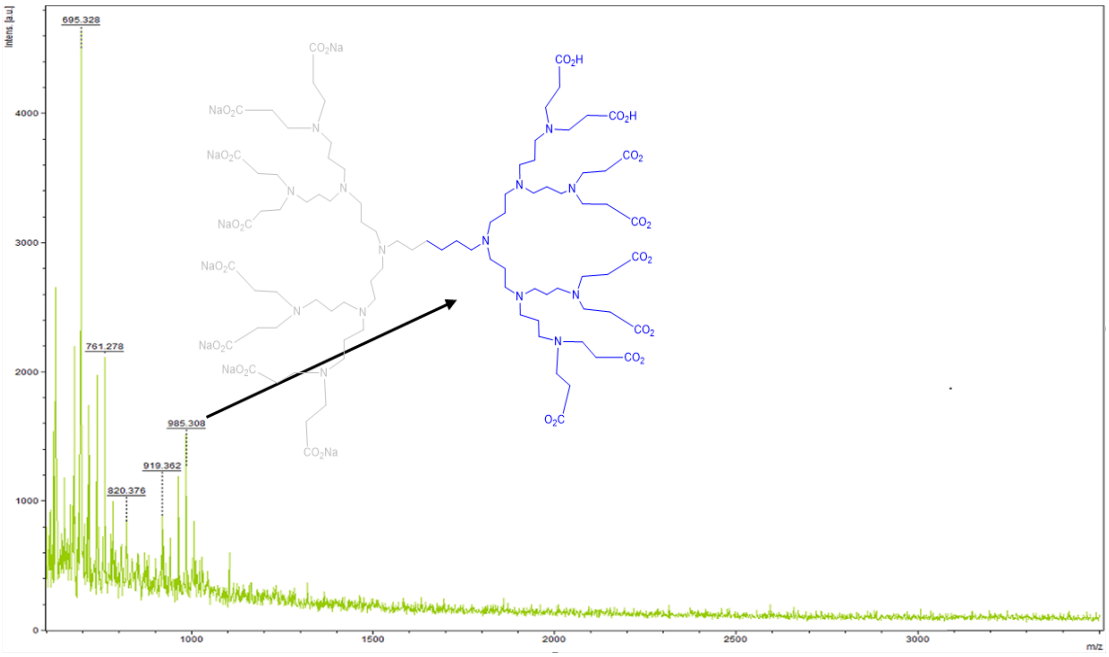

Figure 41- MS spectrum of the G2C (matrix: 2,5-DHB dissolved in methanol).

Zeta potential is usually employed to monitor the successful surface functionalization or modification of materials.[298] Also, the charge of the surface will provide information about the stability of the nanoparticles in solution since values greater than + 30 mV or less than -30 mV represent high degrees of stability. On the contrary, when the values are between +25 mV and -25 mV, the particles tend to agglomerate due to van der Walls, hydrophobic interactions, and hydrogen bonding.[298]

As expected, all the carboxylate dendrimers presented a negative surface charge (Table 5). So, from the experimental data, we can say that the G1C (-51.8 ± 0.6 mV) and G2C (-52.7 ± 0.8 mV) have good stability, and G3C (-32.4 ±2.5 mV) and G4C (-38.6 ±0.4 mV) have moderate stability in aqueous solutions.[298-300]

The terminal carboxylate groups were responsible for the anionic character of the dendrimers. Due to the negative surface charge, dendrimers are not attracted when they find a negative charge, like in the cell membrane. This will reduce toxicity and increase cytocompatibility without seriously compromising cellular uptake due to the different and alternative endocytosis mechanisms.[301,302]

Table 5- Zeta potential data of the carboxylate dendrimers. The data are expressed as the mean ± SD of three independent experiments.

	G1C	G2C	G3C	G4C
Zeta potential (mV)	-51.8 ± 0.6	-52.7 ± 0.8	-32.4 ±2.5	-38.6 ±0.4

Through the DLS technique, we obtained information about the size of our nanoparticles. The DLS measurement is the most versatile and useful set of techniques for measuring *in situ* sizes, size distributions, and, in some cases, the shapes of nanoparticles in liquids. This hydrodynamic technique can directly measure hydrodynamic quantities, usually translational and/or rotational diffusion coefficients, which are then related to sizes and shapes *via* theoretical relations.[303]

All samples were dissolved in a solution of NaCl and filtered. Before measurement, the samples were filtered to exclude lumps and large particles from the preparation, such as some particles aggregate.[300,304] This technique is a low-resolution method that often cannot separate closely related molecules.[304] So, a NaCl solution was used because the ions shielded the particles from interactions with others, reducing the aggregations of the dendrimers in the solution and giving us better results.[300]

The size of the nanoparticles should increase with the generation. Considering the hydrodynamic diameter, the size distribution of the G1C, G2C, and G3C are between 21-44 nm, 140-323 nm, and 2-9 nm, respectively (figure 42). According to the zeta potential analyses, G1C and G2C, presented good stability. Contrarily, G3C and G4C are less stable and, therefore, can agglomerate and deposit in the bottom of the cuvette, not allowing the light to hit the particles. In G4C, we could not obtain any results.

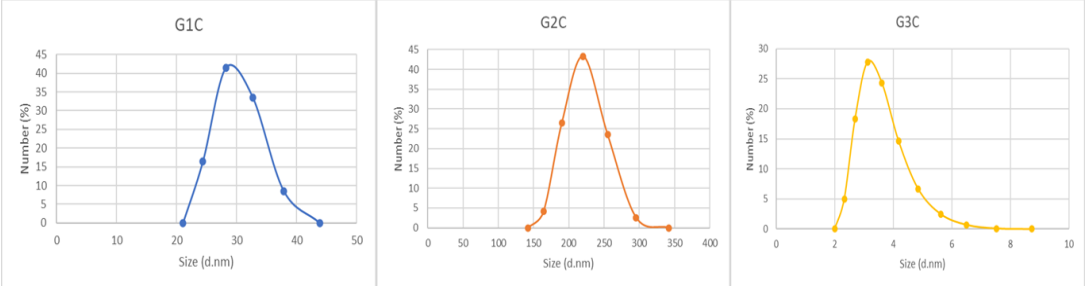

Figure 42- Size distribution of G1C, G2C, and G3C at a concentration of 0.5mg/mL in a solution of 100 µM NaCl.

In conclusion, we can affirm that G1C are in the nanoscale range and have the potential to be used as nanocarriers for achieving the EPR effect. Additional analyses are required to confirm these results and measure the size of the G4C.

Alternative techniques like TEM (transmission electron microscopy) and AFM (atomic force microscopy) could have been applied to determine the size.

Further, G1 to G4 carboxylate dendrimers were synthesized successfully, with yields within the expected. For the first time, G4C has been synthesized. As the generation increases, more time is necessary to purify the final product since it tends to have more impurities. Alternative techniques should be applied, beyond dialysis, to obtain the product more purified. The analytic techniques were applied to confirm the PPI dendrimer's functionalization and the reactions' success.

10.4 Synthesis and characterization of the sulfonate dendrimers

The synthesis of the sulfonate dendrimers was done as described in the experimental section. It was necessary to extend the reaction time due to the doubling of the terminal groups. Moreover, the sulfonate group was added through a Michael-type addition reaction.

The yields obtained for the G1, G2, G3, and G4 sulfonate dendrimers were 78%, 60%, 79% and 98%, respectively. These were related to the yields found in the literature of 90% and 37% for G1, 85% and 48% for G2, and 78% and 76% for G3.[280,296]

In the ^{1}H-NMR spectrum of the G1S (figure 43), the protons near the terminal group appeared as a triplet signal at 3.16-3.12 ppm. The signals of the core appeared at 1.38 ppm, 1.62 ppm, and 3.25-3.22 ppm. The protons of the branches were visible at 1.83 ppm, 2.61 ppm, and 3.01-2.97 ppm. In relation to the ^{13}C-NMR (figure 44), the carbon next to the terminal group was displayed at 46.67 ppm. The signals at 24.13 ppm, 26.01 ppm, and 56.51 ppm corresponded to the carbons of the core. The signals of the branches were displayed at 21.05 ppm, 46.67 ppm, 49.97 ppm, and 52.40 ppm.[280,296]

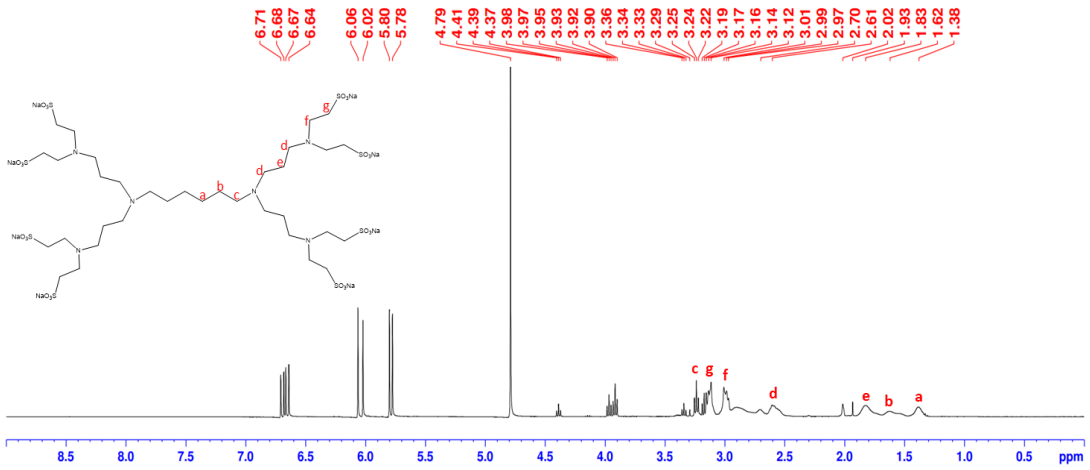

Figure 43- ^{1}H- NMR spectrum of G1S in D_2O.

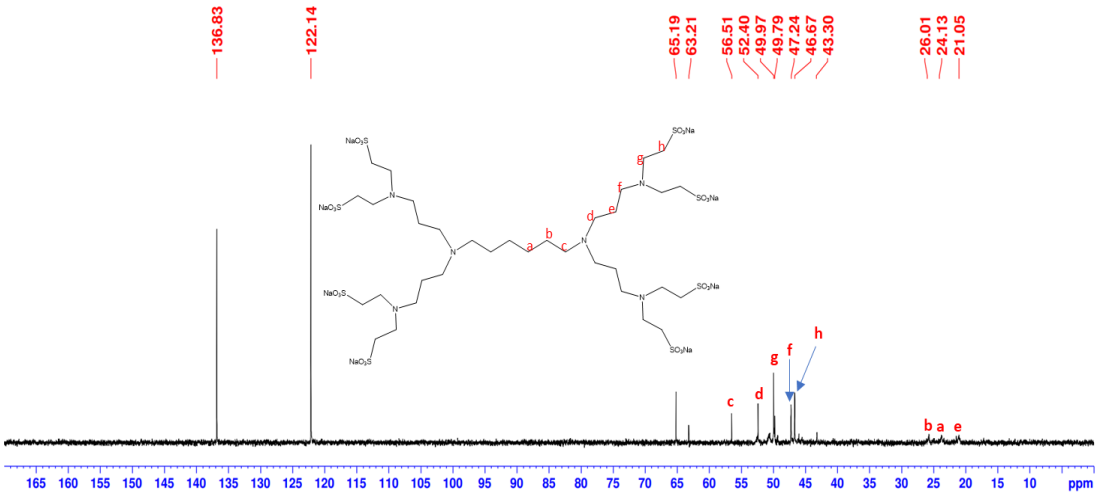

Figure 44- ^{13}C- NMR spectrum of G1S in D_2O.

G2S presented the expected signals. In the ^{1}H-NMR spectrum (figure 45) the signal at 3.16-3.11 ppm represented the protons next to the terminal group. The core signals continued to appear at 1.41 ppm, 1.74 ppm, and 3.24-3.21 ppm. The branch protons was shown at 1.92 ppm, 1.86 ppm, and 3.00-2.96 ppm. The ^{13}C-NMR spectrum (figure 46) showed a signal at 46.63 ppm corresponding to the carbon next to the terminal group. Regarding the carbons of the core, that belonging to the tertiary amine, were detected at 56.51 ppm while, the protons of the core expected between 20-25 ppm were not observed. The remaining signals corresponding to the branches' carbon were visible at 21.74 ppm, 47.23 ppm, 49.97 ppm, and 52.39 ppm.

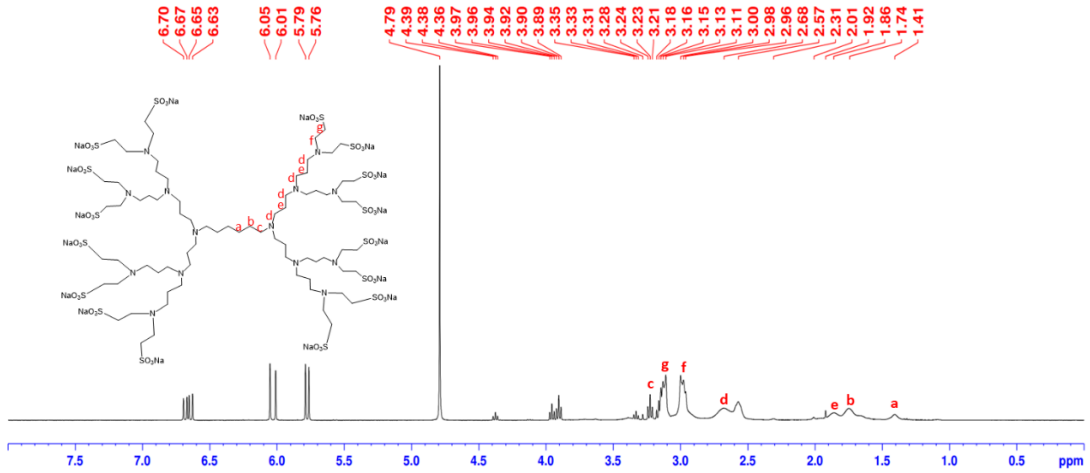

Figure 45- ^{1}H- NMR spectrum of G2S in D_2O.

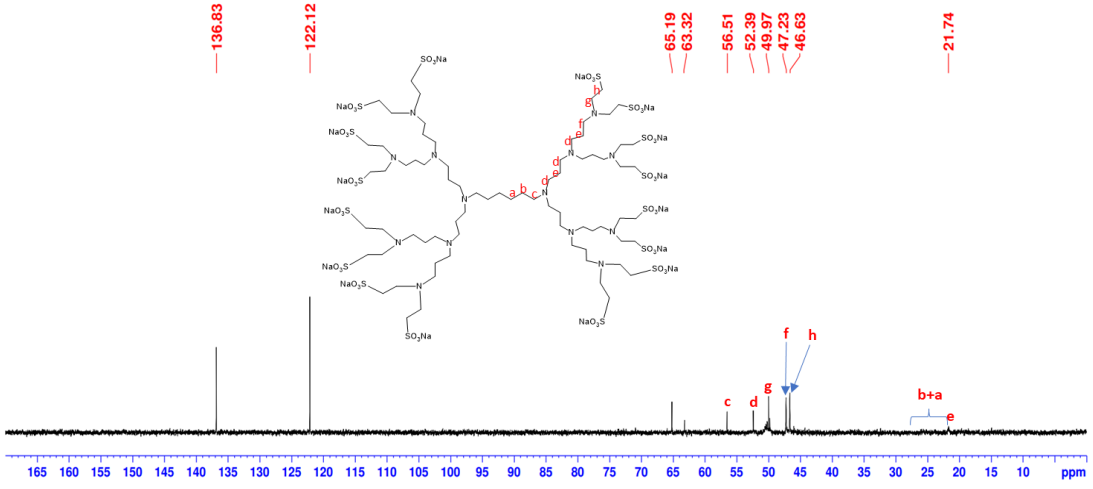

Figure 46- ^{13}C- NMR spectrum of G2S in D_2O.

The ^{1}H-NMR characterization presented the expected signals for G3S (figure 47). The signal at 3.18-3.17 ppm corresponded to the protons next to the sulfonate group. At the same time, the core signals appeared in the upper field, around 1.95 ppm, and as a triplet at 3.37-3.34 ppm. The protons of the branches were visible at 1.97 ppm, 2.70 ppm, and 3.04 ppm. In the ^{13}C-NMR spectrum (figure 48), the signal at 46.67 was from the carbon next to the terminal group. The core signals appeared at 20.34 ppm, 22.97 ppm, and 56.51 ppm. The remaining signals corresponded to the carbons of the branches, precisely at 16.19 ppm, 47.23 ppm, 49.96 ppm, and 52.39 ppm.

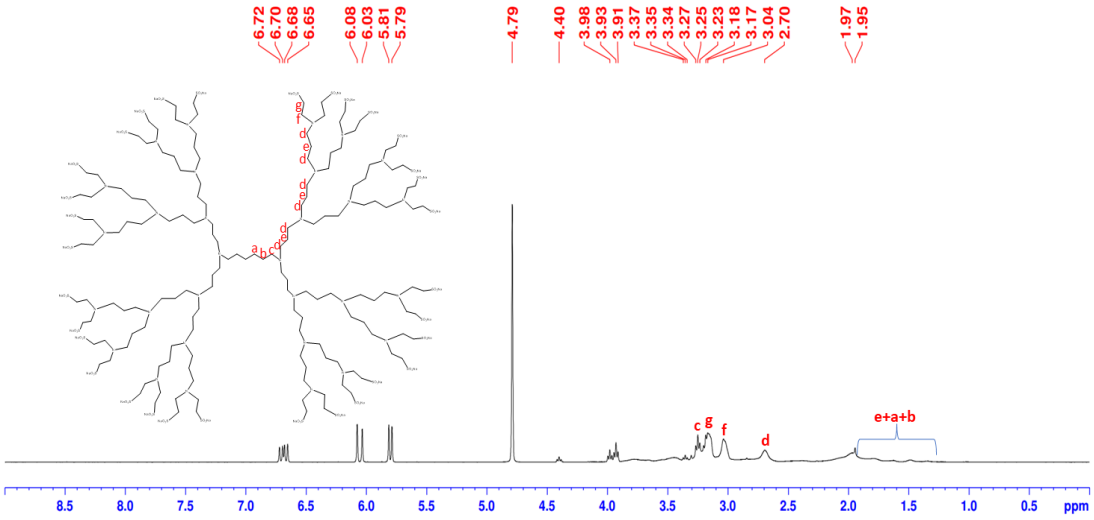

Figure 47- ^{1}H- NMR spectrum of G3S in D_2O.

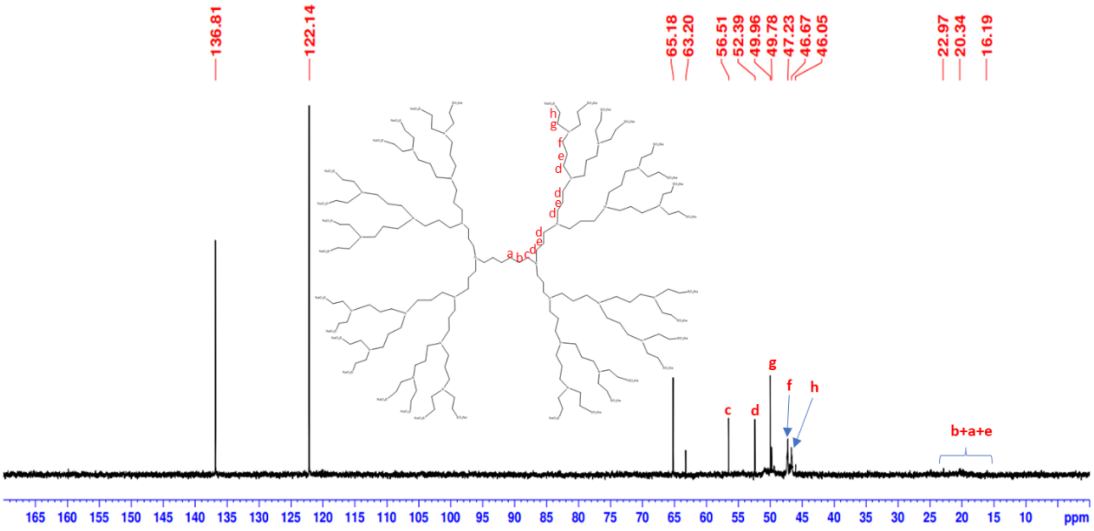

Figure 48- ^{13}C- NMR spectrum of G3S in D_2O.

The last generation synthesized, the G4S dendrimer, was also characterized by ^{1}H- and ^{13}C- NMR. The ^{1}H -NMR spectrum (figure 49) presented the expected signals at 3.15-3.11 ppm, that corresponded to the protons next to the terminal groups. Further, the protons of the core were displayed at 1.57 ppm, 1.73 ppm, and 3.22-3.18 ppm. The signals of the branches appeared at 1.90 ppm, 2.63 ppm, and 2.98 ppm. The ^{13}C-NMR spectrum (figure 50) showed a signal at 46.58 ppm that corresponded to the carbon next to the sulfonate group. The core signals should have appeared in the upper field of the spectrum. The carbons of the branches were shown at 47.19 ppm, 49.90 ppm and 52.33 ppm.

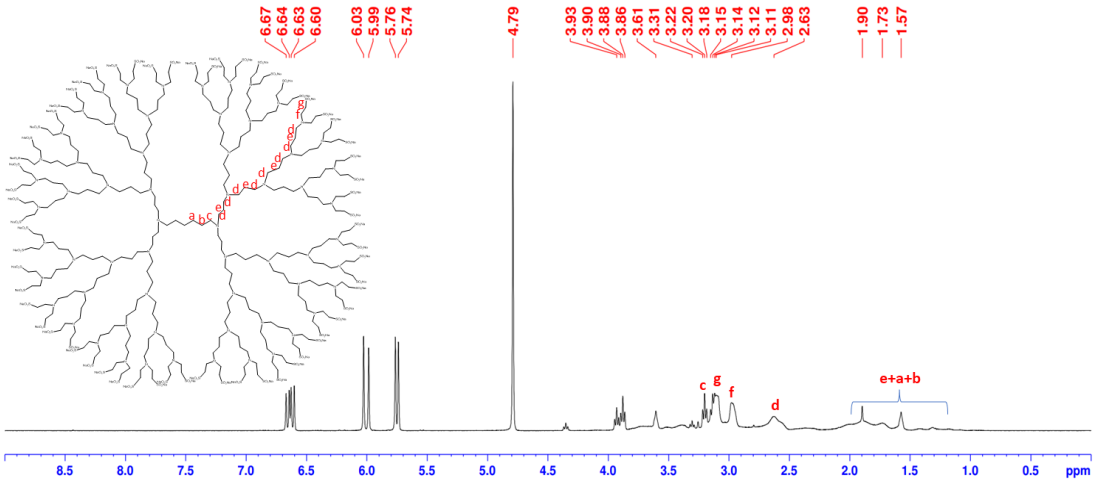

Figure 49- ^{1}H- NMR spectrum of G4S in D_2O.

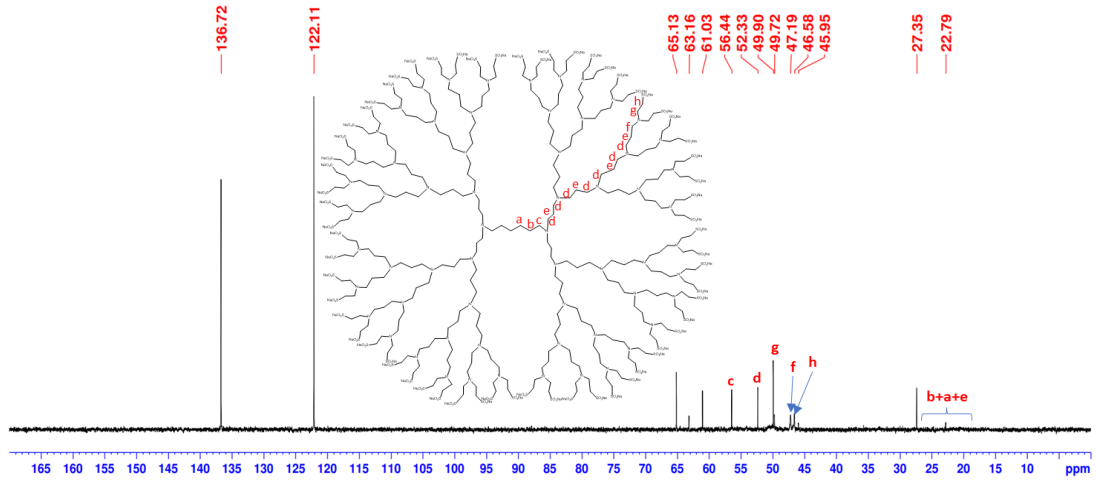

Figure 50- ^{13}C- NMR spectrum of G4S in D_2O.

In the case of the sulfonate dendrimers, NMR did not provide any information about if the functionalization was done. It was supposed that the addition reaction occurred since the signal of the protons to the amine group disappeared in the ^{1}H-NMR spectrum. So, to confirm the functionalization, we performed an ATR-FTIR analysis of the prepared compounds.

According to the ATR-FTIR analysis (figure 51 and table 6), the stretching vibrations characteristic of the sulfonate group (S=O) were detected at 1044 cm^{-1}, 1042.2 cm^{-1}, 1039.4 cm^{-1}, and 1041.6 cm^{-1}, for the G1, G2, G3, and G4 sulfonate dendrimers, respectively. The bands at 1175.5 cm^{-1}, 1176.5 cm^{-1}, 1171.4 cm^{-1}, and 1175.5 cm^{-1}, for the G1, G2, G3, and G4 sulfonate dendrimers, respectively, corresponding to the stretching vibrations of the group S-O.[296]

Table 6- Main characteristic bands for each functional group of the G1S, G2S, G3S, and G4S, obtained by ATR-FTIR

Functional group	band (cm^{-1})				Type of vibration
	G1S	G2S	G3S	G4S	
S=O	1044	1042.2	1039.4	1041.6	str
S-0	1175.5	1176.5	1171.4	1175.5	str

* Str: stretch

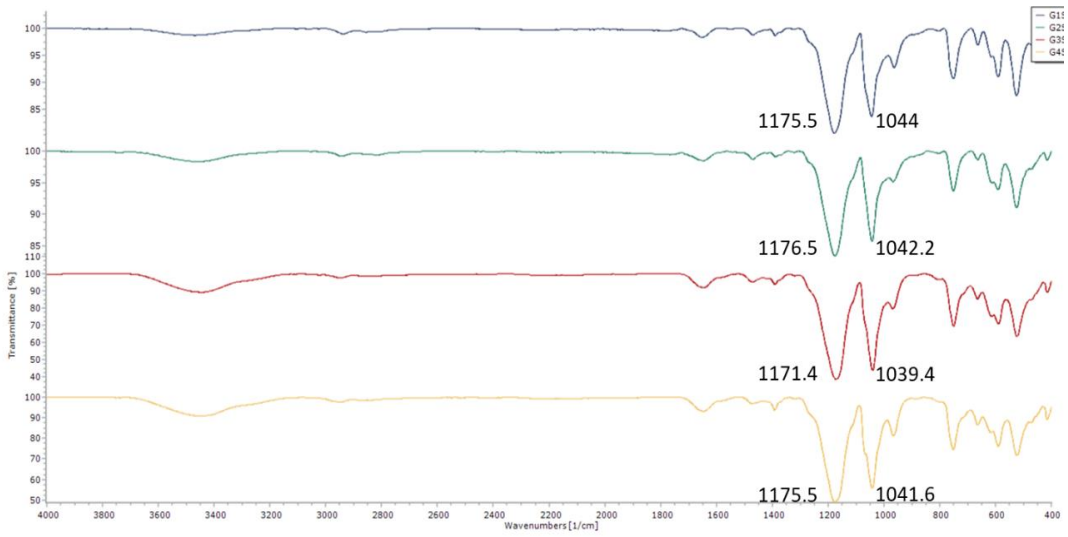

Figure 51- ATR-FTIR spectra of the G1S, G2S, G3S, and G4S, respectively.

The TOF-MS (ESI) analyses (table 7) of the G1S dendrimer presented a peak at m/z= 971.36 $[M- C_5H_{10}NNa_2O_6S_2 – 6\ Na]^{6-}$ that corresponded to the molecule without one terminal branch and Na^+ ions (figure 52). In the G2S dendrimer, a peak at m/z= 2190.62 $[M- C_{17}H_{34}N_3Na_4O_{12}S_4]$ was found and identified as a molecule without a complete branch (figure 53).

Table 7- Molecular weight, m/z calculated, and m/z found in the MS spectra for the G1S and G2S (2,5- DHB dissolved in methanol was used as matrix).

	G1S	**G2S**
Molecular weight	1385.33	2882.84
M/z calculated	971.19	2190.18
M/z found	971.36 $[M- C_5H_{10}NNa_2O_6S_2 – 6\ Na]^{6-}$	2190.62 $[M- C_{17}H_{34}N_3Na_4O_{12}S_4]$

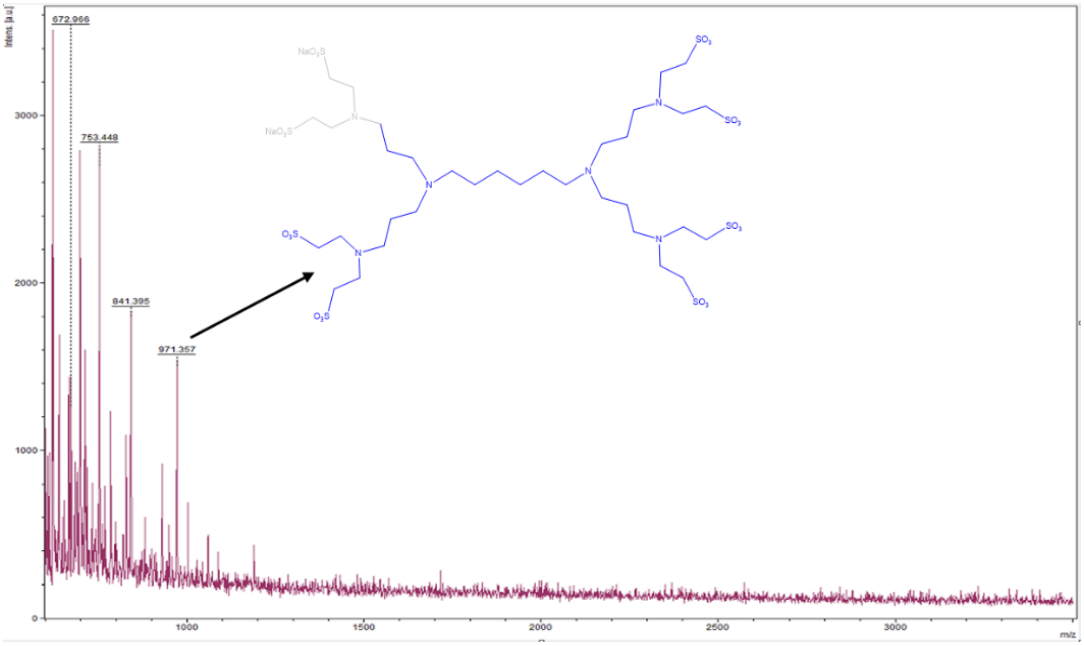

Figure 52- MS spectrum of G1S (matrix: 2,5-DHB dissolved in methanol)

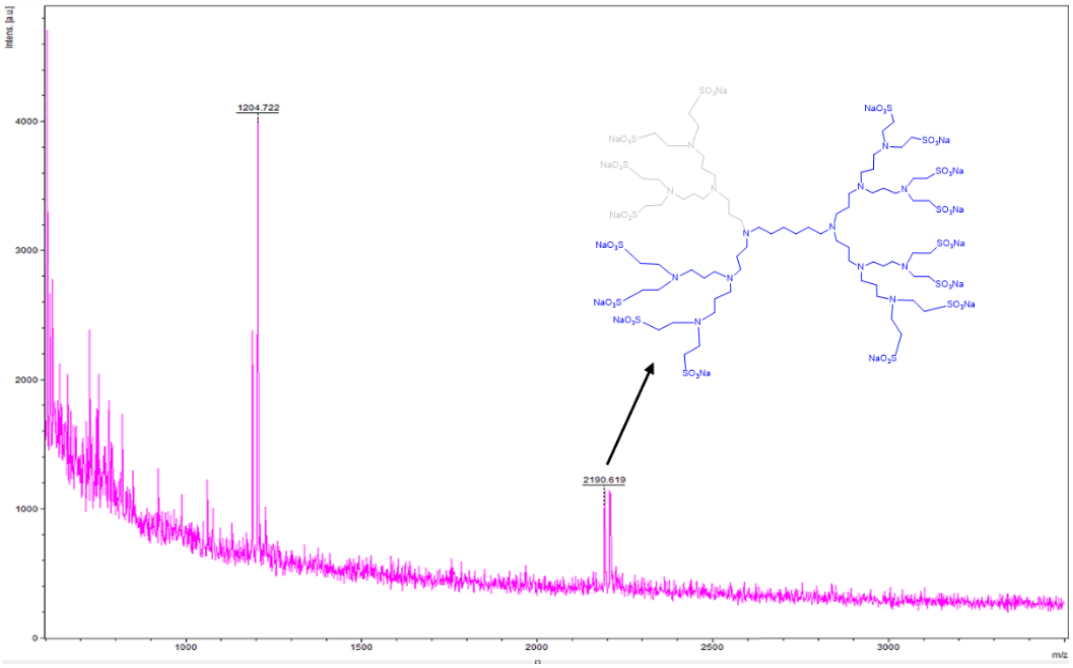

Figure 53- MS spectrum of G2S (matrix: 2,5-DHB dissolved in methanol)

The zeta size analyses showed that all sulfonate dendrimers have a negative surface charge, confirming the functionalization of the terminal groups (table 8). The anionic behaviour will be important for the interaction with the negative membranes.[301,302] Regarding the stability, based only on the zeta potential, we can conclude that, except for G4S which might agglomerate with time, all the sulfonate dendrimers present moderate to good stability in solution.[298-230] We can also say that

compared with carboxylate dendrimers, the zeta potential presents the same trend - a decrease in the zeta potential with the generation, with the sulfonate dendrimers presenting lower zeta potentials but similar stabilities in solution.

Table 8- Zeta potential data of the sulfonate dendrimers. The data are expressed as the mean ± SD of three independent experiments.

	G1S	G2S	G3S	G4S
Zeta potential (mV)	-46.5 ± 1.6	-30.3 ± 0.8	-40.6 ±2.2	-27.0 ±1.6

Relatively to the DLS analyses, as observed in the case of carboxylate dendrimers, the results are difficult to analyse, since they are inconsistent. The hydrodynamic diameter should have increased with the generation, but this only happened separately from generations 1 and 2, and from generations 3 and 4. The last and higher generation is within the limit of equipment detections (figure 54). G1S, G2S, G3S, and G4S presented a hydrodynamic diameter between 11-28 nm, 21-50 nm, 2-8 nm, and 3-11 nm, respectively. Practical issues related to handling the samples, such as filtration, could partly explain the observed behavior. Nevertheless, only TEM and AFM could provide more accurate information about the size of the prepared dendrimers.

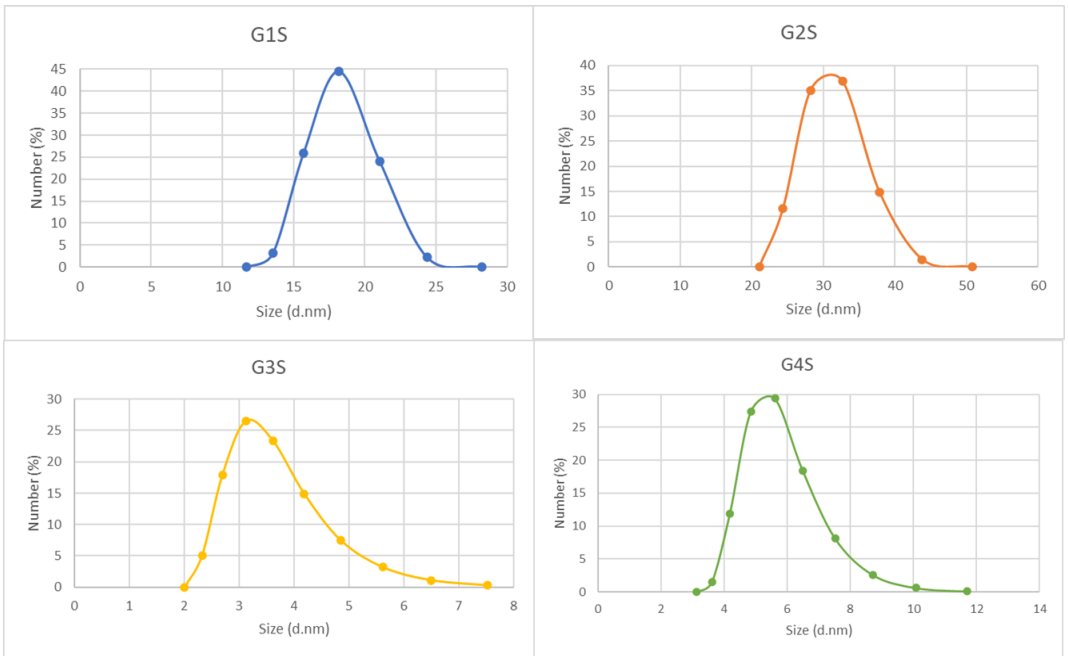

Figure 54- Size distribution of G1S, G2S, G3S, and G4S at a concentration of 0.5mg/mL in a solution of 100 µM NaCl.

However, the sizes of G1S and G2S dendrimers allow potential application in cancer therapeutics since they permit achieving the EPR effect in a nanoscale range of 10-100nm.

In conclusion, the sulfonate dendrimers were synthesized successfully with yields within the expected. For the first time, the G4S have been synthesized. All the final products continued to present residues of the reagent, sodium vinyl sulfonate but did not interfere with the following reactions steps. Based on the information provided by NMR and ATR-FTIR, we can conclude that the sulfonate group was linked with the dendrimers, and the structure was preserved.

10.5 Drug encapsulation of Hydroxychloroquine sulfate (sHCQ)

After all PPI sulfonate and carboxylate dendrimers were characterized, both dendrimers' encapsulation of sHCQ was tested with G1 to G3. The most promising dendrimer generation (G4) was not tested for encapsulation due to a lack of time.

The results of the encapsulation efficiency (EE) and the loading capacity (LC) are presented in the figures below. The EE corresponds to the percentage (w/w) of drug used in the loading process retained inside the dendrimer, and the LC corresponds to the amount of HCQ in the loaded dendrimer.[282]

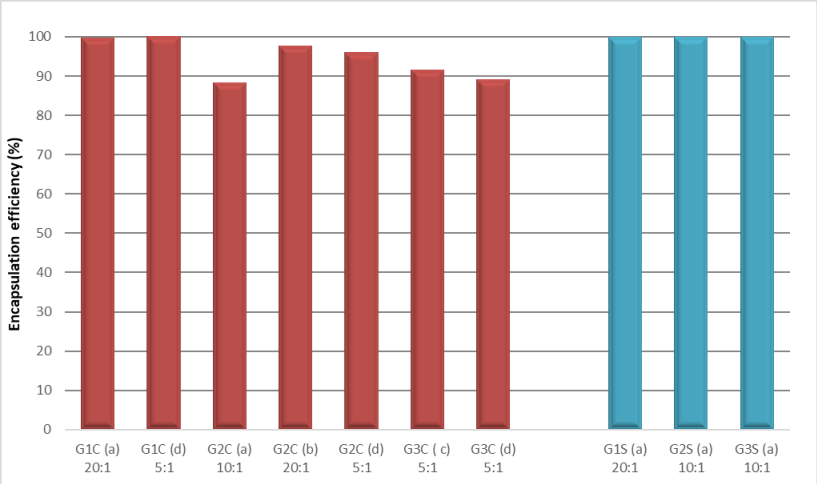

Figure 55- Results of the encapsulation efficiency (%) obtained for the encapsulation of HCQ.

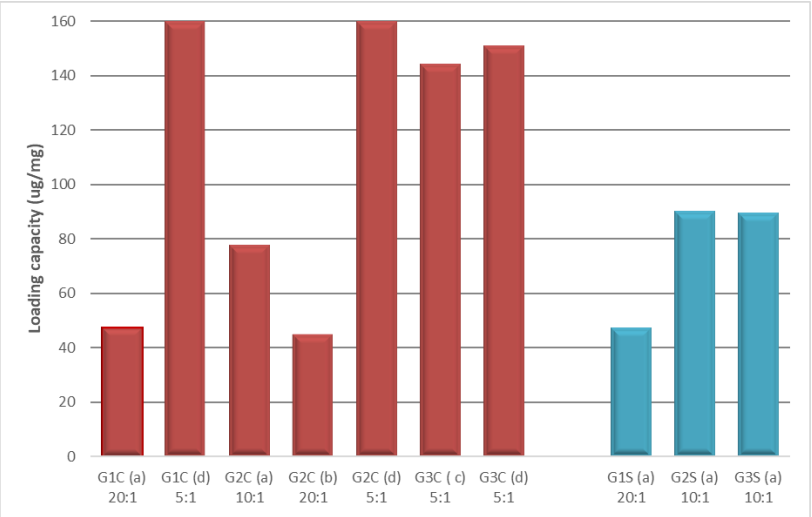

Figure 56- Results of the amount of HCQ loaded in each dendrimer (loading capacity).

In the first attempt (denominated (a) in table 9), we started by encapsulating 100 mg of a dendrimer with 5 mg of HCQ (20:1) for G1C and G1S. For G2S, G3S, and G2C we increased the amount of HCQ to 10 mg (10:1), because it was supposed that there was more space in the interior of the dendrimers for the drug to penetrate.

In all generations of sulfonate dendrimers and G1C, we achieved an EE of 100%. Contrarily, in G2C, only 9 mg of the HCQ was encapsulated, obtaining an EE of 88%. So, by reducing the concentration of HCQ to 5mg (20:1) (see table 9 G2C (b)), the EE increased by 10 %, obtaining about 5 mg of HCQ encapsulated.

When we did the encapsulation of generation G3C (see table 9 G3C (C)), we used 50 mg of dendrimer for 10 mg of HCQ (5:1), the EE was 91% and the amount of HCQ loaded *per* mg of dendrimers was 144 µg. So, we tried to use a carboxylate dendrimer/HCQ ratio of 5:1 (denominated (d) in table 9) to increase the LC, or in other words, the amount of HCQ *per* mg of dendrimers.

Therefore, when we performed the encapsulation of HCQ in sulfonate dendrimers, using a ratio dendrimer/HCQ 20:1 for G1S and 10:1 for the G2S and G3S, the EE was 100%. For the carboxylate dendrimers, using a dendrimer/HCQ ratio of 5:1, we obtained good values for EE and LC, even if their EE was slightly lower when compared with the sulfonate dendrimers. Nevertheless, the sulfonate dendrimers globally presented the best EE and LC without a commensurable generation trend.

Table 9- Results obtained in the drug encapsulation of sHCQ.

Compound	Dendrimer used, mg	HCQ used, mg	Encapsulated, mg	EE (%)	Loading HCQ, ug/mg	LC (%)	
G1C	101	5	5	100	47	5	(a)
	52	10	10	100	160	16	(d)
G1S	101	5	5	100	47	5	(a)
G2C	105	10	9	88	78	8	(a)
	104	5	5	98	45	5	(b)
	50	10	9	96	160	16	(d)
G2S	101	10	10	100	90	9	(a)
G3C	54	10	9	91	144	14	(c)
	50	10	9	89	151	15	(d)
G3S	102	10	10	100	89	9	(a)

To confirm if the HCQ was loaded in the dendrimer, we performed a ^{1}H- and ^{13}C-NMR, ATR-FTIR, and DLS for zeta potential determination.

10.5.1 NMR characterization of the dendrimers encapsulated with sHCQ

Before the drug encapsulation, we performed ^{1}H- and ^{13}C-NMR of the free sHCQ. The ^{1}H-NMR spectrum (figure 57) of sHCQ presented the characteristic signals of the aromatic and pyridine ring between 6.00 ppm and 9.00 ppm. In the ^{13}C-NMR spectrum of sHCQ (figure 58), the carbon signals of these structures appeared between 98 ppm and 155 ppm. So, we used these NMR signals to detect if the HCQ was in the dendrimer.

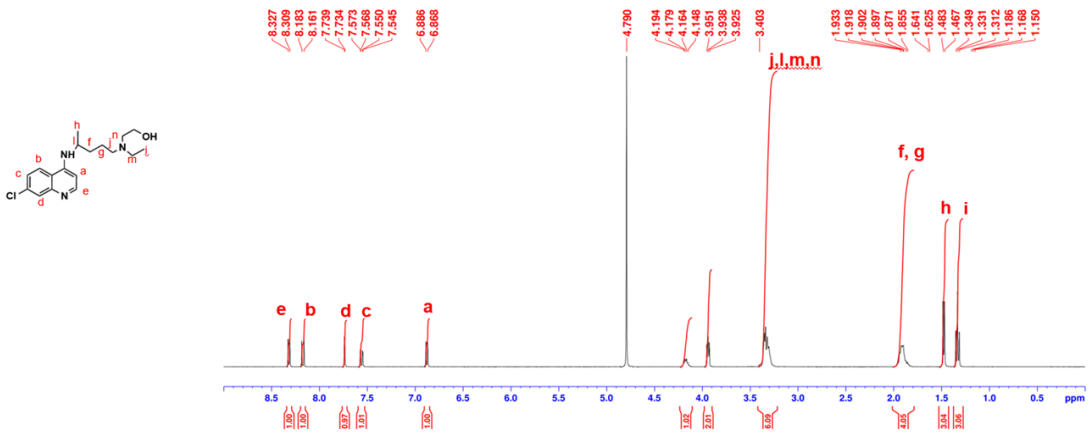

Figure 57- ^{1}H-NMR spectrum of sHCQ in D_2O.

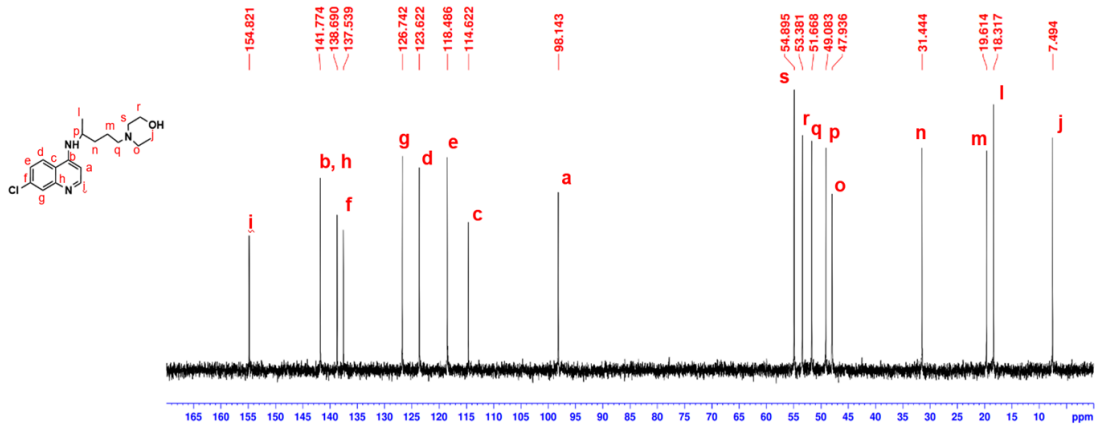

Figure 58- ^{13}C-NMR spectrum of sHCQ in D_2O.

In the ^{1}H-NMR spectrum of G1C, G2C, and G3C dendrimers encapsulated with sHCQ (figures 59, see annex figures A30, A31, A33, A35, A37, A39), it was possible to identify the proton signals of the aromatic and pyridine rings above 6.00 ppm. This indicates the presence of sHCQ in the dendrimers. In the ^{13}C-NMR spectrum (figures 60, see annex figures A32, A34, A36, A38, A40), the characteristic signals of sHCQ only appeared when we had a higher among of drugs encapsulated. From the Figure 60, which represents the ^{13}C-NMR spectrum of G1C when performed the encapsulation with a ratio of 5:1 (dendrimer/sHCQ), it was possible to detect several signals corresponding to the C of the sHCQ, contrary to what was observed when performed the encapsulation with a ratio of 20:1 (figure 61).

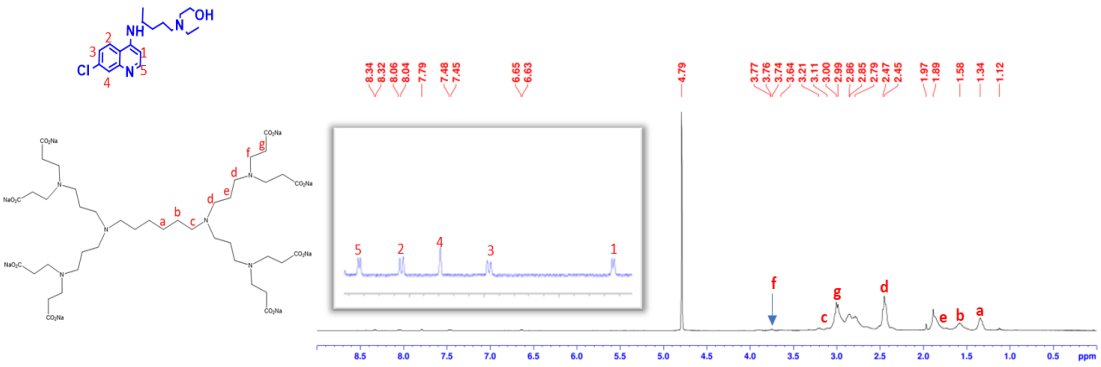

Figure 59- ^{1}H-NMR spectrum of the G1C encapsulated with sHCQ, using a ratio 5:1 (dendrimer/HCQ).

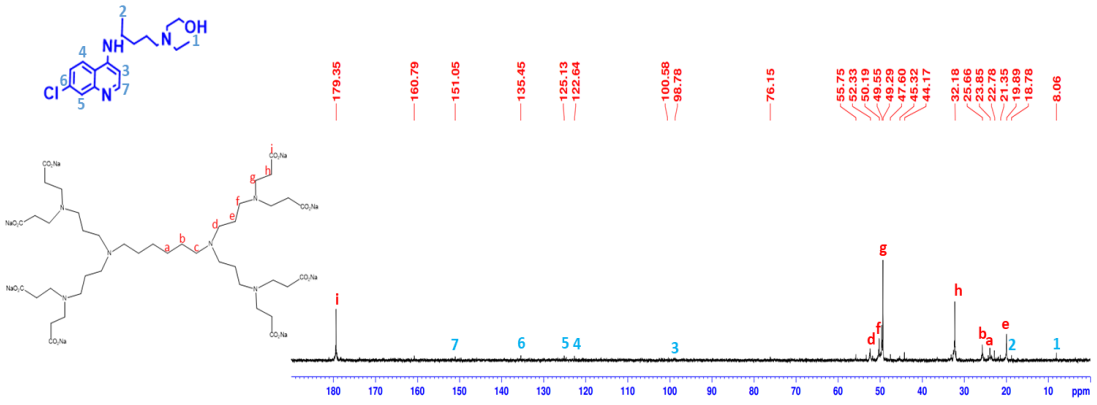

Figure 60- ^{13}C-NMR spectrum of the G1C encapsulated with sHCQ, using a ratio 5:1 (dendrimer/HCQ).

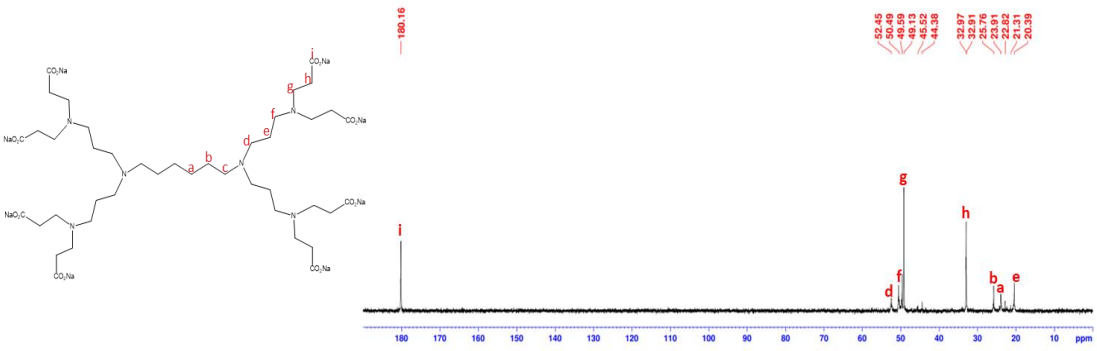

Figure 61- ^{13}C-NMR spectrum of the G1C encapsulated with sHCQ, using a ratio 20:1 (dendrimer/HCQ).

Concerning the encapsulation in the sulfonate dendrimers, in all generations, the signals of the protons of the aromatic and pyridine ring were displayed in all ^{1}H-NMR spectrum (figure 62, see annex figures A41 and A43). Some sodium vinyl sulfonate residues continued to appear around 5.00-6.00 ppm. Also, in the ^{13}C-NMR spectrum (figure 62, see annex figure A42 and A44), some signals of the aromatic ring of HCQ in all sulfonate dendrimers generations were visible. As in the carboxylate dendrimers, some carbon signals did not appear when less drug was encapsulated. Figure 63 represents the ^{13}C-NMR spectrum of the G2S encapsulated with a ratio of 10:1, where various visible signals from the C of the sHCQ are present, contrary to when performed the encapsulation in the G1S (see annex figure A42).

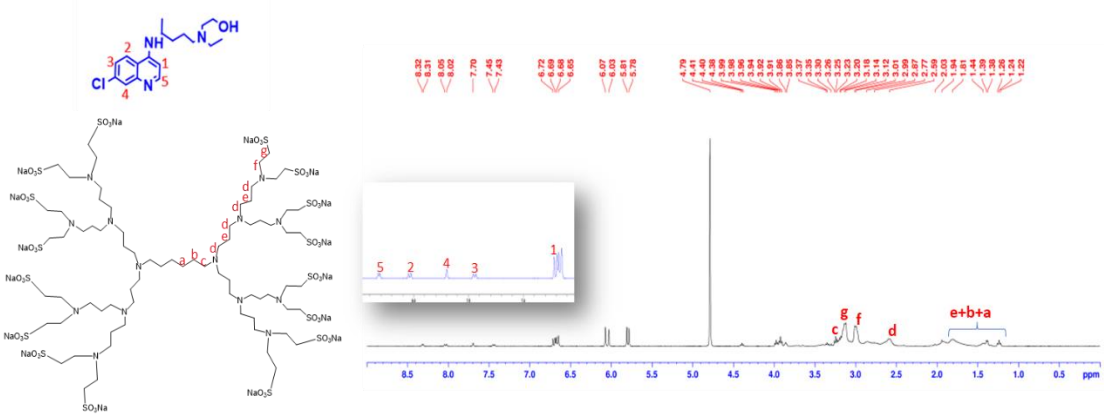

Figure 62- ^{1}H-NMR spectrum of the G2S encapsulated with sHCQ, using a ratio 10:1 (dendrimer/HCQ).

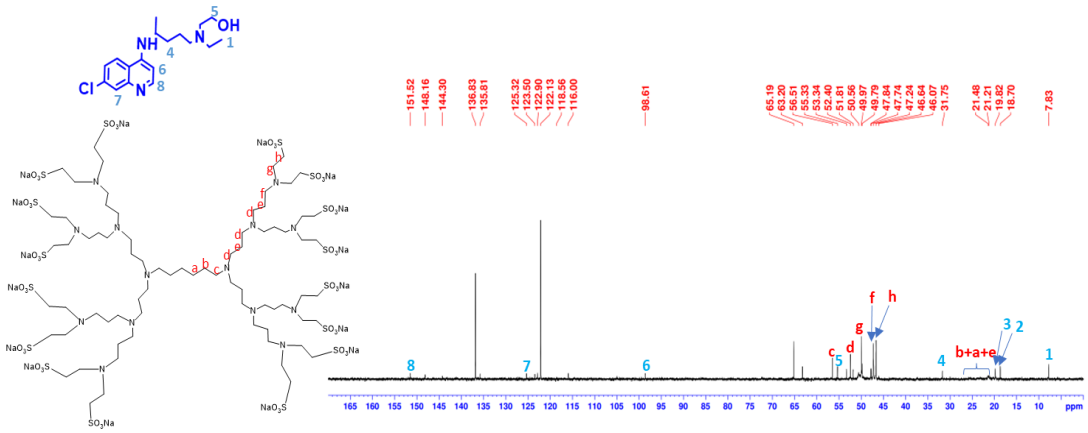

Figure 63- ^{13}C-NMR spectrum of the G2S encapsulated with sHCQ, using a ratio 10:1 (dendrimer/HCQ).

The signals of the sHCQ were not all identified since, with drug encapsulations, some signals can be masked by the carbon signals of the dendrimers.

In conclusion, by the NMR analyses, we can say that the drug was encapsulated in the dendrimers, and the procedure used for the encapsulation of sHCQ was successfully achieved.

10.5.2 ATR-FTIR analyses of the dendrimers encapsulated with sHCQ

We identified some bands corresponding to the drug by analysing the differences between the FTIR spectrum of dendrimers with sHCQ and without sHCQ.

In the ATR-FTIR spectrum of the carboxylate dendrimers (figure 64), it was possible to identify bands at 1128.8 cm $^{-1}$, 1128.9 cm^{-1}, and 1132.6 cm^{-1}, for the G1, G2 and G3, that corresponds to the C-N stretching of HCQ.

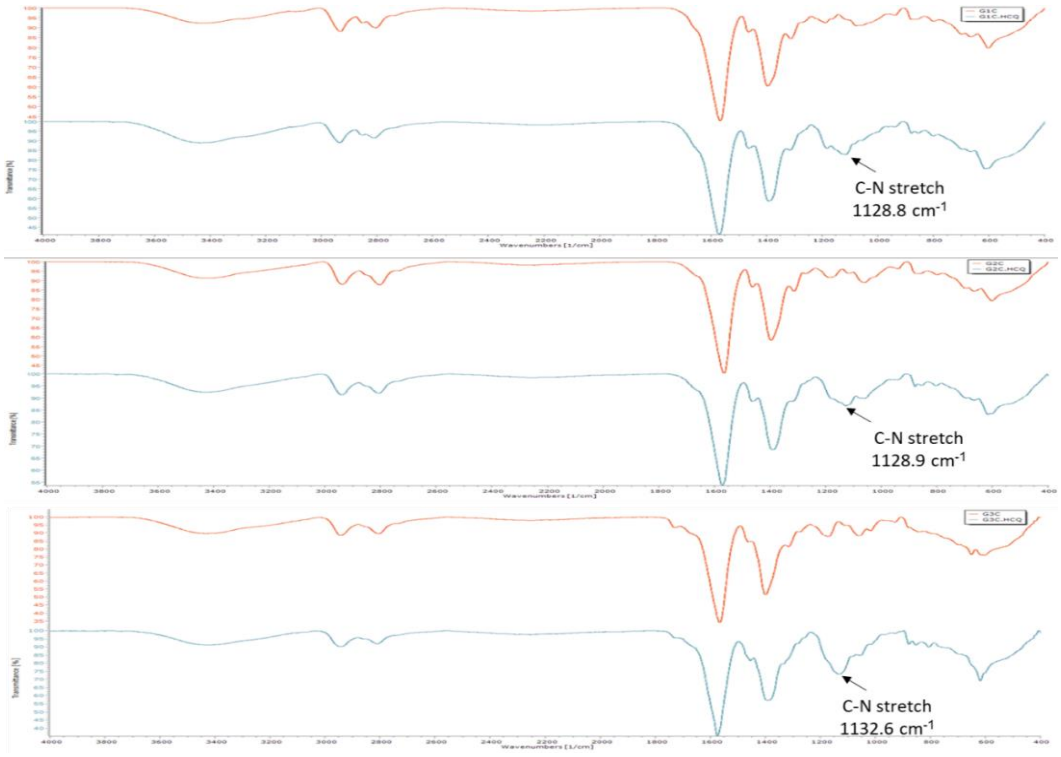

Figure 64- ATR-FTIR spectra of the G1C, G2C and G3C encapsulated with sHCQ, respectively.

In the sulfonate dendrimers, stretching bands at 1579.9 cm^{-1} for G1 and G2, and at 1580.9 cm^{-1} for G3 were observed as a result of the C=C bonding from the aromatic ring of sHCQ (figure 65).

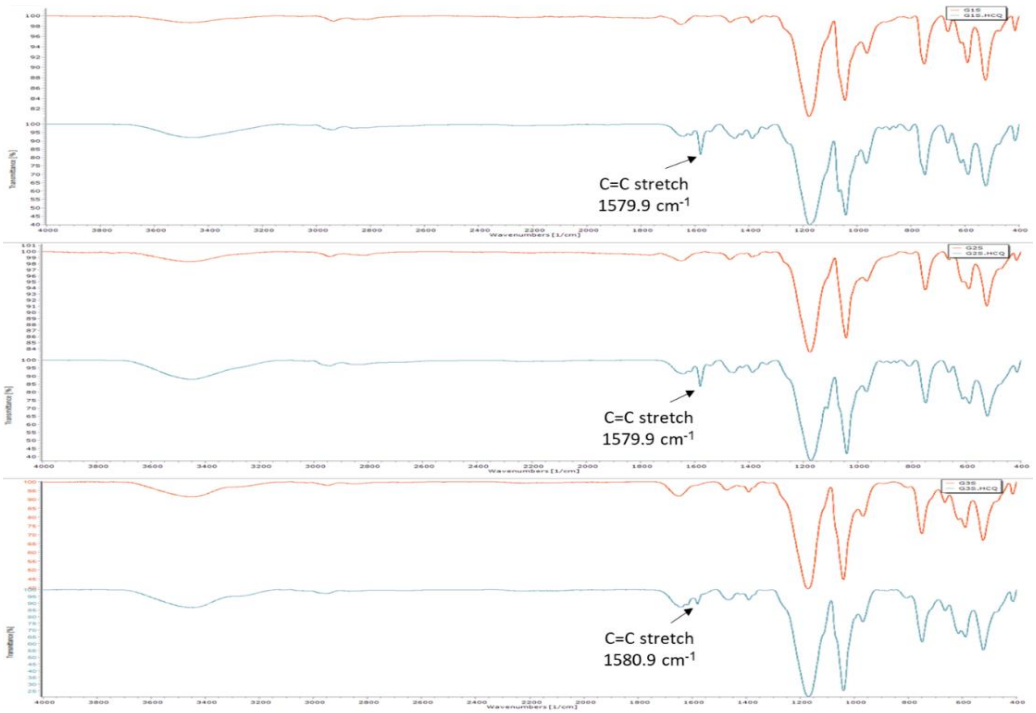

Figure 65- ATR-FTIR spectra of the G1S, G2S and G3S encapsulated with sHCQ, respectively.

Since the other bands of the sHCQ do not appear in the spectrum (see annex figure A45), we predicted that the sHCQ is encapsulated and the dendrimer branches mask the signals.

10.5.3 Zeta potential measurement of the dendrimers with the sHCQ

The zeta potential of the HCQ encapsulated was evaluated to see if the charge differs significantly from the pristine dendrimers (table 10). This information was useful to evaluate the cell uptake and stability and to provide preliminary information about how the encapsulated HCQ affects the double layer and the zeta potential of the dendrimers. Since HCQ presented two positive charges in distilled water, it was expected that the zeta-potential values of the dendrimers with the drug would become slightly less negative. This trend was effectively observed in G1C, G2C, G1S, and G3S. However, in G3C, the differences in the zeta-potential are minimum, and in G2S, zeta-potential becomes more negative after encapsulation.

Table 10- Zeta potential data of the non-loaded and loaded carboxylate and sulfonate dendrimers. The data are expressed as the mean ± SD of three independent experiments.

	G1C	G2C	G3C	G1S	G2S	G3S
Non-loaded HCQ	-51.8 ±0.6	-52.7 ±0.8	-32.4 ±2.5	-46.5 ±1.6	-30.3 ±0.8	-40.6 ±2.2
Loaded HCQ	-46.8±0.9	-47±1.2	-35.6 ±1.2	-36.6 ±1.2	-47.2 ±0.8	-35.6 ±1.2

The techniques used to characterize the dendrimers loaded with the sHCQ were useful for concluding that all dendrimers could encapsulate the drug. The HCQ is composed of both hydrophilic and hydrophobic regions.[305] The HCQ can be partially encapsulated, where only the hydrophobic moiety is encapsulated in the interior, and the hydrophilic moiety is from the exterior.

Also, when encapsulation was performed in distilled water (pH ≈7), the HCQ presented two protonated nitrogen and, consequently, had a more acidic character. Since the PPI dendrimers have a basic and hydrophobic interior (less polar), drugs with a hydrophobic or acidic character should be retained in the dendrimers' interior by hydrophobic interactions when in an aqueous environment.[306]

Another hypothesis proposes that the HCQ are bonded with the dendrimers by hydrogen bonds. The presence of a terminal carboxylate and sulfonate group in the dendrimers allows the -OH or -NH group from the HCQ to establish hydrogen bonds with the dendrimers' terminal groups. Other theory suggests that once at pH 7 the terminal carboxylate and sulfonate groups are deprotonated (negative charge) and the HCQ is protonated (positive charge), the HCQ can be linked with the dendrimers through electrostatic interactions.[246,305]

10.6 Drug release studies

In vitro drug release was performed in PBS at pH 7.4 and 5, for 1 week, at 37°C. PBS at pH 7.4 and 5 were selected to simulate the physiological and tumor environments.

At pH 7.4 (figure 66), G1C and G2C dendrimers showed a more sustained release of sHCQ, after 24h - less than 31 % of the drug was released. After 1 week, less than 50% of the drug was released in both dendrimers. On the other side, G3C had a faster release, and after 24h, it achieved 78% of the drug. After 48h, the cumulative release achieved a maximum value of 88%, remaining practically at the same value (87%) after 1 week. Globally, we can conclude that, at this pH value, the lower carboxylate dendrimer generations present the best-sustained sHCQ release profiles.

Concerning the sulfonate dendrimers, after 24h, the cumulative release was 60%, 77%, and 79%, for the G1S, G2S, and G3S, respectively. These systems have a sustained sHCQ released profile throughout time, but the drug release is faster than in the carboxylate dendrimers.

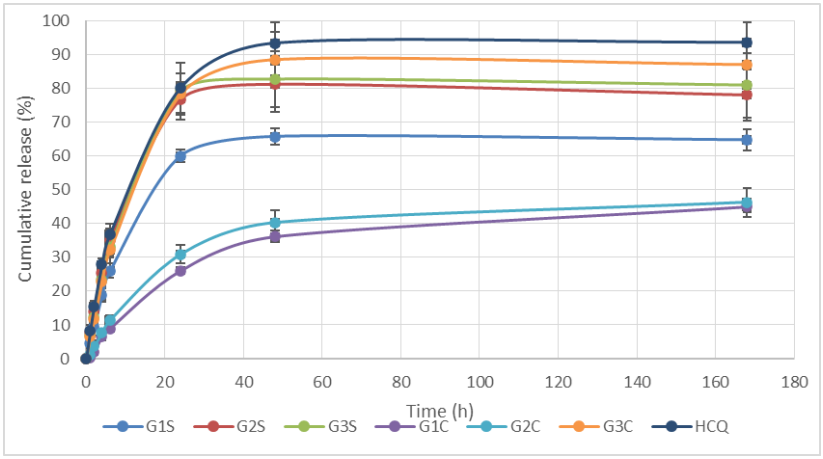

Figure 66- Cumulative release of sHCQ from the carboxylate and sulfonate dendrimers in PBS 7.4 at 37°C. All samples present the same sHCQ content. Data are expressed as a percentage of the total amount of sHCQ content in the samples, mean ±SD (n=3).

When decreased the pH to 5 (figure 67), we expected the release to be faster than pH 7.4, because the PPI dendrimers have many tertiary amines that are protonated at low pH, decreasing the dendrimer inner hydrophobicity. This would facilitate the drug release from the dendrimer at low pH.[307] So, the increased charge would increase the hydrophilicity of the chains, leading to enhanced polymer solubility.[308]

In addition, the carboxylate and sulfonate groups can either accept or donate H^+ in response to the pH alterations. At high pH values (low concentration of H^+ ions), COOH groups start to liberate their H^+ ions (deprotonate), leading to the generation of negatively charged groups of COO^-. On the other hand, at low pH values, the COO^- groups transform into COOH by accepting protons from the surrounding environment. The pH at which an acid becomes ionized depends on its pKa, which is around 5. The protonation/deprotonation changes the ionization degree and the charge, which leads to alterations in the hydrodynamic volume and conformation.[281]

Due to the sulfonate groups, dendrimers have pKa values around 2-3. At pH 5, the carboxylate group is to be protonated, and we expected that the release would be faster in the carboxylate groups than in the sulfonate groups.

In fact, the drug release at pH 5 increases (except for the G2S), after 24h, the cumulative release was 68%.

G1S, also has a notorious difference between pH 5 and 7.4. After 1 week, in the pH 5, it achieved almost 100% of release. G3S system had similar behavior in both pHs.

In G2C, the differences in release in PBS at pH 7.4 and 5 are noticeable. In PBS at pH 5, after 24h, the cumulative release was 86%, and the system achieved a release of 100% after 1 week. The G1C continued to have a sustained release, achieving 38% after 24h, and G3C had a similar release profile in both pHs.

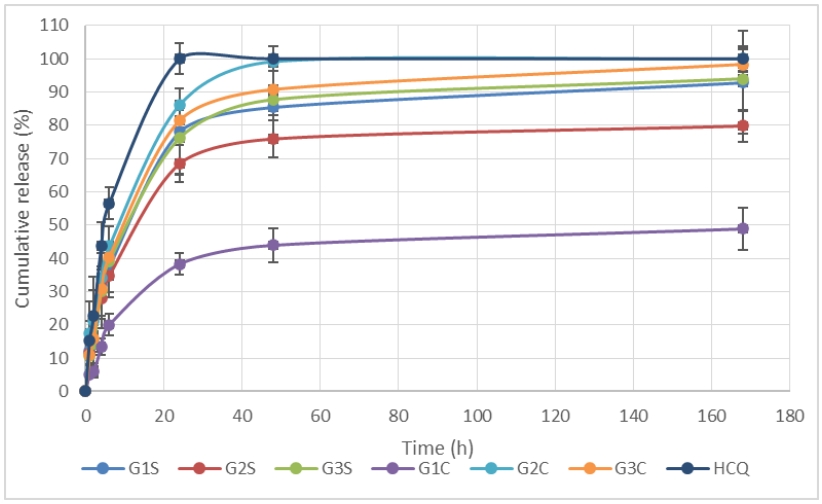

Figure 67- Cumulative release of sHCQ from the carboxylate and sulfonate dendrimers in PBS 5 at 37°C. All samples present the same sHCQ content. Data are expressed as a percentage of the total amount of sHCQ content in the samples, mean ±SD (n=3).

In conclusion, we can point out the following: a) if the objective is obtaining a sustained release of HCQ in the tumor environment, the G1C system is the most indicated; b) If the system is to be administrated in the circulation, the G2C and G1S systems are the most indicated, since the objective is that the dendrimers achieve the tumor site before releasing the drug.

10.7 Hemotoxicity evaluation

Due to their size, the nanomaterials are associated with a risk of interacting at the cellular and sub-cellular levels.[39] As previously seen, the toxicity of dendrimers is associated with the generation and functional group chemistry on the surface. The terminal groups' surface charge and surface chemistry will influence the toxicity. Positively charged dendrimers are known to cause hemotoxicity, resulting in a

generation- and concentration-dependent hemolysis.[309] The free cationic terminal groups of dendrimers interact with the red blood cell membrane leading to hemolysis.[39] Also, they have a high affinity for serum proteins.[310] So, modified amino-terminated dendrimers with negatively charged groups, such as carboxylate and sulfonate, should make the dendrimers less or not hemotoxic.

The red blood cell membrane contains proteins and glycoproteins embedded in a fluid lipid bilayer. The sialylated glycoproteins of the membranes are responsible for a negatively charged surface that creates a repulsive electric zeta potential between cells. This negative charge prevents interactions between the red blood cells and others, and especially between each other.[311,312] So, the negative surface charge of the dendrimers in contact with the red blood cells will be repulsed.

The results obtained for the hemotoxicity of the dendrimers without HCQ and for free sHCQ are presented in figure 68. All generations of carboxylate and sulfonate dendrimers, as free sHCQ, at concentrations ranging of 0.5- 50 µM, did not cause hemolysis.

In conclusion, all the generations of carboxylate and sulfonate dendrimers are not hemotoxic and safe for intravenous administration.

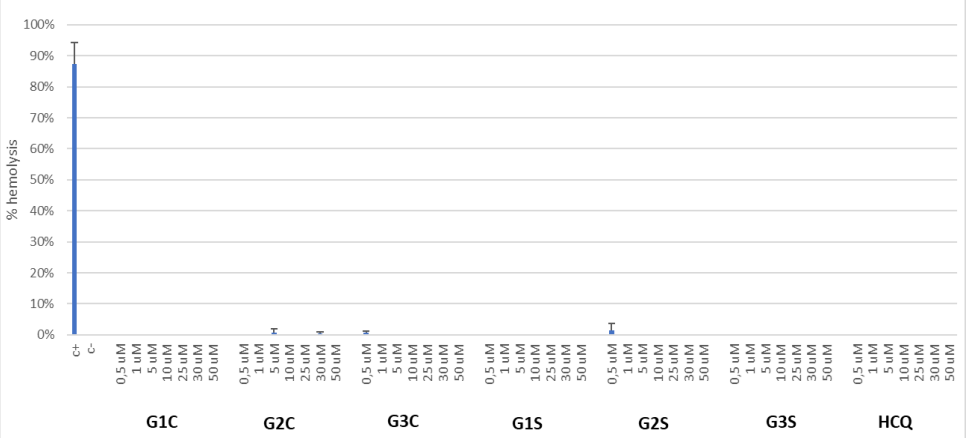

Figure 68- Percentage of hemolysis after the exposure for 3h, at 37 °C, of the non-loaded carboxylate and sulfonate dendrimers and free sHCQ. Cell Data are expressed as the mean ±SD of three independent experiments.

10.8 Cytotoxicity evaluation of the dendrimers- HCQ conjugates

The sulfonate and carboxylate dendrimers G1 to G3 loaded with the sHCQ and without the drug , as the free drug (sHCQ), were tested initially in the MCF-7 cancer

cell line and BJ cells (non-cancer cell line) in a concentration range of 0.5-50 μM. Breast adenocarcinoma cell line (MCF-7) was used because, by the recent statistical analyses, breast cancer is the most prevalent type of cancer in Portugal and in the world.[313, 314]

The resazurin assay was used to evaluate the cytotoxicity indirectly. The test was based on the intracellular reduction of resazurin to resorufin by viable, metabolically active cells. These include reduction by mitochondrial or microsomal enzymes, respiratory chain enzymes, or electron transfer agents.[315] When the resazurin diffuses through cell membranes, it is metabolically reduced by viable cells into resorufin. When excited at a wavelength of 579 nm, resorufin emits a fluorescent signal at 584 nm. The resazurin cannot be determined fluorometrically since only resorufin has fluorescence proprieties.[315] This assay is widely used as an indicator of active metabolism in cell cultures because it is more sensitive and reliable than other assays using tetrazolium dyes.[315]

The results showed that the non-loaded sulfonate and carboxylate dendrimers were less cytotoxic in all concentrations studied for MCF-7 and BJ cells (figure 69 and 70). In the MCF-7 cell line, the sulfonate dendrimers showed slightly higher cytotoxicity than the carboxylate dendrimers (figure 69). As expected, the anionic dendrimers showed lower cytotoxicity because it does not cause disruption and consequent leakage of cellular content or cell death when in contact with the cell membrane. The dendrimers are endocytosed, and the contents are released in the intracellular environment or in the intracellular compartments (lysosomes, endosomes, etc.).[316]

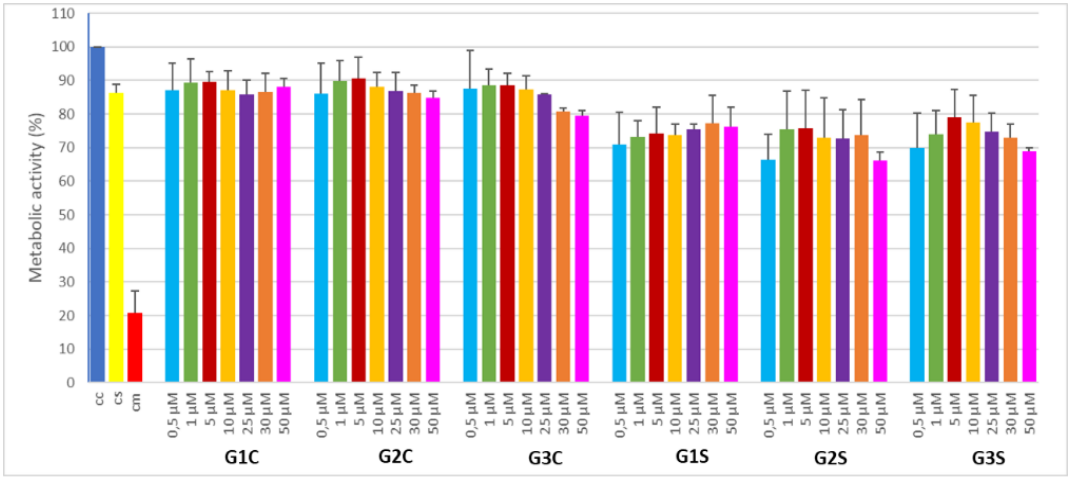

Figure 69- Cell viability of MCF-7 cells after 48h exposure to the non-loaded carboxylate and sulfonate dendrimers (G1, G2 and G3). Data are expressed as the mean ±SD of three independent experiments.

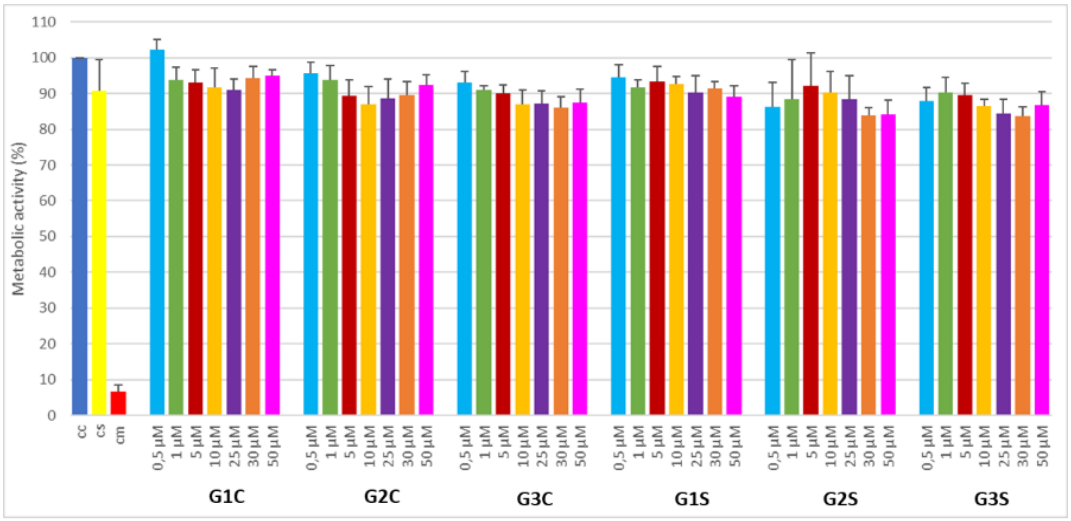

Figure 70- Cell viability of BJ cells after 48h exposure to the non-loaded carboxylate and sulfonate dendrimers (G1, G2 and G3). Data are expressed as the mean ±SD of three independent experiments.

Regarding the free drug, as the concentration of the drug increased, the metabolic activity decreased, as expected (figure 71 e 73). At 50 µM the metabolic activity was 54% for MCF-7 cells. He *et al.*[317] reported an IC50 value of HCQ of 12.47 µM for MCF-7 cells, so we expected the cell viability to be lower. Loh *et al.* exposed MCF-7 cells to 50 µM of HCQ, achieving cell viability of around 70%.[318] So, the cytotoxic effects depend on the cellular line and the cellular passage. To prove this, we performed an assay using a CACO-2 cell line at the same concentrations of HCQ. With 50 µM, the metabolic activity was 72% (annex figure A46). So, the MCF-7 cells seem to be more sensitive to HCQ.

Additionally, in the MCF-7 cells, the cytotoxicity of dendrimers loaded with HCQ was inferior or comparable to free sHCQ with the same drug concentration (figure 71). G1C, G1S and G2C loaded with sHCQ showed less toxicity due to the slow release of the drug into these systems. After 48h, these systems did not release the 50 µM of sHCQ for the medium. The other dendrimers, that had a more instant release, presented similar behavior to the free sHCQ. After 48h, with 50 µM of sHCQ, the G3C, G2S, and G3S had a metabolic activity of 67%, 69%, and 70%, respectively. These systems, after 48h, did not achieve 100% of the drug released. So, if we left the sHCQ in contact for more time, the metabolic activity certainly would decrease.

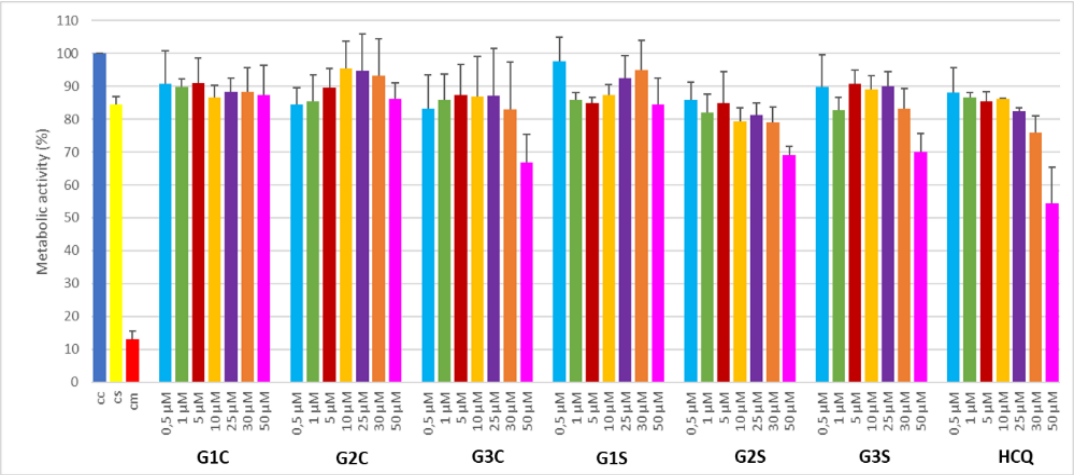

Figure 71- Cell viability of MCF-7 cells after 48h exposure to the sHCQ loaded carboxylate and sulfonate dendrimers (G1, G2 and G3) and free sHCQ. The values of the concentration refer to the amount of the encapsulated drug. Data are expressed as the mean ±SD of three independent experiments.

As it is known, in chemotherapy treatments, the sHCQ is applied in combination with other anti-cancer drugs to enhance tumor killing. So, intending to reduce cellular viability (increasing the cell cytotoxicity), we tested, in the MCF-7 cells, the sHCQ in combination with DOX. The concentration of DOX was fixed at 0.1 µM and the concentration of sHCQ ranged between 25 and 50 µM. We expected the sHCQ to enhance the DOX effect, but no synergetic effect was observed (annex figure A56). Probably our experimental setup was not the best. In fact, Loh *el at.*[291] achieved better results by fixing the concentration of sHCQ at 5uM and varying the concentration of DOX between 0 and 4 µM. With these experimental conditions, the sHCQ enhanced the treatment efficacy of DOX in MCF-7 cells.

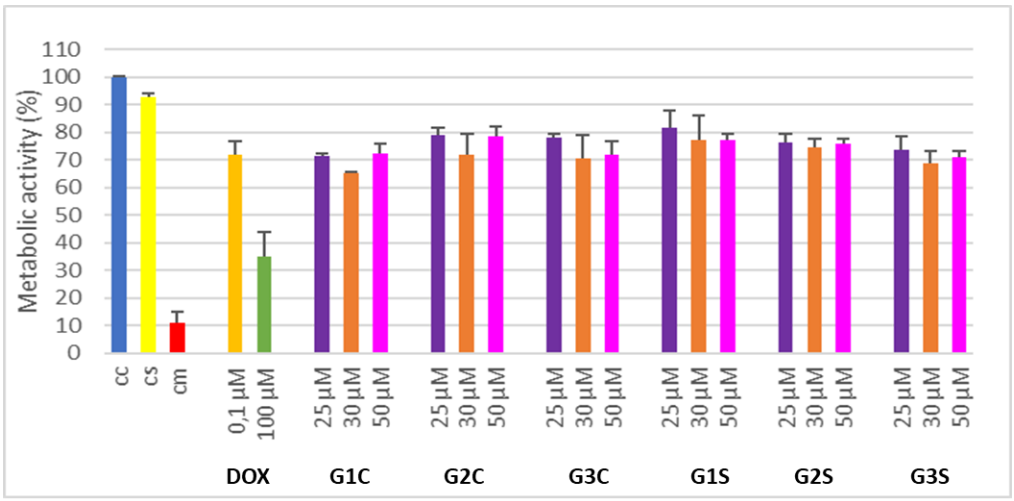

Figure 72- Cell viability of MCF-7 after 48h exposure to the loaded carboxylate and sulfonate dendrimers (G1, G2 and G3) in conjunct with DOX. The values of the concentration refer to the amount of the encapsulated drug. Data are expressed as the mean ±SD of three independent experiments.

With the BJ cells, the free sHCQ are highly toxic in the range of concentrations of 0.5-50 µM. With 50uM, after 48h, the metabolic activity was 12% (figure 73).

The profile of dendrimers loaded with sHCQ metabolic activity following the toxicity of the free drug (figure 73). Again, because of the slow release, the lower dendrimer generations, G1C, G2C, and G1S, induced higher metabolic activity when compared with the other systems and the free sHCQ.

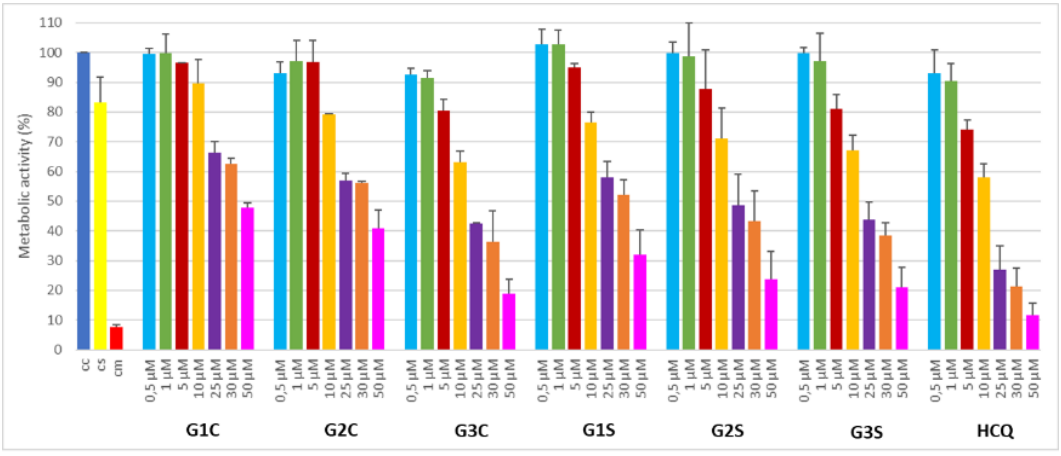

Figure 73- Cell viability of MCF-7 after 48h exposure to the sHCQ loaded carboxylate and sulfonate dendrimers (G1,G2, and G3) and free sHCQ. The values of the concentration refer to the amount of the encapsulated drug. Data are expressed as the mean ±SD of three independent experiments.

We can conclude that the BJ cells were more sensitive to sHCQ than the cancer line MCF-7. In fact, the cancer cells could create multidrug resistance to chemotherapy since it is the leading cause of therapeutic failure and death in women with breast cancer.[292]

The higher cytotoxicity induced in the BJ cells by the sHCQ is associated with secondary effects that can compromise cancer treatment. The use of carboxylate and sulfonate dendrimers has the principal aim of reducing the secondary effects because, as the drug is encapsulated, they do not interact directly with the membranes and direct the drug to the cancer cells.

11 Conclusion and future perspectives

As stated at the beginning of the master thesis, cancer is one of the most deadly diseases now days, and it is estimated that the number of cases will increase over the years. Despite the advances in medicine and healthcare, definitive therapy for successfully eradicating tumors is still not achieved for many types of cancer due to their unique characteristics. The most used treatment is chemotherapy, which causes several side effects in the patient and sometimes leads to treatment failure. Over the years, dendrimers have received increasing attention as drug carriers and tools for diagnosing, imaging, and treatment of different types of cancer. These nanocarriers increase the solubility of anti-cancer drugs, direct drugs to the tumor site, increase the bioavailability, reduce side effects, increase the half-time in circulation, etc.

In this thesis, we took advantage of the most popular characteristics of anionic PPI dendrimers, such as low toxicity, low immunogenicity, and low hemotoxicity, for carrier a drug that was gained some popularity in recent years, hydroxychloroquine. In cancer therapy, the HCQ acts to inhibit the autophagy process that has been proven in a particular stage of tumor growth. This mechanism protects the tumor cells against chemotherapy, radiotherapy, or other cancer treatment. So, by inhibiting autophagy, the cytotoxicity of the other cancer drugs increases since the cells do not have the mechanism for defense. Also, the HCQ administered alone can activate the mitochondrial pathway of apoptosis.

First, we synthesized the nitrile and amine-terminated dendrimers to be used as building blocks to increase the generation. The nitrile-terminated dendrimers were synthesized from G0 to G3 with a yield range between 41% and 88%. As the generation increased, a notorious decrease in yield was verified. The synthesis conditions were optimized since at the higher generations, using methanol as solvent was the better option. The amine-terminated dendrimers were synthesized from G0 to G3 with a yield range between 67% to 99%. By reducing the eq. mol of reagent in the G2 and G3, we achieved yields up to 80%.

After, the amine terminal groups were replaced by anionic carboxylate and sulfonate groups. The sulfonate and carboxylate PPI dendrimers were prepared from

the G1 to G4, and characterized by ^{1}H- and ^{13}C NMR, ATR-FTIR, DLS, zeta potential, and MS. The encapsulation of sHCQ, was successfully performed in both dendrimer families until G3, with encapsulation efficiencies between 88% and 100%. Drug release studies were important for predicting the drug's release *in vivo.* The PPI dendrimers should be pH-responsive (internal stimuli), as observed in the two families of studied dendrimers, particularly at lower generations (G1C, G2C, and G1S), with an advantage for the carboxylates family. The safety of the prepared dendrimers was evaluated *in vitro* as well as their interactions with blood cells. The non-loaded anionic dendrimers and the free sHCQ did not cause hemolysis of the blood red cells. Both anionic dendrimers showed less or no cytotoxicity in MCF-7 and BJ cells, in a range of 0.5-50 μM. The dendrimers loaded with the sHCQ followed the sHCQ cytotoxicity profile, but the MCF-7 were less sensitive to the sHCQ in the studied range of concentrations, showing less cytotoxicity. Contrary, the sHCQ presented higher cytotoxic for the BJ cells. This interaction with the non-cancer cell line resulted in side effects. The objective was that the anionic dendrimers with sHCQ did not release before arriving at the target cells by the EPF effect. No synergetic or antagonist effect was observed when combining the dendrimers with sHCQ and free DOX in the MCF-7 cells.

In conclusion, our dendrimers were synthesized and characterized by different structural techniques and showed potential as a carrier of sHCQ, particularly at low generations. For the first time, G4C and G4S were synthesized, with yields of 50% and 94%, respectively, and characterized by ^{1}H- and ^{13}C- NMR, ATR-FTIR, and DLS. As future work, the new dendrimers deserve to improve their purification (G3 and G4) and to be fully characterized by TEM and AFM. The type of interactions and location of HCQ within dendrimers must also be studied. Regarding the cytotoxicity evaluation, the range of concentrations must be increased to achieve 50% or less of cell viability. To obtain a better overview of the cancer effect of the dendrimers and HCQ, other cancer cells line must be tested. The cytotoxicity of our systems in combination with other anti-cancer drugs should also be studied to verify the eventual synergistic effect caused by sHCQ. Previously to the *in vivo* tests to be developed in selected dendrimers, it would also be interesting to study the interaction of the loaded dendrimers with the DNA.

References

[1] National Nanotechnology Initiative (NNI), What Is Nanotechnology?. https://www.nano.gov/nanotech-101/what/definition (accessed April 30, 2022)

[2] Mignani, S.; Rodrigues, J.; Tomas, H.; Roy, R.; Shi, X.; Majoral, J.P. Bench-to-bedside translation of dendrimers: Reality or utopia? A concise analysis. *Adv Drug Delivery Rev* **2017**, 136-137, 73-81. DOI: https://doi.org/10.1016/j.addr.2017.11.007

[3] Mousa, S.A.; Bharali, D.J. Nanotechnology-based detection and targeted therapy in cancer: Nano-bio paradigms and applications. *Cancers (Basel)* **2011**, 33, 2888-2903. DOI: https://doi.org/10.3390/cancers3032888

[4] Ventola, C.L. The nanomedicine revolution: part 1: emerging concepts. *P T* **2012,** 37, 512-525. Available in URL: https://www.researchgate.net/publication/232248534_The_nanomedicine_revolution_Part_1_Emerging_Concepts

[5] Benelmekki, M. Nanomaterials: The original Product of Nanotechnology. IOP Concise Physics, **2019**. ISBN: 978-1-64327-644-1

[6] Raza, F.; Zafar, H.; You, X.; Khan, A.; Wu, J.; Ge, L. Cancer nanomedicine: focus on recent developments and self-assembled peptide nanocarriers. *J. Mater. Chem. B* **2019**, 7, 7639-7655. DOI: https://doi.org/10.1039/C9TB01842E

[7] Lombardo, D.; Kiselev, M.A.; Caccamo, M.T. Smart Nanoparticles for Drug Delivery Application: Development of Versatile Nanocarrier Platforms in Biotechnology and Nanomedicine, *J. Nanomater.* **2019**, 2019, 1–26. https://doi.org/10.1155/2019/3702518

[8] Jain, A.; Kesharwani, P.; Garg, N. K.; Jain, A.; Jain, S. A.; *et al.* Galactose engineered solid lipid nanoparticles for targeted delivery of doxorubicin, *Colloids Surfaces B: Biointerfaces* **2015**, 134, 47–58. DOI: https://doi.org/10.1016/j.colsurfb.2015.06.027

[9] Seigneuric, R.; Markey, L.; Nuyten, D.S.; *et al.* From nanotechnology to nanomedicine: Applications to cancer research. *Curr Mol Med.* **2010**, 10, 640–652. DOI: https://doi.org/10.2174/156652410792630634

[10] Wickens, J.M.; Alsaab, H.O.; Kesharwani, P.; Bhise, K.; Amin, M.C.I.M.; *et al*. Recent advances in hyaluronic acid-decorated nanocarriers for targeted cancer therapy. *Drug Discov Today* **2017,** 22, 665-680. DOI: https://doi.org/10.1016/j.drudis.2016.12.009

[11] Ventola, C.L. Progress in nanomedicine: approved and investigational nanodrugs. *P T* **2017**, 42, 742-755. Available in URL: https://www.researchgate.net/publication/321805304_Progress_in_Nanomedicine_Approved_and_Investigational_Nanodrugs

[12] Leon, L.; Chung, E.J.; Rinaldi, C. A brief History of Nanotechnology and Introduction to Nanoparticles for biomedical Applications. *Nanoparticles for Biomedical Applications: Fundamental Concepts, Biological Interactions and Clinical Applications* **2020**, 1-4. DOI: https://doi.org/10.1016/B978-0-12-816662-8.00001-1

[13] Kesharwani, P; Amin, M. C. I. M.; Giri, N.; Jain, A.; Gajbhiye, V. Dendrimers in Targeting and Delivery of Drugs. *Nanotechnology-Based Approaches for Targeting and Delivery of Drugs and Genes* **2017***,* 363–388. DOI: https://doi.org/10.1016/B978-0-12-809717-5.00013-0

[14] Strobl G. The Physics of Polymers: Concepts for Understanding Their Structures and Behavior. Springer Berlin Heidelberg **2007**. DOI: https://doi.org/10.1007/978-3-540-68411-4

[15] Huang, D.; Wu, D. Biodegradable dendrimers for drug delivery. *Mater. Sci. Eng. C* **2018,** 90, 713-727. DOI: https://doi.org/10.1016/j.msec.2018.03.002

[16] Buhleier, E.; Wehner, W.; Vögtle, F. "Cascade"- and "non-skid-chain-like" Syntheses of molecular cavity topologies. *Synthesis (Stuttg)* **1978**, 1978, 155-158. DOI: https://doi.org/10.1055/s-1978-24702

[17] Tomalia, D. A.; Baker, H.; Dewald, J.; Hall, M.; Kallos, G.; Martin, S.; Roeck, J.; Ryder, J.; Smith, P. A New Class of Polymers: Starburst-Dendritic Macromolecules. *Polym. J.* **1985**, 17, 117–132. DOI: https://doi.org/10.1295/polymj.17.117

[18] Newkone, G.R.; Yao, Z.; Baker, G.R.; Gupta, V.K. Cascade molecules: a new approach to micelles. A [27]-arborol. *J. Org*. Chem. **1985**, 50, 2003–2004. DOI: https://doi.org/10.1021/jo00211a052

[19] Hawker, C.J.; Frechet, J.M.J. Preparation of polymers with controlled molecular architecture - a new convergent approach to dendritic macromolecules. *J. Am. Chem. Soc.* **1990**, 112, 7638–7647. DOI: https://doi.org/10.1021/ja00177a027

[20] Klajnert, B.; Bryszewska, M. Dendrimers: properties and applications, *Acta Biochimi. Pol.* **2001**, 48, 199-208. DOI: https://doi.org/10.1016/B978-0-444-53349-4.00162-X

[21] Lee, C.C.; MacKay, J.A.; Fréchet, J.M.J.; Szoka, F.C. Designing dendrimers for biological applications. *Nat. Biotechnol* **2005**, 23, 1617-1526. DOI: https://doi.org/10.1038/nbt1171

[22] Boas U, Heegaard P.M.H. Dendrimers in drug research. *Chem. Soc. Rev*. **2004**, 33,43-63. DOI: https://doi.org/10.1039/b309043b

[23] Svenson, S.; Tomalia D.A. Dendrimers in biomedical applications - reflections on the field. *Adv. Drug Deliv. Rev.* **2005**, 57, 2106-2129. DOI: https://doi.org/10.1016/j.addr.2005.09.018

[24] Nanjwade,B.K.; Bechra H.M.; Derkar G.K.; Manvi, F.V., Nanjwade V.K. Dendrimers: Emerging polymers for drug-delivery systems. *Eur. J. Pharm. Sci*. **2009**, 38, 185-196. DOI: https://doi.org/10.1016/j.ejps.2009.07.008

[25] Santos, A.; Veiga, F.; Figueiras A. Dendrimers as Pharmaceutical Excipients: Synthesis, Properties, Toxicity and Biomedical Applications. *Materials* **2020**, 13, 65. DOI: https://doi.org/10.3390/ma13010065

[26] Mintzer M.A.; Grinstaff M.W. Biomedical applications of dendrimers: A tutorial. *Chem. Soc. Rev.* **2011**, 40, 173-190. DOI: https://doi.org/10.1039/b901839p

[27] Trinchi A.; Muster, T.H. A review of surface functionalized amine terminated dendrimers for application in biological and molecular sensing. *Supramol. Chem.* **2007**, 19, 431-445.DOI: https://doi.org/10.1080/10610270601120363

[28] Inoue, K. Functional dendrimers, hyperbranched and star polymers. *Prog. Polym. Sci.* **2000**, 25, 453–571. DOI: https://doi.org/10.1016/S0079-6700(00)00011-3

[29] Liu, M.; Kono, K.; Fréchet, J.M.J. Water-soluble dendritic unimolecular micelles: their potential as drug delivery agents. *J. Control. Release* **2000**, 65, 121–131. DOI: https://doi.org/10.1016/S0168-3659(99)00245-X

[30] Stevelmans, S.; Hest, van, J. C. M.; Jansen, J. F. G. A.; Boxtel, van, D.; Berg, van den, E. M. M.; Meijer, E. W Synthesis, characterization, and guest-host properties of inverted unimolecular dendritic micelles. *J. Am. Chem. Soc.* **1996**, 118, 7398–7399. DOI: https://doi.org/10.1021/ja954207h

[31] Gupta, U.; Agashe, H.B.; Asthana, A.; Jain, N.K. Dendrimers: Novel Polymeric Nanoarchitectures for solubility Enhancement. *Biomacromolecules* **2006**, 7, 649-658. DOI: https://doi.org/10.1021/bm050802s

[32] Choudhary, S.; Gupta, L.; Rani, S.; Dave, K; Gupta, U. Impacto f Dendrimers on solubility of Hydrophobic Drug Molecules. *Front. Pharmacol.* **2017**, 8, 261-283. DOI: https://doi.org/10.3389/fphar.2017.00261

[33] Rolland, O.; Turrin C. O.; Camide, A.M.; Majoral; J.P. Dendrimers and nanomedicine: multivalency in action. *New J. Chem.* **2009**, 33, 1890-1824. DOI: https://doi.org/10.1039/B901054H

[34] Kesharwani, P.; Jain, K.; Jain, N.K. Dendrimer as nanocarrier for drug delivery. *Prog. Polym. Sci.* **2014**, 39, 268-307. DOI: https://doi.org/10.1016/j.progpolymsci.2013.07.005

[35] Hong, S.; Bielinska, A.U.; Mecke, A.; Keszler, B.; Beals, J.L.; et al. Interaction of poly(amidoamine) dendrimers with supported lipid bilayers and cells: hole formation and the relation to transport. *Bioconjug. Chem.* **2004**, 15, 774–782. DOI: https://doi.org/10.1021/bc049962b

[36] Kuo, J.H.S.; Jan, M.S.; Chiu, H.W. Mechanism of cell death induced by cationic dendrimers in RAW 264.7 murine macrophage-like cells. *J. Pharm. Pharmacol.* **2005**, 57, 489–495. DOI: https://doi.org/10.1211/0022357055803

[37] Zhang, Z.Y.; Smith, B.D. High-generation polycationic dendrimers are unusually effective at disrupting anionic vesicles: membrane bending model. *Bioconjugate Chem.* **2000**, 11, 805-814. DOI: https://doi.org/10.1021/BC000018Z

[38] Mecke, A.; Uppuluri, S.; Sassanella, T.M.; Lee, D.K.; Ramamoorthy A.; Baker, J.R. *et al.* Direct observation of lipid bilayer disruption by poly(amidoamine) dendrimers. *Chem. Phys. Lipids* **2004**, 132, 3-14. DOI: https://doi.org/10.1016/j.chemphyslip.2004.09.001

[39] Jain, K.; Kesharwani, P.; Gupta, U.; Jain, N.K. Dendrimer toxicity: Let´s meet the challenge. *Int. J. Pharm.* **2010**, 394, 122-142. DOI: https://doi.org/10.1016/j.ijpharm.2010.04.027

[40] Svenson, S. Dendrimers as a versatile platform in drug delivery applications. *Eur. J. Pharm. Biopharm.* **2009**, 71, 445– 464. DOI: https://doi.org/10.1016/j.ejpb.2008.09.023

[41] Fischer, D.; Li,Y.; Ahlemeyer, B.; Krieglstein, J.; Kissel, T. *In vitro* cytotoxicity testing of polycationic: Influence of polymer structure on cell viability and hemolysis. *Biomaterials* **2003**, 24, 1121–1131. DOI: https://doi.org/10.1016/S0142-9612(02)00445-3

[42] Zinselmeyer, B.H.; Mackay, S.P.; Schatzlein, A.G.; Uchegbu, I.F. The lower-generation polypropylenimine dendrimers are effective gene-transfer agents. *Pharm. Res.* **2002**, 19, 960-967. DOI: https://doi.org/10.1023/A:1016458104359

[43] Malik. N.; Wiwattanapatapee, R.; Klopsch, R.; Lorenz, K.; Frey, H.; Weener, J.W.; *et al.* Dendrimers: relationship between structure and biocompatibility *in vitro*, and preliminary studies on the biodistribution of 125I-labelled polyamidoamine dendrimers *in vivo*. *J. Contro.l Release* **2000**, 65, 133-48. DOI: https://doi.org/10.1016/s0168-3659(99)00246-1

[44] Jones, C.F.; Campbell, R.A.; Brooks, A.E.; Assemi, S.; Tadjiki, S.; Thiagarajan, G.; et al. Cationic PAMAM dendrimers aggressively initiate blood clot formation. *ACS Nano* **2012**, 6, 9900–9910. DOI: https://doi.org/10.1021/nn303472r

[45] Roberts, J.C.; Bhalgat, M.K.; Zera, R.T. Preliminary biological evaluation of polyamidoamine (PAMAM) Starburst dendrimers. *J. Biomed. Mater. Res.* **1996**, 30, 53–65. DOI: https://doi.org/10.1002/(SICI)1097-4636(199601)30:1<53::AID-JBM8>3.0.CO;2-Q

[46] Jevprasesphant, R.; Penny, J.; Attwood, D.; McKeown, N.B.; D`Emanuele, A. The influence of surface modification on the cytotoxicity of PAMAM dendrimers. *Int. J. Pharm.* **2003**, 252, 263–266. DOI: https://doi.org/10.1016/S0378-5173(02)00623-3

[47] Thakur, S.; Kesharwani, P.; Tekade, R.K.; Jain, N.K. Impact of pegylation on biopharmaceutical properties of dendrimers. *Polymer (Guildf)* **2015**, 59, 67-92. DOI: https://doi.org/10.1016/j.polymer.2014.12.051

[48] Kobayashi, H.; Kawamoto, S.; Saga, T.; Sato, N.; Hiraga, A.; Ishimori, T.; et al. Positive effects of polyethylene glycol conjugation to generation-4 polyamidoamine dendrimers as macromolecular MR contrast agents. *Magn. Reson. Med.* **2001**, 46, 781–788. DOI: https://doi.org/10.1002/mrm.1257

[49] Abbasi, E.; Aval, S.F.; Akbarzadeh ,A.; Milani, M.; Nasrabadi, H.T.; Joo, S.W.; *et al.* Dendrimers: Synthesis, Applications, and Properties. *Nanoscale Res. Lett.* **2014**, 9, 247. DOI: https://doi.org/10.1186/1556-276X-9-247

[50] Madaan, K.; Kumar, S.; Poonia, N.; Lather, V.; Pandita D. Dendrimers in drug delivery and targeting: Drug-dendrimer interactions and toxicity issues. *J. Pharm. Bioallied Sc.* **2014**, 6, 139-150. DOI: https://doi.org/10.4103/0975-7406.130965

[51] Li, Y.; Cheng, Y.; Xu, T. Design, Synthesis and Potent Pharmaceutical Applications of Glycoden-Drimers: A Mini Review. *Curr. Drug Discov. Technol.* **2007**, 4, 246-254. DOI: https://doi.org/10.2174/157016307783220503

[52] Sampathkumar, S.; Yarema, K.J..Dendrimers in Cancer Treatment and Diagnosis. *Nanotechnologies for the Life Sciences* **2007**, 7, 1-43. DOI: https://doi.org/10.1002/9783527610419.ntls0071

[53] Najafi, F.; Salami-Kalajahi, M.; Roghani-Mamaqani, H. A review on synthesis and applications of dendrimers. *J. Iran. Chem. Soc.* **2021**, 18, 503-517. DOI: https://doi.org/10.1007/s13738-020-02053-3

[54] Esfand, R.; Tomalia, D.A. Poly(amidoamine) (PAMAM) dendrimers: from biomimicry to drug delivery and biomedical applications. *Drug Discov. Today* **2001**, 6, 427–436. DOI: https://doi.org/10.1016/S1359-6446(01)01757-3

[55] Liu, X.; Liu, C.; Catapano, C.V.; Peng, L.; Zhou, J.; Rocchi, P. Structurally fexible triethanolamine-core poly(amidoamine) dendrimers as efective nanovectors to deliver RNAi-based therapeutics. *Biotechnol. Adv.* **2014**, 32, 844–852. DOI: https://doi.org/10.1016/j.biotechadv.2013.08.001

[56] Tomalia, D.A.; Baker, H.; Dewald, J.; Hall, M.; Kallos, G.; Martin, S.; *et al.* Dendritic macromolecules: synthesis of starburst dendrimers. *Macromolecules* **1986**, 19, 2466–2468. DOI: https://doi.org/10.1021/ma00163a029

[57] Cowie, J.M.G. Polymers: chemistry & physics of modern materials. *Polym. Int.* **1991**, 28, 95. DOI: https://doi.org/10.1002/pi.4990280115

[58] Kaur, D.; Jain, K.; Mehra, N.K.; Kesharwani, P.; Jain, N.K.; Kumar, N. A Review on Comparative Study of PPI and PAMAM dendrimers. *J. Nanopart. Res*. **2016**, 18, 1-14. DOI: https://doi.org/10.1007/s11051-016-3423-0

[59] Koper, G.; Genderen, M. V.; Elissen-Roman, C.; Baars, M.; Meijer, E.W.; Borkovec, M. Protonation mechanism of poly (propylene imine) dendrimers and some associated oligo amines. *J. Am. Chem. Soc.* **1997**, 119, 6512–6521. DOI: https://doi.org/10.1021/ja970442j

[60] Shao, N.; Su, Y.; Hu, J.; Zhang, J.; Zhang, H.; Cheng Y. Comparison of generation 3 polyamidoamine dendrimer and generation 4 polypropylenimine dendrimer on drug loading, complex structure, release behavior, and cytotoxicity. *Int. J. Nanomed*. **2011**, 6, 3361–3372. DOI: https://doi.org/10.2147/ijn.s27028

[61] Kesharwani, P.; Tekade, R.; Gajnhiye, V.; Jain, K.; Jain, N.K. Cancer targeting potential of some ligand-anchored poly(propylene imine) dendrimers: a comparison. *Nanomedicine* **2011**, 7, 295–304. DOI: https://doi.org/10.1016/j.nano.2010.10.010

[62] Akhter, S.; Ahmed, I.; Ahmad, M.Z.; Ramazani, F.; Singh, A.; Rahman, Z.; *et al.* , Nanomedicines as cancer therapeutics: current status. *Curr. Cancer Drug Targets* **2013**, 13, 362–378. DOI: https://doi.org/10.2174/1568009611313040002

[63] Avti, P.k.; Kakkar, A. Dendrimers as anti-inflammatory agent. *Braz. J. Pharm. Sci*. **2013**, 49, 57–65. DOI: https://doi.org/10.1590/S1984-82502013000700006

[64] García-Gallego, S.; Díaz, L.; Jiménez, J.L.; Gómez, R.; de la Mata, F.J.; Muñoz-Fernández, M. HIV-1 antiviral behavior of anionic PPI metallo-dendrimers with EDA core. *Eur. J. Med. Chem.* **2015**, 98, 139–148. DOI: https://doi.org/10.1016/j.ejmech.2015.05.026

[65] Majoros, I.J.; Williams, C.R.; Tomalia, D.A.; Baker Jr., J.R. New dendrimers: synthesis and characterization of POPAM −PAMAM hybrid dendrimers. *Macromolecules* **2008**, 41, 8372–8379. DOI: https://doi.org/10.1021/ma801843a

[66] Berg E.V.D.; Meijer, E.W. Poly (propylene imine) dendrimers: large scale synthesis by hetrogenously catalyzed hydrogenation. *Angew* **1993**, 32, 1308–1311. DOI: https://doi.org/10.1002/anie.199313081

[67] Sherje, A.P.; Jadhav, M.; Dravyakar, B.R.; Kadam, D. Dendrimers: A versatile nanocarrier for drug delivery and targeting. *Int. J. Pharm.* **2018**, 548, 707-720. DOI: https://doi.org/10.1002/anie.199313081

[68] Vaidya, A.; Jain, S.; Pathak, K.; Pathak, D. Dendrimers: Nanosized Multifunctional Platform for Drug Delivery. *Drug. Deliv. Lett.* **2017**, 8, 3-19. DOI: https://doi.org/10.2174/2210303107666171109112523

[69] Maciejewski, M. Concepts of trapping topologically by shell molecules. *Macromol. Sci. Chem. A* **1982**, 17, 689-703. DOI: https://doi.org/10.1080/00222338208062416

[70] Cloninger, M.J. Biomedical applications of dendrimers. *Curr. Opin. Chem. Biol.* **2002**, 6, 742-748. DOI: https://doi.org/10.1016/S1367-5931(02)00400-3

[71] Owens, D.E.; Peppas, N.A. Opsonization, biodistribution, and pharmacokinetics of polymeric nanoparticles. *Int. J. Pharm.* **2006**, 307, 93-102. DOI: https://doi.org/10.1016/j.ijpharm.2005.10.010

[72] Peracchia, M.T.; Harnisch, S.; Pinto-Alphandary, H.; Gulik, A.; Dedieu, J.C.; Desmaele, D.; *et al.* Visualization of in vitro protein-rejecting properties of PEGylated

stealth polycyanoacrylate nanoparticles. *Biomaterials* **1999**, 20, 1269–1275. DOI: https://doi.org/10.1016/S0142-9612(99)00021-6

[73] Brigger, I.; Dubernet, C.; Couvreur, P. Nanoparticles in cancer therapy and diagnosis. *Adv. Drug Deliv. Rev.* **2002**, 54, 631-651. DOI: https://doi.org/10.1016/s0169-409x(02)00044-3

[74] Storm, G.; Belliot, S.O; Daemen, T.; Lasic, D.D. Surface modification of nanoparticles to oppose uptake by the mononuclear phagocyte system. *Adv. Drug Deliv. Rev.* **1995**, 17, 31–48. DOI: https://doi.org/10.1016/0169-409X(95)00039-A

[75] Torchilin, V.P; Trubetskoy, V.S. Which polymers can make nanoparticulate drug carriers long-circulating?. *Adv. Drug Deliv. Rev.* **1995**, 16, 141–155. DOI: https://doi.org/10.1016/0169-409X(95)00022-Y

[76] Peracchia, M. T.; Fattal, E.; Desmaële, D.; Besnard, M.; Noël, J. P.; Gomis, J.M. Stealth® PEGylated polycyanoacrylate nanoparticles for intravenous administration and splenic targeting. *J. Control. Release* **1999**, 60, 121–128. DOI: https://doi.org/10.1016/S0168-3659(99)00063-2

[77] Wijagkanalan, W.; Kawakami, S.; Hashida, M. Designing dendrimers for drug delivery and imaging: Pharmacokinetic considerations. *Pharm. Res.* **2011**, 28, 1500-1519. DOI: https://doi.org/10.1007/s11095-010-0339-8

[78] Kaminskas, L.M.; Boyd, B.J; Porter, C.J.H. Dendrimer pharmacokinetics: the effect of size, structure and surface characteristics on ADME proprieties. *Nanomedicine* **2011**, 6, 1063-1084. DOI: https://doi.org/10.2217/NNM.11.67

[79] Moghimi, S.M.; Hedeman, H.; Muir, I.S.; Illum, L.; Davis, S.S. An investigation of the filtration capacity and the fate of large filtered sterically-stabilized microspheres in rat spleen. *Biochin. Biophys.* **1993**, 1157, 233–240. DOI: https://doi.org/10.1016/0304-4165(93)90105-H

[80] Porter, C.J.H.; Moghimi, S.M.; Illum, L.; Davis, S.S. The polyoxyethylene polyoxypropylene block copolymer Poloxamer-407 selectively redirects intravenously

injected microspheres to sinusoidal endothelial-cells of rabbit bone-marrow. *FEBS Lett.* **1992**, 305, 62–66. DOI: https://doi.org/10.1016/0014-5793(92)80655-Z

[81] Malik, N.; Evagorou, E.G.; Duncan, R. Dendrimer-platinate: a novel approach to cancer chemotherapy. *Anticancer Drugs* **1999**, 10, 767–776. DOI: https://doi.org/10.1097/00001813-199909000-00010

[82] Margerum, L.D.; Campion, B.K.; Koo, M.; Shargill, N.; Lai, J.; Marumoto, A;, *et al.* Gadolinium (III)DO3A macrocycles and polyethylene glycol coupled to dendrimers: Effect of molecular weight on physical and biological properties of macromolecular magnetic resonance imaging contrast agents. *J. Alloys Compd*. **1997,** 249, 185–190. DOI: https://doi.org/10.1016/S0925-8388(96)02830-7

[83] Xiao, K.; Li, Y.; Luo, J.; Lee, J.S.; Xiao, W.; Gonik, A.M.; *et al.* The effect of surface charge on in vivo biodistribution of PEG-oligocholic acid based micellar nanoparticles. *Biomaterials* **2011**, 32, 3435-3446. DOI: https://doi.org/10.1016/j.biomaterials.2011.01.021

[84] Maeda, H. Tumor-selective delivery of macromolecular drugs via the EPR effect: background and future prospects. *Bioconjug. Chem.* **2010**, 21, 797–802. DOI: https://doi.org/10.1021/bc100070g

[85] Abedi-Gaballu, F.; Dehghan, G.; Ghaffari, M.; Yekta, R.; Abbaspour-Ravasjani, S.; Baradaran, B.*; et al.* PAMAM dendrimers as efficient drug and gene delivery nanosystems for cancer therapy. *Appl. Mater. Today* **2018**, 12, 177-190. DOI: https://doi.org/10.1016/j.apmt.2018.05.002

[86] Chauhan, A.S. Dendrimers for Drug Delivery. *Molecules* **2018**, 23, 938-946. DOI: https://doi.org/10.3390/molecules23040938

[87] Kumar, A.S.P.; Latha, S.; Selvamani, P.; Dendrimers: multifunctional drug delivery carriers. *Int. J. Technol. Res. Engine.* **2015***,* 2, 1569–1575. Available in URL: https://www.researchgate.net/publication/341895126_Dendrimers_Multifunctional_Drug_Delivery_Carriers

[88] Singh, J.; Jain, K.; Kumar, N.; Jain, N.K. Dendrimers in anticancer drug delivery: mechanism of interaction of drug and dendrimers. *Artif. Cells Nanomed. Biotechnol.* **2016**, 44, 1626–1634. DOI: https://doi.org/10.3109/21691401.2015.1129625

[89] Hughes, G. A. Nanostructure-mediated drug delivery. *Nanomedicine: Nanotechnology, Biology and Medicine,* **2015***, 1, 22–30.* DOI: https://doi.org/10.1016/j.nano.2004.11.009

[90] Cheng, Y.; Xu, Z.; Ma, M., Xu, T. Dendrimers as drug carriers: Applications in different routes of drug administration. *J. Pharm. Sci.* **2008**, 97, 123-143. DOI: https://doi.org/10.1002/jps.21079

[91] Liu, M.; Fréchet, J.M. Designing dendrimers for drug delivery. *Pharm. Sci. Technol. Today* **1999**, 2, 393–401. DOI: https://doi.org/10.1016/s1461-5347(99)00203-5

[92] Devarakonda, B.; Hill, R.A.; de Villiers, M.M. The effect of PAMAM dendrimer generation size and surface functional group on the aqueous solubility of nifedipine. *Int. J. Pharm.* **2004**, 284, 133-140. DOI: https://doi.org/10.1016/j.ijpharm.2004.07.006

[93] Caminade, A.M.; Turrim, C.O. Dendrimers for drug delivery. *J. Mater. Chem. B* **2014**, 2, 4055–4066. DOI: https://doi.org/10.1039/c4tb00171k

[94] Jain, K.; Jain, N.K. Dendrimers as Nanobiopolymers in Cancer ChemoTherapy. *Nanobiomedicine* **2015**, 65–90. DOI: https://doi.org/10.1201/9781315364513-9

[95] Milhem, O.M.; Myles, C.; McKeown, N.B.; Attwood, D.; D'Emanuele, A. Polyamidoamine Starburst dendrimers as solubility enhancers. *Int. J. Pharm.* **2000,** 197, 239-41. DOI: https://doi.org/10.1016/s0378-5173(99)00463-9

[96] Patri, A.K.; Kukowskalatallo, J.F.; Baker, J.R. Targeted drug delivery with dendrimers: comparison of the release kinetics of covalently conjugated drug and non-covalent drug inclusion complex. *Adv. Drug Deliv. Rev*. **2005**, 57, 2203–2214. DOI: https://doi.org/10.1016/j.addr.2005.09.014

[97] V. Patel; Rajani, C.; Paul, D.; Borisa, P.; Rajpoot, K; Youngren-Ortiz, S.R.; *et al.* Dendrimers as novel drug-delivery system and its applications. *Adv. Pharmacol.* **2020**, 333–392. DOI: https://doi.org/10.1016/B978-0-12-814487-9.00008-9

[98] Mignani, S.; El Kazzouli, S.; Bousmina, M.; Majoral, J.P. Expand classical drug administration ways by emerging routes using dendrimer drug delivery systems: A concise overview. *Adv. Drug Deliv. Rev.* **2013**, 65, 1316-1330. DOI: https://doi.org/10.1016/j.addr.2013.01.001

[99] Moghimi, S.M.; Bonnemain, B. Subcutaneous and intravenous delivery of diagnostic agents to the lymphatic system: Applications in lymphoscintigraphy and indirect lymphography. *Adv. Drug Deliv. Rev.* **1999**, 37, 295–312. DOI: https://doi.org/10.1016/s0169-409x(98)00099-4

[100] Gebbia, V.; Puozzo, C. Oral versus intravenous vinorelbine: Clinical safety profile. *Expert. Opin. Drug Saf.* **2005**, 4, 915–928. DOI: https://doi.org/10.1517/14740338.4.5.915

[101] Yellepeddi, V.K.; Ghandehari, H. Pharmacokinetics of oral therapeutics delivered by dendrimer-based carriers. *Expert. Opin. Drug Deliv.* **2019**, 16, 1051–1061. DOI: https://doi.org/10.1080/17425247.2019.1656607

[102] Csaba, N.; Garcia-Fuentes, M.; Alonso, M.J. The performance of nanocarriers for transmucosal drug delivery. *Expert. Opin. Drug Deliv.* **2006**, 3, 463–78. DOI: https://doi.org/10.1517/17425247.3.4.463

[103] Malingre, M.M.; Beijnen, J.H.; Schellens, J.H.M. Oral delivery of taxanes. *Invest. New Drugs* **2001**, 19, 155–62. DOI: https://doi.org/10.1023/a:1010635000879

[104] Kitchens, K.M; Kolhatkar, R.B.; Swaan, P.W.; Eddington, N.D.; Ghandehari, H. Transport of poly (amidoamine) dendrimers across Caco-2 cell monolayers: infuence of size, charge and fluorescent labeling. *Pharm. Res.* **2006**, 23, 2818–2826. DOI: https://doi.org/10.1007/s11095-006-9122-2

[105] Yellepeddi, V.K.; Mohammadpour, R.; Kambhampati, S.P.; Sayre, C.; Mishra, K.; Kannan, R.M.; *et al.* Pediatric oral formulation of dendrimerN-acetyl-l-cysteine conjugates for the treatment of neuroinfammation. *Int. J. Pharm.* **2018**, 545, 113–116. DOI: https://doi.org/10.1016/j.ijpharm.2018.04.040

[106] Sardo, H.S.; Saremnejad, F.; Bagheri, S.; Akhgari, A.; Garekani, A.; Sadeghi, F. A review on 5-aminosalicylic acid colon-targeted oral drug delivery systems. *Int. J. Pharm.* **2019**, 558, 367–379. DOI: https://doi.org/10.1016/j.ijpharm.2019.01.022

[107] Ramachandran, C.; Fleisher, D. Transdermal delivery of drugs for the treatment of bone diseases. *Adv. Drug Deliv. Rev.* **2000**, 42, 197–223. DOI: https://doi.org/10.1016/s0169-409x(00)00062-4

[108] Argenta, D.F.; Martelli, S.M.; Caon, T. Dendrimer as a platform for drug delivery in the skin. *Biomed. Mater. Eng.* **2019**, 331–36. DOI: https://doi.org/10.1016/B978-0-12-818433-2.00010-8

[109] Cheng, Y.; Man, N.; Xu, T.; Fu, R.; Wang, X.; Wang, X.; Wen, L. Transdermal delivery of nonsteroidal anti-inflammatory drugs mediated by polyamidoamine (PAMAM) dendrimers. *J. Pharm. Sci.* **2007**, 96, 595–602. DOI: https://doi.org/10.1002/jps.20745

[110] Thomas, B.J.; Finnin, B.C. The transdermal revolution. *Drug Discov. Today* **2004**, 9, 697–703. DOI: https://doi.org/10.1016/S1359-6446(04)03180-0

[111] Movliya, R.V.; Patel, P.M. Role of dendrimer in drug solubilisation—a review. *Drug Deliv. Lett.* **2019**, 9, 265–276. DOI: https://doi.org/10.2174/2210303109666190319165209

[112] Manikkath, J.; Hedge, A.R.; Kalthur, G.; Perekh, H.S.; Mutalik, S. Infuence of peptide dendrimers and sonophoresis on the transdermal delivery of ketoprofen. *Int. J. Pharm.* **2017**, 521, 110–119. DOI: https://doi.org/10.1016/j.ijpharm.2017.02.002

[113] Manikkath, J.; Manikkath, A.; Shavi, G.V.; Bhat, K.; Mutalik, S. Low frequency ultrasound and PAMAM dendrimer facilitated transdermal delivery of ketoprofen. *J. Drug Deliv. Sci. Technol.* **2017**, 41, 334–343. DOI: https://doi.org/10.1016/j.jddst.2017.07.021

[114] Huang, B.; Dong, W.; Yang, G.; Wang, W.; Ji, C.; Zhou, F. Dendrimer-coupled sonophoresis-mediated transdermal drug-delivery system for diclofenac. *Drug Des. Dev. Ther.* **2015**, 9, 3867-3876. DOI: https://doi.org/10.2147/DDDT.S75702

[115] Mulligan, R.C. The basic science of gene therapy. *Science* **1993**, 260, 926–932. DOI: https://doi.org/10.1126/science.8493530

[116] Santos, J.L; Rodrigues, J.; Pêgo, A.; Granja, P.; Tomás, H. Non-viral gene delivery to mesenchymal stem cells: methods, strategies and application in bone tissue engineering and regeneration. *Curr. Gene Ther.* **2011**, 111, 46-57. DOI: https://doi.org/10.2174/156652311794520102

[117] Kane, N.M.;McRae, S.; Denning, C.; Baker, A.H. Viral and non-viral gene delivery and its role in pluripotent stem cell engineering. *Drug Discov. Today: Technol.* **2008**, 5, 107-115. DOI: https://doi.org/10.1016/j.ddtec.2008.10.002

[118] Li, S.D.; Huang, L. Non-viral is superior to viral gene delivery. *J. Control. Release* **2007**, 123, 181-83. DOI: https://doi.org/10.1016/j.ddtec.2008.10.002

[119] Mastrobattista, E.; Bravo, S.A.; van der Aa, M.; Crommelin, D. Nonviral gene delivery systems: from simple transfection agents to artificial viruses. *Drug Discov. Today: Technol.* **2005**, 2, 103-109. DOI: https://doi.org/10.1016/j.ddtec.2005.04.002

[120] N. Tomar, Dendrimers as nanocarriers in cancer chemotherapy. *Int. J. Chem. Eng.* **2019**, 5, 14 – 32. Available in URL: https://www.researchgate.net/publication/341911619_Dendrimers_as_Nanocarriers_in_Cancer_Chemotherapy

[121] Hu, J.; Hu, K.; Cheng, Y. Tailoring the dendrimer core for efficient gene delivery. *Acta Biomater*. **2016**, 35, 1–11. DOI: https://doi.org/10.1016/j.actbio.2016.02.031

[122] Amreddy, N.; Babu, A.; Panneerselvam, J.; Srivastava, A.; Muralidharan, R.; Chen, A.; *et al.* Chemo-biologic combinatorial drug delivery using folate receptor-targeted dendrimer nanoparticles for lung cancer treatment. *Nanomed. Nanotechnol. Biol. Med.* **2018**, 14, 373–384. DOI: https://doi.org/10.1016/j.nano.2017.11.010

[123] Haensler, F.C.; Szoka, Jr. Polyamidoamine cascade polymers mediate efcient transfection of cells in culture. *Bioconjugate Chem*. **1993**, 4, 372–379. DOI: https://doi.org/10.1021/bc00023a012

[124] Wang, H; Zhao, X.; Guo, C., Ren, D.; Zhao, Y.; Xiao, W.; Jiao, W. Aptamer-dendrimer bioconjugates for targeted delivery of miR34a expressing plasmid and antitumor efects in non-small cell lung cancer cells. *PLoS ONE* **2015**, 10, 1-15 DOI: https://doi.org/10.1371/journal.pone.0139136

[125] Kukowska-Latallo, J.F.; Raczka, E.; Quintana, A.; Chen, C.; Rymaszewski, M.; Baker, J.R. Intravascular and endobronchial DNA delivery to murine lung tissue using a novel, nonviral vector. *Hum. Gene Ther.* **2000**, 11, 1385–1395. DOI: https://doi.org/10.1089/10430340050057468

[126] Ramalingam, K.; Castro, R.; Pires, P.; Shi, X.; Rodrigues, J.; Xiao, S.; *et al.* Gene delivery using dendrimer/pDNA complexes immobilized in electrospun fibers using the Layer-By-Layer technique. *RSC ADV*. **2016**, 6, 97116-97128. DOI: https://doi.org/10.1039/C6RA22444J

[127] Xiao, S.; Castro, R.; Rodrigues, J.; Shi, X.; Tómas, H. PAMAM Dendrimer/pDNA Functionalized-Magnetic Iron Oxide Nanoparticles for Gene Delivery. *J. Biomed*. **2015**, 11, 1370-1384. DOI: https://doi.org/10.1166/jbn.2015.2101

[128] Wolinsky, J.B.; Grinstaff, M.W. Therapeutic and diagnostic applications of dendrimers for cancer treatment. *Adv. Drug Deliv. Rev.* **2008**, 60, 1037-1055. DOI: https://doi.org/10.1016/j.addr.2008.02.012

[129] Oliveira, J.M.; Salgado, A.J.; Sousa, N.; Mano, J.F.; Reis, R.L. Dendrimers and derivatives as a potential therapeutic tool in regenerative medicine strategies-A review. *Prog. Polym. Sci.* **2010**, 35, 1163–1194. DOI: https://doi.org/10.1016/J.PROGPOLYMSCI.2010.04.006

[130] Jang, W.D.; Selim, K.M.K. Lee C.H.; Kang, I.K. Bioinspired application of dendrimers: from bio-mimicry to biomedical applications. *Prog. Polym. Sci.* **2009**, 34, 1–23. DOI: https://doi.org/10.1016/j.progpolymsci.2008.08.003

[131] Noriega-Luna, B.; Godínez, L.A.; Rodríguez, F.J.; Rodriguez, A.; Larrea, G.Z.; Sosa-Ferreyra, C.F.; *et al.* Applications of dendrimers in drug delivery agents, diagnosis, therapy, and detection. *J. Nanomater*. **2014**, 2014, 1-19. DOI: https://doi.org/10.1155/2014/507273

[132] Patri, A.K.; Majoros, I.J.; Baker Jr., J.R. Dendritic polymer macromolecular carriers for drug delivery. *Curr. Opin. Chem. Biol.* **2002**, 6, 466–471. DOI: https://doi.org/10.1016/s1367-5931(02)00347-2

[133] Wiener, E.; Brechbiel, M.W.; Brothers,H.; Magin, R.L.; Gansow,O.A.; Tomalia, D.A.; Lauterbur, P.C. Dendrimer-based metal chelates: a new class of magnetic resonance imaging contrast agents. *Magn. Reson. Med.* **1994**, 31, 1–8. DOI: https://doi.org/10.1002/mrm.1910310102

[134] Kalender, W.A. X-ray computed tomography. *Phys. Med. Biol.* **2006**, 51. R29-43 DOI: https://doi.org/10.1088/0031-9155/51/13/R03

[135] Peng, C.; Wang, H.; Guo, R.; Shen, M.; Cao, X.; Zhu, M., *et. al.* Acetylation of dendrimer-entrapped gold nanoparticles: synthesis, stability, and X-ray attenuation properties. *J. Appl. Polym. Sci.* **2011**, 119, 1673–1682. DOI: https://doi.org/10.1002/app.32845

[136] Liu, H.; Wang, H.; Guo, R.; Cao, X.; Zhao,Z.; Luo, Y.; *et al.* Size controlled synthesis of dendrimer-stabilized silver nanoparticles for X-ray computed tomography imaging applications. *Polym. Chem.* **2010**, 1, 1677–1683. DOI: https://doi.org/10.1039/C0PY00218F

[137] Umeda, Y.; Kojima, C.; Harada, A.; Horinaka, H.; Kono, K. PEGattached PAMAM dendrimers encapsulating gold nanoparticles: growing gold nanoparticles in the dendrimers for improvement of their photothermal properties. *Bioconjug. Chem.* **2010**, 21, 1559– 1564. DOI: https://doi.org/10.1021/bc1001399

[138] Kojima, C.; Umeda, Y.; Ogawa, M.; Harada, A.; Magata, Y.; Kono, K. X-ray computed tomography contrast agents prepared by seeded growth of gold nanoparticles in PEGylated dendrimer. *Nanotechnology* **2010**, 21, 245104. DOI: https://doi.org/10.1088/0957-4484/21/24/245104

[139] Kojima, C.; Cho, S.H.; Higuchi, E. Gold nanoparticle-loaded PEGylated dendrimers for theragnosis. *Res. Chem. Intermed*. **2012**, 38, 1279–1289. DOI: https://doi.org/10.1007/s11164-011-0466-9

[140] Zhu, Z.; Zheng, L.; Wen, S.; Tang, Y.; Shen, M.; Zhang, G.; Shi, X. Targeted cancer theranostics using alpha-tocopheryl succinate-conjugated multifunctional dendrimer-entrapped gold nanoparticles. *Biomaterials* **2014**, 35, 7635–7646. DOI: https://doi.org/10.1016/j.biomaterials.2014.05.046

[141] Singh, V.; Sahebkar, A.; Kesharwani, P. Poly (propylene imine) dendrimer as an emerging polymeric nanocarrier for anticancer drug and gene delivery. *Eur. Polym. J.* **2021**, 158, 110683. DOI: https://doi.org/10.1016/j.eurpolymj.2021.110683

[142] Sung, H.; Ferlay, J.; Siegel, R.L.; Laversanne, M.; Soerjomataram, I.; Jemal, A.; Bray, F. Global cancer statistics 2020: GLOBOCAN estimates of incidence and mortality worldwide for 36 cancers in 185 countries, *CA, Cancer J. Clin.* **2021**, 71, 209–249, DOI: https://doi.org/10.3322/caac.21660

[143] Sutradhar, K.B.; Amin, Md.L. Nanotechnology in Cancer Drug Delivery and Selective Targeting. *ISRN Nanotechnology* **2014**, 2014, 1-12. DOI: https://doi.org/10.1155/2014/939378

[144] Singh, O.P., Nehru, R.M. Nanotechnology and cancer treatment. *Asian J Exp Sci.* **2008**, 22, 6. DOI: https://doi.org/10.4236/anp.2013.22023

[145] DeVita, V.T.; Chu, E. A History of Cancer Chemotherapy. *Cancer Res.* **2008**, 68, 8643−8653. DOI: https://doi.org/10.1158/0008-5472.CAN-07-6611

[146] Jabir, N.R.; Tabrez, S.; Ashraf, G.M.; Shakil, S.; Damanhouri, G.A.; Kamal, M.A Nanotechnology-based approaches in anticancer research. *Int. J. Nanomedicine* **2012**, 7, 4391–4408. DOI: https://doi.org/10.2147/IJN.S33838

[147] Chidambaram, M.; Manavalan, R.; Kathiresan, K. Nanotherapeutics to overcome conventional cancer chemotherapy limitations. *J Pharm Pharm Sci.* **2011**, 14, 67–77. DOI: https://doi.org/10.18433/J30C7D

[148] Tannock, I.F.; Lee, C.M.; Tunggal, J.K.; Cowan, D.S.M.; Egorin, M.J. Limited penetration of anticancer drugs through tumor tissue: a potential cause of resistance of solid tumors to chemotherapy. *Clin. Cancer Res.* **2002**, 8, 878– 884. Available in URL: https://aacrjournals.org/clincancerres/article/8/3/878/289217/Limited-Penetration-of-Anticancer-Drugs-through

[149] Clemons, T.D.; Singh, R.; Sorolla, A.; Chaudhari, N.; Hubbard, A.; Iyer, K.S. Distinction between Active and Passive Targeting of Nanoparticles Dictate Their Overall Therapeutic Efficacy. *Langmuir* **2018**, 34, 15343-15349. DOI: https://doi.org/10.1021/acs.langmuir.8b02946

[150] Praetorius, N.P.; Mandal, T.K. Engineered nanoparticles in cancer therapy. *Recent Pat. Drug Deliv. Formul.* **2007**, 1, 37–51. DOI: https://doi.org/10.2174/187221107779814104

[151] Park, K. Nanotechnology: what it can do for drug delivery. *J. Control. Release* **2007**, 120, 1–3. DOI: https://doi.org/10.1016/j.jconrel.2007.05.003

[152] Folkman, J. Angiogenesis in cancer, vascular, rheumatoid and other disease. *Nat. Med*. **1995**, 1, 27–31. DOI: https://doi.org/10.1038/nm0195-27

[153] Iyer, A.K.; Khaled, G.; Fang, J.; Maeda, H. Exploiting the enhanced permeability and retention effect for tumor targeting. *Drug Discov. Today*. **2006**, 11, 812-818. DOI: https://doi.org/10.1016/j.drudis.2006.07.005

[154] Matsumura, Y.; Maeda, H. A new concept for macromolecular therapeutics in cancer chemotherapy: mechanism of tumoritropic accumulation of proteins and the antitumor agent smancs. *Cancer Res.* **1986**, 46, 6387–6392. Available in URL: https://aacrjournals.org/cancerres/article/46/12_Part_1/6387/490212/A-New-Concept-for-Macromolecular-Therapeutics-in

[155] Ganoth, A., Merimi, K.C.; Peer, D. Overcoming multidrug resistance with nanomedicines. *Expert Opin. Drug Deliv.* **2015**, 12, 223-238. DOI: https://doi.org/10.1517/17425247.2015.960920

[156] Davis, M.E; Chen, Z.G.; Shin, D.M. Nanoparticle therapeutics: an emerging treatment modality for cancer. *Nat. Rev. Drug Discov.* **2008**, 7, 771-782. DOI: https://doi.org/10.1038/nrd2614

[157] Morales-Cruz, M.; Delgado, Y.; Castillo, B.; Figueroa, C.M.; Molina, A.M.; Torres, A.; *et al.* Smart targeting to improve cancer therapeutics. *Drug Des. Devel. Ther.* **2019**, 13, 3753-3772. DOI: https://doi.org/10.2147/DDDT.S219489

[158] Jain, R.K. Transport of molecules, particles, and cells in solid tumors. *Annu. Rev. Biomed. Eng*. **1999**, 1, 241-263. DOI: https://doi.org/10.1146/annurev.bioeng.1.1.241

[159] Forster, J. C.; Harriss-Phillips, W.M.; Douglass M.J.; Bezak, E.; *et al.* A review of the development of tumor vasculature and its effects on the tumor microenvironment. *Hypoxia* **2017**, 5, 21–32. DOI: https://doi.org/10.2147/HP.S133231

[160] Liu, D.; Mori, A.; Huang, L. Role of liposome size and RES blockade in controlling biodistribution and tumor uptake of GM1-containing liposomes. *Biochim. Biophys. Acta* **1992**, 1104, 95–101. DOI: https://doi.org/10.1016/0005-2736(92)90136-a

[161] Nagayasu, A.; Shimooka, T, Kinouchi, Y.; Uchiyama, K.; Takeichi, Y.; Kiwada, H. Effects of fluidity and vesicle size on antitumor activity and myelosuppressive activity of liposomes loaded with daunorubicin. *Biol. Pharm. Bull.* **1994**, 17, 935–939. DOI: https://doi.org/10.1248/bpb.17.935

[162] Nagahara, L.A.; Lee, J.S.H.; Molnar, L.K.; Panaro, N.; Farrell, D.; Ptak, K.; *et al.* Strategic workshops on cancer nanotechnology. *Cancer Res.* **2010**, 70, 4265–4268. DOI: https://doi.org/10.1158/0008-5472.CAN-09-3716

[163] Jain, R. K. Barriers to Drug-Delivery in Solid Tumors. *Sci. Am.* **1994**, 271, 58−65. DOI: https://doi.org/10.1038/scientificamerican0794-58

[164] Peer, D.; Karp, J. M.; Hong, S.; FarokHzad, O. C.; Margalit, R.; Langer, R. Nanocarriers as an emerging platform for cancer therapy. *Nat. Nanotechnol*. **2007**, 2, 751−760. DOI: https://doi.org/10.1038/nnano.2007.387

[165] Bazak, R.; Houri, M.; el Achy, S.; Kamel, S.; Refaat, T. Cancer active targeting by nanoparticles: a comprehensive review of literature. *J. Cancer Res. Clin. Oncol.* **2015**, 141, 769-784. DOI: https://doi.org/10.1007/s00432-014-1767-3

[166] Dong, X.; Mumper, R.J. Nanomedicinal strategies to treat multidrugresistant tumors: current progress. *Nanomedicine* (*Lond*) **2010**, 5, 597–615. DOI: https://doi.org/10.2217/nnm.10.35

[167] Kohler, G.; Milstein, C. Continuous cultures of fused cells secreting antibody of predefined specificity. *Nature* **1975**, 256, 495–497. DOI: https://doi.org/10.1038/256495a0

[168] Drugs. Orthoclone OKT3. https://www.drugs.com/pro/orthoclone-okt3.html (accessed June 16, 2022)

[169] Thistlethwaite, J.R; Cosimi, A.B.; Delmonico, F.L.; Rubin, R.H.; TalkoffRubin, N.; Nelson, P.W.; *et al.* Evolving use of OKT3 monoclonal antibody for treatment of renal allograft rejection. *Transplantation* **1984**, 38, 695–701. Available in URL: https://journals.lww.com/transplantjournal/Abstract/1984/12000/EVOLVING_USE_OF_OKT3_MONOCLONAL_ANTIBODY_FOR.29.aspx

[170] Alexis, F.; Basto, P.; Levy-Nissenbaum, E.; Radovic-Moreno, A.F.; Zhang, L.; Pridgen, E.; *et al.* HER-2-targeted nanoparticle-affibody bioconjugates for cancer therapy. *Chem. Med. Chem.* **2008**, 3, 1839–1843. DOI: https://doi.org/10.1002/cmdc.200800122

[171] Puri, A.; Kramer-Marek, G.; Campbell-Massa, R.; Yavlovich, A.; Tele, S.C.; Lee, S.; et al. HER2-Specific Affibody-Conjugated Thermosensitive Liposomes (Affisomes) for Improved Delivery of Anticancer Agents. *J. Liposome Res.* **2008**, 18, 293 - 307. DOI: https://doi.org/10.1080/08982100802457377

[172] Reddy, J.A.; Allagadda, V.M.; Leamon, C.P. Targeting therapeutic and imaging agents to folate receptor positive tumors. *Curr. Pharm. Biotechnol*. **2005**, 6, 131-50. DOI: https://doi.org/10.2174/1389201053642376

[173] Leamon, C.P.; Reddy, J.A. Folate targeted chemotherapy. *Adv. Drug Delivery Rev.* **2004**, 56, 1127–1141. DOI: https://doi.org/10.1016/j.addr.2004.01.008

[174] Nahta, R.; Yu, D.; Hung, M.C.; Hortobagyi, G.N.; Esteva, F.J. Mechanisms of disease: understanding resistance to HER2- targeted therapy in human breast cancer. *Nat. Clin. Pract. Oncol.* **2006**, 3, 269–280. DOI: https://doi.org/10.1038/ncponc0509

[175] Spector, N.L.; Blackwell, K.L. Understanding the mechanisms behind trastuzumab therapy for human epidermal growth factor receptor 2-positive breast cancer. *J. Clin. Oncol.* **2009**, 27, 5838–584. DOI: https://doi.org/10.1200/JCO.2009.22.1507

[176] Wartlick, H.; Michaelis, K.; Balthasar, S.; Strebhardt, K.; Kreuter, J.; Langer, K. Highly specific HER2-mediated cellular uptake of antibody-modified nanoparticles in tumour cells. *J. Drug Target*. **2004**, 12, 461–471. DOI: https://doi.org/10.1080/10611860400010697

[177] Thorne, A.H.; Zanca, C.; Furnari, F. Epidermal growth factor receptor targeting and challenges in glioblastoma. *Neuro. Oncol*. **2016**, 18, 914–918. DOI: https://doi.org/10.1093/neuonc/nov319

[178] Harding, J.; Burtness, B. Cetuximab: an epidermal growth factor receptor chemeric human-murine monoclonal antibody. *Drugs Today (Barc)* **2005**, 41, 107–127. DOI: https://doi.org/10.1358/dot.2005.41.2.882662

[179] Hrkach, J.; Von Hoff, D.; Mukkaram, Ali, M.; Andrianova, E.; Auer, J.; Campbell, T.; et al. Preclinical development and clinical translation of a PSMA-targeted docetaxel nanoparticle with a differentiated pharmacological profile. *Sci. Transl. Med.* **2012**, 4, 128ra39. DOI: https://doi.org/10.1126/scitranslmed.3003651

[180] Taylor, R.M.; Huber, D.L.; Monson, T.C.; Ali, A.M.; Bisoffi M; Sillerud, L.O. Multifunctional iron platinum stealth immunomicelles: targeted detection of human prostate cancer cells using both fluorescence and magnetic resonance imaging. *J. Nanopart. Res.* **2011**, 13, 4717–4729. DOI: https://doi.org/10.1007/s11051-011-0439-3

[181] Ni, X., Castanares, M.; Mukherjee, A.; Lupold, S.E. Nucleic acid aptamers: clinical applications and promising new horizons. *Curr. Med. Chem.* **2011**, 18, 4206–4214. DOI: https://doi.org/10.2174/092986711797189600

[182] White, B.D.; Duan, C., Townley, H.E. Nanoparticle activation methods in cancer treatment. *Biomolecules* **2019**, 9, 202. DOI: https://doi.org/10.3390/biom9050202

[183] Justus, C.R.; Dong, L.; Yang, L.V. Acidic tumor microenvironment and pH-sensing G protein-coupled receptors. *Front. Physiol.* **2013**, 4, 354. DOI: https://doi.org/10.3389/fphys.2013.00354

[184] Barar, J.; Omidi, Y. Dysregulated pH in tumor microenvironment checkmates cancer therapy. *Bioimpacts* **2013**, 3, 149–162. DOI: https://doi.org/10.5681/bi.2013.036

[185] Kato, Y.; Ozawa, S.; Miyamoto, C.; Maehata, Y.; Suzuki, A.; Maeda, T.; *et al.* Acidic extracellular microenvironment and cancer. *Cancer Cell Int.* **2013**, 13, 89. DOI: https://doi.org/10.1186/1475-2867-13-89

[186] Glunde, K.; Guggino, S.E.; Solaiyappan, M.; Pathak, A.P.; Ichikawa, Y.; Bhujwalla, Z.M. Extracellular acidification alters lysosomal trafficking in human breast cancer cells. *Neoplasia* **2003**, 5, 533–545. DOI: https://doi.org/10.1016/s1476-5586(03)80037-4

[187] Griset, A.P.; Walpole, J.; Liu, R.; Gaffey, A.; Colson, Y.L.; Grinstaff, M.W. Expansile Nanoparticles: Synthesis, Characterization, and in Vivo Efficacy of an Acid-Responsive Polymeric Drug Delivery System. *J. Am. Chem. Soc.* **2009**, 131, 2469–2471. DOI: https://doi.org/10.1021/ja807416t

[188] Muniswamy, V.J.; Raval, N.; Gondaliya, P.; Tambe, V.; Kalia, K.; Tekade, R.K. 'Dendrimer-Cationized-Albumin' encrusted polymeric nanoparticle improves BBB penetration and anticancer activity of doxorubicin. *Int. J. Pharm*. **2019**, 555, 77–99. DOI: https://doi.org/10.1016/j.ijpharm.2018.11.035

[189] Kim, D.; Lee, E.S.; Park, K.; Kwon, I.C.; Bae, Y.H. Doxorubicin loaded pH-sensitive micelle: antitumoral efficacy against ovarian A2780/DOXR tumor. *Pharm. Res.* **2008**, 25, 2074–2082. DOI: https://doi.org/10.1007/s11095-008-9603-6

[190] Mannaris, C.; Teo, B.M.; Seth, A.; Bau, L.; Coussios, C.; Stride, E. Gas-Stabilizing Gold Nanocones for Acoustically Mediated Drug Delivery. *Adv. Healthc. Mater*. **2018**, 7, 1800184. DOI: https://doi.org/10.1002/adhm.201800184

[191] Decock, J.; Obermajer, N.; Vozelj, S.; Hendrickx, W.; Paridaens, R.; Kos, J. Cathepsin B, cathepsin H, cathepsin X and cystatin C in sera of patients with early-stage and inflammatory breast cancer. *Int. J. Biol. Mark*. **2008**, 23, 161–168. DOI: https://doi.org/10.5301/JBM.2008.3270

[192] Villar-Alvarez, E.; Cambón, A.; Pardo, A.; Mosquera, V.X.; Bouzas-Mosquera, A.; Topete, A.; *et al.* Gold Nanorod-Based Nanohybrids for Combinatorial Therapeutics. *ACS Omega* **2018**, 3, 12633–12647. DOI: https://doi.org/10.1021/acsomega.8b01591

[193] Davies, G.; Henrissat, B. Structures and mechanisms of glycosyl hydrolases. *Structure* **1995**, 3, 853–859. DOI: https://doi.org/10.1016/S0969-2126(01)00220-9

[194] Dzamukova, M.R.; Naumenko, E.A.; Lvov, Y.M.; Fakhrullin, R.F. Enzyme-activated intracellular drug delivery with tubule clay nanoformulation. *Sci. Rep.* **2015**, 5, 10560. DOI: https://doi.org/10.1038/srep10560

[195] Shin, W.S.; Kwon, J.; Lee, H.W.; Kang, M.C.; Na, H.-W.; Lee, S.-T.; Park, J.H. Oncogenic role of protein tyrosine kinase 7 in esophageal squamous cell carcinoma. *Cancer Sci.* **2013**, 104, 1120–1126. DOI: https://doi.org/10.1111/cas.12194

[196] Huang, F.; You, M.; Chen, T.; Zhu, G.; Liang, H.; Tan, W. Self-assembled hybrid nanoparticles for targeted co-delivery of two drugs into cancer cells. *Chem. Commun*. **2014**, 50, 3103. DOI: https://doi.org/10.1039/C3CC49003C

[197] Chipman, S; Oldham, F; Pezzoni, G; Singer, J.W. Biological and clinical characterization of paclitaxel poliglumex (PPX, CT-2103), a macromolecular polymer-drug conjugate. *Int. J. Nanomedicine* **2006**; 1, 375–383. DOI: https://doi.org/10.2147/nano.2006.1.4.375

[198] Lushchak, V.I. Glutathione homeostasis and functions: potential targets for medical interventions. *J Amino Acids* **2012**, 2012, 1–26. DOI: https://doi.org/10.1155/2012/736837

[199] Mortera, R.; Vivero-Escoto, J.; Slowing, I.I.; Garrone, E.; Onida, B.; Lin, V. Cell-induced intracellular controlled release of membrane impermeable cysteine from a mesoporous silica nanoparticle-based drug delivery system. *Chem. Commun*. **2009,** 22, 3219–3221. DOI: https://doi.org/10.1039/b900559e

[200] Hong, R.; Han, G.; Fernández, J.M.; Kim, B.; Forbes, N.S.; Rotello, V.M. Glutathione-mediated delivery and release using monolayer protected nanoparticle carriers. *J. Am. Chem. Soc.* **2006,** 128, 1078–1079. DOI: https://doi.org/10.1021/ja056726i

[201] Figueroa, C.M.; Suárez, B.N.; Molina, A.M.; Fernández, J.C.; Torres, Z.; Griebenow, K. Smart release nanoformulation of cytochrome C and hyaluronic acid induces apoptosis in cancer cells. *J. Nanomed. Nanotechnol*. **2017**, 8, 427. DOI: https://doi.org/10.4172/2157-7439.1000427

[202] Do, H.D; Couillaud, B.M.; Doan, B.T.; Corvis, Y.; Mignet, N. Advances on noninvasive physically triggered nucleic acid delivery from nanocarriers. *Adv. Drug Deliv. Rev*. **2019**, 138, 3–17. DOI: https://doi.org/10.1016/j.addr.2018.10.006

[203] Ponce, A.M.; Vuujaskovic, Z.; Yuan, F.; Needham, D.; Dewhirst, M. Hyperthermia mediated liposomal drug delivery. *Int. J. Hyperthermia* **2006,** 22, 205–213. DOI: https://doi.org/10.1080/02656730600582956

[204] Nakayama, M.; Akimoto, J.; Okano, T. Polymeric micelles with stimuli-triggering systems for advanced cancer drug targeting. *J. Drug Target.* **2014**, 22, 584-599. DOI: https://doi.org/10.3109/1061186X.2014.936872

[205] Pillai G. Nanomedicines for cancer therapy: an update of FDA approved and those under various stages of development. *SOJ Pharm. Pharm. Sci.* **2014**, 1, 1–13. DOI: https://doi.org/10.15226/2374-6866/1/2/00109

[206] Kwiatkowski, S.; Knap, B.; Przystupski, D.; Saczko, J.; Kędzierska, E.; Knap-Czop, K.; *et al.* Photodynamic therapy - mechanisms, photosensitizers and combinations. *Biomed. Pharmacother.* **2018**, 106, 1098-1107. DOI: https://doi.org/10.1016/j.biopha.2018.07.049

[207] Wang, G.; Tong, X.; Zhao, Y. Preparation of azobenzene-containing amphiphilic diblock copolymers for light-responsive micellar aggregates. *Macromolecules* **2004**, 37, 8911–8917. DOI: https://doi.org/10.1021/MA048416A

[208] Starpharma, VivaGel®. https://www.starpharma.com/vivagel (accessed 3 August, 2022)

[209] Dendris Molecular Diagnosis. https://dendris.fr/technology/ (accessed August 3, 2022)

[210] Dias, A.P; Santos, S.S.; Silva, J.V.; Parise-Filho, R.; Ferreira, E.I.; Seoud, O. Dendrimers in context of nanomedicine. *Int. J. Pharm*. **2020**, 573, 118814. DOI: https://doi.org/10.1016/j.ijpharm.2019.118814

[211] Siemens Healthineers. Stratus CS Acute Care - Siemens Healthineers Portugal (siemens-healthineers.com) (accessed August 3, 2022).

[212] QIAGEN. https://www.qiagen.com/us/product-categories/discovery-and-translational-research/functional-and-cell-analysis/transfection/ (accessed August 3, 2022).

[213] Starpharma, DEP® dozetaxel. https://www.starpharma.com/drug_delivery/dep_docetaxel (accessed August 3, 2022).

[214] Starpharma, DEP® cabazitaxel. https://starpharma.com/news/356 (accessed 3 August, 2022)

[215] Runge, V.M.; Heverhagen, J.T. Advocating the Development of Next-Generation High-Relaxivity Gadolinium Chelates for Clinical Magnetic Resonance. *Investig. Radiol*. **2018**, 53, 381–389. DOI: https://doi.org/10.1097/RLI.0000000000000454

[216] Herborn, C.U.; Schmidt, M.; Bruder, O.; Nagel, E.; Shamsi, K.; Barkhausen, J. MR Coronary Angiography with SH L 643 A: Initial Experience in Patients with Coronary Artery Disease. *Radiology* **2004**, 233, 567–573. DOI: https://doi.org/10.1148/radiol.2332031545

[217] Starpharma. https://starpharma.com/drug_delivery/dep-azd0466 (accessed August 15, 2022)

[218] Laubreton, D.; Bay, S.; Sedlik, C.; Artaud, C.; Ganneau, C.; Dérlaud, E.; et alThe fully synthetic MAG-Tn3 therapeutic vaccine containing the tetanus toxoid-derived TT830-844 universal epitope provides anti-tumor immunity. *Cancer Immunol. Immunother.* **2016**, 65, 315–325. DOI: https://doi.org/10.1007/s00262-016-1802-0

[219] Sharma, R.; Sharma, A.; Kambhampati, S.P.; Reddy, R.R.; Zhang, Z.; Cleland, J.L.; Kannan, S.; Kannan, R.M. Scalable synthesis and validation of PAMAM dendrimer-N-acetyl cysteine conjugate for potential translation. *Bioeng. Transl. Med*. **2018**, 3, 87–101. DOI: https://doi.org/10.1002/btm2.10094

[220] Camide, A.M. Dendrimers, an emerging opportunity in personalized medicine?. *J. Pers. Med*. **2022**, 12, 1334. DOI: https://doi.org/10.3390/jpm12081334

[221] Starpharma, VIRALEZE. https://www.starpharma.com/viraleze/spl7013 (accessed September 9, 2022)

[222] Castellarnau, A.; Heery, G.P.; Seta, A.; Luscombe, C.A.; Kinghorn, G.R.; Button, P.; McCloud, P.; Paull, J.R.A. Astodrimer sodium antiviral nasal spray for reducing respiratory infections is safe and well tolerated in a randomized controlled trial. *Sci. Rep*. **2022**, 12, 10210. DOI: https://doi.org/10.1038/s41598-022-14601-3

[223] Shippey, E.; Wagler, V.; Collamer, A. Hydroxychloroquine: An old drug with new relevance. *Cleveland Clinic Journal of Medicine* **2018**, 85, 459-467. DOI: https://doi.org/10.3949/ccjm.85a.17034

[224] Ashutosh, M.; Aparna W. Expanding horizons for clinical applications of chloroquine, hydroxychloroquine, and related structural analogues. *Drugs context*, **2019**, 8. DOI: https://doi.org/10.7573/dic.2019-9-1

[225] Mizushima, N. Autophagy: process and function. *Genes Dev*. **2007**, 21, 2861–2873. DOI: https://doi.org/10.1101/gad.1599207

[226] Ravikumar, B.; Sarkar, S.; Davies, J.E.; Futter, M.; Garcia-Arencibia, M.; Green-Thompson; Z.W.; *et al.* Regulation of mammalian autophagy in physiology and pathophysiology. *Physiol. Rev.* **2010**, 90, 1383–1435. DOI: https://doi.org/10.1152/physrev.00030.2009

[227] Choi, A.M.; Ryter, S.W.; Levine, B. Autophagy in human health and disease. *N. Engl. J. Med.* **2013**, 368, 651- 662. DOI: https://doi.org/10.1056/NEJMra1205406

[228] Mizushima, N.; Komatsu, M. Autophagy: renovation of cells and tissues. *Cell* **2011**,147, 728-41. DOI: https://doi.org/10.1016/j.cell.2011.10.026

[229] Amaravadi, R.; Kimmelman, A.C.; White, E. Recent insights into the function of autophagy in cancer. *Genes Dev.* **2016**, 30, 1913–1930. DOI: https://doi.org/10.1101/gad.287524.116

[230] White, E. Deconvoluting the context-dependent role for autophagy in cancer. *Nat. Rev. Cancer* **2012**, 12, 401–410. DOI: https://doi.org/10.1038/nrc3262

[231] Morselli, E.; Galluzzi, L.; Keep, O.; Mariño, G.; Michaud, M.; Vitale, I.; *et al.* Oncosuppressive functions of autophagy. *Antioxid. Redox Signal* **2011**, 14, 2251-2269. DOI: https://doi.org/10.1089/ars.2010.3478

[232] Yang, Z.J.; Chee, C.E.; Huang, S.; Sinicrope, F.A. The role of autophagy in cancer: therapeutic implications. *Mol. Cancer Ther*. **2011**, 10, 1533–1541. DOI: https://doi.org/10.1158/1535-7163.MCT-11-0047

[233] Levy, J.M.M.; Towers, C.G.; Thorburn, A. Targeting autophagy in cancer. *Nat. Rev. Cancer* **2017**, 17, 528–542. DOI: https://doi.org/10.1038/nrc.2017.53

[234] Mizushima, N.; Levine, B.; Cuervo, A.M.; Klionsky, D.J. Autophagy fights disease through cellular self-digestion. *Nature* **2008**, 451, 1069-1075. DOI: https://dx.doi.org/10.1038/nature06639

[235] Thorburn, A.; Thamm, D.H.; Gustafson, D.L. Autophagy and cancer therapy. Mol. Pharmacol. **2014**, 85, 830–838. DOI: https://doi.org/10.1124/mol.114.091850

[236] Altman, J.K,; Szilard, A.; Goussetis, D.J.; Sassano, A.; Colamonici, M.; Gounaris, E.; *et al.* Autophagy is a survival mechanism of acute myelogenous leukemia precursors during dual mTORC2/mTORC1 targeting. *Clin. Cancer Res.* **2014**, 20, 2400–2409. DOI: https://doi.org/10.1158/1078-0432.CCR-13-3218

[237] Masui, A.; Hamada, M.; Kameyama, H.; Wakabayashi, K.; Takasu, A.; Imai, T.; *et al*. Autophagy as a survival mechanism for squamous cell carcinoma cells in endonuclease Gmediated apoptosis. *PLoS One* **2016**, 11, e0162786. DOI: https://doi.org/10.1371/journal.pone.0162786

[238] Tan, Q.; Wang, M.; Yu, M.; Zhang, J.; Bristow, R.; Tannock, I.; *et al.* Role of autophagy as a survival mechanism for hypoxic cells in tumors. *Neoplasia* **2016**, 18, 347–355. DOI: https://doi.org/10.1016/j.neo.2016.04.003

[239] Debnath, J. The multifaceted roles of autophagy in tumors—implications for breast cancer. *J. Mammary Gland. Biol. Neoplasia* **2011**, 16, 173–187. DOI: https://doi.org/10.1007/s10911-011-9223-3

[240] Shi, T.; Yu, X.; Yan, L.; Xiao, H. Research progress of hydroxychloroquine and autopagy inhibitors on cancer. *Cancer Chemother. Pharmacol*. **2017**, 79, 287-294. DOI: https://doi.org/10.1007/s00280-016-3197-1

[241] Levy, J.M.; Thorburn, A. Targeting autophagy during cancer therapy to improve clinical outcomes. *Pharmacol. Ther.* **2011**, 131, 130–141. DOI: https://doi.org/10.1016/j.pharmthera.2011.03.009

[242] Yang, Y.P.; Hu, L.F.; Zheng, H.F.; Mao, C.; Hu, W.; Xiong, K.; *et al.* Application and interpretation of current autophagy inhibitors and activators. *Acta Pharmacol. Sin.* **2013**, 34, 625–635. DOI: https://doi.org/10.1038/aps.2013.5

[243] Poole, B.; Ohkuma, S. Effect of weak bases on the intralysosomal pH in mouse peritoneal macrophages. *J. Cell Biol.* **1891**, 90, 665–669. DOI: https://doi.org/10.1083/jcb.90.3.665

[244] Kazmi, F.; Hensley, T.; Pope, C.; Funk, R.S.; Loewen, G.J.; Buckley, D.B.; *et al.* Lysosomal sequestration (trapping) of lipophilic amine (cationic amphiphilic) drugs in immortalized human hepatocytes (Fa2N-4 cells). *Drug Metab. Dispos.* **2013**, 41, 897–905. DOI: https://doi.org/10.1124/dmd.112.050054

[245] MacIntyre, A.C.; Cutler, D.J. The potential role of lysosomes in tissue distribution of weak bases. *Biopharm. Drug Dispos.* **1988,** 9, 513–526. DOI: https://doi.org/10.1002/bod.2510090602

[246] Derendorf, H. Excessive lysosomal ion-trapping of hydroxychloroquine and azithromycin. *Int. J. Antimicrob*. **2020**, 55, 106007. DOI: https://doi.org/10.1016/j.ijantimicag.2020.106007

[247] Pellegrini, P.; Strambi, A.; Zipoli, C.; Hagg-Olofsson, M.; Buoncervello, M.; Linder, S., *et al.* Acidic extracellular pH neutralizes the autophagy-inhibiting activity of chloroquine: Implications for cancer therapies. *Autophagy* **2014**, 10, 562-571; DOI: https://doi.org/10.4161/auto.27901

[248] Brannon-Peppas, L.; Blanchette, J.O. Nanoparticle and targeted systems for cancer therapy. *Adv. Drug Deliv. Rev.* **2012**, 64, 206-212. DOI: https://doi.org/10.1016/j.addr.2012.09.033

[249] Allen, T.M.; Cullis, P.R. Drug delivery systems: entering the mainstream. *Science* **2004**, 303, 1818-1822. DOI: https://doi.org/10.1126/science.1095833

[250] Solomon, V.R.; Lee, H. Chloroquine and its analogs: a new promise of an old drug for effective and safe cancer therapies. *Eur. J. Pharmacol*. **2009**, 625, 220–233. DOI: https://doi.org/10.1016/j.ejphar.2009.06.063

[251] Boya, P.; Gonzalez-Polo, R.A.; Poncet, D.; Andreau, K.; Vieira, H.L.; Roumier, T.; *et al.* Mitochondrial membrane permeabilization is a critical step of lysosome-initiated apoptosis induced by hydroxychloroquine. *Oncogene* **2003**, 22, 3927-3936; DOI: https://doi.org/10.1038/sj.onc.1206622

[252] Galluzzi, L.; Keep, O.; Kroemer, G. Mitochondria: master regulators of danger signalling. *Nat. Rev. Mol. Cell Biol*. **2012**, 13, 780-788. DOI: https://doi.org/10.1038/nrm3479

[253] Pan, Y.; Gao, Y.; Chen, L.; Gao, G.; Dong, H.; Yang, Y.; *et al.* Targeting autophagy augments in vitro and in vivo antimyeloma activity of DNA-damaging chemotherapy. *Clin. Can. Res.* **2011**, 17, 3248–3258. DOI: https://doi.org/10.1158/1078-0432.CCR-10-0890

[254] Yang, Z.J.; Chee, C.E.; Huang, S.; Sinicrope, F. The role of autophagy in cancer: therapeutic implications. *Mol. Cancer Ther.* **2011**, 10,1533–1541. DOI: https://doi.org/10.1158/1535-7163.MCT-11-0047

[255] Bray, K.; Mathew, R.; Lau, A.; Kamphorst, J.J.; Fan, J.; Chen, J.; *et al.* Autophagy suppresses RIP kinaseYdependent necrosis enabling survival to mTOR inhibition. *PLoS ONE* **2012**, 7, e4183. DOI: https://doi.org/10.1371/journal.pone.0041831

[256] Lee, H.O.; Mustafa, A.; Hudes, R.G.; Kruger, Q.D. Hydroxychloroquine destabilizes phospho-S6 in human renal carcinoma cells. *PLoS ONE* **2015**, 10, e0131464. DOI: https://doi.org/10.1371/journal.pone.0131464

[257] Dragowska, W.H.; Weppler, S.A.; Wang, J.C.; Womg, L.Y.; Kapanem, A.I.; Rawji, J.S.; et al. Induction of autophagy is an early response to gefitinib and a potential therapeutic target in breast cancer. *PLoS ONE* **2013**, 8, e76503. DOI: https://doi.org/10.1371/journal.pone.0076503

[258] Li, J.; Yang, B., Zhou, Q.; Wu, Y.; Shang, D.; Guo, Y.; *et al.* Autophagy promotes hepatocellular carcinoma cell invasion through activation of epithelial-mesenchymal transition. *Carcinogenesis* **2013**, 34, 1343–1351. DOI: https://doi.org/10.1093/carcin/bgt063

[259] Wei, Y.; Zou, Z.; Becker, N.; Anderson, M.; Sumpter, R.; Xiao, G.; *et al.* XEGFR-mediated Beclin 1 phosphorylation in autophagy suppression, tumor progression, and tumor chemoresistance. *Cell* **2013**, 154, 1269-1284. DOI: https://doi.org/10.1016/j.cell.2013.08.015

[260] Bareford, M.D.; Park, M.A.; Yacoub, A.; Hamed, H.A.; Tang, Y.; Cruickshanks, N.; *et al*. Sorafenib enhances pemetrexed cytotoxicity through an autophagydependent mechanism in cancer cells. *Cancer Res*. **2011,** 71, 4955-4967. DOI: https://doi.org/10.1158/0008-5472.CAN-11-0898

[261] Elgendy, M., Sheridan, C.; Brumatti, G.; Martin, S.J. Oncogenic Ras-induced expression of Noxa and Beclin-1 promotes autophagic cell death and limits clonogenic survival. *Mol. Cell* **2011**, 42, 23-35. DOI: https://doi.org/10.1016/j.molcel.2011.02.009

[262] Gump, J.M.; Staskiewicz, L.; Morgan, M.J.; Bamberg, A.; Riches, D.W.; Thorburn, A. Autophagy variation within a cell population determines cell fate through selective degradation of Fap-1. *Nat. Cell Biol.* **2014**, 16, 47- 54. DOI: https://doi.org/10.1038/ncb2886

[263] Kohli, L.; Kaza, N.; Coric, T.; Byer, S.J.; Brossier, N.M.; Klocke, B.J.; *et al.* 4-Hydroxytamoxifen induces autophagic death through K-Ras degradation. *Cancer Res.* **2013,** 73, 4395-4405. DOI: https://doi.org/10.1158/0008-5472.CAN-12-3765

[264] Voss, V.; Senft, C.; Lang, V.; Ronellenfitsch, M.W.; Steinbach, J.P.; Seifert, V.; *et al.* The pan-Bcl-2 inhibitor (-)-gossypol triggers autophagic cell death in malignant glioma. *Mol. Cancer Res*. **2010**, 8, 1002-1016. DOI: https://doi.org/10.1158/1541-7786

[265] Manic, G.; Obrist, F.; Kroemer, Vitale, I.; Galluzzi, L. Chloroquine and Hydroxychloroquine for cancer therapy. *Molecular & Cellular Oncology* **2014**, 1, e29911. DOI: https://doi.org/10.4161/mco.29911

[266] Wang, X.; Teng, Z.; Wang, H.; Wang, C.; Liu, Y.; Tang, Y.; et al. Increasing the cytotoxicity of doxorubicin in breast cancer MCF-7 cells with multidrug resistance using a mesoporous silica nanoparticle drug delivery system. *Int. J. Exp. Pathol.* **2014**, 7, 1337-1347. Available in URL: https://www.ncbi.nlm.nih.gov/pmc/articles/PMC4014214/

[267] Rivankar, S. An overview of doxorubicin formulations in cancer therapy. *J. Cancer Res. Ther.* **2014**, 10, 853-858. DOI: https://doi.org/10.4103/0973-1482.139267

[268] Cutts, S.; Parsons, P.; Sturm, R.; Phillips, D. Adriamycin-induced DNA adducts inhibit the DNA interactions of transcription factors and RNA polymerase. *J. Biol. Chem*. **1996**, 271, 5422-5429. DOI: https://doi.org/10.1074/jbc.271.10.5422

[269] Cutts, S.; Swift, L.; Rephaeli, A.; Nudelman, A.; Phillips, D. Recent advances in understanding and exploiting the activation of anthracyclines by formaldehyde. *Curr. Med. Chem. AntiCancer Agents* **2005**, 5, 431-447. DOI: https://doi.org/10.2174/1568011054866964

[270] Carvalho, C.; Santos, R.X.; Cardoso, S.; Correia, S.; Oliveira, P.J.; Santos M.S. Doxorubicin: The good, the bad and the ugly effect. *Curr. Med. Chem*. **2009**, 16, 3267-3285. DOI: https://doi.org/10.2174/092986709788803312

[271] Waterhouse, D.N.; Tardi, P.G.; Mayer, L.D.; Bally, M.B. A comparison of liposomal formulations of doxorubicin with drug administered in free form: Changing toxicity profiles. *Drug Saf.* **2001**, 24, 903-920. DOI: https://doi.org/10.2165/00002018-200124120-00004

[272] Birtle, A.J. Anthracyclines and cardiotoxicity. *Clin Oncol (R Coll Radiol)* **2000**, 12, 146-152. DOI: https://doi.org/10.1053/clon.2000.9141

[273] Seymour, L.; Bramwell, V.; Moran, L.A. Use of dexrazoxane as a cardioprotectant in patients receiving doxorubicin or epirubicin chemotherapy for the treatment of cancer. The Provincial Systemic Treatment Disease Site Group. *Cancer Prev Control* **1999**, 3, 145-159. Available in URL: https://pubmed.ncbi.nlm.nih.gov/10474762/

[274] He, X.; Alves, C.S.; Oliveira, N.; Rodrigues, J.; Zhu, J.; Bányai, I.; *et al.* RGD peptide-modified multifunctional dendrimer platform for drug encapsulation and targeted

inhibition of cancer cells. *Colloids Surf.* **2015**, 125, 82-89. DOI: https://doi.org/10.1016/j.colsurfb.2014.11.004

[275] Liao, H.; Liu, H.; Li, Y.; Zhang, M.; Tómas, H.; Shen, M.; *et al*. Antitumor efficacy of doxorubicin encapsulated within PEGylated poly(amidoamine) dendrimers. *J. Appl. Polym.* **2014**, 131, 40358. DOI: https://doi.org/10.1002/app.40358

[276] Singh, V.; Kesharwani, P. Dendrimer as a promising nanocarrier for the delivery of doxorubicin as an anticancer therapeutics. *Journal of Biomaterials Science, Polymer Edition* **2021**, 32, 1882-1909. DOI: https://doi.org/10.1080/09205063.2021.1938859

[277] Zhang, M.; Guo, R.; Kéri, M.; Bányai, I.; Zheng, Y.; Cao, M.; *et al.* Impact of Dendrimer Surface Functional Groups on the Release of Doxorubicin from Dendrimer Carriers. *J. Phys. Chem. B* **2014**, 118, 1696–1706. DOI: https://doi.org/10.1021/jp411669k

[278] Jardim, M.G.; Rissanen, K.; Rodrigues, J. Preparation and Characterization of Novel Poly(alkylidenamine) Nitrile Ruthenium Metallodendrimers. *Eur. J. Inorg. Chem.* **2010**, 1729– 1735. DOI: https://doi.org/10.1002/ejic.200901187

[279] Pan, H.; Grow; M. E.; Wilson, O.; Daniel, M.C. A new poly (propylene imine) dendron as potential convenient building-block in the construction of multifunctional systems. *Tetrahedron,* **2013**, 69, 2799–2806. DOI: https://doi.org/10.1016/j.tet.2013.01.070

[280] García-Gallego, S.; Cangiotti, M.; Fiorani, L.; Fattori, A.; Muñoz-Fernández, M.A.; Gomez, R.; *et al.* Anionic sulfonated and carboxylated PPI dendrimers with the EDA core: synthesis and characterization of selective metal complexing agents. *Dalton Trans.* **2013**, 42, 5874-89. DOI: https://doi.org/10.1039/c3dt32870h

[281]Agrawal, P.; Gupta, U.; Jain, N.K. Glycoconjugated peptide dendrimers-based nanoparticulate system for the delivery of chloroquine phosphate. *Biomaterials* **2007**, 28, 3349- 3359. DOI: https://doi.org/10.1016/j.biomaterials.2007.04.004

[282] Gonçalves, M.; Kairys, V.; Rodrigues, J.; Tomás, H. Polyester Dendrimers Based on Bis-MPA dor Doxorubicin Delivery. *Biomacromolecules* **2022**, 23, 20-33. DOI: https://doi.org/10.1021/acs.biomac.1c00455

[283] Deng, H.; Zhao, X.; Liu, J.; Zhang, J; Deng, L.; Liu, J.; *et al.* Synergistic dual-pH responsive copolymer micelles for pH-dependent drug release. *Nanoscale* **2016**, 8, 1437-1450. DOI: https://doi.org/10.1039/c5nr06745f

[284] International Committee for Standardization in Haematology. International Committee for Standardization in Haematology Recommendations for reference method for haemoglobinometry in human blood (ICSH Standard EP 6/2: 1977) and specifications for international haemiglobincyanide reference preparation (ICSH Standard EP 6/3: 1997). *J. Clin. Pathol*. **1978**, 31, 139–143. DOI: https://doi.org/10.1136/jcp.31.2.139

[285] Jain, K. Dendrimers: Smart nanoengineered polymers for bioinspired applications in drug delivery. *Biopolymer-Based Composites* **2017**, 169-220. DOI: https://doi.org/10.1016/B978-0-08-101914-6.00007-7

[286] Mather, B.; Viswanathan, K.; Miller, K.; Long, T. Michael addition reactions in macromolecular design for emerging technologies. *Prog. Polym. Sci*. **2006**, 31, 487–531. DOI: https://doi.org/10.1016/j.progpolymsci.2006.03.001

[287] De Brabander-Van Den Berg, E. M. M.; Nijenhuis, A.; Mure, M.; Keulen, J.; Reintjens, R.; Vandenbooren, F.; *et al.* Large-scale production of polypropylenimine dendrimers. *Macromol. Symp*. **1994**, 77, 51–62. DOI: https://doi.org/10.1016/j.progpolymsci.2006.03.001

[288] Camide, A. Laurent, R.; Majoral, J. Characterization of dendrimers. *Adv. Drug Deliv. Rev.* **2005**, 57, 2130-2146. DOI: https://doi.org/10.1016/j.addr.2005.09.011

[289] Jayamurugan, G.; Jayaraman, N. Synthesis of large generation poly(propyl ether imine) (PETIM) dendrimers. *Tetrahedon* **2006**, 62, 9582-9588. DOI: https://doi.org/10.1016/j.tet.2006.07.094

[290] Golshan, M.; Salami-Kalajahi, M.; Roghani-Mamaqani, H.; Mohammadi, M. Synthesis of poly(propylene imine) dendrimers via homogeneous reduction process using lithium aluminium hydride: Bioconjugation with folic acid and doxorubicin release kinetics. *Appl. Organometal. Chem.* **2017**, 31, e3789. DOI: https://doi.org/10.1002/aoc.3789

[291] Maciel, Dina. Metallodendrimers as HIV Antiviral and Anticancer Agents. PhD thesis, University of Madeira, Portugal, 2020. Available in URL: https://digituma.uma.pt/handle/10400.13/3146?mode=full

[292] Boas, U.; Christensen, J. B.; Heegaard, P. M. H. Dendrimers: design, synthesis and chemical properties. *J. Mater. Chem.* **2006**, 16, 3785. DOI: https://doi.org/10.1039/b611813p

[293] Zhou, W.; Zhang, D.; Wang, Y.; Peng, X. Preparation of Rh metallic nanoparticle stabilized by 15-membered nitrogen-containing triolefinic macrocycle-ended poly(propylene imine) dendrimer and its catalytic hydrogenation for nitrile-butadiene rubber. *Colloid. Polym. Sci.* **2017**, 295, 767–772. DOI: https://doi.org/10.1007/s00396-017-4060-6

[294] Thakur, S.; Tekade, R.K.; Kesharwani, P.; Jain, N.K. The effect of polyethylene glycol spacer chain length on the tumor-targeting potential of folate-modified PPI dendrimers. *J. Nanopart. Res*. **2013**, 15, 1625. DOI: https://doi.org/10.1007/s11051-013-1625-2

[295] Rasines, B.; Sánchez-Nieves, J.; Maiolo, M.; Maly, M.; Chonco, L.; Jiménez, J.L; *et al*. Synthesis, structure and molecular modelling of anionic carbosilane dendrimers. *Dalton Trans*. **2012**, 41, 12733-12748. DOI: https://doi.org/10.1039/C2DT31099F

[296] Maciel, D., Beltrán-Guerrero, C.; Cenã-Diez, R.; Tómas, H.; Munoz-Fernandez, M.A.; Rodrigues, J. New anionic poly(alkylideneamine) dendrimers as microbicide agents against HIV-1 infection. *Nanoscale*, **2019**, 11, 9679-9690. DOI: https://doi.org/10.1039/C9NR00303G

[297] Öztürk, K. Ertürk, A.S.; Sarısözen, C.; Tulu, M.; Çalış, S. Cytotoxicity and in vitro characterization studies of synthesized Jeffamine-cored PAMAM dendrimers. *Journal of Microencapsulation* **2014**, 31, 127–136. DOI: https://doi.org/10.3109/02652048.2013.814727

[298] Kumar, A.; Dixit, C.K. Methods for characterization of nanoparticles. *Advances in Nanomedicine for the Delivery of Therapeutic Nucleic Acids* **2017**, 43-58. DOI: https://doi.org/10.1016/B978-0-08-100557-6.00003-1

[299] Patel, V.R., Agrawal, Y.K. Nanosuspension: an approach to enhance solubility of drugs,. *J. Adv. Pharm. Technol. Res*. **2011**, 2, 81–87. DOI: https://doi.org/10.4103/2231-4040.82950

[300] Bhattacharjee, S. DLS and zeta potential- What they are and what they are not?. *J. Control. Release* **2016**, 235, 337-351. DOI: https://dx.doi.org/10.1016/j.jconrel.2016.06.017

[301] Zhao, F.; Zhao, Y.; Liu, Y.; Chang, X.; Chen, C.; Zhao, Y. Cellular uptake, intracellular trafficking, and cytotoxicity of nanomaterials. *Small* **2011**, 7, 1322-1337. DOI: https://doi.org/10.1002/smll.201100001

[302] Donahue, N.D.; Acar, H.; Wilhelm, S. Concepts of nanoparticle cellular uptake, intracellular trafficking, and kinetics in nanomedicine. *Adv. Drug. Del. Rev.* **2019**, 143, 68-96. DOI: https://doi.org/10.1016/j.addr.2019.04.008

[303] Pecora, R. Dynamic light scattering measurement of nanometer particles in liquids. *J. Nanopart. Res*. **2000**, 2, 123-131. DOI: https://doi.org/10.1023/A:1010067107182

[304] Stetefeld, J.; McKenna, S.A.; Patel, T.R. Dynamic light scattering: a practical guide and applications in biomedical sciences. *Biophys. Rev.* **2016**, 8, 409-427. DOI: https://doi.org/10.1007/s12551-016-0218-6

[305] Sandhu, V.K.; Weisman, M.H. Hydroxychloroquine- How Much Is Too Much?. *The J. Rheumatol.* **2019**, 46, 340-342. DOI: https://doi.org/10.3899/jrheum.180639

[306] Kojima, C.; Kono, K.; Maruyama, K.; Takagishi, T. Synthesis of Polyamidoamine Dendrimers Having Poly(ethylene glycol) Grafts and Their Ability To Encapsulate Anticancer Drugs. *Bioconjugate Chem.* **2000**, 11, 910–917. DOI: https://doi.org/10.1021/bc0000583

[307] Kojima, C. Design of stimuli-responsive dendrimers. *Expert. Opin. Drug Deliv.* **2010**, 7, 307-319. DOI: https://doi.org/10.1517/17425240903530651

[308] Bazban-Shatorbani, S.; Hasani- Sadrabadi, M.M.; Karkhaneh, A. Serpooshan, V.; Jacob, K.I.; Moshaverinia, A.; et al. Revisiting structure- propriety relationship of pH-

responsive polymers for drug delivery applications. *J. Control. Release* **2017**, 253, 46-63. DOI: https://doi.org/10.1016/j.jconrel.2017.02.021

[309] Jones, C. F.; Campbell, R. A.; Franks, Z., Gibson, C.C.; Thiagarajan, G.; Vieira-de-Abreu, A.; *et al.* Cationic PAMAM dendrimers disrupt key platelet functions. *Mol. Pharm*. **2012**, 9, 1599–1611. DOI: https://doi.org/10.1021/mp2006054

[310] Ziemba, B.; Matuszko, G.; Bryszewska, M.; Klajnert, B. Influence of dendrimers on red blood cells. *Cellular & Molecular Biology Letters* **2012**, 17, 21-35. DOI: https://doi.org/10.2478/s11658-011-0033-9

[311] Fernandes, H.P.; Cesar, C.L.; Barjas-Castro; M.L. Electrical proprieties of the red blood cell membrane and immunohematological investigation. *Rev. Bras Hematol. Hemoter.* **2011**, 33, 297-301. DOI: https://doi.org/10.5581/1516-8484.20110080

[312] Boulton-Jones, T.M.; Chandrachud, L. Variation in charge on red cells of patients with different glomerulopathies. *Lancet* **1986**, 2, 186-189. DOI: https://doi.org/10.1016/s0140-6736(86)92488-8

[313] Liga Portuguesa contra o Cancro. https://www.ligacontracancro.pt/outubrorosa (accessed July 28, 2022).

[314] World Cancer Research Found International. Worldwide cancer data. https://www.wcrf.org/cancer-trends/worldwide-cancer-data/ (accessed September 6, 2022

[315] Präbst, K.; Engelhardt, H.; Ringgeler, S.; Hübner, H. Basic Colorimetric Proliferation Assays: MTT, WST, and Resazurin. *Cell Viability Assays* **2017**, 1–17. DOI: https://doi.org/10.1007/978-1-4939-6960-9_1

[316] Janaszewska, A; Lazniewska, J.; Trzepinski, P.; Marcinkowska, M.; Klajnert-Maculewicz, B. Cytotoxicity of dendrimers. *Biomolecules* **2019**, 9, 330. DOI: https://doi.org/10.3390/biom9080330

[317] He, Y.; Xu, Y.; Huang, Y.; Quang, H.; Xia, X.; Zhao, H. Redox sensitive nano-capsules self-assembled from hyaluronic acid-hydroxychloroquine conjugates for CD44-targeted

delivery of hydroxychloroquine to combat breast cancer metastasis *in vitro* and *in vivo*. *Colloids Surf.* **2022**, 210, 112249. DOI: https://doi.org/10.1016/j.colsurfb.2021.112249

[318] Loh, J.S.; Rahim, N.A.; Tor, Y.S.; Foo, J.B. Simultaneous proteasome and autophagy inhibition synergistically enhances cytotoxicity of doxorubicin in breast cancer cells. *Cell Biochem. Funct.* **2022**, 40, 403-416. DOI: https://doi.org/10.1002/cbf.3704

Supplementary material

Annex 1. Synthesis and characterization of the nitrile dendrimers

Annex 1.1. NMR characterization of G1CN

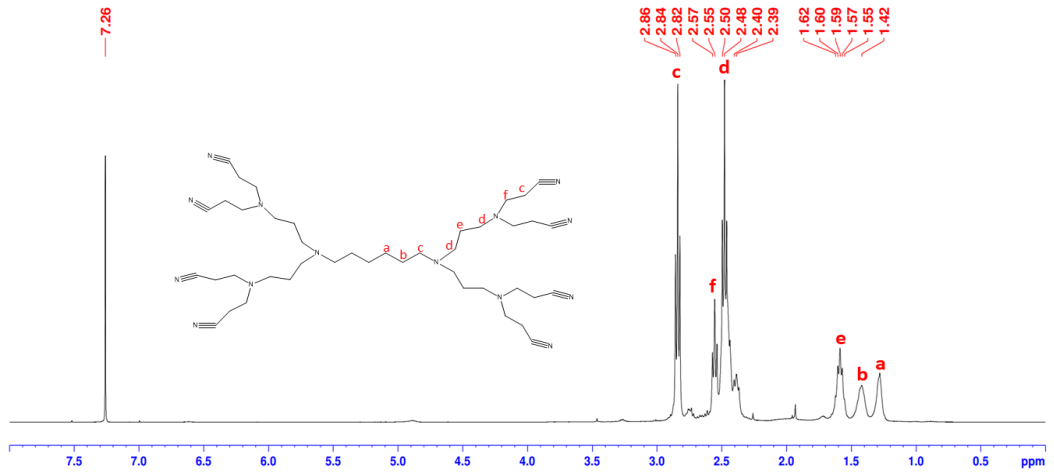

Figure A1- ^{1}H-NMR spectrum of G1CN in $CDCl_3$, second batch.

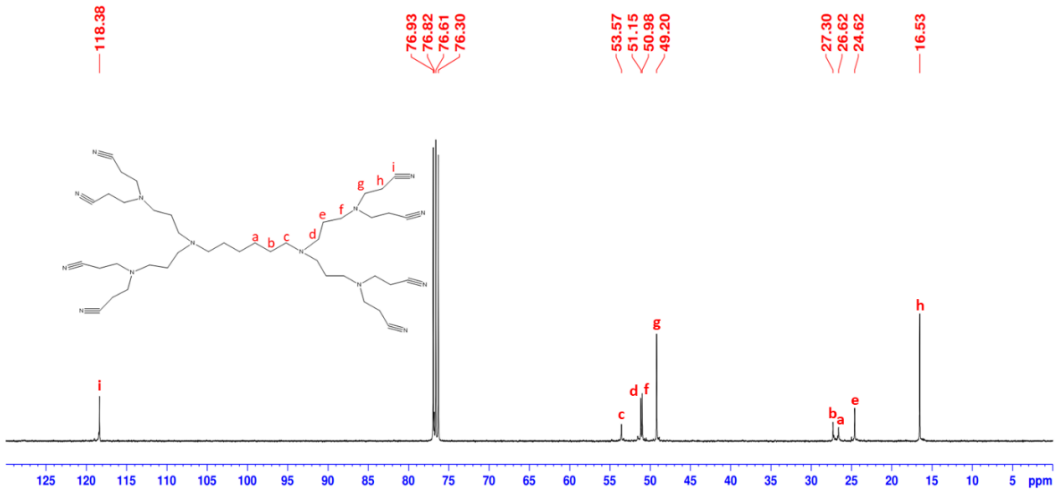

Figure A2- ^{13}C-NMR spectrum of G1CN in $CDCl_3$, second batch.

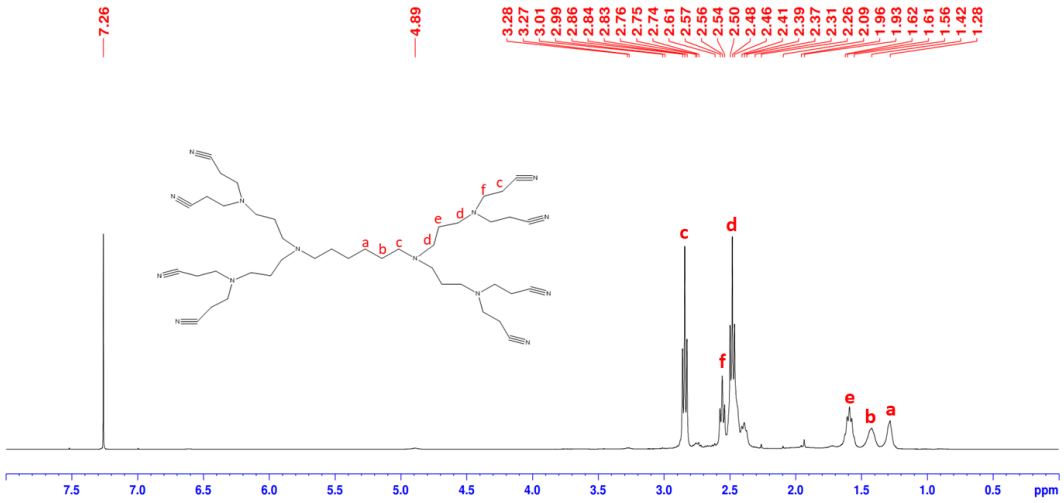

Figure A3- ^{1}H-NMR spectrum of G1CN in $CDCl_3$, third batch.

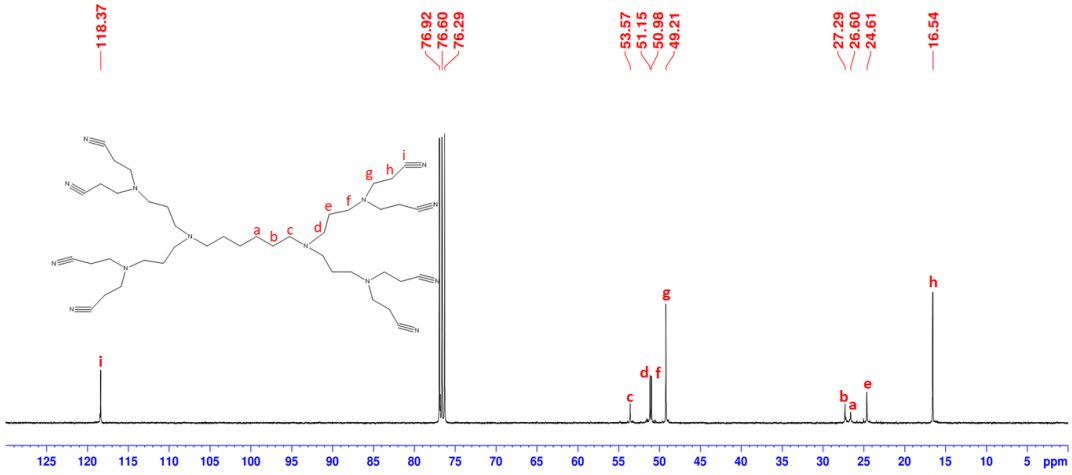

Figure A4- ^{13}C-NMR spectrum of G1CN in $CDCl_3$, third batch.

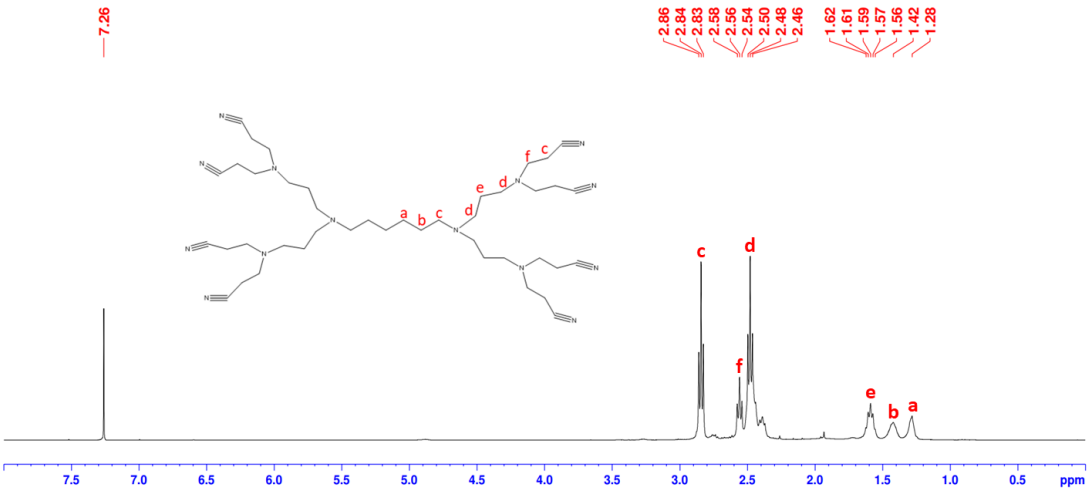

Figure A5- ^{1}H-NMR spectrum of G1CN in $CDCl_3$, fourth batch.

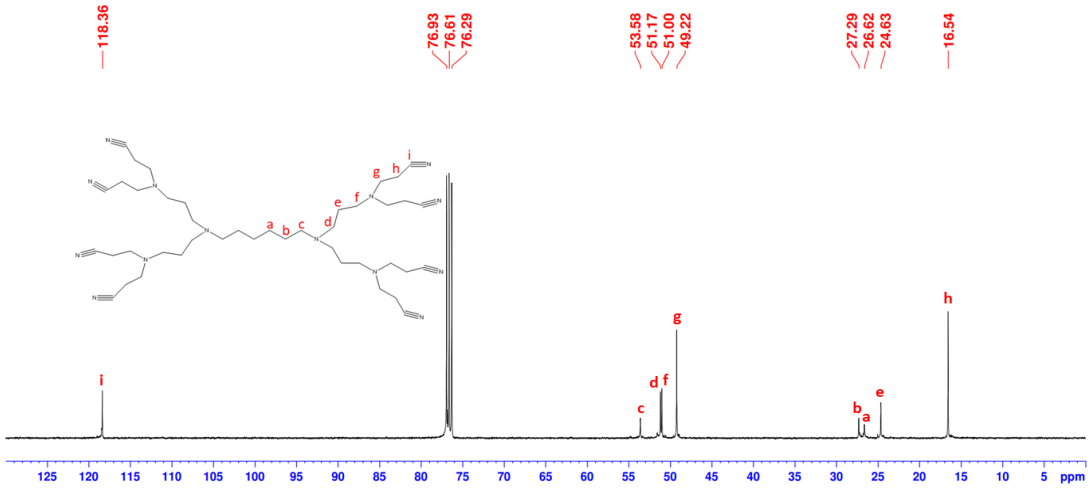

Figure A6- ^{13}C-NMR spectrum of G1CN in $CDCl_3$, fourth batch.

Annex 1.2. NMR characterization of G2CN

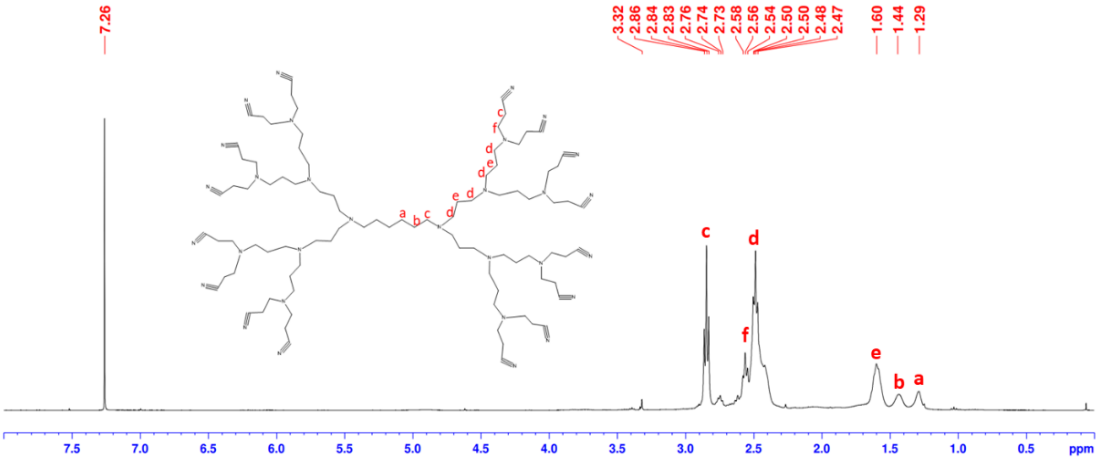

Figure A7- ^{1}H-NMR spectrum of G2CN in $CDCl_3$, second batch.

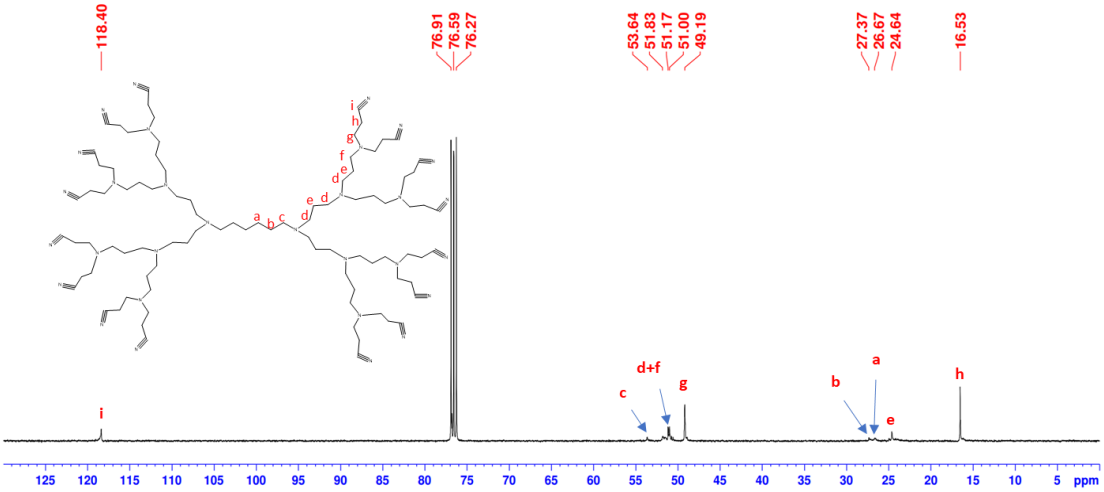

Figure A8- ^{13}C-NMR spectrum of G2CN in $CDCl_3$, second batch.

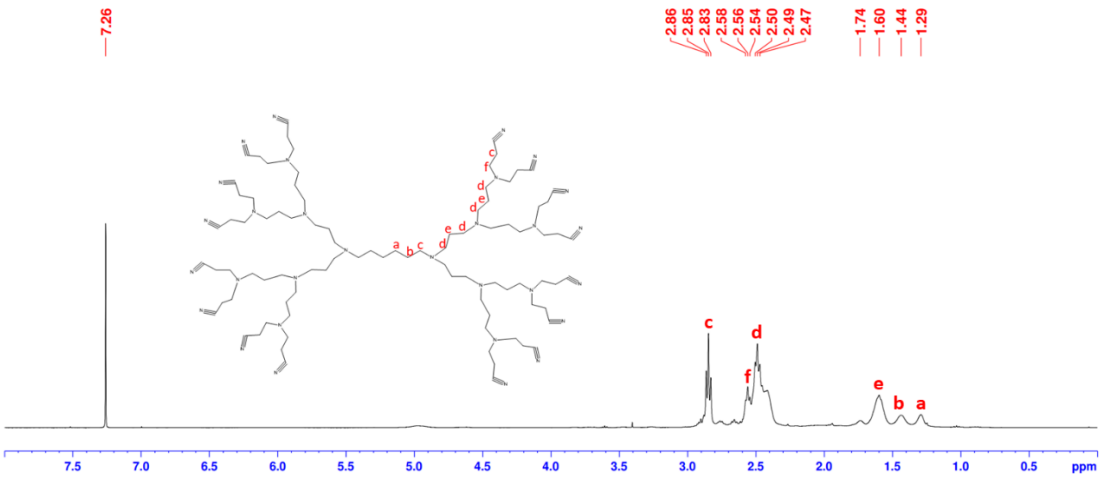

Figure A9- ^{1}H-NMR spectrum of G2CN in $CDCl_3$, third batch.

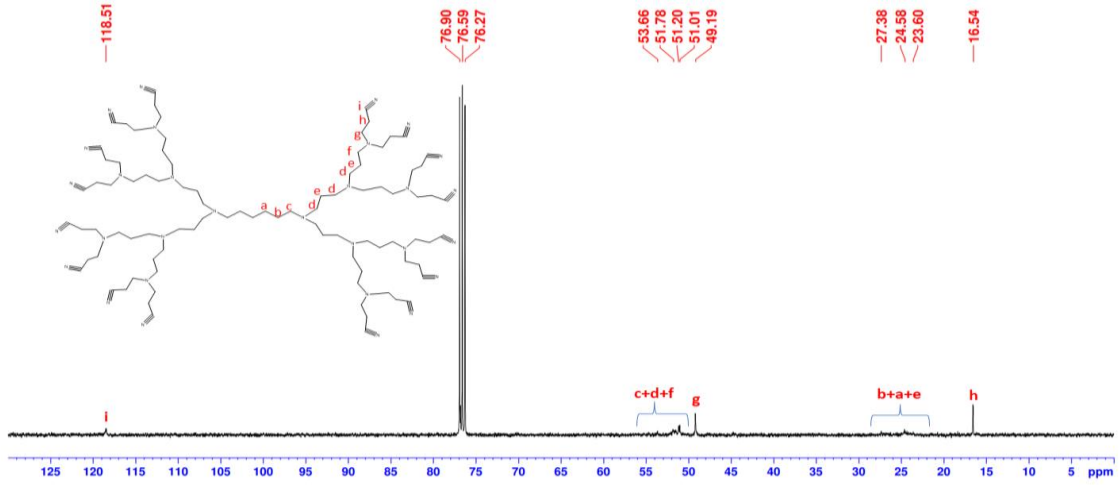

Figure A10- ^{13}C-NMR spectrum of G2CN in $CDCl_3$, third batch.

Annex 1.3. NMR characterization of G3CN

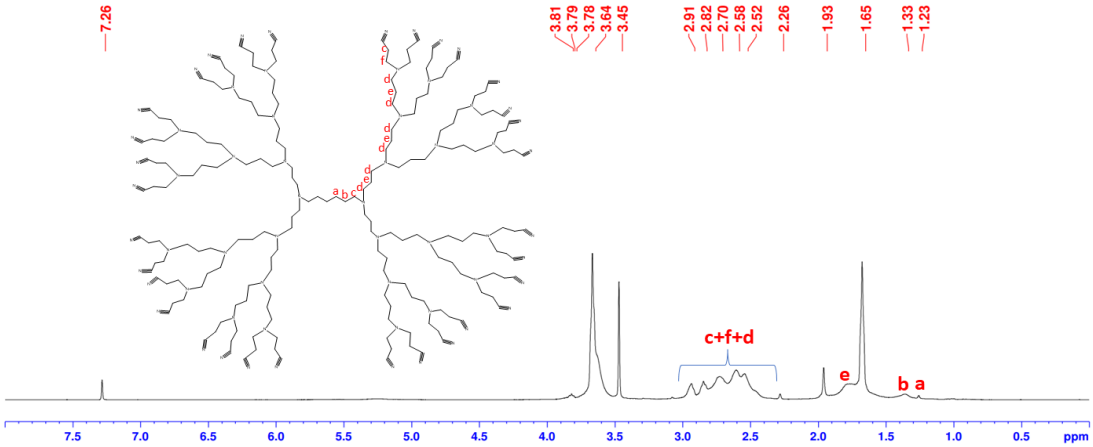

Figure A11- ^{1}H-NMR spectrum of G3CN in $CDCl_3$, second batch.

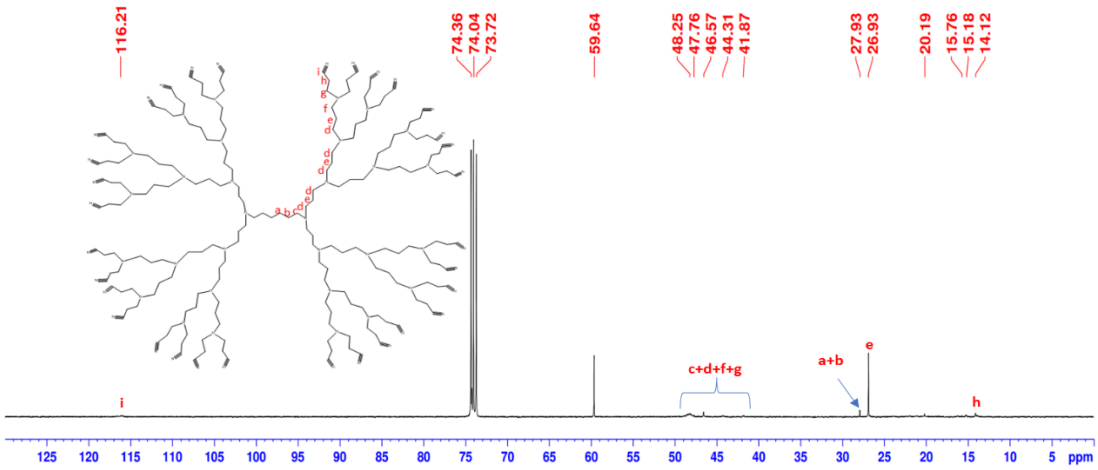

Figure A12- ^{13}C-NMR spectrum of G3CN in $CDCl_3$, second batch.

Annex 2. Synthesis and characterization of the amine dendrimers

Annex 2.1. NMR characterization of G0NH$_2$

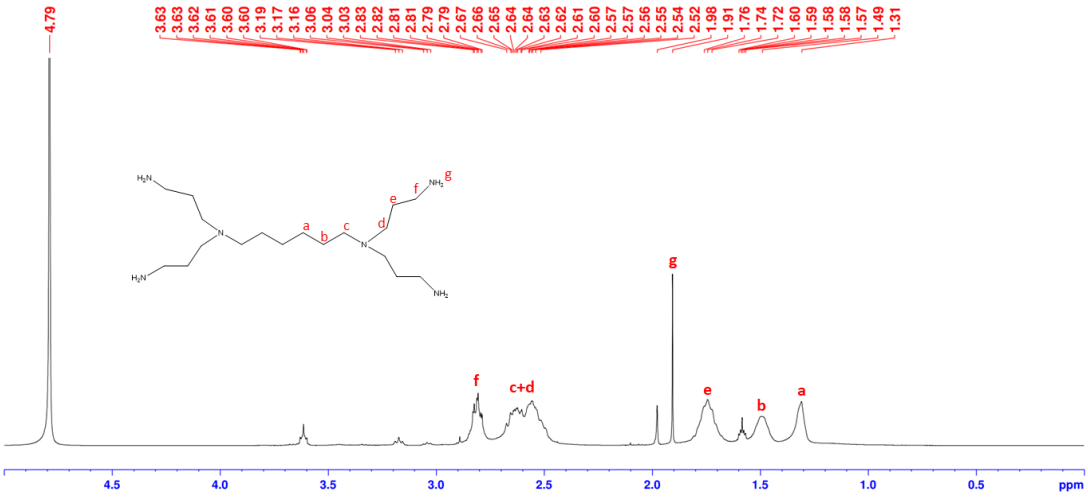

Figure A13- ^{1}H-NMR spectrum of G0NH$_2$ in D_2O, second batch.

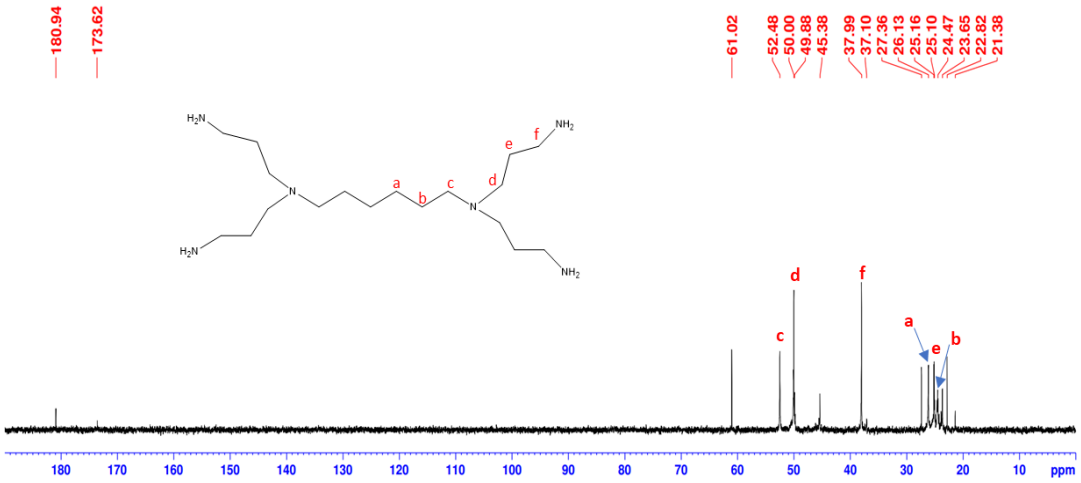

Figure A14- ^{13}C-NMR spectrum of G0NH$_2$ in D$_2$O, second batch.

Annex 2.2. NMR characterization of G1NH$_2$

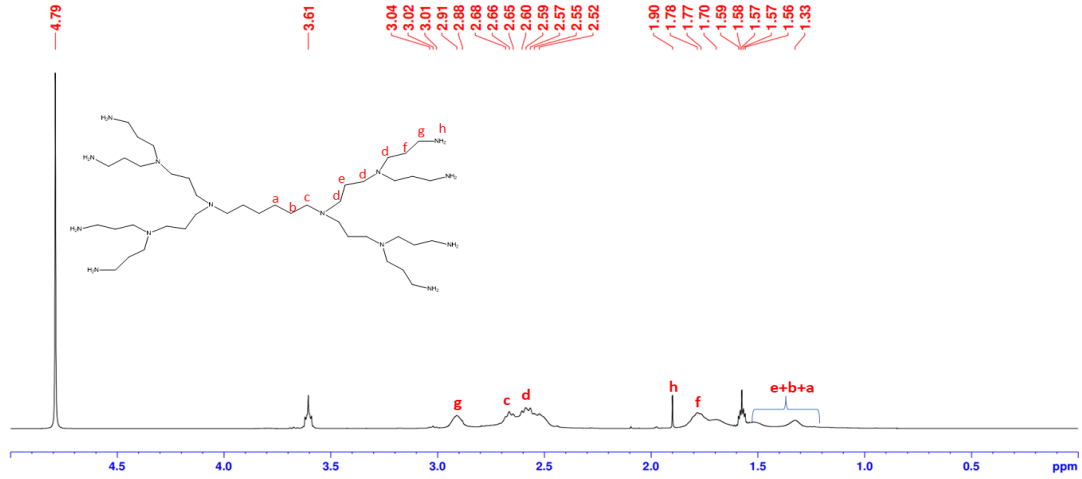

Figure A15- ^{1}H-NMR spectrum of G1NH$_2$ in D$_2$O, second batch.

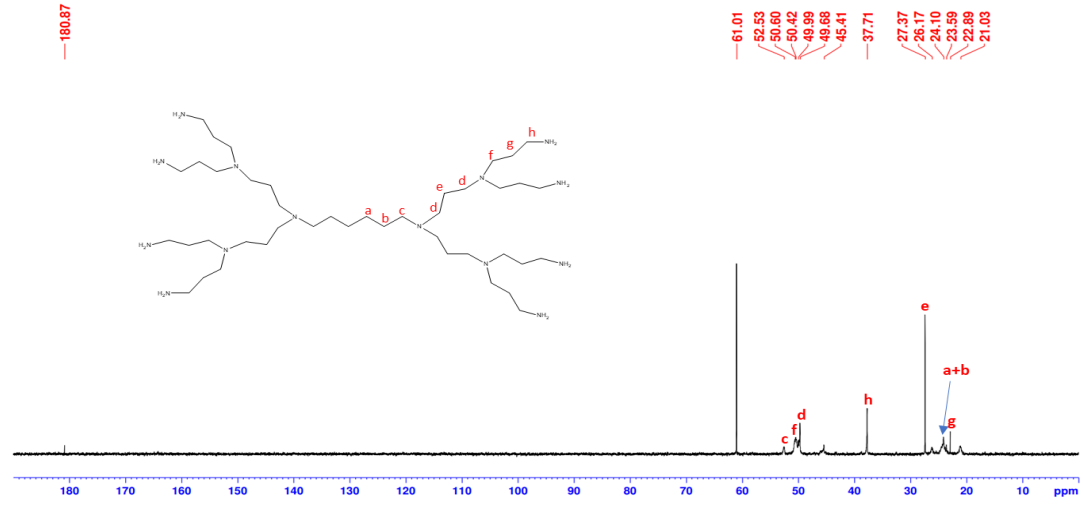

Figure A16- ^{13}C-NMR spectrum of G1NH$_2$ in D$_2$O, second batch.

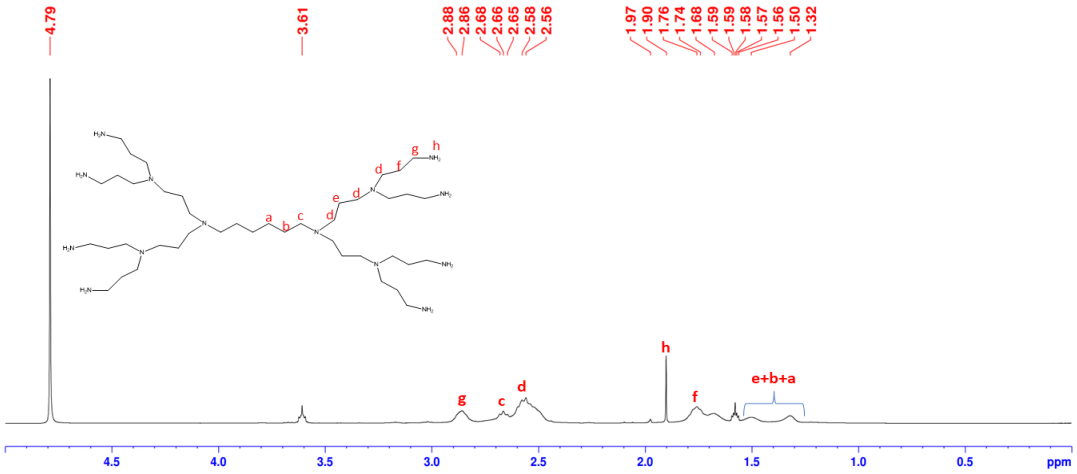

Figure A17- ^{1}H-NMR spectrum of G1NH$_2$ in D$_2$O, third batch.

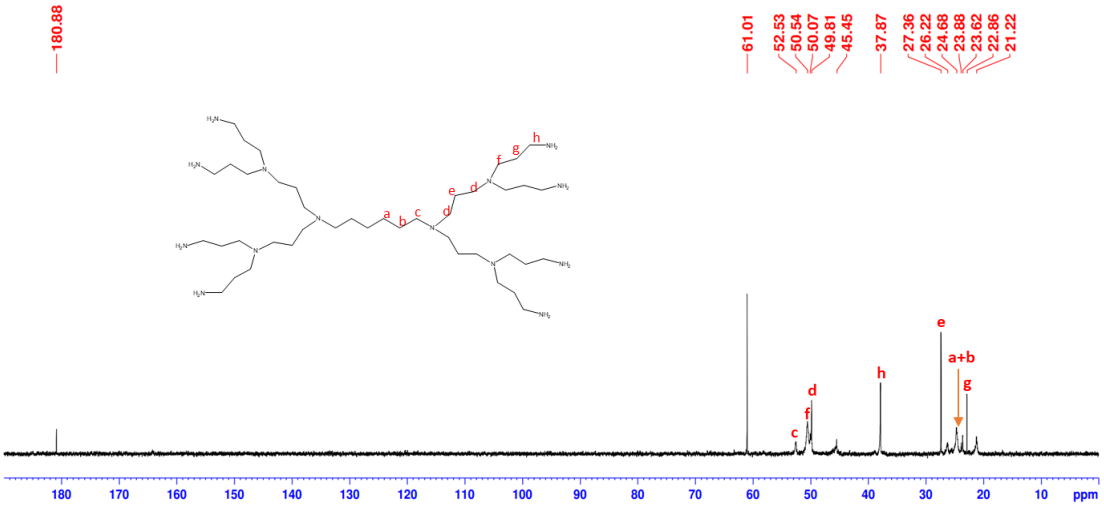

Figure A18- ^{13}C-NMR spectrum of G1NH$_2$ in D$_2$O, third batch.

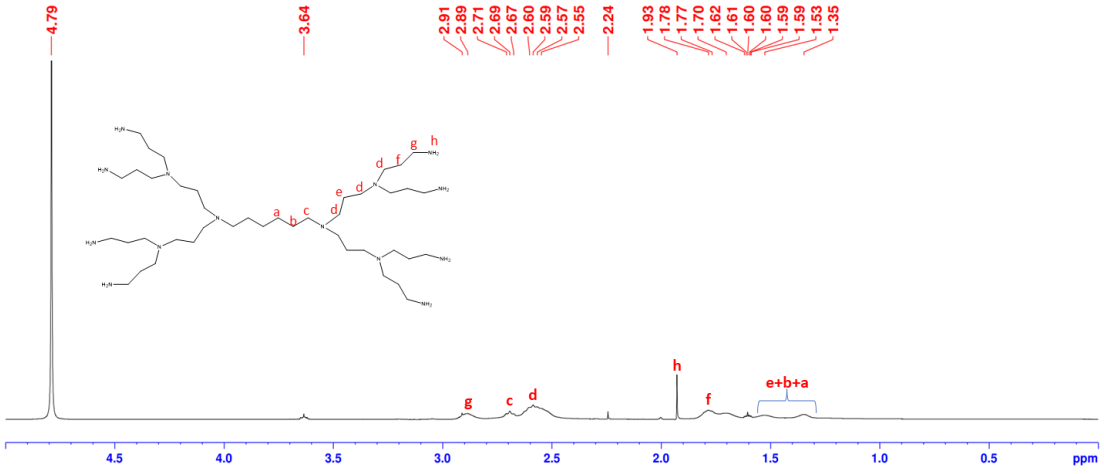

Figure A19- ^{1}H-NMR spectrum of G1NH$_2$ in D$_2$O, fourth batch.

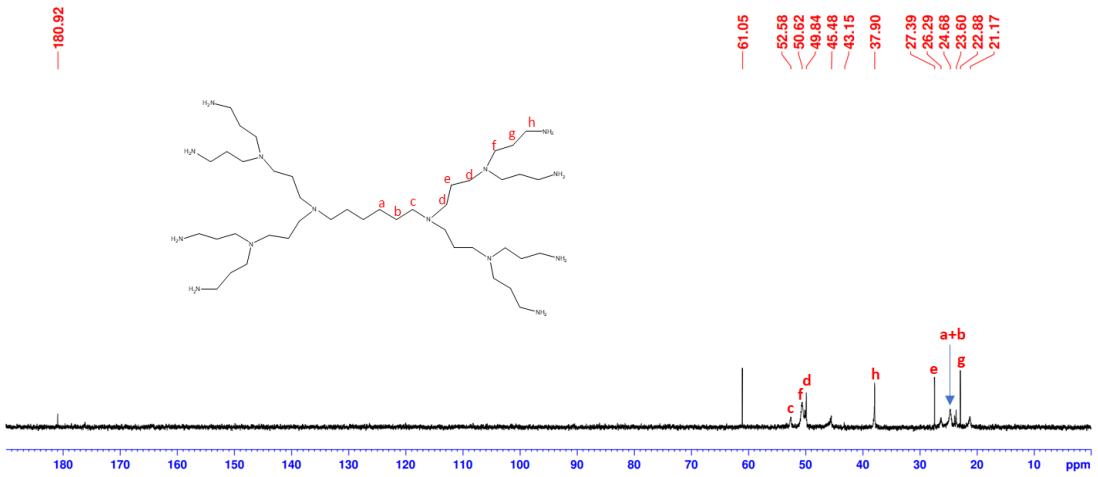

Figure A20- ^{13}C-NMR spectrum of G1NH$_2$ in D$_2$O, fourth batch.

Annex 2.3. NMR characterization of G2NH$_2$

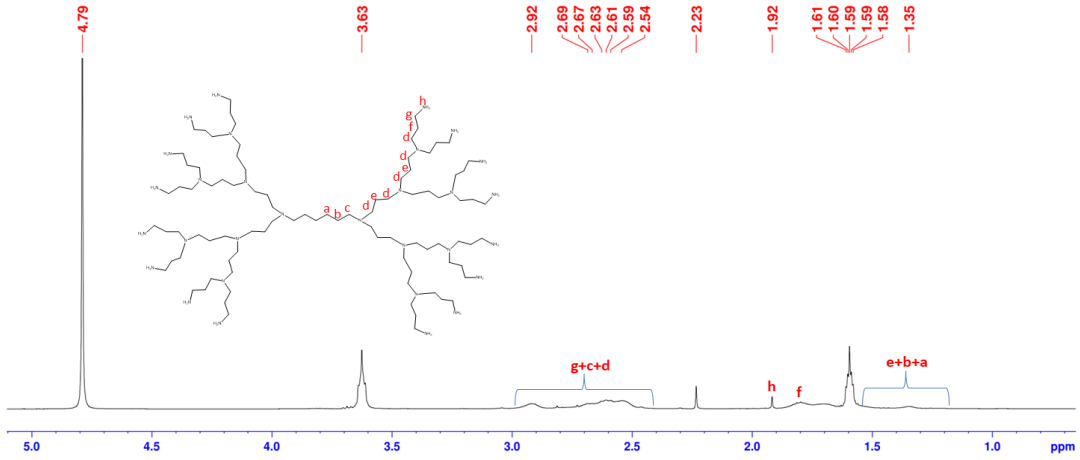

Figure A21- ^{1}H-NMR spectrum of G2NH$_2$ in D$_2$O, second batch.

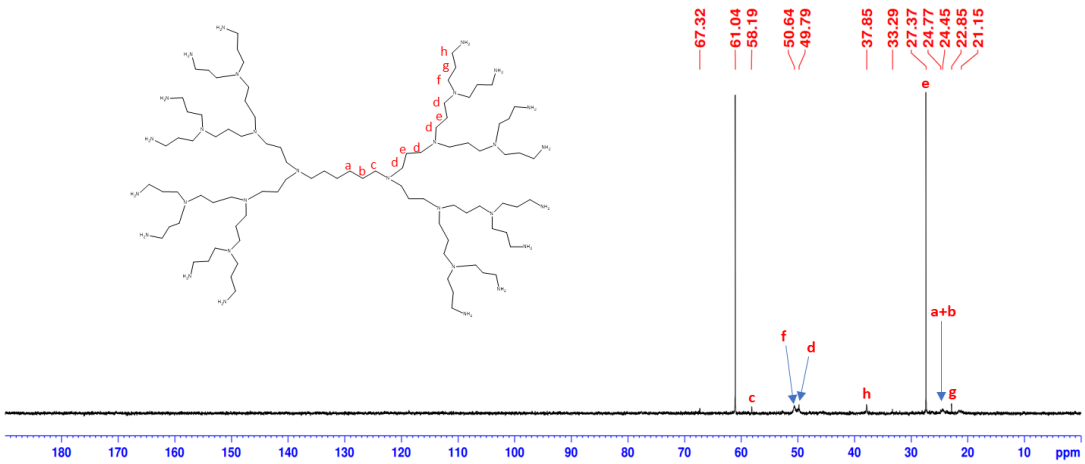

Figure A22- ^{13}C-NMR spectrum of G2NH$_2$ in D$_2$O, second batch.

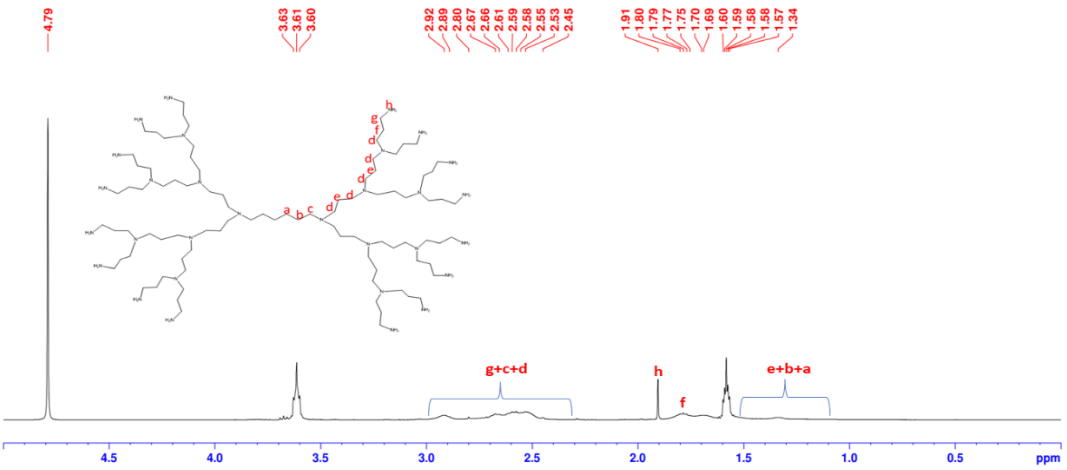

Figure A23- ^{1}H-NMR spectrum of G2NH$_2$ in D$_2$O, third batch.

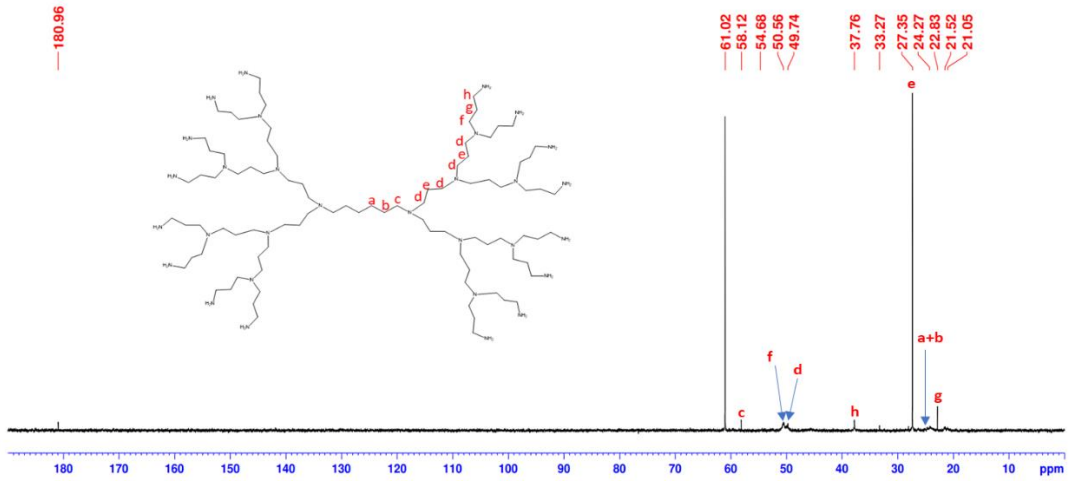

Figure A24- ^{13}C-NMR spectrum of G2NH$_2$ in D$_2$O, third batch.

Annex 2.4. NMR characterization of G3NH$_2$

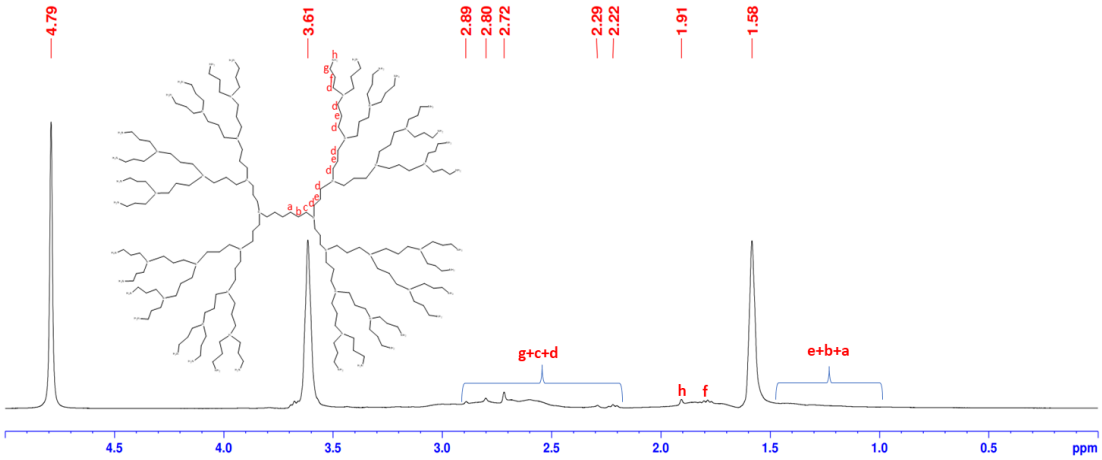

Figure A25- ^{1}H-NMR spectrum of G3NH$_2$ in D$_2$O, second batch.

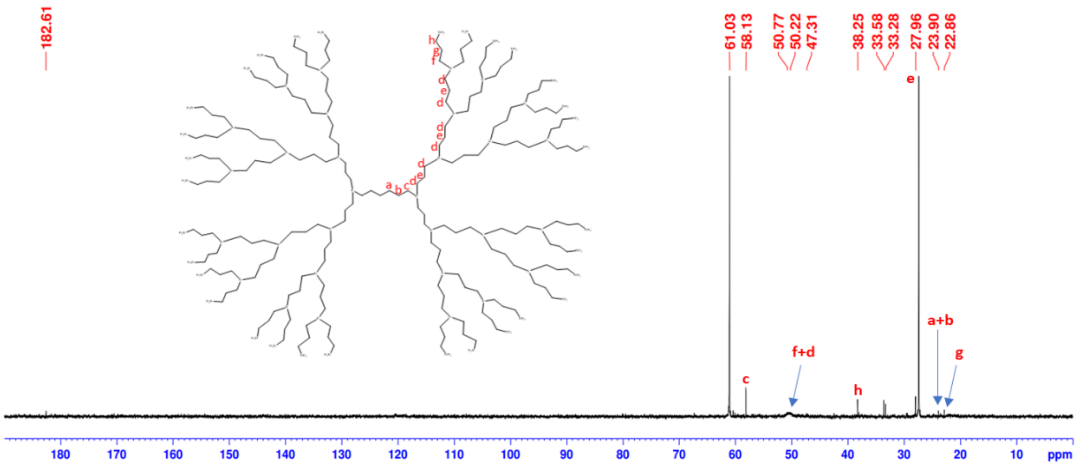

Figure A26- ^{1}H-NMR spectrum of G3NH$_2$ in D$_2$O, second batch.

Annex 3. Synthesis of the methyl ester dendrimers

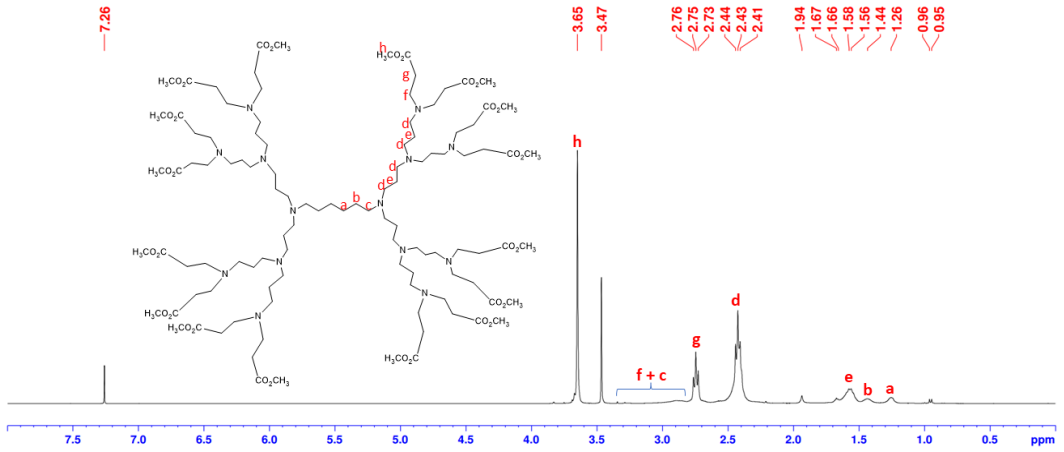

Figure A27- ^{1}H-NMR spectrum of G2CO$_2$Me in CDCl$_3$.

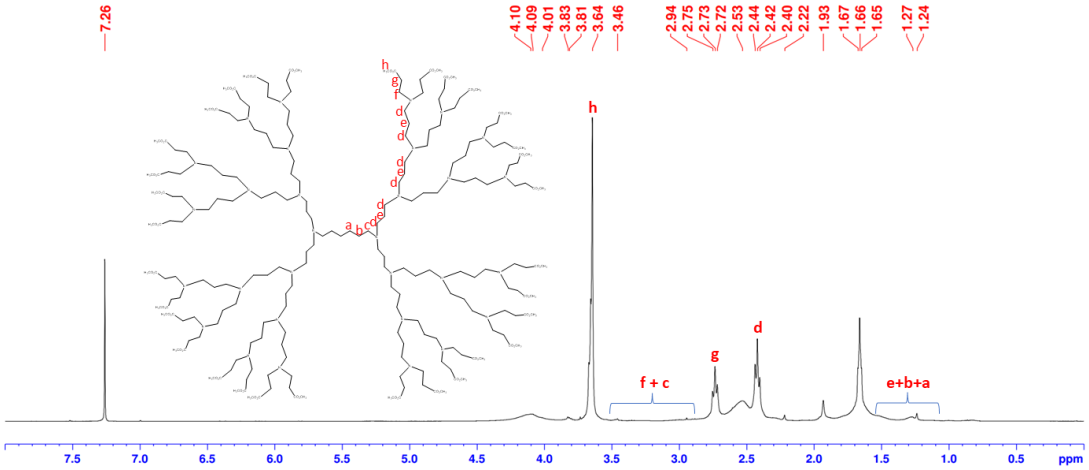

Figure A28- ^{1}H-NMR spectrum of G3CO$_2$Me in CDCl$_3$.

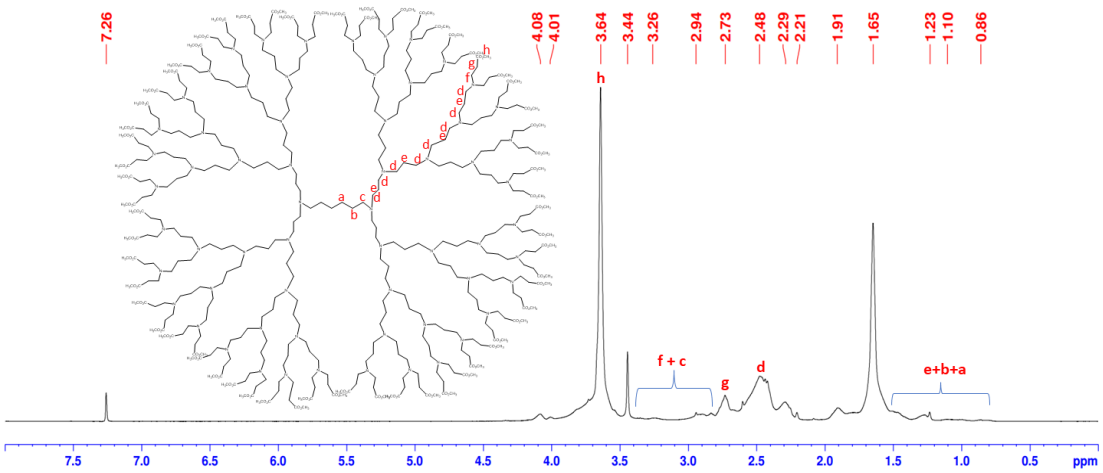

Figure A29- ^{1}H-NMR spectrum of G4CO_2Me in $CDCl_3$

Annex 4. Characterization of the dendrimers encapsulated with the sHCQ

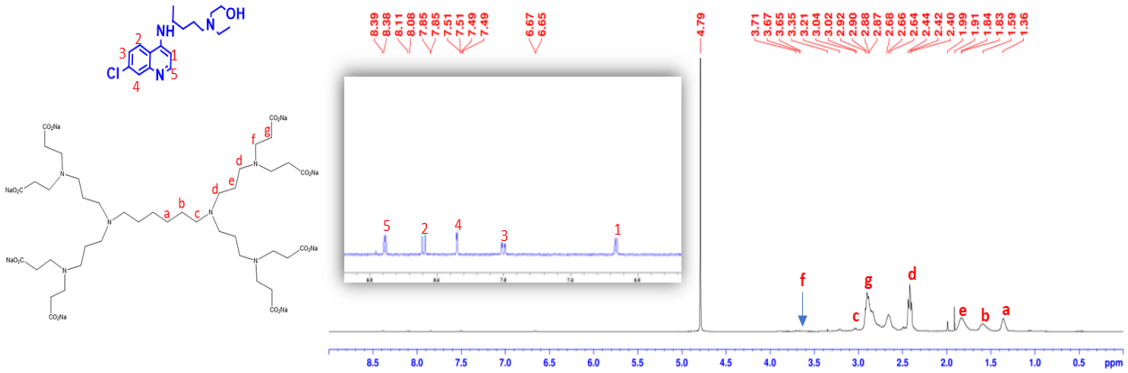

Figure A30- ^{1}H-NMR spectrum of the G1C encapsulated with sHCQ, using a ratio 20:1 (dendrimer/HCQ).

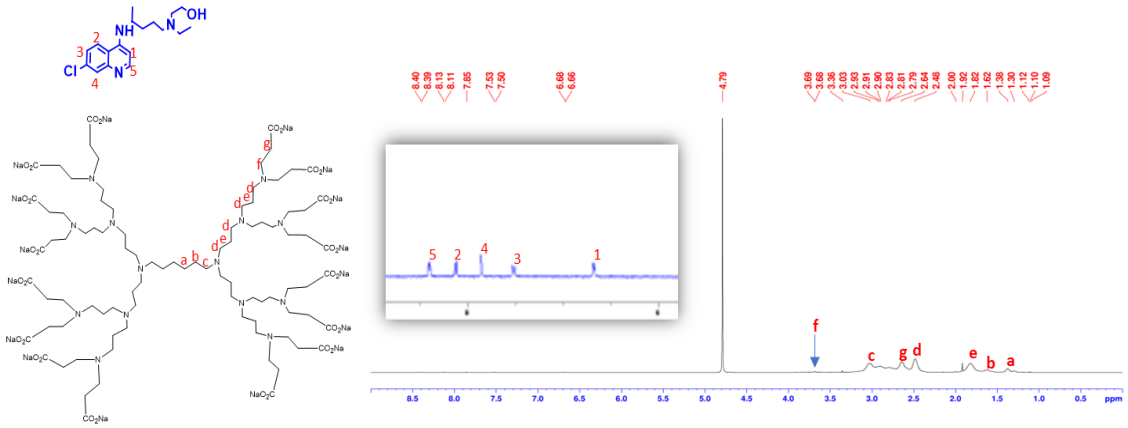

Figure A31- ^{1}H-NMR spectrum of the G2C encapsulated with sHCQ, using a ratio 10:1 (dendrimer/HCQ).

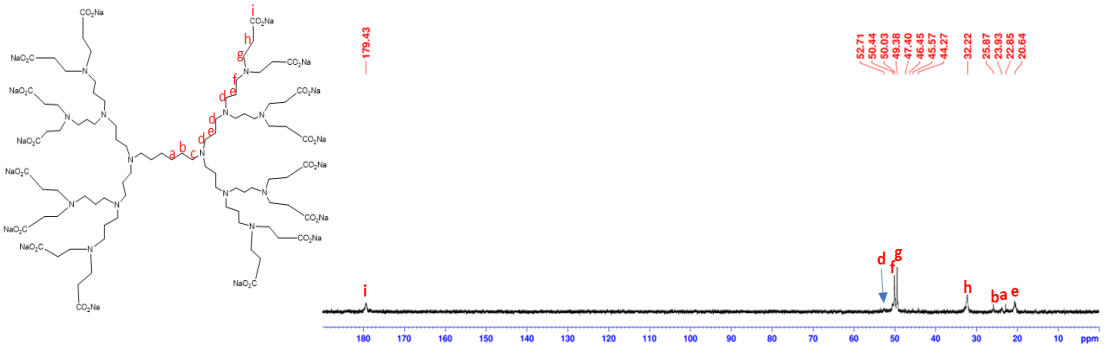

Figure A32- ^{13}C-NMR spectrum of the G2C encapsulated with sHCQ, using a ratio 10:1 (dendrimer/HCQ).

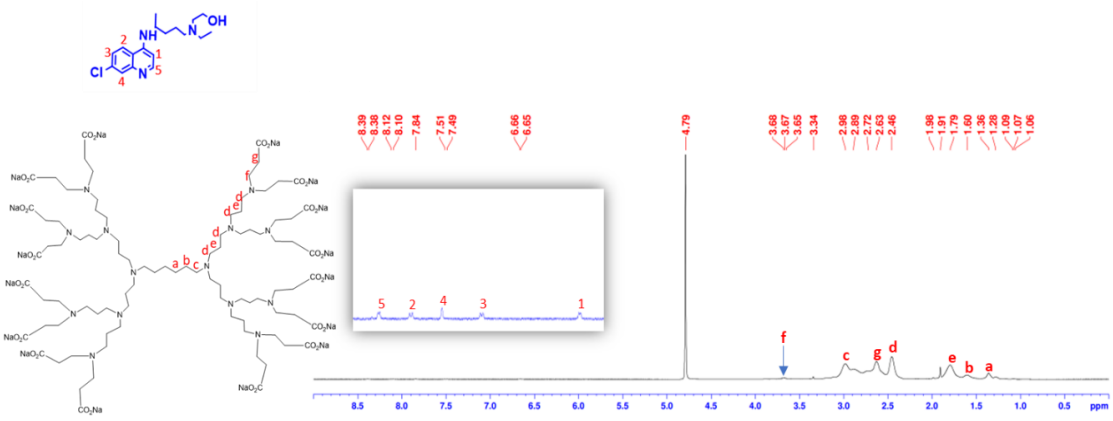

Figure A33- ^{1}H-NMR spectrum of the G2C encapsulated with sHCQ, using a ratio 5:1 (dendrimer/HCQ).

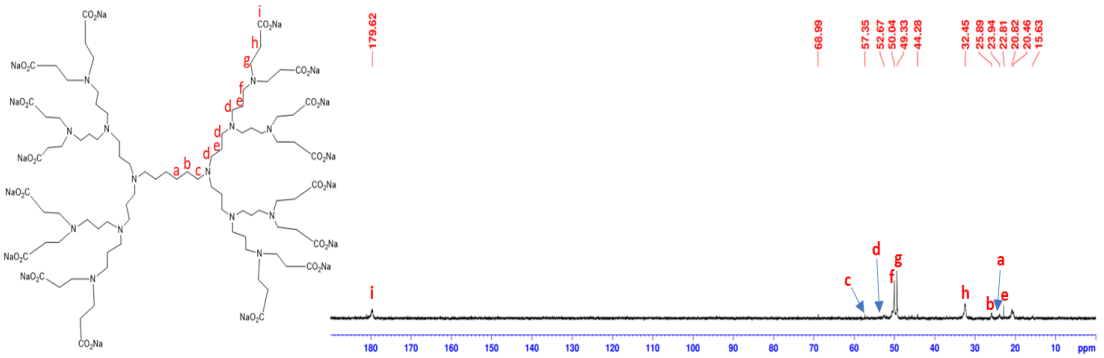

Figure A34- ^{13}C-NMR spectrum of the G2C encapsulated with sHCQ, using a ratio 5:1 (dendrimer/HCQ).

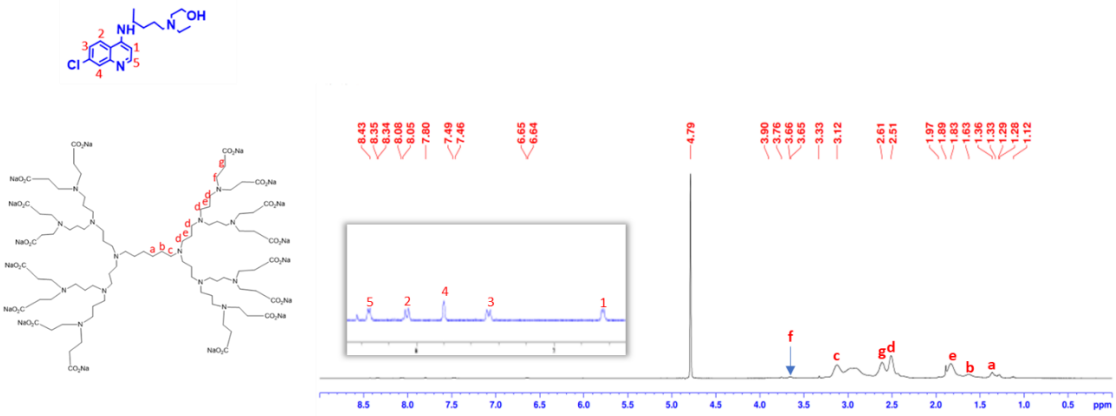

Figure A35- ^{1}H-NMR spectrum of the G2C encapsulated with sHCQ, using a ratio 5:1 (dendrimer/HCQ).

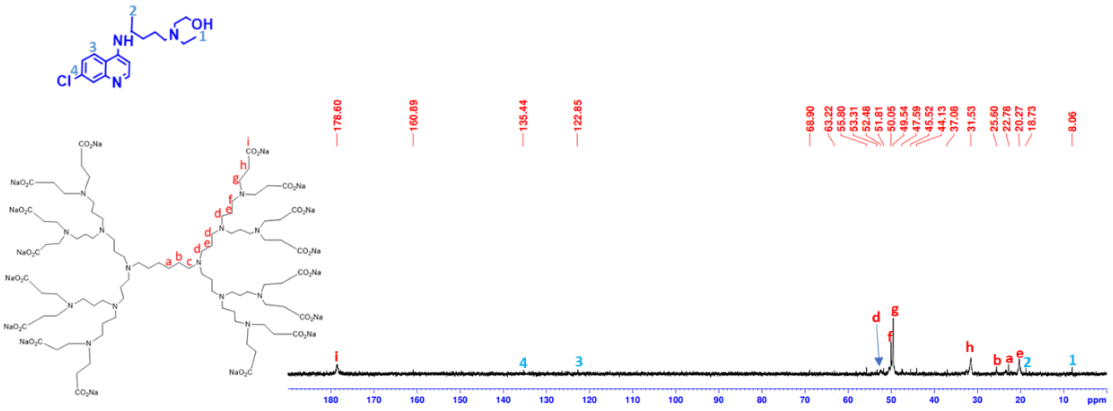

Figure A36- ^{13}C-NMR spectrum of the G2C encapsulated with sHCQ, using a ratio 5:1 (dendrimer/HCQ).

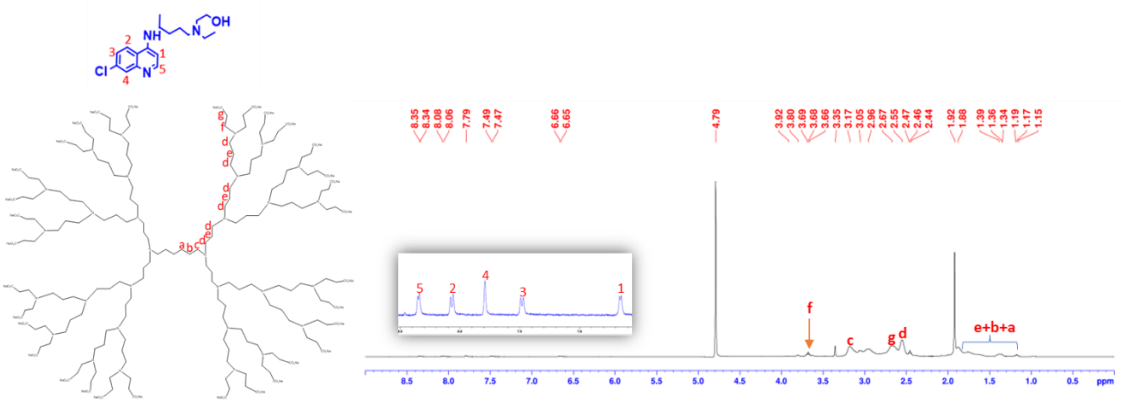

Figure A37- ^{1}H-NMR spectrum of the G3C encapsulated with sHCQ, using a ratio 5:1 (dendrimer/HCQ).

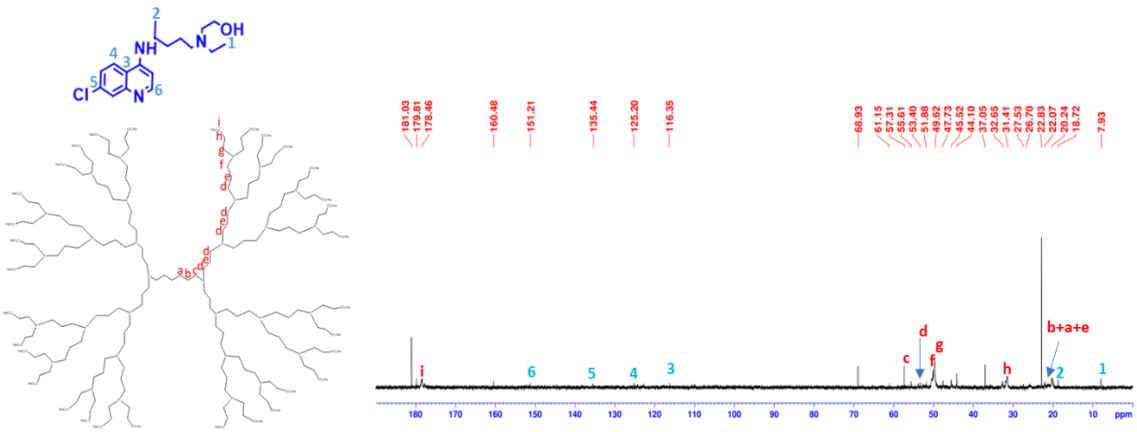

Figure A38- ^{13}C-NMR spectrum of the G3C encapsulated with sHCQ, using a ratio 5:1 (dendrimer/HCQ).

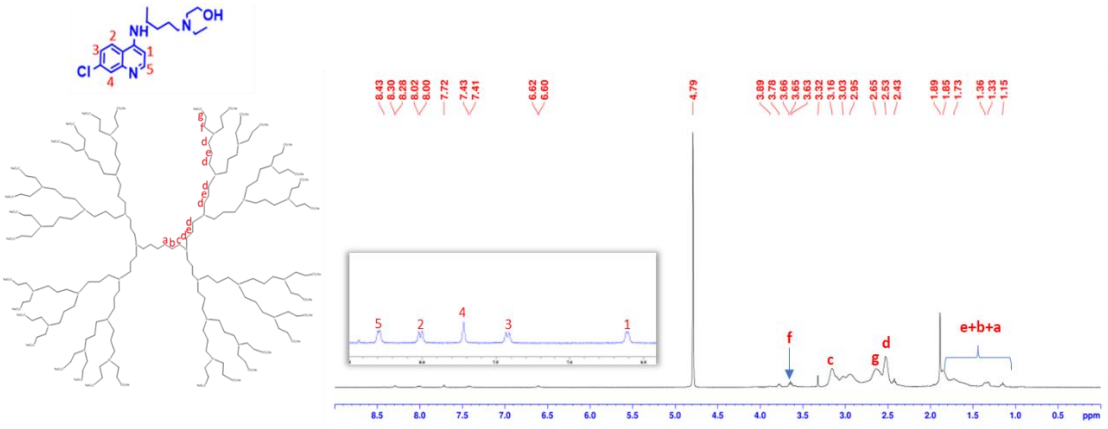

Figure A39- ^{1}H-NMR spectrum of the G3C encapsulated with sHCQ, using a ratio 5:1 (dendrimer/HCQ).

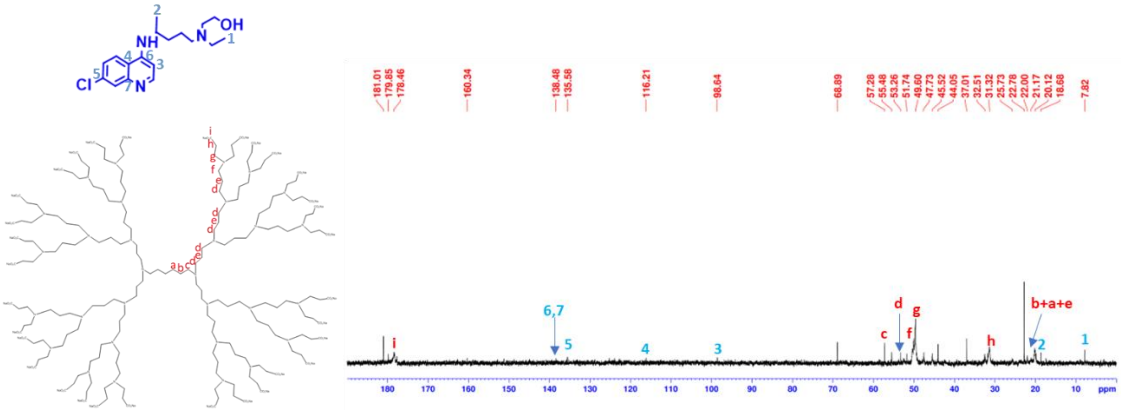

Figure A40- ^{13}C-NMR spectrum of the G3C encapsulated with sHCQ, using a ratio 5:1 (dendrimer/HCQ).

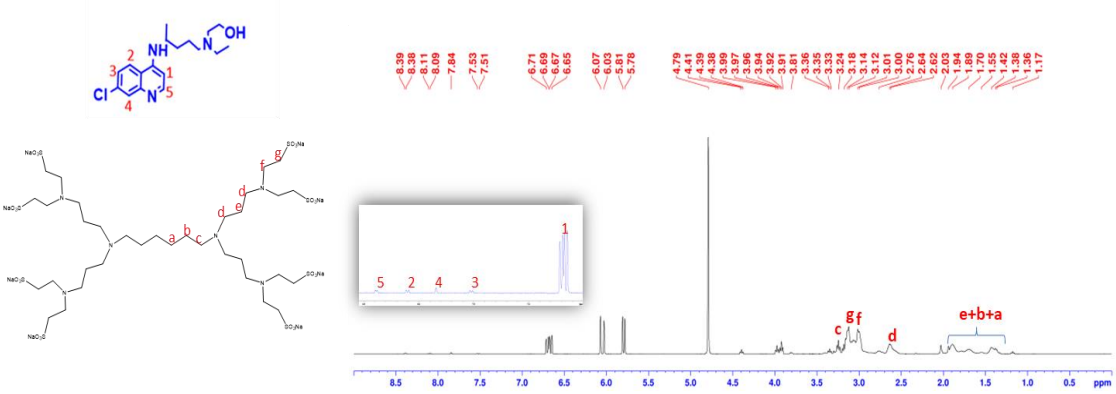

Figure A41- ^{1}H-NMR spectrum of the G1S encapsulated with sHCQ, using a ratio 20:1 (dendrimer/HCQ).

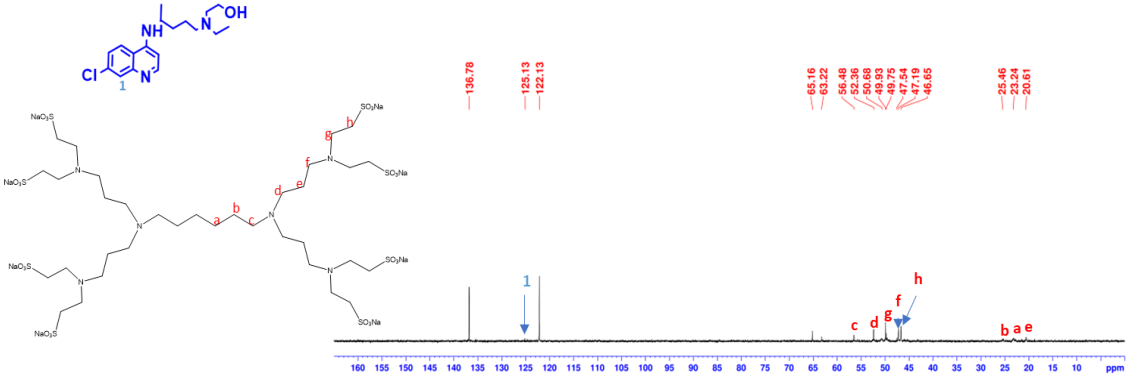

Figure A42- ^{13}C-NMR spectrum of the G1S encapsulated with sHCQ, using a ratio 20:1 (dendrimer/HCQ).

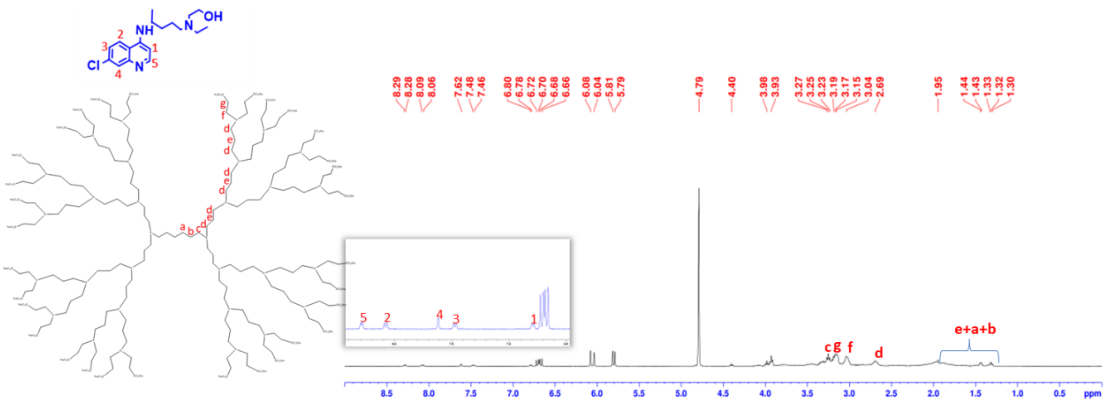

Figure A43- ^{1}H-NMR spectrum of the G3S encapsulated with sHCQ, using a ratio 10:1 (dendrimer/HCQ).

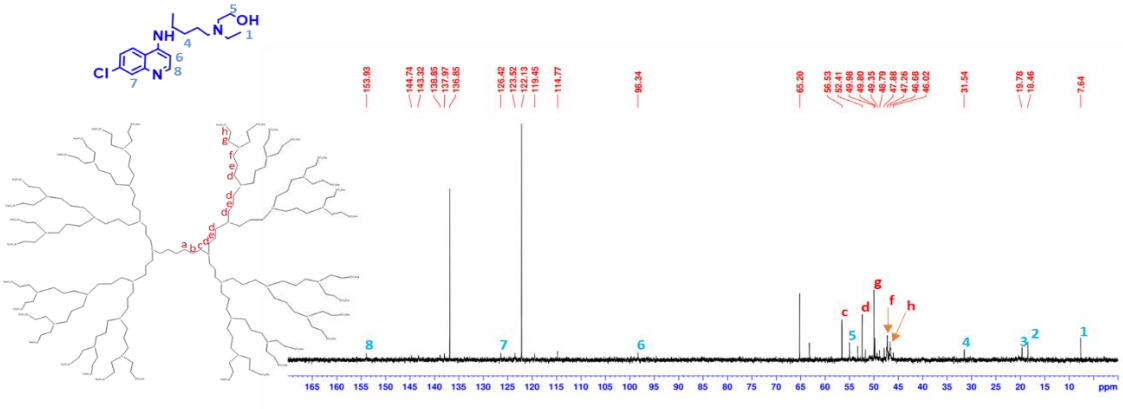

Figure A44- ^{1}H-NMR spectrum of the G3S encapsulated with sHCQ, using a ratio 10:1 (dendrimer/HCQ).

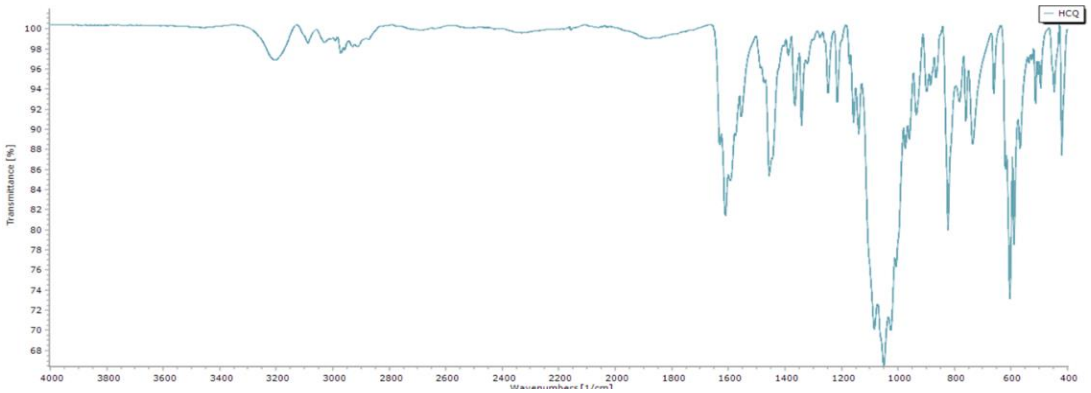

Figure A45- ATR-FTIR spectra of sHCQ

Annex 5. Cytotoxicity of the dendrimers loaded with sHCQ

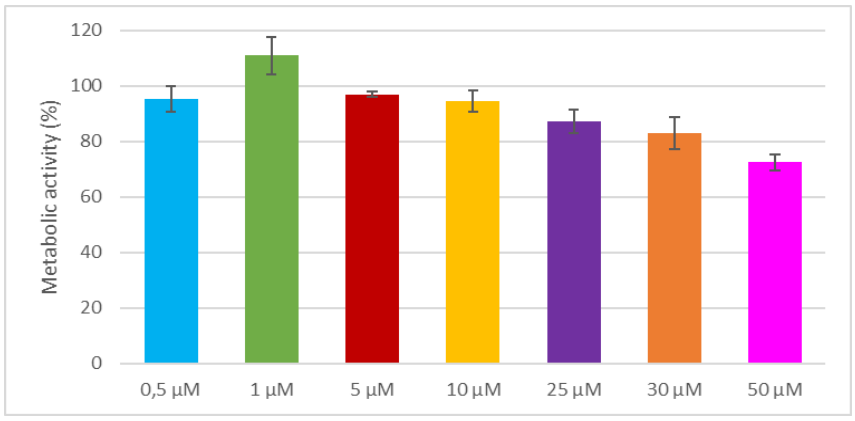

Figure A46- Cell viability of the CACO-2 cells after 48h exposure to the free sHCQ. Data are expressed as the mean ±SD of three independent experiments.

This thesis was written using Microsoft Word Office 365, font Calibry (Body) (font sizes 28, 16, 14, 12, and 9), generally with line spacing of 1.5 lines. For data process and treatment were also used the following software from Microsoft Office 365: Excel (data and graph processing), PowerPoint (images process and processing), ChemDraw Professional 15.0 (images and structures drawing), Topspin® 4.1.3 (software for NMR data processing from BRUKER), SpectraGryph 1.2 (software for FT-IR data processing), Zetasizer software (software for zeta and size data processing), BioRender (on-line free version) (images drawing), Mendeley version 2.74.0 (references).

Fundação para a Ciência e a Tecnologia

CQM Base Fund - UIDB/00674/2020
Programmatic Fund - UIDP/00674/2020

arditi agência regional para o desenvolvimento da investigação tecnologia e inovação

PROEQUIPRAM (M1420-01-0145-FEDER-000008)
M1420-01-0145-FEDER-000005 - CQM+
(Madeira 14-20 Program)

Molecular Materials® RESEARCH GROUP MADEIRA ISLAND · PORTUGAL

OPERAÇÃO CQM+ OPERATION CQM+

Cofinanciado por:

MADEIRA 14-20 · REGIÃO AUTÓNOMA DA MADEIRA · PORTUGAL 2020 · UNIÃO EUROPEIA Fundo Europeu de Desenvolvimento Regional